UNIVERSITY OF LIVERPOOL

Role of provenance on clay minerals and their distribution in modern estuaries

Thesis submitted in accordance with the requirements of the University of Liverpool for degree of Doctor in Philosophy by

Ehsan Daneshvar

March 2011

Dedication

To Professor R.H. Worden

My friend, my teacher, my inspiration

Acknowledgments

This PhD could not have been completed without the help and assistance of many people. At this point I would like to add a general note of thanks to everyone I know. Emotional assistance is just as valued as academic assistance!

First and foremost I would like to thank my heart and soul, my support in my entire life, my dearest Goli, or in an official way, Dr. Golrokh Sepasdar. I would not be able to be here without your support. I love you.

I would like to thank and appreciate my little one, Mana for being patient and lovely. I love you sweetheart.

I would like to express my deep and sincere gratitude to Richard, Professor Richard H. Worden, my supervisor. His wide knowledge and his logical way of thinking have been of great value for me. His understanding, encouragement and personal guidance have provided a good basis for the present thesis. Your continued help for years has been invaluable and I consider you much more than a supervisor. You are my friend.

I am deeply grateful to my supervisor, Doctor Dave Hodgson, for his detailed and constructive comments, and for his important support throughout this work. Thank you so much Dave, you are a brilliant man and friend.

I owe my most sincere gratitude to James Utley who directed me in X-ray diffraction method and technique. His kind support and guidance have been of huge value in this study. He gave me untiring help during my difficult moments.

My sincere thanks to colleagues Gemma and Paddy for all their support and companionship, you are very precious to me. Thank you very much.

I warmly thank Professor Richard Holme, for his valuable advice and friendly help.

Special thanks to Carmel. Your continued help throughout the SEM analysis has been very important to me.

For all lab and further academic support, thanks go to Steve, Keese, Kav, Alan, Chris, Anu, Martin, George, Stan, Jim and Ian. Thanks to the office staff: Helen, Paula, Jeanette, Moira and my best Mo.

To all the postgrads at Liverpool who made me feel great: Mohammad Bukar, Salah, Ben Shatwan, Liz and Dr. Shanvas.

I would like to thank people at chlorite consortium **(ExxonMobil, Chevron, ConoccoPhilips, Eni, Petrobras, BP, Shell and Statoil)** for all their supports and academic comments.

Lastly, I would like to thank all at University of Liverpool and ORSAS team for funding me and believing in me!

Table of Contents

Abstract

A multi-disciplinary investigation into the role of provenance on clay distribution in Ravenglass estuary in north west England employed a range of techniques including clay mineralogy, process sedimentology, surface water and sediment geochemistry and wash load analysis. The results reveal that the hinterland has a specific role in clay mineral distribution across the estuarine systems in association with the other factors such as chemical weathering and alteration, iron elimination and cation behaviour within the estuary, sediment grain size and the physical properties of estuaries. The role of the hinterland is defined as a source of detrital and slightly weathered particles in fluvial sediments through the suspended load into the estuary. The Ravenglass estuary is fed by two different types of rocks which are drained through two rivers. Irt River to the north drains the St. Bees Triassic Sandstones and Esk River to the south drains the Eskdale granite. St. Bees Triassic Sandstones are dominated by feldspar, quartz and minor muscovite in carbonate cement. Pink-coloured Eskdale granite is quartz and feldspars dominated and minor muscovite. Fluvial bedload sediment and wash load (suspension and solute) beyond the estuary are chlorite-dominated in both arms of the estuary with vermiculite and minor illite. Comparison between fluvial and estuarine sediments shows a considerable variation in clay mineral quantification and qualification. X-ray diffraction scans revealed the main chlorite beyond the estuary is dioctahedral chlorite. Fe-Mg chlorite and illite are a minor component in the fluvial sediment and suspended materials. Absence of kaolinite and minor illite in hinterland shows chemical weathering is not advanced and illite can be a muscovite alteration product. Berthierine and kaolinite were absent beyond the estuary system, however, kaolinite is a major clay mineral within the estuary and berthierine also was reported as well. The X-ray diffraction (XRD) method discriminates berthierine with a strong peak at ~7Å (12.5°). Kaolinite can be discriminated at 7.15Å (12.3°), and sample heating to 400°C causes a maximum 50% fall in intensity of the ~7Å (12.5°) for berthierine, while the behavior of the trioctahedral chlorite (002) is unchanged in a berthierine free sample. This amount of loss is decreased for a mix of berthierine with types of chlorite samples. Chlorite is fed to the estuary from the hinterland via river waters and in association with eliminated iron from the river. Berthierine is formed within the estuary in a cold temperature shallow-marine environment. On the other hand, surface water chemistry analysis showed a non-conservative behaviour of Fe in estuary and almost all of the dissolved iron (~90%) precipitates and aggregates inside the estuary. Chemical weathering and alteration had a great opportunity in estuary to form new minerals. In addition to berthierine, role of Fe in estuary to transform Fe-Mg chlorite to Fe-rich chlorite has been considered. In oxidised state and a good source of iron, chlorite shows a vertical variation of increasing Fe-rich chlorite downward in south arm of the estuary.

Sand grains in the estuary surface sediments are coated with a fine layer of clay minerals including chlorite, illite, mix of illite-chlorite and kaolinite in the Irt estuary and Fe-rich chlorite, berthierine, chlorite-illite and kaolinite in the Esk estuary. This suggests that estuaries are sites for not only Fe-clay creation and accumulation but also for the generation of coated grains, which upon subsequent burial and diagenesis, would become chlorite-coated sand grains. Grain-coating clay mineralss are variably present on sand grains from this estuary. Finer grained sand tends to have more complete clay mineral coats than coarser-grained sand. The degree of coating decreases up-section in the Irt Estuary cores. The degree of grain coating is more variable in the Esk estuary but tends to increase up-section.

Chapter 1

Chapter 1 Introduction

The principal purpose of this research is to integrate various sources of data relevant to clay mineral distribution and to critically assess alteration processes in terms of water-sediment interactions in estuarine sedimentary environments. These objectives have been achieved through detailed investigations of the Ravenglass estuary in Cumbria, North West of England. The research has focussed on estuary and river water chemistry and clay minerals from hinterland and soil stream samples, suspended sediments, estuary water sediments, and surface sediments down to a 1m depth.

1.1 Estuarine sedimentary system

An estuary (Fig. 1.1) can be defined as a tidal mouth of a river or marine marginal location where marine salinity is measurably diluted by local freshwater discharge (Fairbridge 2002). Estuaries vary in size, depth, and morphology and can be confined by bedrock and/or alluvium. Tidal processes tend to dominate the pattern of sedimentation within an estuary (Thom et al. 1975; Komar and Enfield 1987). Sediment deposition is controlled by the complicated interplay of various factors including tidal currents, tidal range over different periodicities, wind waves, river discharge, precipitation, temperature and local flora and fauna (Burton and Liss 1976; Wiley 1978; FitzGerald et al. 2005). These factors differ noticeably among the world's estuaries, so that sedimentation patterns and environments of deposition vary widely. The tides shape the interior of most estuaries into marginal tidal flats with run-off channels, and axial tidal channels, which extend well below the position of the lowest tides.

Figure 1.1: The Ravenglass estuary north west England as example of small estuaries. Scale bar in lower right is 10493ft or 3182 metres.

1.2 Estuary waters

From a geochemical standpoint, an estuarine environment may be defined as one in which seawater is substantially diluted with fresh water supplied from the hinterland drainage basin (Perillo 1995). An estuary will typically contain waters in a mixing series from river water, which has an estimated average T.D.S of 120 mg/L (Domenico et al. 1998), to sea water with a salinity about 35,000 mg/L (Drever 1982). One approach, which has proved of value in studying the fate of a dissolved constituent material entering an estuarine system, is to compare its observed distribution with that predicted for conservative mixing of river water with seawater. If the behaviour of a compound or ion is such that there is a linear relationship between its concentration and the degree of mixing between the end members of the mixing series then its behaviour is correctly described as conservative. For non-conservative behaviour there is either net addition or removal of the species and the graph of constituent concentration against salinity will deviate from a simple straight line(Burton and Liss 1976).

For aqueous iron behaviour in estuaries, physical-chemical considerations suggest that iron (III) entering estuaries or formed by oxidation of iron (II) should largely precipitate as the

hydrous oxide. Such an effect can be seen where slightly acidic river waters, potentially carrying large amounts of iron, mix with the slightly alkaline seawater (Mayer, 1982). The non-conservative behaviour of dissolved iron during estuarine mixing has been reasonably well-documented (e.g. (Boyle et al. 1974; Boyle et al. 1977a; Sholkovitz 1978; Sholkovitz et al. 1978; Mayer 1982). Riverine dissolved iron is mostly in a colloidal form (Sholkovitz 1978; Sholkovitz et al. 1978). On mixing with saline seawater in an estuary, these colloids aggregate to form particles larger than the filter pore size (Mayer, 1982). Natural riverine Fe colloids, typically in association with organic matter, are more stable and resistant to aggregation by salt than synthetic iron hydroxide colloids (Mosley et al., 2003). Therefore, full compatibility between the non-conservative behaviour of Fe in natural riverine systems with experiments may not necessarily be expected. It has been suggested that if organic matter were absent from river water, it is likely that Fe colloids would precipitate long before reaching the estuarine mixing zone (Mosley et al. 2003). However, once in the presence of more concentrated seawater, aggregation of Fe colloids accelerates (Boyle et al. 1977a; Mosley et al. 2003). Coagulation and precipitation of Fe colloids can occur in the absence of particulate materials; however the association of humic acids and clay minerals can also help precipitate hydrous ferric oxide (Sholkovitz et al. 1978).

1.3 Sedimentary environments, diagenesis, and clay minerals

1.3.1 Sedimentary environments

Non-marine sedimentary environments of deposition, such as alluvial fans, rivers and floodplains, lakes, and deserts, are important indicators of ancient climate and paleogeography. These settings are preserved in the stratigraphic record in subsiding basins (Prothero and Schwab 2004).

Marine sedimentary deposits make up most of the stratigraphic record, since they are commonly deposited below the base level of erosion and have a high preservation potential. In fact, the sediments of the deep sea are formed by a steady "rain" of clays and microfossils from the surface. Many important economic deposits, including most of the world's oil, as well as clays, diatomite, and other economically valuable sedimentary rocks, are produced in the marine realm. Coastal sedimentary environments such as deltas, tidal flats, and barrier islands are highly dynamic systems. They migrate both offshore and

onshore in response to relative sea level changes, and up and down the coast in response to currents, and prograde due to high sediment supply. Many coastal areas have extensive wetlands, or salt marshes, particularly on the borders of estuaries. Salt marshes are highly stressed environments, dominated by a few organisms that can tolerate the extreme ranges of salinity. The documentation of diagenesis and clay mineral alteration and distribution in marine sedimentary depositional system has been started but remains in its infancy as a science (Aller et al. 1986; Bailey 1988; Abu-Zeid and Stanley 1990; Bokuniewicz 1995; Petschick et al. 1996; Bjolykke 1998; Velde and Church 1999; Belzunce-Segarra et al. 2002; Burley et al. 2003). Mineral distribution in estuaries is largely unstudied. There are no means of predicting mineral distribution in estuaries.

1.3.2 Sediment-animal interactions

During the mineral alteration and mineral weathering, sediment reworking is a potential result of animals living in the sediments. There some evidence that show some invertebrate species such as earth worms (Carpenter-Boggs et al. 2000; Carpenter et al. 2007) and marine lugworms (McIlroy et al. 2003; Needham 2004; Needham et al. 2004) can induce significantly mineral weathering.

Sediment reworking results from various activities of benthic infauna (e.g. burrowing, feeding and locomotion), and strongly affects the physical, chemical and biological characteristics of marine sediments (Meadows 1991; Aller and Aller 1998; Rowden et al. 1998). Sediment reworking strongly influences organic matter mineralization (Kristensen 2000), the structure and porosity of the sediment matrix (Maire et al. 2007; Volkenborn et al. 2007) and the release of nutrients from the sediment to the water column (Hylleberg 1975; Volkenborn et al. 2007). The rate of sediment reworking directly depends on the characteristics of the dominant macrobenthic species (i.e., size, density and feeding ethology), and on the intensity of infaunal activity, which depends on environmental parameters such as food availability and temperature (Maire et al., 2007).

Lugworms

Lugworms are the marine equivalent of the earthworms. They take in sand through the body during feeding; any organic matter is digested in the gut. To keep the burrows clear, lugworms are required to reverse up the burrow to the surface to defecate the sand, and so form the cast. The common lugworm, *Arenicola marina* (Fig. 1.2), a large polychaete found in great abundance in intertidal areas of northwestern Europe (Beukema and De

Vlas 1979; De Wilde and Berghuis 1979), modifies the bed in several ways (Cadee 1976). As a deposit feeder, it indiscriminately ingests particles from the head-shaft, digests organic matter, and excretes a characteristic coiled faecal cast at the top of the tail-shaft. Oxygenated water, pumped in at the tail-shaft for respiration, is then driven into the sediment in

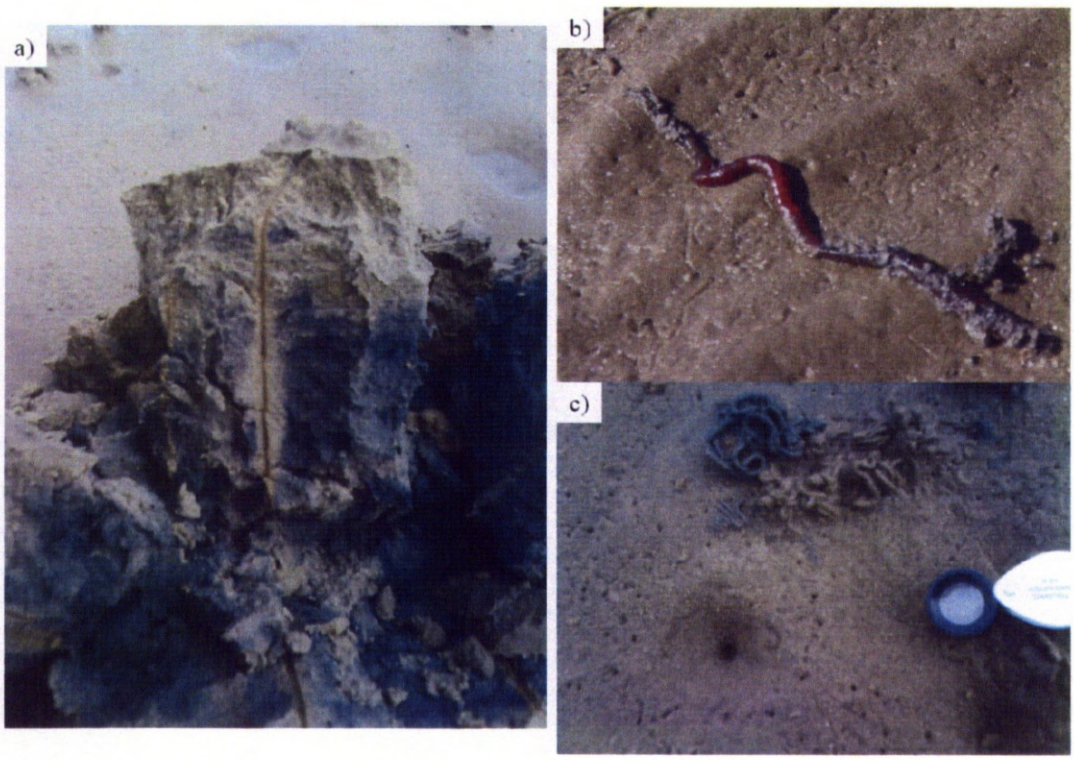

Figure 1.2: Lugworms and burrows in modern sedimentary environments. a) a burrow in estuary surface sediments and reworking by lugworm (field of view 18 cm), b) an adult lugworm (field of view 15 cm) and c) a plan view of a burrow hole and faecal cast (hand-lens for scale).

the head-shaft, causing bed liquefaction and grain settlement, and thus maintaining a fresh supply of grains from the surface. This "conveyor belt" system permits the adult organism to remain in one place throughout its life span, living within its large U-shaped burrow that extends 150 mm or more into the sediment (Cadee 1976; Beukema and De Vlas 1979; De Wilde and Berghuis 1979). *A. marina* exhibits preference for sandy substrates: coarse sands are too large for ingestion while fine sediments (muds) are unsuitable for maintaining burrow structure; unwanted coarse or shelly material can build up at the base of the head shaft, leading to a graded deposit (Hylleberg 1975; Cadee 1976; Volkenborn et al. 2007).

Bioturbation

In fine grained sand, lugworm activities significantly limit the accumulation of clay grade particles and associated organic material. Fine grained sediments, which typically occur between sand flats in the low intertidal and mud flats near the high water mark, are most susceptible to the ecosystem engineering effects of *Arenicola marina*. Coarse grained sediments, with a median above 300μm, are less efficient in accumulating clay grade particles and less susceptible to sediment clogging (Volkenborn et al. 2007). The sedimentary system is shifted from mud towards sand flats in the presence of lugworms. The most obvious change is the accumulation of clay grade particles and associated organic matter in the upper 5cm in the absence of *Arenicola marina*, coupled with a decrease in sediment permeability. Lugworm defecation at the surface followed by a re-suspension of clay size material when casts are washed away is presumably an important mechanism preventing fine particle accumulation in the presence of lugworms (Volkenborn et al., 2007). Cadee (1976) suggested a depth of 0.1m is the most active area for lugworms and Hylleberg (1975) reported fine sands, silt and clay grade particles have a greater chance to be swallowed than larger ones and are returned to the sediment surface with the faecal casts (Baumfalk 1979). In shallow waters, tidal currents and wave action are the main forces of lateral particle fluxes. Faecal casts of *Arenicola marina* may persist for several tidal cycles under calm conditions but are usually washed away by waves and winds. During this process clay grade particles are likely to be re-suspended and removed from the sediment. Bioturbation by benthic organisms redistributes particles during feeding, burrowing, and burrow construction. This activity can profoundly affect the physical, chemical, and biological properties of the estuarine surface. Links between animal population, bioturbation and clay mineral distribution in estuaries are presently unexplored.

1.3.3 Origin of estuarine sediments

Sediment deposited in estuaries can originate from the upstream drainage basin, the marine basin (offshore to onshore), the alluvium and or bedrock at the estuary margins, and aeolian sources (Allan and Komar 2009). Sedimentary particles in suspension in estuaries are of relatively small size, 2 μm in diameter, and are mainly clay minerals and colloids which carry a negative surface charge. These are charge-balanced by a double layer of hydrated cations. The stability of this shell of hydrated cations is directly dependant on the ionic concentrations in the bulk water and as ionic strength increases there is a tendency

for the particles to flocculate as the charge equilibrium is disturbed. The flocculation of clay mineral particles has been studied by various authors (Biggs 1970; Gibbs 1977; Arthur et al. 1978; Eisma 1986; Abu-Zeid and Stanley 1990) and they have shown that in general, river waters contain un-flocculated, dispersed clay mineral particles, but that floccules develop in saline waters where an increase in the total ionic concentration occures. The transport of suspended and bedload material in estuarine system is complicated; it is a function of the circulation and stratification of the estuarine waters. It is difficult to distinguish the bedload from suspended load in an estuary because what at one stage of the tidal cycle may be bedload can become re-suspended at another stage.

1.3.4 Weathering

A combination of processes causes the breakdown of rocks, either to form new minerals that are stable on the surface of the Earth, or to break down the rocks into smaller particles to liberate sediment. Minerals can be broken down, dissolved or converted to new minerals by a range of processes which are defined as physical, chemical (Skinner et al. 2004) and biological (microbial) weathering processes (Konhauser 2007).

Physical weathering is disintegration of rocks or minerals with a variety of physical and mechanical processes. This includes the processes of thermal action (expansion due to heat or freezing), roots and animal activity. These mechanical processes can initiate chemical and biological weathering processes by weakening the parent rocks, increasing the effective surface and improve the joints and cracks for a better circulation of water.

Chemical weathering includes processes such as dissolution, oxidation, hydration and hydrolysis (White and Brantley 1995). In these reactions, ions can be added to or removed from a mineral structure. Most rocks and minerals were formed at conditions different to the Earth's surface temperature and pressure. Therefore, minerals in rocks react with their new environment to produce new minerals that are stable under conditions near the surface (Nahon 1991). The most important agents in the chemical weathering processes are water and natural weak acids.

Dissolution occurs when cations or anions are removed from a mineral structure (leaching) by dissolution into water (Meybeck 1987; White and Brantley 1995). When atmospheric CO_2 is dissolved in water it is converted to carbonic acid. H^+ ions from dissolved carbonic

acid (the most abundant weak acid in surface waters) increase its ability to dissolve minerals more eagerly, particularly those containing calcium, magnesium, sodium and potassium. Limestone is particularly subject to this process. Calcite can be leached from the rock.

$$CaCO_3 + H_2CO_3 \rightarrow Ca^{2+} + 2HCO_3^-$$

Redox reactions occur when the oxidation state of the mineral change due to an exchange of electrons between reactant and product assemblages (McSween et al. 2003). This is common in Fe (iron) bearing minerals, and also it is an important pH-based process in the alteration of iron and magnesium rich minerals. Oxidation processes convert the Fe^{2+} to Fe^{3+}. Iron oxide minerals can be common in sandstone, with haematite and goethite common weathering products in this sedimentary rock. These Fe^{3+} minerals are highly insoluble and the reaction typically involves creation of silica (Krauskopf and Bird 1995)

$$Fe_2SiO_4 + 1/2O_2 + 2H_2O \rightarrow Fe_2O_3 + H_4SiO_4$$

Hydrolysis is a water-mineral interaction, resulting in H^+ or OH^+ ions in solution and is primarily a silicate weathering processes. Potassium feldspars are common minerals in granite and sandstones, and chemical weathering alters the feldspars to kaolinite. Leaching K^+ out from K-feldspar and forming kaolinite or from muscovite and forming dioctahedral vermiculite (Essington 2004) is an example of hydrolysis in association with ion exchange example in hinterlands. This chemical reaction occurs when there is H^+ in solutions and these reactions are irreversible.

Biomineralization and microbiological weathering processes is another type of the chemical weathering. In this issue microorganisms have a fundamental role on mineral dissolution and mineral oxidation, and the role of microorganisms in the weathering processes has been recently re-evaluated (Banfield et al. 1999; Skidmore et al. 2005). Needham et al. (2005) have shown that microbiological and macrobiological processes have an effect on the dissolution, the structure and the composition of minerals and also the rate of alteration of minerals. Bacteria or microbes have a significant role on weathering processes while they are the only organisms that inhabit almost every environment on and near the Earth's surface. Biomimeralization forms a mineral phase by micro-organism is in two ways: (1) biomineralization, which is induced by

microorganisms or precipitation in the open environment without any control by the cell over the mineral product (Lowenstam and Weiner 1983). In this process, new minerals are formed as a by-product of either cell metabolic activity or through its interactions with the surrounding aqueous environment. (2) biologically-controlled biomineralizartion (Konhauser 2007), which is completely regulated and controlled by the organism in order to precipitate minerals as a main product for cell and metabolism. Nucleation is the fundamental step in new mineral formation in terms of biomineralization. Micro-organisms contribute significantly to the development of extremely fine grained (<1μm in diameter) mineral precipitates (Konhauser 2007). Biomineralization can be influenced in two ways: surface reactivity, which contains ionized surfaces for better absorption reactivity, and metabolism. In metabolism, the excretion and metabolism of microbes affect the mineral saturation states. Ferric hydroxide ($Fe(OH)_3$) is an example of biomineral precipitation in sedimentary environments, for which the presence of the Fe^{2+}-bearing water in association with microbial bio-mass is essential. Transported dissolved iron into an estuarine environment where pH is increased with dissolved oxygen (Boyle et al. 1977b), can be precipitated inorganically as ferric hydroxide on available nucleation surfaces. This surface has a microbiological role at the iron precipitation phase in order to result in passive iron mineralization (Konhauser 2007).

1.3.5 Clay minerals in the estuaries

The role of clay minerals in association with diagenesis in sediments is well known especially in controlling the quality of sandstone reservoirs (Rossel 1982; Worden and Morad 2003a; Worden and Morad 2003b). Therefore, it is important to understand the mechanisms which control clay mineral formation and distribution. Sandstone properties, such as permeability and porosity, are influenced by clay mineral content. Worden and Morad (2003) discussed how clay coating on the sand grains can affect the permeability particularly in fine-grained sandstones. The effect of clay minerals, predominantly smectite, illite, illite-smectite, kaolinite and chlorite, on reservoir properties are not universal and local conditions will govern the effect of a clay mineral on reservoir quality (Edzwald and O'Melia 1975; Rossel 1982; Petschick et al. 1996; Worden and Morad 2003a). Some early studies (Griffin and Ingram 1954) suggested that clay mineral distribution is controlled by diagenetic processes in coastal plain estuaries. Gibbs (1977) has shown that the grain size and physical circulation in estuarine –marine systems have a

major role. In this research, clay mineral distribution is ascribed to controlling parameters such as diagenetic processes, grain size of sediments and source area variation.

1.4 Clay minerals

Clay minerals are hydrous aluminosilicates that belong to the phyllosilicate group of minerals (Deer et al. 1997). In addition to the aluminium and silicon, they also may contain other cations (Bailey 1980). Where layers of silicon cations are linked to oxygen anions, the immediate geometry of the oxygen around the cation is in the form of a tetrahedron (Velde 1985; Worden and Morad 2003b). In the clay mineral terminology, the silica tetrahedron (Fig. 1.3)

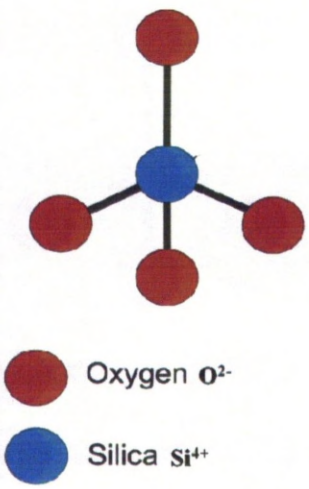

Figure 1.3: The silica tetrahedron; the basic unit of the tetrahedral sheet in layered silicates (Chamley, 1989).

is the basic unit of the tetrahedral sheet (Chamley 1989). Packing of six anions forms octahedra (Fig. 1.4). This is dominated by oxygen but can include some hydroxyl (OH) ions.

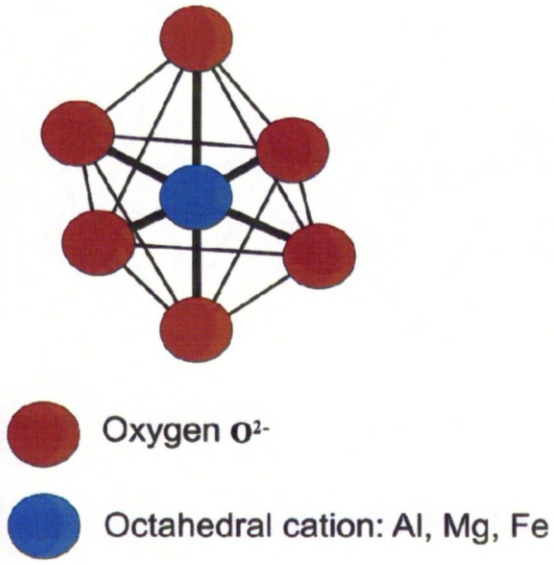

Figure 1.4: The polyhedral that comprises the octahedral sheet utilizes a cation with 6 oxygens. The basic unit is called the octahedral.

Al and Si are the main cations that occupy the space between oxygen layers. However, some other cations such as Fe, Mg, Ca, K, Na are necessary in terms of charge balance to occupy the spaces (Velde 1985; Worden and Morad 2003b). A clay mineral's crystal is made of varying numbers of the tetrahedral and octahedral layers coordinated to oxygen ions. The crystal is a succession of repeating sequences of the basic tetrahedral-octahedral layers (Krauskopf and Bird 1995). These are the basic units of the clay mineral crystal. Tetrahedral and octahedral sheets are bound to each other in layers and layers are stacked on top of each other. The tetrahedral and octahedral ionic basic units, which form sheet structures of great lateral dimension, have a given and constant thickness. This is called the fundamental repeat distance of the mineral. There are three basic combinations of tetrahedral-octahedral coordinated ion layers in clays (Velde, 1985) that are formed by (1) one tetrahedral plus one octahedral layer make a 7 Å (12.5° angle when analysed by Cu k_{α} X-rays) unit layer which is a 1:1 structure; (2) two tetrahedral plus one octahedral layer make 10 Å (9.9° angle) unit layer, which is a 2:1 structure; and (3) if two tetrahedral are added to two octahedral layers they will make a 14 Å (6.2° angle) unit layer which is a 2:1+1 structure (Velde 1985; McSween et al. 2003; Worden and Morad 2003a). The repeat distances are generally identified by X-ray diffraction. In clay mineralogy, the basic

repeat distance, such as a 14Å, 10Å, or 7Å represents different clay minerals (Srodon et al. 2001). Clay minerals can be classified based on the types of ions occupying the octahedral sites. The trivalent ions like Al^{3+} and Fe^{3+} can make dioctahedral units because only two ions are needed to provide six positive charges. The divalent ions like Mg^{2+} and Fe^{2+} make trioctahedral units because three ions are needed to provide six positive charges. Typically Mg-Fe^{2+} rich clay minerals are trioctahedral and Al-Fe^{3+} rich clay minerals are dioctahedral. Interlayer cations are dominated by potassium (Weaver and Pollard 1973; Velde 1985; Worden and Morad 2003b). There are five dominant groups of clay minerals in the sandstones and estuarine sedimentary systems: kaolin, illite, chlorite, smectite and mix-layer varieties.

1.4.1 Chlorite

Chlorite can be described as a 2:1:1 structure including a tetrahedral-octahedral-tetrahedral layered structure interlayered with an additional octahedral layer. For a charge balanced stable structure, positively charged cations (Fe, Mg, Al) and hydroxyl ions can join the negatively charged sheets and interlayer. A solid solution on all sites of the cations is possible and they produce a large variety of chlorite group minerals (Worden and Morad 2003a). These minerals are similar in composition to 7Å berthierine (see later). In low-temperature environments, chlorites are predominantly trioctahedral, with di-trioctahedral-type substitutions in up to half of the octahedral sites (Velde, 1985). This substitution is also found in the berthierine-serpentines (7Å minerals). Some exchange of trivalent ions (Al^{3+}) in the tetrahedral site also occurs, which compensates the trivalent ion substitution in the octahedral site. Thus, the chlorite compositions are the result of simultaneous substitutions which present several types of ionic replacement. Chlorites are found in low-temperature environments, such as in soils and on the ocean bottom, where they can be very rich in iron (Essington 2004). As temperature increases (in arid climates and deserts) chlorites have been reported to become more magnesium-rich (Velde, 1985). Chlorite occurs in a variety of environments and especially in ancient, deeply buried estuarine sedimentary rocks where it occurs as grain coating around the sand grains. In XRD patterns, odd and even order peaks for Mg-rich chlorite will be more equal in intensity while in Fe-rich chlorite, the odd-order peaks are broadened relative to the even orders and intensity of the even-order peaks are about twice than odd-order peaks (Hillier 2003). Dioctahedral chlorites in XRD patterns are identified by unusual relative greater intensity of chlorite (003) compared with the chlorite (002) and (004) peaks, also the chlorite (002)

peak should be almost equal to chlorite (001) peak (Hillier 2003; Worden and Morad 2003a).

1.4.2 Berthierine

Berthierine is an aluminium-bearing, Fe-rich clay belonging to the kaolinite-serpentinite series of 1:1 clay minerals (Bailey 1980). Berthierine has a ~7Å basal (001) spacing and typically has approximately the same chemical composition as Fe-rich chlorite (Brindley 1982b). Some recent studies (Odin 1988; Hornibrook and Longstaffe 1996; Baker et al. 2000a; De Hon et al. 2001) have attempted to address the origin of berthierine concluding that it tends to be found in sediments deposited in shallow marine, marginal-marine and estuarine environments, thus potentially helping to pin down its location within the rock record. Berthierine is commonly, but not always, associated with oolitic ironstones (Odin 1988); although this presents an interesting problem since there seem to be no modern environments where this type of sediment is accumulating. Some consider that Fe^{2+}-rich berthierine transforms from an earlier Fe^{3+}-rich odinite phase (aka phyllite-V) during early diagenesis (Odin 1988) and is part of the tropically-associated verdine facies. However, berthierine has been reported, albeit rarely, from mid to high latitudes casting doubt on the role of latitude and climate (Rohrlich et al. 1969). Fe-rich chlorite is of great interest since it can lead to anomalously high porosity in sandstones since it can coat sand grains and inhibit the growth of porosity-destroying quartz cement (e.g. (Ehrenberg 1993). Berthierine has been reported to transform to Fe-rich chlorite during diagenesis (Aagaard et al. 2000; Worden and Morad 2003a) and has been cited as one of the most important sources of porosity-preserving Fe-rich chlorite. Therefore understanding the origin of berthierine may help to predict the occurrence of anomalously high porosity in the subsurface, which is of obvious relevance to resource exploration and exploitation.

1.4.3 Illite

Illite is a K-rich dioctahedral clay mineral which comprises one octahedral layer packed in between two tetrahedral layers in other word 2:1 clay mineral. Illite is a non-expandable dioctahedral clay mineral in which ionic substitution occurs in both octahedral and tetrahedral layers (Worden and Morad 2003a; Meunier and Velde 2004). In the illite structure, there are some substitution of Fe^{3+}, Mg, and Fe^{2+} in the octahedral site and some Al^{3+} in the tetrahedral site. Illite is characterised by a series of peaks mainly at 10Å in the XRD pattern and in terms of the precise definition of the mineral species illite, glycolation

and heating to 550°C show no change on peak intensity (Hillier, 2003), shape and position. Illite can be a chemical weathering product of muscovite and mica in general and/or K-feldspars from parent rocks in the hinterland or in shallow burial sediments and also in deep burial diagenesis. Illite also can be a product of kaolinite, feldspar or smectite diagenesis as well (Lanson et al. 2002).

1.4.4 Kaolinite

Kaolinite is a ~7 Å (12.3°) 1:1 clay mineral with one tetrahedral layer linked to one octahedral layer and there is no cation interlayer. The chemical formula is $Al_2Si_2O_5(OH)_4$ (Worden and Morad 2003a). Serpentine has a similar structure but is a trioctahedral 1:1 clay with Mg being the dominant divalent cation ($Mg_3Si_2O_5(OH)_4$). XRD can discriminate kaolinite at peaks 7.15Å (kaolinite (001)) or 12.3° and 3.58Å or 24.9° as kaolinite (002) (Hillier, 2003). Problems in distinguishing kaolinite from chlorite and berthierine in XRD pattern have been reported (Hillier 2003; Gould et al. 2010). Kaolinite can be difficult to distinguish from chlorite due to overlap of the kaolinite (001) and chlorite (002) peaks but the analytical approach adopted in this research was sufficient to clearly differentiate the two minerals. A peak at 12.3° is the kaolinite (001) peak while a peak at 12.5° is either solely due to the chlorite (002) peak or is a combination of chlorite (002) and berthierine (001) (Brindley, 1982). The kaolinite peak after glycolation and heating up to 375°C remains unchanged (Hillier, 2003) and if heating continues to 400°C it will either show unchanged or a small decrease in intensity (Starkey et al. 1984; Hillier 2003). Kaolinite during heating up to 550°C is destroyed and will turn to an amorphous phase (Starkey et al. 1984; Hillier 2003). The origin and diagenetic behaviour of the kaolinite is poorly understood and still debated (Worden and Morad, 2003a), however kaolinite stability and kaolinite dissolution-precipitation experiments has been pointed out (Huang 1993; Nagy and Lasaga 1993; Manning 2003). On the other hand, formation of the kaolinite from chemical weathered feldspars, precipitation of gibbsite from the kaolinite dissolution and alteration, all are the issues which have been addressed separately in the estuarine sedimentary environments (Drever and Hurcomb 1986; Drever and Zobrist 1992; Velde and Church 1999; Worden and Burley 2003; Worden and Morad 2003a).

1.4.5 Smectite

The property of absorbing cations and water into the clay structure defines the major classification of clay minerals with their swelling properties (expanding minerals and nonexpanding minerals) and the basic crystallographic repeat unit of the layer structures

(Velde, 1985). All swelling or expanding clays have a 2:1 structure, with two tetrahedral layers and one octahedral layer. Trioctahedral smectite has octahedral layers dominated by divalent metals like Fe^{2+}, Mg^{2+} and Ca^{2+}, whereas dioctahedral smectite has octahedral layers dominated by trivalent metals (Fe^{3+}, Al^{3+}) (Velde 1985; Krauskopf and Bird 1995; Worden and Morad 2003a). These swelling clays are called smectites, which are defined by their tendency to swell when exposed to glycols which can be absorbed between interlayers (Velde 1985; Moore and Reynolds 1989). Vermiculite is characterized by material that comes from rather special, non clay environments, hydrothermal alteration, and soils with a low degree of swelling. In XRD patterns, smectite is identified by a strong peak at about 17Å following glycolation which collapses to about 10Å after heating (Starkey et al. 1984; Hillier 2003).

1.4.6 Vermiculite

Vermiculite is a high-charge, expandable 2:1 clay mineral, meaning it has 2 tetrahedral sheets for every one octahedral sheet, which are separated by layers of water molecules. Vermiculites are the common chemical weathering and alteration product of muscovite, biotite or chlorite which controls the final structure of vermiculite (Essington, 2004). A number of water molecules are related to the hydration state of cations located at the interlayer sites. Therefore, the basal spacing of vermiculite changes from about 10.5 to 15.7 Å (Velde, 1985), depending on relative humidity and the kind of interlayer cation. Heating vermiculite to temperatures (depending on its crystal size) as high as 550° C takes the water out from between the layers (Starkey et al., 1984). Vermiculite can be seen as either dioctahedral vermiculite or trioctahedral vermiculite, with two or three octahedral sites occupied per formula unit, (Scholle and Spearing 1982; Worden and Morad 2003a; Essington 2004; Meunier 2007). Trioctahedral vermiculite is a 2:1 clay mineral with a fundamental unit similar to that of mica. An octahedral sheet forms the basis of the layer and is sandwiched between two opposing tetrahedral sheets. The chemical formula of vermiculite is close to biotite where, instead of the Fe^{2+}, there is Fe^{3+} in its structure and due to reducing of layer charge (Fe^{2+} to Fe^{3+}), hydrated ions in the interlayer space, balance the layer charges (Moore and Reynolds, 1989; Worden and Morad, 2003a). Potassium ions between the molecule sheets are replaced by magnesium and iron ions. Identification of vermiculite using XRD patterns can be difficult due to variable characteristics. Due to the original source, vermiculites have some interlayers of their precursor as interstratified layers. Three types of vermiculite based on its origins have

been addressed: (1) trioctahedral vermiculite as a product of biotite weathering (2) dioctahedral vermiculite from weathered muscovite and (3) vermiculite (dioctahedral and dioctahedral) from trioctahedral and/or dioctahedral chlorite (Moore and Reynolds 1989; Essington 2004).

1.4.7 Mix-layer clay minerals

Interstratifications of different mineral layers in a single structure can make a mix-layer clay mineral (Srodon 1999). Since the clays are phyllosilicates, the mixed layering occurs in the layer plane. For example, a layer of mica can be substituted by a smectite layer in a mineral. These minerals are called interlayered or mixed layered minerals, terms that refer to their composite structure, which consists of a series of different layers of compositions corresponding to mineral species. The main mix-layer clay minerals are expandable clay minerals such; illite-smectite, chlorite-smectite, and hydroxyl interlayered minerals (HIMs). Mix-layer clay minerals often occur in geologically dynamic environments where mineral change is evident, and hence, they are often considered to be transitional or intermediate phases (Velde, 1985). Hydroxyl-interlayered minerals have shown similar basal spacing (14.2Å or 6.2°) as relatively narrow peaks in the air dried scans (Moore and Reynolds, 1989). Hydroxyl interlayer minerals (HIMs) based on their XRD pattern can be categorised in aluminium chlorite, hydroxyl-interlayered smectite and hydroxyl-interlayered vermiculites (HIV) (Meunier, 2007). After saturation with bivalent cations like Mg (Mg-saturation treatment), low-charge smectites under ambient conditions in the air-dried and ethylene glycol salvation state, respectively expand to 15Å and 17Å , while XRD patterns do not show any shift or change in the peak positions and intensity for dioctahedral chlorite and hydroxyl-interlayer vermiculite in same condition. Potassium saturation treatment has an effective change on smectite in which this treatment shifts the smectite XRD peak to 10Å, although has no impact on HIV and dioctahedral chlorite (Barnhisel and Bertsch 1989; Righi et al. 1993; Maes et al. 1999). Heating to 300°C (Fig. 1.5) and then scanning the sample can discriminate the HIV from dioctahedral chlorite, in this way, shifting peak from 14.2Å to ~13Å can be likely a sign of HIV presence rather persistence of dioctahedral peak at 14.2Å (Barnhisel and Bertsch 1989). Higher thermal treatment

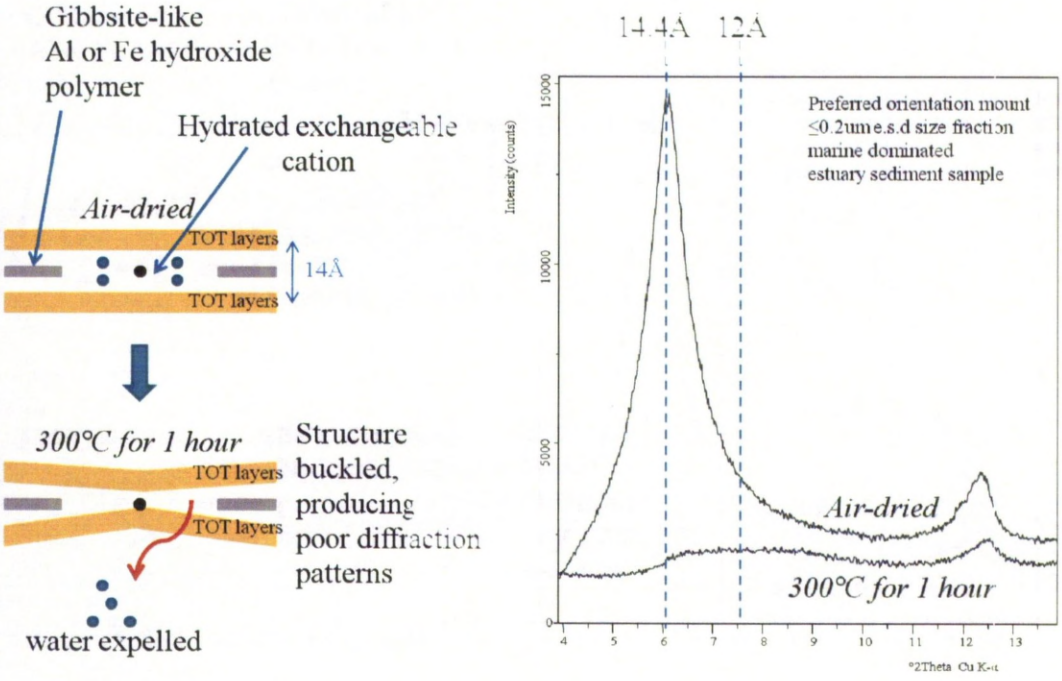

Figure 1.5: Indicative behaviour of Hydroxy-Interlayered-Vermiculite on heating to 300°C.

(400 and 550°C) can shift the peak toward ~10-11Å (Barnhisel and Bertsch 1989; Righi et al. 1993; Meunier 2007). In summary, hydroxy-interlayer vermiculite characteristic behaviour with treating states on XRD patterns can be concluded as: (1) no change with Mg saturation, (2) no expansion with glycerol and/or glycolation (3) no collapse with K saturation (4) 14.2Å partial collapse to ~13Å upon heating to 300°C for 1 hour (5) shifting ~13Åto ~12Å after heating to 400°C and (6) shifting the ~12Å to ~11-10Å upon heating to 550°C.

1.5 Key scientific questions to be addressed

The major scientific questions that have framed this research are presented below with their rationale. These questions are addressed in the final chapter using results and interpretations from core chapters where applicable.

<u>Question 1</u>: How do estuarine sedimentary processes impact clay distributions, and potentially influence reservoir quality in analogous estuarine rocks?

Rationale: Clay minerals and their role on the reservoir quality have been well documented (Rossel 1982; Curtis et al. 1985; Bjolykke 1998; Aagaard et al. 2000; Baker et al. 2000b; Worden and Morad 2003a; Worden and Morad 2003b; Pache et al. 2008; Sionneau et al. 2008) so understanding the mechanisms that control the formation and distribution of the clay minerals is important. Based on the recent studies the ways in which clay minerals affect reservoir quality is broadly known (Aagaard et al., 2000; Worden and Morad, 2003b). Clay minerals can strongly alter porosity and permeability. The effects of clay minerals, especially kaolinite, illite, and chlorite, on reservoir properties are not always uniform (Edzwald and O'Melia 1975; Eberl et al. 1993; Worden and Morad 2003a). Local characteristics, such as crystal shape, distribution and amount, govern the specific effect of a clay mineral on reservoir quality. Estuaries are proficient sediment traps and their deposits have high preservation potential (Dalrymple et al. 1992; Ruggiero et al. 2001). Estuarine systems are commonly interpreted in the stratigraphic record, and typically are associated with incised valley-fills or parts of fluvio-deltaic systems. Estuarine sedimentology and sedimentary processes that influence clay mineral distribution in estuaries are controlled by various processes such as differential settling, diagenesis, flocculation, source area variation and physical properties of estuaries (Feuillet and Fleischer 1980). The distribution and types of clay minerals in ancient estuarine rocks cannot be predicted with present levels of understanding. The distribution and types of clay minerals in modern estuarine systems is also largely unknown so modern systems cannot be used as way to help understand ancient estuarine rock clay mineral distribution.

<u>Question 2</u>: How does fluvial iron form floccules and aggregates in suspended materials in estuary waters and how can affect these affect clay minerals and so influence reservoir quality?

Rationale: Mixing of saline-water and freshwater in an estuary is well documented in terms of chemical and physical properties that change salinity, pH and redox potential (Sholkovitz 1976; Sholkovitz 1978; Sholkovitz 1979; Officer 1981; Mayer 1982). Estuarine waters also contain suspended sediment derived from the in-flowing river and seawater or by re-suspension of settled sediment as a result of tidal currents. Iron occurs at higher concentrations in river water than in seawater (Mayer, 1982). The non-conservative behaviour of dissolved iron during estuarine mixing is moderately well documented (Boyle

et al. 1974; Boyle et al. 1977a; Sholkovitz 1978; Mayer 1982). The physical state of iron in river waters, whether it is truly dissolved, is a complex question. Much "dissolved" iron is actually in a colloidal form, possibly as Fe-organic complexes. Truly dissolved iron can be defined as the fraction which passes through a 0.2μm filter but this only describes a lesser part of the iron being transported by a river (Sholkovitz, 1978). On mixing with the seawater in an estuary, the dominant form of Fe, as colloids, aggregates to form larger particles. The aggregation of the Fe colloids appears due to interaction between the Fe colloids and cations such as Mg^{2+} and Ca^{2+} ions, which have been introduced to the estuary by the seawater end-member (Eckert and Sholkovitz 1976; Boyle et al. 1977a). The most important physical process is flocculation. Clay minerals, organic matter, and colloidal hydroxides of iron all tend to form stable suspensions in fresh water, but tend to flocculate in seawater (Boyle et al., 1977a; Sholkovitz, 1978). Floccules then either sink and are carried landward along the bottom or they are carried out to the sea, depending on the type of estuary and mixing of saline and fresh water models in estuary (Drever 1982). Clay minerals and organic materials in association with iron colloids are transported to estuaries by rivers. During typically non-conservative behaviour in estuaries, Fe colloids become immobilised in presence of cations during the mixing of freshwater and seawater in association with organic matter, thus estuaries are suitable places for both clay mineral accumulation and iron trapping. Links between Fe accumulation and clay mineral type in estuaries have been suspected (e.g. Odin, 1988; Ehrenberg, 1990) but there is no knowledge of processes and links between the sites and timescales of Fe flocculation and clay mineral accumulation.

<u>Question 3</u>: What clay minerals are transported into, formed in (neo-formation) and transported out of the estuary?

Rationale: There are three major locations where clay mineral formation take place: (1) *in situ* during physical and chemical bedrock weathering, (2) during transport and in the depositional environment, and (3) during diagenesis (Tucker 2001; Burley et al. 2003; Worden and Morad 2003b) . Practically all clay minerals can form and develop within soils and regolith. Clay minerals form by alteration and replacement of other silicate minerals such as feldspars and micas, transformation of other detrital clay minerals, and direct precipitation (Velde 1985; Tucker 2001). Illite and kaolinite are common

weathering products of the feldspar minerals (Tucker 2001). After neoformation and transformation in the hinterland, clay minerals are available for erosion, transportation and deposition in estuaries (Wilson 1999). Estuaries are sedimentary systems that receive material via bedload, in suspension and as solute from weathered hinterland material via rivers. During depositional settling some alteration and diagenesis can occur. Clay minerals can precipitate directly from water or pore waters in the surficial sediments and also within coarser siliciclastic sediment during diagenesis (Worden and Morad 2003b). Some clay minerals can also be transformed to form other clay minerals. For example, transformation of precursor Fe-rich clay minerals to chlorite (chloritization) as coated grains during early diagenesis (Worden and Morad, 2003b) or dissolution of kaolinite and precipitation of illite or chlorite-smectite (Lanson et al. 2002) have been reported. Chlorite coating in the estuarine sediments can be a variety of chlorite types, Mg-rich chlorite, Fe-rich chlorite, dioctahedral chlorite and mix-layer chlorites (Hillier, 2003). The aqueous iron load of rivers decreases suddenly once rivers enter estuaries and the salinity starts to increase (Boyle et al., 1977b). The factors that control iron-loss from rivers may explain the source of the elevated Fe-content of chlorite in estuarine rocks (Ehrenberg, 1990). Neoformation of berthierine within marine and estuarine macrofauna (lug worms, *Arenicola marina*) has also reported (Needham et al. 2004; Needham et al. 2005). It seems likely that berthierine will form in the estuarine sediment by interaction between the flocculated and deposited fluvial Fe and detrital and neoformed alumina-silicate phases. Despite the disparate studies that have allowed these conclusions to be made, there have been no holistic studies of clay creation in hinterlands, transport and accumulation in estuaries or then subsequent loss from estuaries.

<u>Question 4</u>: How do hinterland geology, diagenetic and alteration processes, grain-size, and biological activity impact clay mineral distribution in the estuary, and can these controls by discriminated?

Rationale: Estuarine sedimentary systems and clay mineral distribution studies in estuaries have begun to be addressed in recent studies (Edzwald and O'Melia 1975; Feuillet and Fleischer 1980; Abu-Zeid and Stanley 1990; Petschick et al. 1996). Explaining the mechanism of clay distributions in coastal sedimentary systems has been argued in different ways. Some researchers have stated that the distribution of clays in estuaries is

controlled by various mechanisms such as differential settling, diagenesis, flocculation, hinterland geology and physical processes in the estuary (Feuillet and Fleischer, 1980). Other studies on the clay mineralogy of estuarine and coastal sediments have emphasised the role of diagenetic processes in coastal plain estuaries on clay mineral distribution (Chamley, 1989). Gibbs et al. (1989) ascribed the main control on the distribution of clay minerals in the estuary as grain size and physical circulation in estuarine–marine systems. The distribution of clay minerals in modern sediments is largely a reflection of the climate and weathering pattern of the source area (Rossel 1982; Velde and Church 1999; Sionneau et al. 2008). Clay mineral transformation and grain size of the sediments are the other important factors which control the clay mineral distribution (Gibbs 1977; Rossel 1982; Michalopoulos and Aller 1995; Petschick et al. 1996; Velde and Church 1999; Tucker 2001; Needham et al. 2005; Worden et al. 2006). Despite the studies cited above, there have been few studies that have attempted to discriminate the range of controls on clay mineral type and distribution in estuaries.

Question 5: What are the quality, quantity, and mineralogy of grain coats across an estuary?

Rationale: The occurrence, amount and type of clay minerals can alter the porosity and permeability of a reservoir (Worden and Morad, 2003b). Chlorite and illite are the most dominant clay minerals in estuarine sediments. Illite is good example of a clay mineral which affects the porosity of the reservoirs (Ehrenberg 1993). The fibrous shape of some type of illite leads to a high surface area and enables illitic clay minerals to grow outward as coats from a host grain into pore space. This reduces the pore spaces for fluids (petroleum) but more importantly has a disproportionate impact on permeability (Hillier and Velde 1992; Ehrenberg 1993). Chlorite can have the opposite effect on the reservoir quality. The most important process which decreases porosity and permeability of sandstone reservoirs at great depth is quartz nucleation and cementation during the burial diagenesis (Hillier 1993). Chlorite has been identified as quartz cement inhibitor. Chlorite coats significantly inhibit the quartz nucleation and can anomalously preserve porosity and also permeability to great depths of burial (Hillier and Velde 1992; Ehrenberg 1993; Hillier 1993; Hillier 1994). It is important to develop an understanding of the mode of occurrence and the mechanism which generates clay mineral coatings to enable their

prediction. Transformation of precursor Fe rich-phases into chlorite during burial diagenesis has been reported (Aagaard et al., 2000). There is more than one origin of clay as coated materials on sand grains in reservoirs. The origins may be the diagenetic transformation of inherited clay coated sand grains or direct precipitation from pore fluid forming authigenic clay coats (Hillier 1993; Hillier 1994; Aagaard et al. 2000; Worden and Morad 2003b). There is currently no basis for understanding or predicting the amount of inherited grain coats in sedimentary environments (including estuarine environments). Thus the measurement of grain coating in modern estuarine systems may help provide the basis for the prediction of the distribution of grain coating clays and anomalously high porosity in the reservoirs.

Chlorite coats or early chlorite coating are most likely the product of the transformation of a variety of precursor phases ranging from verdine minerals, mix-layer minerals, to berthierine and smectite (Worden and Morad, 2003b). Berthierine is an aluminium-bearing, Fe-rich clay belonging to the kaolinite-serpentinite series of 1:1 clay minerals (Bailey, 1980). Berthierine has a ~7Å basal (001) spacing and typically has approximately the same chemical composition as Fe-rich chlorite (Brindley 1982b). A combination of precursor aluminosilicate minerals and an available cation (Fe and Mg) source is needed to form a diagenetic chlorite coat. Berthierine can transform to chlorite (Aagaard et al., 2000; Hillier, 1994; Worden and Morad, 2003) since they have very similar composition (the difference is their crystal structure, see later). This is rather simpler than a transformation from kaolinite to chlorite since these have very different compositions (Velde 1985). A potentially important precursor to grain-coating chlorite is smectite or chlorite-smectite but the progressive transformation may require a source of aluminium and Fe^{2+} (Worden and Morad, 2003b). An experimental approach to making chlorite coats from berthierine-coated precursor grains in burial diagenesis simulation has been reported (Aagaard et al., 2000). Berthierine has been cited as one of the most important sources of porosity-preserving Fe-rich chlorite. Therefore understanding the origin of berthierine may help to predict the occurrence of anomalously high porosity in the subsurface. Some recent studies (Odin 1988; Hornibrook and Longstaffe 1996; Baker et al. 2000b; De Hon et al. 2001) have attempted to address the origin of berthierine concluding that it tends to be found in sediments deposited in shallow marine, marginal-marine and estuarine environments, thus potentially helping to pin down its location within the rock record. This work seeks to link together observations about the degree and type of grain coating

with clay mineral, and specifically Fe-clays such as berthierine, distribution in estuarine sediments.

1.6 Thesis structure

This thesis includes five independent manuscripts that have been, or are going to be, submitted to international journals. The background, methodology, results and discussion of each manuscript is presented in each chapter (chapter 2 to 6). An integrated and extended discussion and final conclusion and suggestions for further work are located in chapter 7. All data, figures and tables are collected in appendices at the end of the thesis. The content of each chapter is summarised as follows:

Chapter 2 introduces berthierine forming in a cold temperate estuary: a broad clay mineral investigation such as SEM/BSE/EDAX, XRD, and FTIR techniques for one cored sample from the Ravenglass estuary (northwest England) has revealed the formation of berthierine within the estuary, however alter of this type of clay minerals has not been reported in such environments so far.

Chapter 3 presents clay mineral distribution and origin of the clay minerals in surface sediments in the Ravenglass estuary and related river systems. Samples from stream sediments, and surface estuary sediments have been analyzed in order to a surface distribution clay mineral pattern. In this manuscript, the origin of the clay mineral (transported from hinterland or forming within the estuary) and type of clay mineral across the estuary are discussed.

Chapter 4 introduces the stratigraphic distribution (depth-controlled) of clay minerals in the Ravenglass estuary and also alteration and early diagenetic processes. In this manuscript, neo-formation of Fe-chlorite and alteration of kaolinite to gibbsite in the oxidation zone at the south arm of the Ravenglass estuary and pyritization in the north arm are discussed.

Chapter 5 explains the Fe-behaviour in estuary waters all across the Ravenglass estuary as a function of time during tide cycles. Elimination of Fe from the waters and relationship with salinity change during the tide in association with pH changes are mapped.

Chapter 6 introduces the suspended matters in the marine and non-marine system in the Ravenglass estuary and rivers respectively. Clay minerals as suspended materials in the estuary water and end-members are discussed. The results of this manuscript expand the idea of clay mineral origins in the chapters 2, chapter 3 and chapter 4.

Chapter 7 contains an integrated and extended discussion of the chapters 2, 3, 4, 5 and 6 to an overall explanation of the all parameters control the clay mineral distribution in the Ravenglass estuary, origin of the clay minerals, grain coating, diagenesis in modern sedimentary systems and transported systems for the clay minerals toward the estuary and marine system. For example the role of Fe to form new Fe-bearing grain coats and/or pyritization is explained. This chapter also tries to answer the questions and expand the hypothesises which have been discussed in chapter 1 and also tries to address new suggestion and research target for future regarding discussed contexts.

1.7 Author contributions

At the time of thesis submission, the statuses of the manuscripts collated in this thesis were as follows:

Chapter 2: Daneshvar, E., Worden, R. H., Hodgson, D. M. and Utley, J., Berthierine on clay-coated sand grains in the Ravenglass estuary, NW England, UK

Author contribution: Daneshvar, E.: Principal investigator and author. All primary data collection, processing and interpretation

Worden, R. H.: Discussion and detailed manuscript review

Hodgson, D. M.: Discussion and detailed manuscript review

Utley, J.: XRD diffractometer assistance, discussion and manuscript review

Chapter 3: Daneshvar, E., Worden, R. H., Hodgson, D. M., Clay mineral distribution in surface sediments from the Ravenglass estuary

Author contribution: Daneshvar, E.: Principal investigator and author. All primary data collection, processing and interpretation

Worden, R. H.: Discussion and detailed manuscript review

Hodgson, D. M.: Discussion and detailed manuscript review

Chapter 4: Daneshvar, E., Worden, R. H., Hodgson, D. M., Stratigraphic variations in clay mineralogy, grain coating pattern and clay mineral alteration in the Ravenglass estuary

Author contribution: Daneshvar, E.: Principal investigator and author. All primary data collection, processing and interpretation

Worden, R. H.: Discussion and detailed manuscript review

Hodgson, D. M.: Discussion and detailed manuscript review

Chapter 5: Daneshvar, E., Worden, R. H., Hodgson, D. M., Dissolved iron behaviour in the Ravenglass estuary waters

Author contribution: Daneshvar, E.: Principal investigator and author. All primary data collection, processing and interpretation

Worden, R. H.: Discussion and detailed manuscript review

Hodgson, D. M.: Discussion and detailed manuscript review

Chapter 6: Daneshvar, E., Worden, R. H., Hodgson, D. M., Suspended clay minerals in the Ravenglass estuary; origin of the clay minerals, their variation during tide cycles and comparison to fluvial suspended clay minerals

Author contribution: Daneshvar, E.: Principal investigator and author. All primary data collection, processing and interpretation

Worden, R. H.: Discussion and detailed manuscript review

Hodgson, D. M.: Discussion and detailed manuscript review

Chapter 2

Chapter 2 Berthierine on clay-coated sand grains in the Ravenglass estuary, NW England, UK

2.1 Abstract

Berthierine, a Fe-bearing clay mineral of the kaolinite-serpentine series with a ~7Å basal spacing for (001), and approximately the same chemical composition as Fe-rich chlorite, can be transformed to chlorite during diagenesis. Berthierine formation has been reported in hot (tropical) sedimentary environments. However, formation of berthierine in the Ravenglass estuary (~54° N, Cumbria, northwest England) is reported here. The X-ray diffraction (XRD) method discriminates berthierine with a strong peak at ~7Å (12.5°). Kaolinite (001) and chlorite (002) are two clay minerals that also have a ~7Å basal spacing. However, berthierine can be identified because kaolinite can be discriminated at 7.15Å (12.3°), and sample heating to 400°C causes a maximum 50% fall in intensity of the ~7Å (12.5°) for berthierine, while the behavior of the trioctahedral chlorite (002) is unchanged in a berthierine-free sample. This amount of loss is decreased for a mix of berthierine with types of chlorite samples. Chlorite is fed to the estuary from hinterland sources (bedrock) via rivers, and in association with eliminated iron from the river, berthierine is formed within the estuary in a cold temperature shallow-marine environment.

2.2 Introduction

Berthierine is an aluminium-bearing, Fe-rich clay belonging to the kaolinite-serpentinite series of 1:1 clay minerals (Bailey 1980). Berthierine has a ~7Å basal (001) spacing and typically has approximately the same chemical composition as Fe-rich chlorite (Brindley 1982b).

Some recent studies (Odin 1988; Hornibrook and Longstaffe 1996; Baker et al. 2000b; De Hon et al. 2001) have attempted to address the origin of berthierine concluding that it tends to be found in sediments deposited in shallow marine, marginal-marine and estuarine environments, thus potentially helping to pin down its location within the rock record. Berthierine is commonly, but not always, associated with oolitic ironstones (Odin 1988); although this presents an interesting problem since there seem to be no modern environments where this type of sediment is accumulating. Some consider that Fe^{2+}-rich berthierine transforms from an earlier Fe^{3+}-rich odinite phase (aka phyllite-V) during early diagenesis and is part of the verdine facies, which is closely associated with tropical

climates (Odin 1988). However, berthierine has been reported, albeit rarely, from mid to high latitudes casting doubt on the role of latitude and climate on the formation of berthierine (Rohrlich et al. 1969).

Fe-rich chlorite is of interest as it can lead to anomalously high porosity in deeply buried sandstones as a coating on sand grains that inhibits the growth of porosity-destroying quartz cement (Ehrenberg 1993). Berthierine has been reported to transform to Fe-rich chlorite during diagenesis (Aagaard et al. 2000; Worden and Morad 2003a) and has been cited as one of the most important sources of porosity-preserving Fe-rich chlorite. Therefore, understanding the origin of berthierine may help to predict the occurrence of anomalously high porosity in the subsurface; of obvious relevance to resource exploration and exploitation. It has been proposed that chlorite with a high iron content in ancient, deeply buried sedimentary environments reflects syndepositional concentration of Fe-rich marine clays, with mineralisation being localised where Fe-rich river water (Boyle et al. 1977b) discharged into the sea (Ehrenberg 1993).

X-ray diffraction (XRD) is the most commonly employed technique in the detection and discrimination clay minerals. Berthierine, with a ~7Å basal (001) spacing, and Fe-chlorite, with a ~14Å basal spacing, are theoretically distinguishable by the absence or presence respectively of a 14Å reflection. However, the 14Å reflection of Fe chlorite is relatively weak to very weak, and therefore berthierine with a small admixture of chlorite may easily be overlooked with the mixture simply being labelled as chlorite (Brindley 1982b).

A pragmatic approach to the identification of berthierine during X-ray diffraction analysis is best adopted (Starkey et al. 1984). This is especially important when chlorite and kaolinite are also present in a sample. Historically, the peak equivalent to about 7Å (~12.5° using Cu kα radiation) was labelled "K+Chl" since kaolinite and chlorite could not be discriminated using older types of X-ray equipment. However, by using an efficient X-ray source, Soller slits, a slow X-ray scan and a high-efficiency, multistrip detector, kaolinite(001) can now be easily distinguished from chlorite(002). Kaolinite has a (001) spacing of 7.15Å while chlorite(002) has a spacing equal to 7.07Å. The best practical way to distinguish berthierine(001) from chlorite(002) is by step-wise heating with X-ray diffraction analysis between each step. Heating to 400°C typically leads to a small change (~20% reduction) in intensity of the berthierine(001) peak at 7.07Å and no change for the chlorite(002) peak. Heating to 550°C typically leads to complete destruction of the

berthierine(001) peak at 7.07Å and almost complete destruction of the chlorite (002) peak but with a commensurate *increase* in intensity of the chlorite (001) peak at about 14Å (Starkey et al. 1984; Hillier 2003).

This research was aimed to identifying clay minerals in a modern, marginal marine (estuarine) environment that likely had an Fe-rich fluvial input into the marine waters. The estuary selected was the Ravenglass estuary in Cumbria (UK) (Fig. 2.1) that drained Fe-rich Triassic sandstones and Fe-rich Palaeozoic granite and andesite. The specific objectives were (1) to use X-ray diffraction techniques to identify clay minerals in the sedimentary column and compare them to clay minerals suspended in the estuary and (2) to determine which, if any, Fe-rich clay minerals are present in this mid-latitude estuary sitting at about 54.3° north.

2.3 Background geology

The Ravenglass estuary in northwest England (Figure 2.1) lies near the small town of Ravenglass located on the west coast of Cumbria. The Ravenglass estuary is fed by two main arms; the southerly River Esk drains the Palaeozoic Eskdale granite; northerly River Irt drains the Triassic Sherwood Sandstone Group (Fig. 2.1). The Fe-rich Eskdale granite (Moseley 1978) is a Lower Ordovician intrusion and was a result of the Caledonian orogeny. There are two main types of granite; an earlier biotite-granodiorite in the south and a later pink muscovite-granite in the north (Rundle 1979). Tourmaline occurs as joint coating and as replacement of feldspar. Biotite, where present, is typically chloritized or replaced by hematite. Overall, the Eskdale granite shows intense chloritization (Moseley 1978). This study focused on clay minerals in the southern arm of the estuary and its river, the Esk. It is assumed that the stream sediment sample reflects the average mineralogy of the fluvial part of the Esk river valley. It is also assumed that the net flux of sediment is downstream towards the open sea from the upper reach of the estuary (i.e. the sampling point) and that, at the present time, there is no significant offshore to onshore input of material. The northern part of the UK (including Cumbria) is undergoing limited isostatic recovery after the last glacial maximum (Bousher 1999).

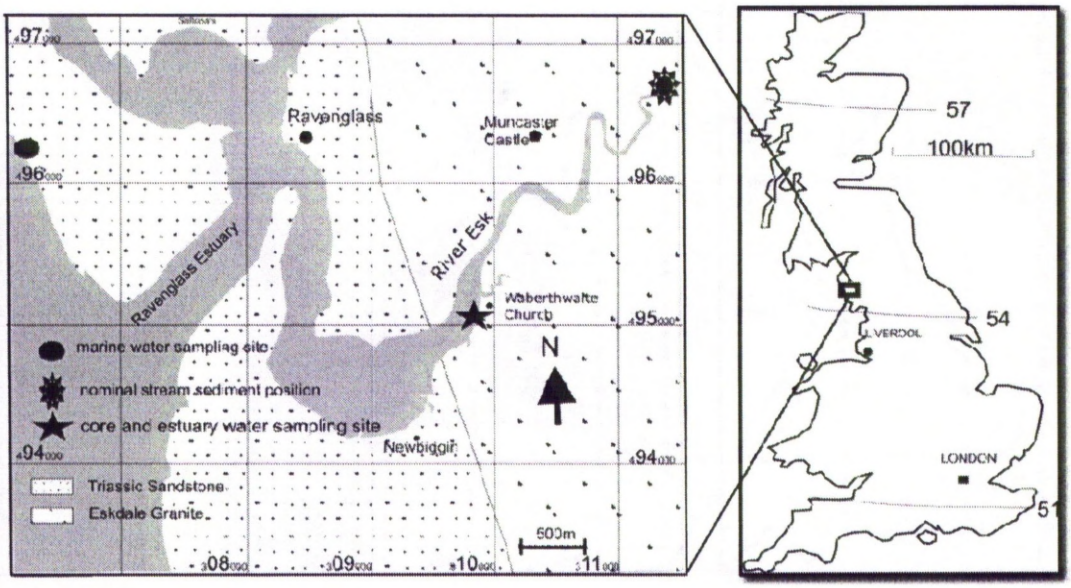

Figure 2.1. Map of the study area, showing the location of the Esk arm of the Ravenglass estuary and coring point just north of 54° latitude.

2.4 Methods of sampling and analysis

2.4.1 Sediment sampling

A sediment core was obtained from the upper-middle part of the Esk arm of the Ravenglass estuary (Fig. 2.1) in October 2009 by using a Van Walt coring window sampler. The window sampler takes cores of up to 1m that are preserved in a polythene sleeve that is retracted over the core as the sampler is forced into the sediment. This method preserves the fine sedimentary structures in the core and isolates the sediment from the atmosphere. The window sampler was driven into the sediment with an Atlas Copco Cobra TT percussion hammer. Once the polythene sleeve was sliced open, sub-samples were taken every 0.1m, preserved in sealed plastic jars and then stored in a refrigerator before preparation for mineral and petrological analysis. The whole cores (Figure 2.2) were about 0.9m in length due to ~10% compaction during coring. The core consisted of a variation of sand, silt and clay with the redox zone apparent at about 5cm below the sediment surface. Bioturbation was visible due to the mixing of primary sedimentary layers by burrowing creatures. A sample from a depth 5-10cm was chosen for the detailed investigation of clay minerals and sediment fabrics. A sediment sample was

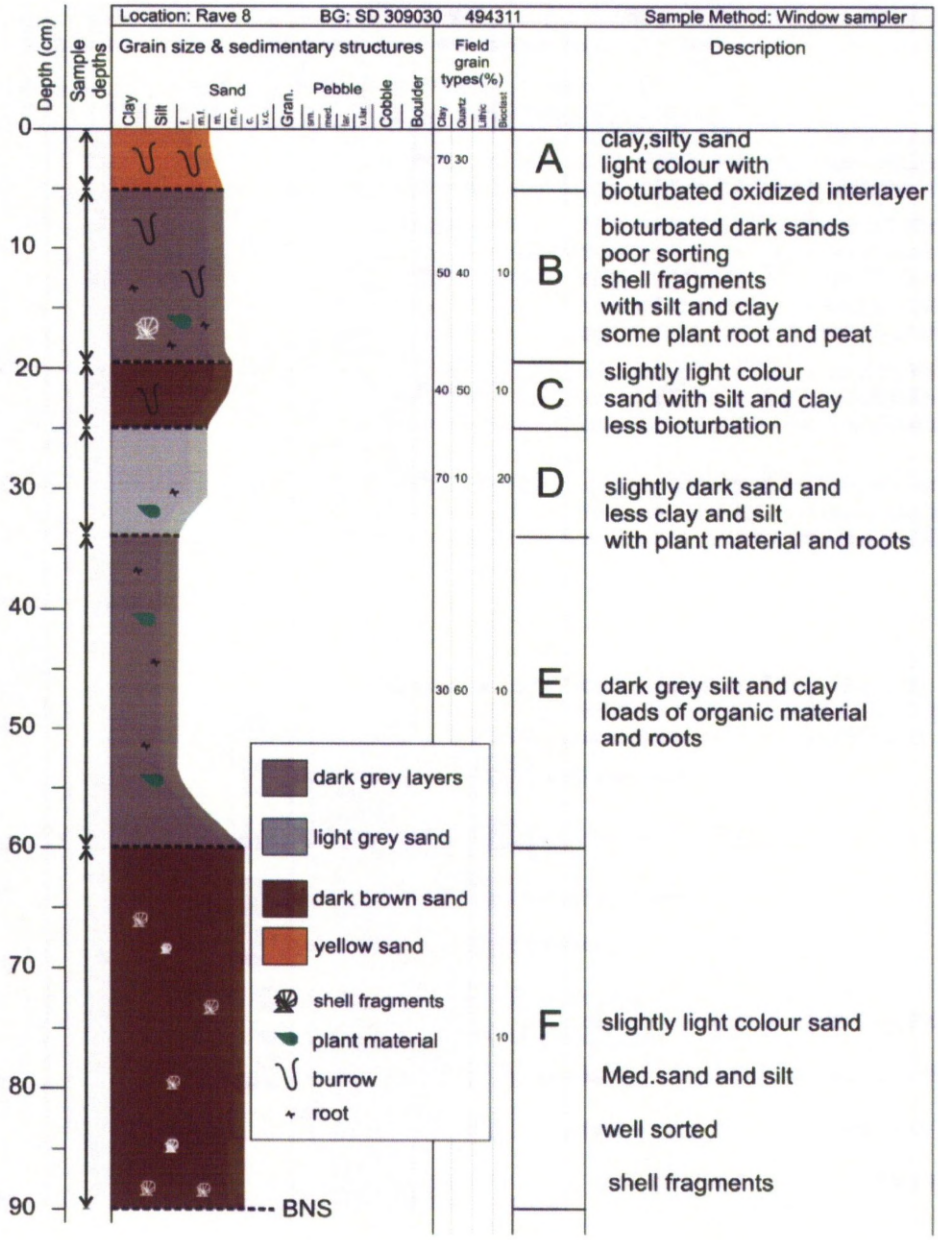

Figure 2.2: Detailed stratigraphy of the core from the Ravenglass estuary. Core log shows bioturbation at the top of the core which decreases with depth

also collected from the River Esk above the tidal range (Fig. 1) to reveal differences between the fluvial and estuarine sediments.

Water sampling and clay filtration methods

A water sample was collected from the Irish Sea about 1000 m north of where the Ravenglass estuary meets the sea (Fig. 2.1). Water samples from the Ravenglass estuary were collected at various sites regularly through the tidal cycle. One of the sites was adjacent to the coring point at the upper-middle part of the Esk estuary (Fig. 2.1). Twelve water samples were taken at the rate of one an hour to cover the full range of tidal conditions within the estuary. The samples were stored in air-tight polyethylene jars that were filled to the brim. All water samples were filtered in the field, using 0.2μm Whatman cellulose nitrate filters, under pressure using vacuum pumps. Suspended particles remained on the filter paper and the filtered water samples were frozen for further geochemical analysis in the laboratory. Filter papers were analysed directly using XRD techniques. Several samples of untreated (unacidified, unfiltered) river water were filtered in the laboratory, using 0.2μm Sterlitech silver filters. The filtrate on these filters were also analysed directly by X-ray diffraction. X-ray diffraction analysis of the cellulose filter papers led to a noisy background and contributed to a broad pair of humps between about 9 and 50° 2theta using Cu kα radiation. In contrast, the silver filters resulted in no additional background noise and only a few, very sharp peaks, derived the metallic silver. The silver filters could be glycolated and heated to at least 550°C enabling a full characterisation of the clay minerals while the cellulose filters could not withstand these clay treatment steps. The extra cost of the silver filters is their only disadvantage relative to the cellulose filters. Only the results of X-ray diffraction analysis of silver filters are presented in this paper.

2.4.2 Clay fraction preparation from sediment samples

Clay fractions from the cored sediment sample were suspended by ultrasonic disaggregation in distilled water. Suspended materials were then separated using a centrifuge on 3500 rev/minute for 30 minutes. Finally they were dried out in an oven at 55°C for 12 hours. The separated clay fraction nominally consists of the <2μm fraction although there is considerable variability given the role of grain shape and its effects on

settling velocities. Clay fractions of sediment samples were prepared for X-ray diffraction in four ways: (1) air dried, (2) Mg-saturated and then glycolated, (3) heated for one hour at 400°C and (4) heated for one hour at 550°C.

2.4.3 XRD analysis and sample treatments

Separated clay samples and silver filters were analysed with a PANalytical X'Pert Pro X-ray diffractometer fitted with an X'Celerator, solid state, multi-strip detector. A copper X-ray tube was used at 40kV and 40mA. A nickel filter was used to reduce the incident beam to Cu kα X-rays. Powder samples of the clay separates were back loaded into cavity holders and rotated continuously during the scan, completing one rotation every 2 seconds. Programmable anti-scatter slits and a fixed mask maintained an irradiated sample area of 10x15mm, with an additional 2° incident beam, anti-scatter slit producing a uniformly flat background. Scans covered the 2Theta range of 3.66-70.00° with a step size of 0.0167113°. With the multistrip detector, the overall integrated time per step was 165.735 seconds leading to an overall scan time of nearly 99 minutes. The XRD used 0.02 rad Soller slits in both the incident and diffracted beam paths. The X'Celerator detector was set to scan in continuous mode with full length active and pulse-height discrimination levels set to 45-80%.

There is no reported XRD scan for berthierine and its behavior through heating treatment in the literature. Therefore a berthierine sample from the Cleveland Ironstone Formation in Yorkshire, UK, as a standard berthierine sample, was analyzed and treated with glycolation, and heated to 400°C and finally 550°C (Fig. 2.3). Table 2.1 has been derived from XRD investigations (Starkey et al. 1984; Moore and Reynolds 1989; Hillier 2003; Meunier 2007) on the behavior of the clay minerals during heating treatments and glycolation. The Cleveland Ironstone Formation is a lower Jurassic formation from Cleveland Basin. A series of ironstone seams alternating with mudstones are main characteristics of this formation. Half of the all Fe-bearing minerals in this formation is berthierine and the rest are siderite (Jeans 2006; Jeans and Merriman 2006).

2.4.4 SEM examination

A whole sediment fraction was washed with distilled water and freeze-dried for examination in a Philips XL 30 scanning electron microscopy. Samples were prepared as grain mounts by setting them in resin under vacuum. These mounted samples were then

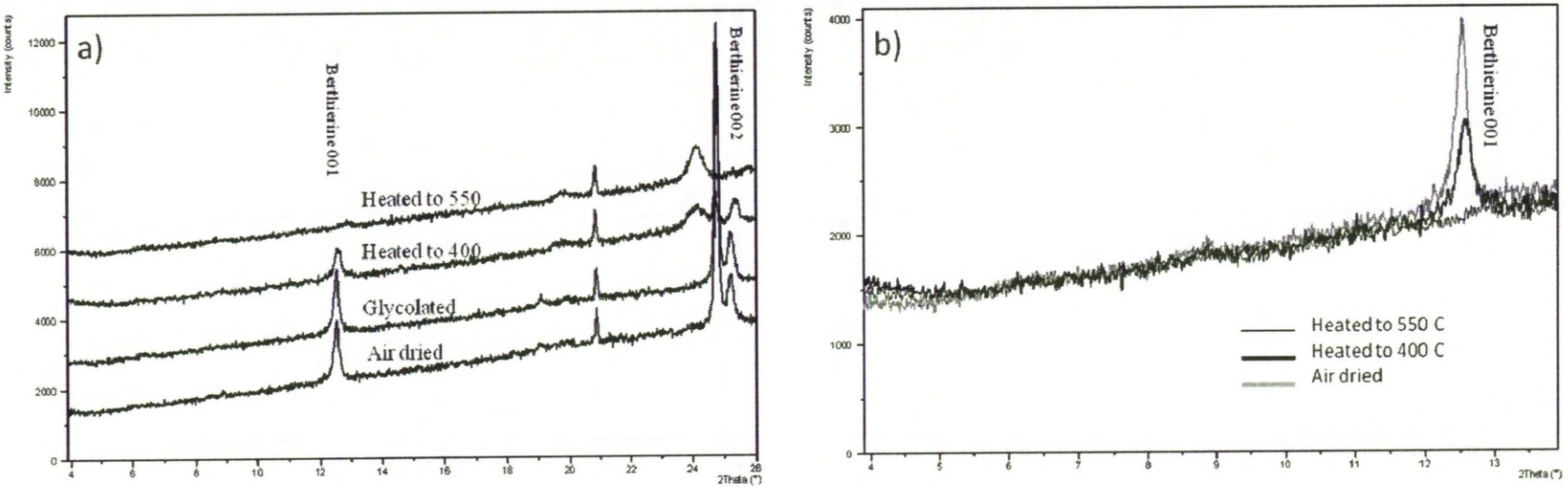

Figure 2.3:. XRD patterns of the <2μm fraction of a berthierine standard sample from Cornelian formation, Yorkshire, England (a) Collection of patterns arranged from the base: air dried, glycolated, heated to 400°C and heated to 550°C at the top of the stack. b) Overlapping of the XRD data from the low angle end of the pattern to illustrate the lack of any peak 7.15. The 7Å peak seems to disappear at heating to 550°C. Note there is no any considerable peaks at ~10Å and ~14Å in this sample. This sample seems to be predominantly berthierine.

sliced and prepared as ordinary polished thin sections. Secondary electron imaging was used on the whole sediment samples. Backscattered electron imaging was used on the polished grain mounts. An EDAX detector was used for the point chemical analysis of secondary X-rays detectors.

2.5 Results

2.5.1 SEM examination of cored sediment

SEM images reveal moderately to poorly-sorted sediment with sand grains that are variably coated with clay minerals (Figs. 2.4a and 2.4b). The sediment contains a combination of clastic grains and marine, mostly siliceous, bioclasts such as radiolarians and diatoms. The clay minerals present are very fine grained, tending to be less than a few micrometres in size. They do not occur as masses of monominerallic material, rather they seem to be intergrown with other clay minerals given their variable backscatter responses (Figs. 2.4c and 2.4d). They are largely too fine-grained to give high quality, single mineral EDAX spectra. Most EDAX spectra of coating minerals on sand grains contain Fe and some certainly resemble EDAX spectra of chlorite analysis on the coated mineral having abundant Si, somewhat less Al and much less Mg. However, most spectra seem to contain K, implying either the presence of intergrown illite and chlorite-like material or some sort of K- and Fe-rich smectite phase. Kaolinite can be identified in places (equal Al and Si peaks and no K or any other cations). Illite has also been identified with abundant Si, somewhat less Al and a sizeable K peak. The SEM, BSE and EDAX investigations therefore revealed that the clay minerals present seem to be: kaolinite, illite, chlorite, and combinations of these. It is possible that smectite is present (accounting for the apparent presence of K in chlorite); this was then investigated using X-ray diffraction.

	~ 6.2°(~14Å)					001:002 ratio	12.3° and 12.5°(~7Å)				
Treatment minerals	Air dried	Glycol.	300°	400°	550°		Air dried	Glycol.	300°	400°	550°
kaolinite	N/A	N/A	N/A	N/A	N/A		Strong peak at 12.3°	No change	No change	Fall in intensity	destroyed
berthierine	N/A	N/A	N/A	N/A	N/A		Strong peak at 12.5°	No change	No change	Fall in intensity	destroyed
Fe-rich chlorite	smaller than 12.5°	No change	No change	No change	Increase in intensity	~1:4	Bigger than 6.2°	No change	No change	No change	destroyed
Fe-Mg chlorite	Smaller than 12.5°	No change	No change	No change	Increase in intensity	~1:2	Bigger than 6.2°	No change	No change	No change	destroyed
Al-rich chlorite	Strong peak	No change	No change	Fall in intensity	Increase in intensity	~1:1	Strong peak at 12.5°	No change	No change	Fall in intensity	destroyed
smectite	Strong peak	Expand to ~17Å	Collapse to 10Å	Collapse to 10Å	Collapse to 10Å		N/A	N/A	N/A	N/A	N/A
hydroxy-interlayer vermiculite (HIV)	Strong peak	No change	Collapse to 12-13Å	Collapse to 11Å	Collapse to 10Å		Nil to weak peak	No change	No change	Fall in intensity	destroyed

Table 2.1: behaviour of the <2µm fraction of clay minerals through treatment such as glycolation, heating to 300°, 400° and 550°C for peaks at ~14Å and ~7Å ((Hillier, 2003; Meunier, 2007; Moore and Reynolds, 1989; Starkey et al., 1984)

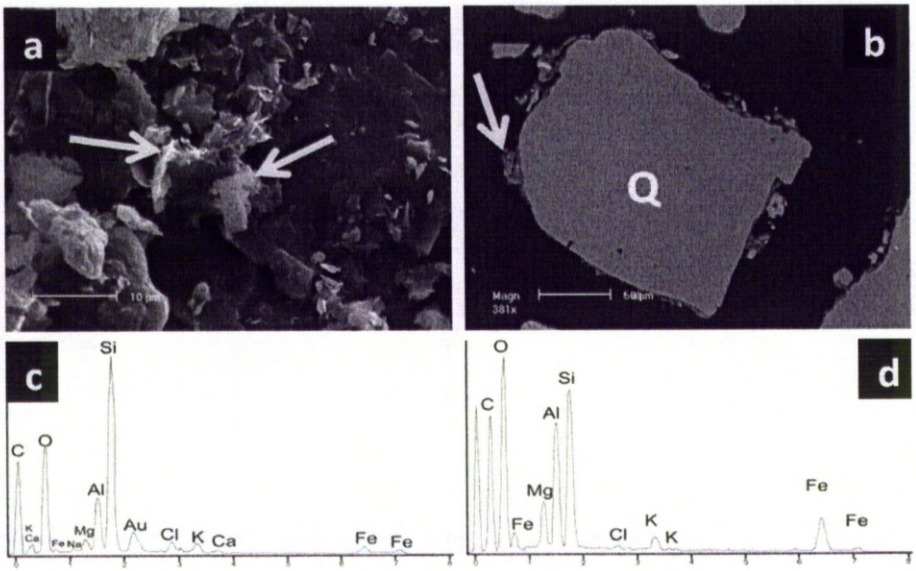

Figure 2.4: Electron microscope data from core samples. SEM/BSE analysis: a) Secondary electron image of a dried sample, showing a detrital quartz grain that is substantially coated with fine material including flaky chlorite-illite clay minerals and debris from marine fauna. b) Backscattered electron image of a polished section grain mount; a quartz sand grain in the middle is almost fully coated with clay grade material. c) EDAX spectrum analysis of the flaky shape clays which Si, Al, Mg, K and Fe are dominant. The high peak for Si is due to the active volume for X-ray generation including a quartz grain and siliceous marine fauna. d) EDAX spectrum analysis of the area indicated in Figure 3.1.3b showing a Fe-rich chlorite-like phase probably in association with illite.

2.5.2 XRD analysis of cored sediment

The X-ray diffraction analysis of the <2μm fraction from the cored sediment revealed a moderately complex trace for the air-dried sample (Fig. 2.5) with peaks at 6.2°, 8.9° and a pair of peaks at 12.3° and 12.5°. The peak at 6.2° is from chlorite (001) while the peak at 8.9° is from illite. Gould et al. (2010) reported that kaolinite can be difficult to distinguish from chlorite due to overlap of the kaolinite(001) and chlorite(002) peaks but the analytical approach adopted here was sufficient to clearly differentiate the two minerals. The peak at 12.3° is the kaolinite(001) peak while the peak at 12.5 is either solely due to the chlorite(002) peak or is a combination of chlorite(002) and berthierine(001) (Brindley 1982b). The relative heights of the (001) and (002) peaks suggests that the chlorite in the sediment core is Fe-rich (Hillier 2003). Scans of the glycolated sample showed no discernable changes in peak intensity suggesting that smectite is negligible in this sediment. Chlorite(002) peaks are reportedly unaffected when heated to 400°C (Starkey et al. 1984). In contrast, berthierine(001) and kaolinite(001) peaks typically show a decrease

in intensity on heating to 400°C. A scan of the cored sediment sample when heated up to 400°C revealed a distinct decrease in intensity for the peaks at 12.3° and 12.5° (equivalent to 7.15Å and 7.07Å respectively). This confirms the presence of kaolinite but further suggests that the peak at 12.5° is not solely due to the chlorite (002) peak. The implication is that berthierine is present in this sample. For the 400°C scan, the intensities of the peaks at 6.2° and 8.9° remain unchanged further confirming that illite and chlorite are present. A scan of the sample heated up to 550°C shows a significant collapse for both the 12.3° and 12.5° peaks while the intensity of the peak at 6.2° increased slightly and sharpened, typical of chlorite (Starkey et al. 1984; Moore and Reynolds 1989; Hillier 2003). This combination of X-ray diffraction analyses confirms the presence of kaolinite, illite and chlorite. These refute the presence of smectite suspected from the EDAX analyses (Fig. 2.4d), rather they apparently represent intergrowth of illite and chlorite. Finally, the X-ray diffraction data suggest the substantial presence of berthierine in these sediments, not initially suspected from the SEM/EDAX analyses.

2.5.3 XRD analysis of the suspended sediment

The X-ray diffraction analyses of the suspended sediment material, separated using silver filters, are presented in Figures 2.6 and 2.7, taken from seawater and estuary-low tide conditions respectively. These were also each analysed using air-drying, glycolation and heating to 400°C and then 550°C. The air-dried scans from both seawater and low tide filtrates reveal peaks at 6.2°, 8.9° and a pair of peaks at 12.3° and 12.5°. The peak at 6.2° is from chlorite(001) while the peak at 8.9° is from illite. The peak at 12.3° is the clearly discerned kaolinite(001) peak while the bigger peak at 12.5 is either solely due to the chlorite(002) peak or is a combination of chlorite(002) and berthierine(001) (Brindley, 1982). The relative heights of the (001) and (002) peaks from the low tide sample (about 1:2) suggests that the chlorite has a mixed Mg-Fe composition (Hillier 2003). In contrast the seawater filtrate sample has a lower (001) to (002) ratio suggesting that this chlorite is Fe-rich (Hillier 2003). Glycolation had negligible effect on either filtrate sample

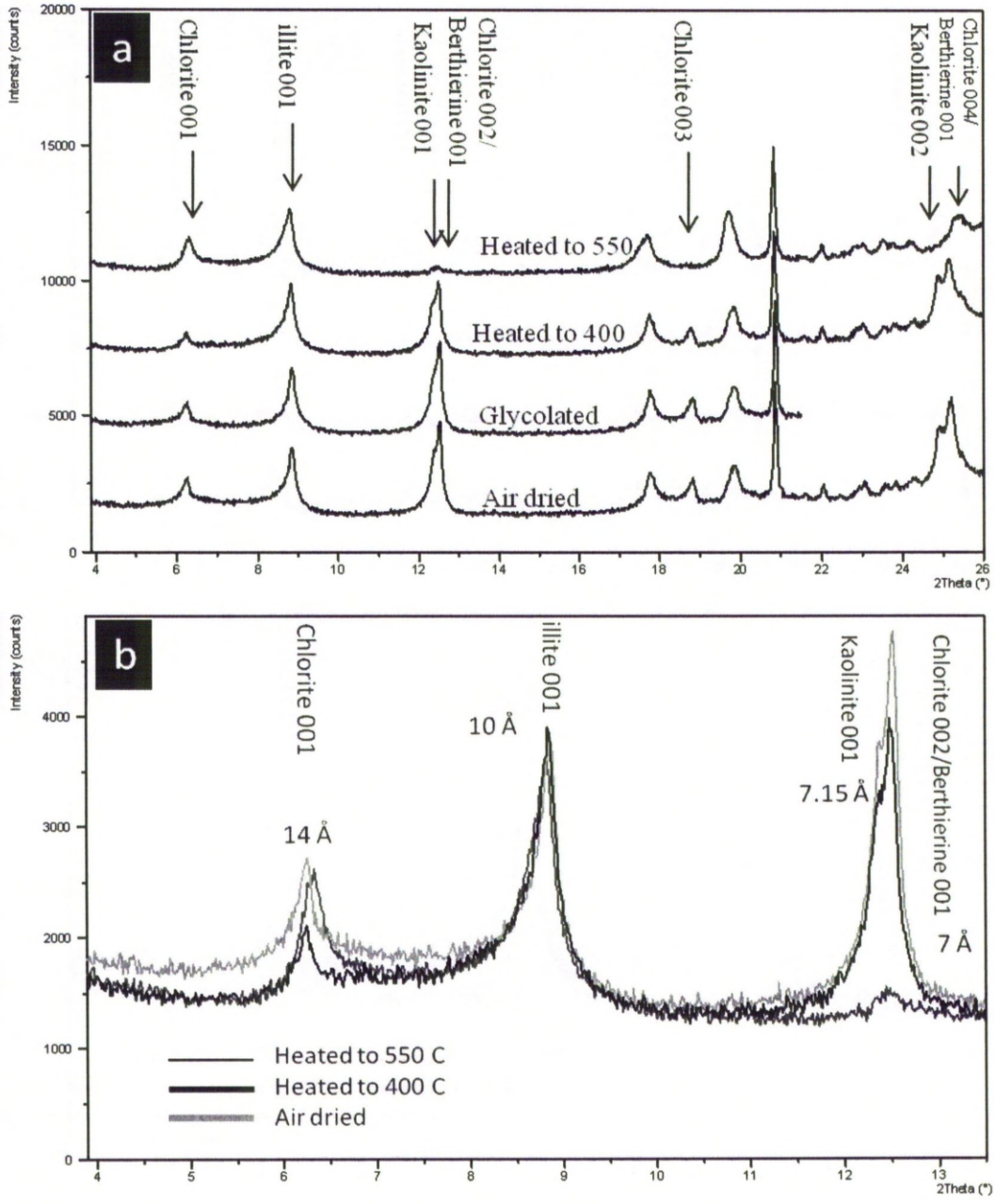

Figure 2.5: XRD patterns of the <2μm fraction of the cored sediment sample taken at a depth of 5-10cm (Fig. 3.1.1). a) Collection of patterns arranged from the base: air dried, glycolated, heated to 400°C and heated to 550°C at the top of the stack. b) Overlapping of the XRD data from the low angle end of the pattern to illustrate the drop in intensity of the 7.15 and 7Å peaks during heating to 400°C and their near total collapse at 550°C. Glycolation seems to have little effect on the sample. Note also the broadening of the chlorite(001) peak. The sediment seems to be composed of illite, chlorite, kaolinite and berthierine with negligible smectite present.

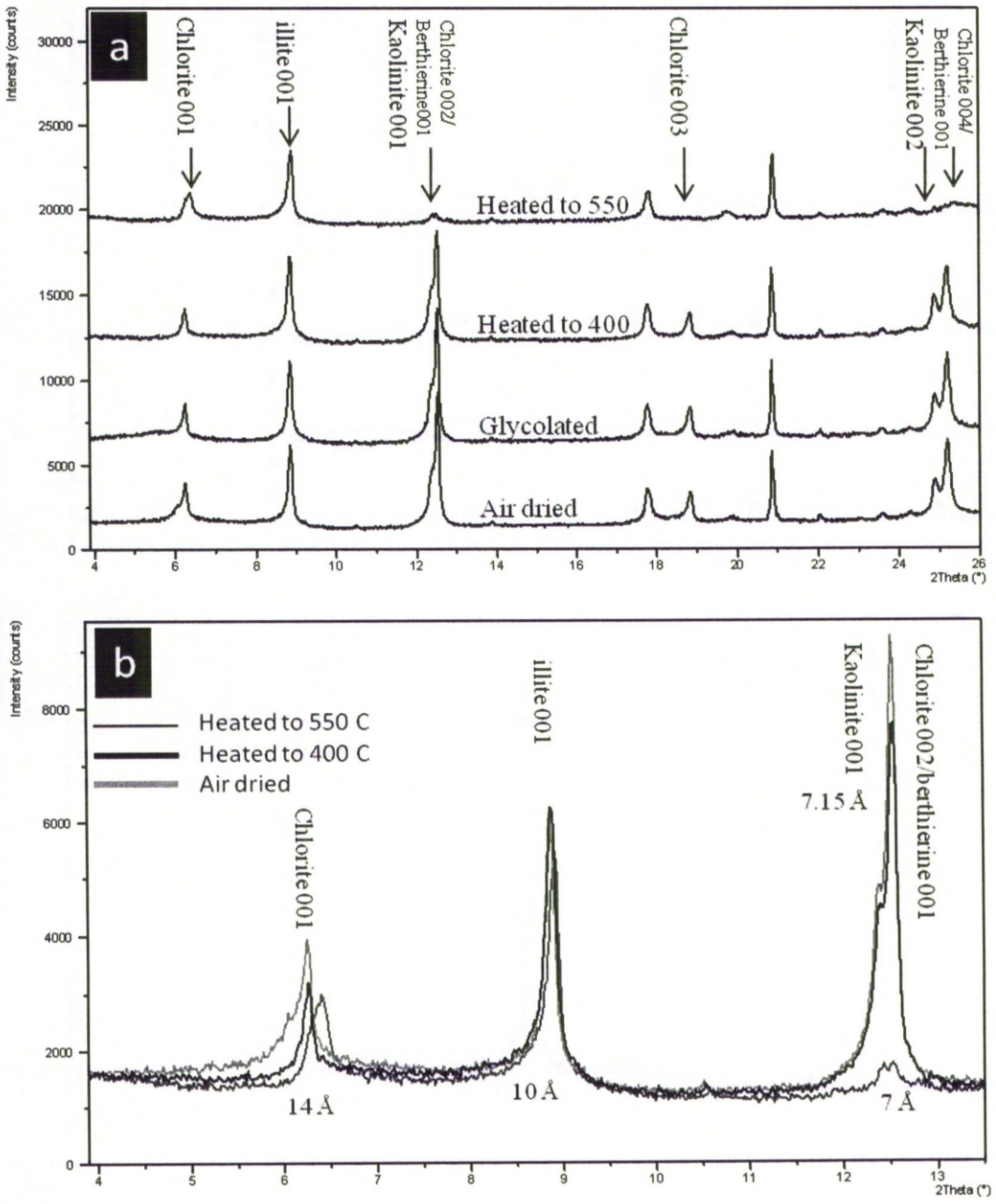

Figure 2.6: XRD patterns of the <2μm fraction of the filtered suspended sediment taken from sea water ~1000m north of where the Ravenglass estuary meets the Irish Sea (Fig. 3.1.1). a) Collection of patterns arranged from the base: air dried, glycolated, heated to 400°C and heated to 550°C at the top of the stack. b) Overlapping of the XRD data from the low angle end of the pattern to illustrate the drop in intensity of the 7.15 and 7Å peaks during heating to 400°C and their near total collapse at 550°C. Glycolation seems to have little effect on the sample.

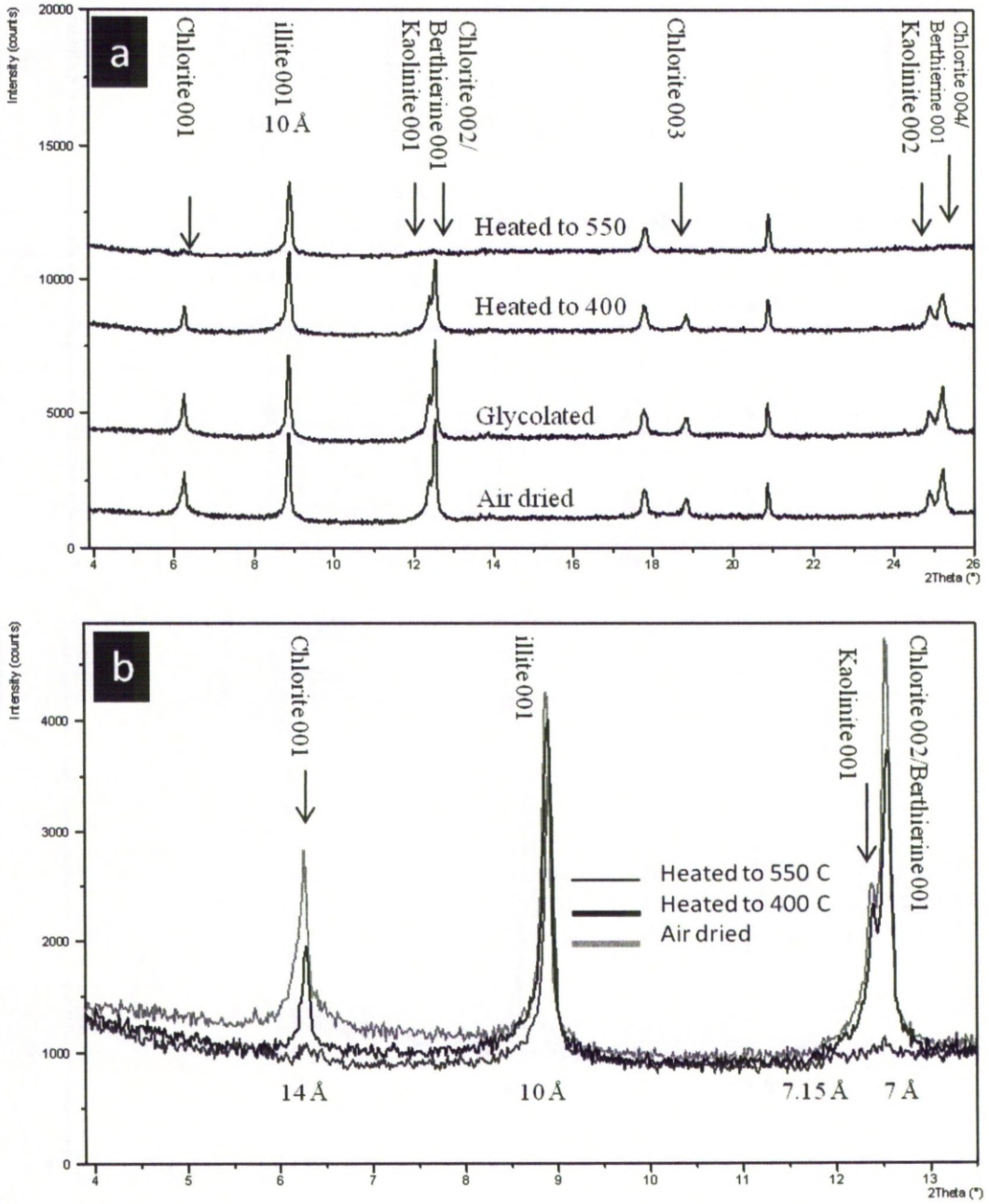

Figure 2.7: XRD patterns of the <2μm fraction of the filtered suspended sediment taken from the river at low tide at the point at which the core was taken (Fig. 3.1.1). a) Collection of patterns arranged from the base: air dried, glycolated, heated to 400°C and heated to 550°C at the top of the stack. b) Overlapping of the XRD data from the low angle end of the pattern to illustrate the drop in intensity of the 7.15 and 7Å peaks during heating to 400°C and their near total collapse at 550°C. Note also the unexpected collapse of the chlorite(001) peak.

Peaks	Samples	Berthierine (the Cleveland Ironstone Fm.)		Sediment core sample		Stream sediment sample		Low tide suspended matters		Marine suspended matters	
	Treatment	Area	Changes of area (%)	Area	Changes of area (%)	Area	Changes of area (%)	Area	Changes of area (%)	Area	Changes of area (%)
~14Å	Air dried	n/a	n/a	212	100	418	100	231	100	486	100
	400°C	n/a	n/a	191	90.09	174	41.63	183	79.22	327	67.27
~7Å	Air dried	1119	100	583	100	699	100	310	100	875	100
	400°C	697	62.29	497	85.25	628	89.84	272	90.66	668	76.34

Table 2.2: peak decomposition measurement at ~14Å (6.2°) and 7Å (12.5°) using The X'Pert HighScore Plus software. This measurement has been done for berthierine from the Cleveland Ironstone formation (Yorkshire, England), estuarine sediment, low tide suspended matters, marine suspended matters and stream sediment beyond the Esk River high tide line based on the XRD scans.

suggesting there was little smectite in the suspended sediment. Scans of these samples heated up to 400°C revealed a distinct decrease in the intensity for the peaks at 12.3° and 12.5. This clearly confirms the presence of kaolinite but shows that the peak at 12.5° is not solely due to the Fe-Mg rich chlorite (002) peak. The scan of the seawater filtrate sample heated up to 550°C shows a total collapse for the 12.3° peak and substantial collapse of the 12.5° peak. In contrast, the intensity of the peak at 6.2° slightly decreased but sharpened for the seawater filtrate sample, follows behaviour typical of chlorite (Moore and Reynolds 1989; Hillier 2003). The scan of the estuary-low tide filtrate sample heated up to 550°C shows a total collapse for both the 12.3° and 12.5° peaks while the intensity of the peak at 6.2° strongly decreased. Referring to Table 2.1 and the behavior of the 12.5° peak during the heating treatment up to 550°C (Fig. 2.7) predominantly dioctahedral type of chlorite or weak chlorite (Al-rich chlorite) can be present in the samples. The fall in intensity of the 12.5° peak after heating to 400°C (Fig. 2.7) in the XRD scans of the suspended materials at low tide is interpreted to indicate the presence of the dioctahedral type of chlorite rather than berthierine (Starkey et al. 1984; Moore and Reynolds 1989; Hillier 2003). Seawater data (Fig. 2.6) are very similar to the diffraction traces of the cored sediment sample (Fig. 2.5) in terms of both initial peak height ratios and response to different treatments. Low tide (Fig. 2.7) has similarities to the cored sediment sample (Fig. 2.5) but the near total collapse of the peak at 6.2° and 12.5° at 550°C and the higher illite (8.9°) peak suggest this is somewhat different to the cored sediment sample.

2.5.4 XRD analysis of stream sediments

The stream sediment sample, from the River Esk (beyond the tidal reach), had prominent peaks at 6.2° and 12.5° probably associated with chlorite and rather small peaks at 8.9 and 10.5 associated with, respectively, illite and possibly zeolite (or amphibole). There is no peak at 12.3° showing that there is no kaolinite present (Fig. 2.8). The relative heights of the (001) and (002) peaks from the stream sediment sample suggests that the chlorite has a mixed Mg-Fe composition (Hillier 2003). Glycolation led to a slightly bigger effect for this sample than the suspended sediments or cored sediment samples. This suggests that some sort of expandable phase such as smectite, or possibly hydroxyl-interlayered vermiculite (Meunier 2007), is present in this sample but is absent in the estuarine part of this sedimentary system. More treatment to identify the expandable phase has been done

for this sample such as cation saturation (Mg and K) (Fig. 2.8). Based on the results from Meunier 2007, and the XRD scans of the stream sediment sample, hydroxyl-interlayer vermiculite (HIV) can be detected in this sample. However sequential heating to 300°, 400° and finally 550°C did produce a change in the diffraction pattern, with a gradual collapse and slight shift of a portion of the 14Å peak towards ~10Å at 550°C. This behaviour follows the prescribed behaviour of hydroxyl-interlayer vermiculite (HIV) (Starkey et al. 1984; Meunier 2007), although unique identification is made difficult by the presence of dioctahedral and trioctahedral chlorite. Heating to 400°C had relatively little effect around (~14% loss) (Table 2.2) on the peak at 12.5° suggesting that there is likely dioctahedral type of the chlorite (table 2.1) (Moore and Reynolds 1989) in this sample. Heating to 550°C led to substantial collapse of the peak at 12.5° and, as mentioned, a commensurate increase in intensity of the peak at 6.2° suggesting that chlorite is the dominant clay mineral in this sediment.

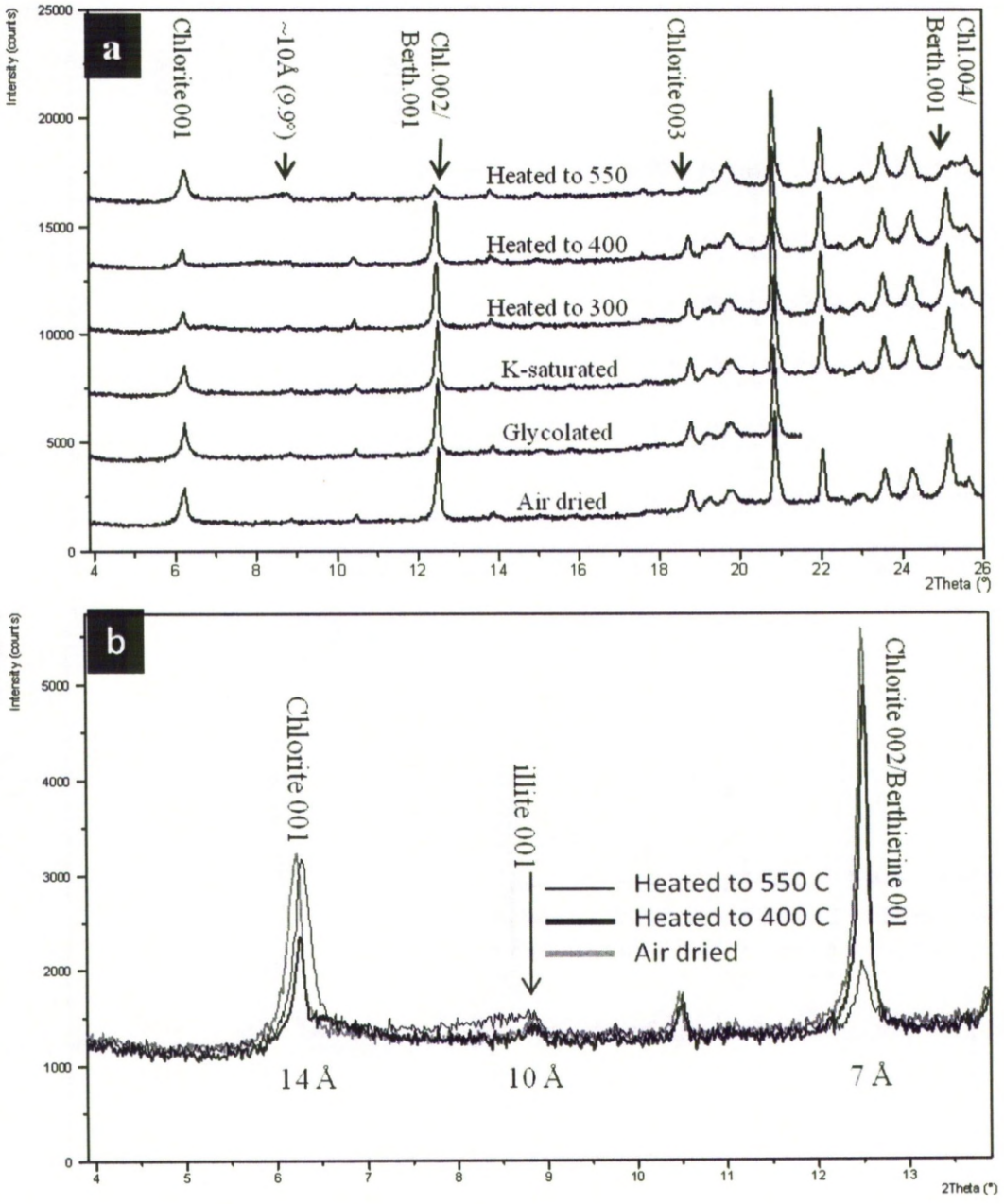

Figure 2.8. XRD patterns of the <2μm fraction of a stream sediment sample taken well beyond the tidal reach of the river (Fig. 3.1.1). a) Collection of patterns arranged from the base: air dried, glycolated, K-saturated, heated to 300°C, heated to 400°C and heated to 550°C at the top of the stack. b) Overlapping of the XRD data from the low angle end of the pattern to illustrate the lack of any peak at 7.15 and the general persistence of the 7Å peaks during heating to 400°C. The 7Å and 14Å peaks seem to survive heating to 550°C better than the estuary core or suspended sediment samples. Note also the lack of a peak at ~10Å in this sample. The stream sediment seems to be predominantly chlorite with negligible berthierine and illite and kaolinite and smectite are below detection limit. Sequential heating treatment shows a collapse from ~14Å toward ~10Å which indicates hydroxyl-interlayer vermiculite (Table 2.1)(Meunier 2007).

2.6 Discussion

2.6.1 Clay minerals present in the Ravenglass estuary sedimentary system

The most common clay mineral in the samples studied here is chlorite, present throughout the estuary in (1) stream sediments beyond the tidal reach, (2) estuarine deposits, (3) suspended material in the estuary at low tide, and (4) suspended material in the immediate marine environment close to the estuary mouth. Illite, kaolinite and, by reference to the systematic reduction in intensity of the peak at 12.5° on heating to 400°C, berthierine are all present in estuarine deposits and in the immediate marine environment close to the estuary mouth. Little smectite is found in the Ravenglass sedimentary system although there is some minor effect of glycolation on the stream sediments beyond the tidal reach. There is a distinct difference between the sediment found in the non-marine and marine parts of the system. Dioctahedral chlorite and hydroxyl interlayer vermiculite are other clay minerals which are abundant in the stream sediments and dioctahedral chlorite in estuarine suspended load at low tide.

2.6.2 Origins of illite and kaolinite in the Ravenglass estuary sedimentary system

Illite and kaolinite are common weathering products of the feldspar minerals that are abundant in the Eskdale granite exposed in the Esk drainage basin. The absence of kaolinite in the stream sediment sample (Fig. 2.8) suggests a limited degree of chemical weathering in the hinterland. The presence of kaolinite in the estuarine and near-estuary marine environments (Figs. 2.5-7) suggests that chemical weathering has had more opportunity to progress. There is a small illite peak in the stream sediment (Fig. 2.7) sample also suggesting a limited degree of chemical weathering in the hinterland although this might be due to white mica (Burley et al. 2003), which is present in Eskdale granite (Branney and Soper 1988). The much greater presence of illite in the estuarine and near estuary marine environments suggests, as for kaolinite, that chemical weathering of the granite feldspar minerals has had more opportunity to progress. The greater abundance of illite and kaolinite in the estuary relative to the stream sediments might simply be a function of the increased residence time (more time for weathering) of the sediment in the lower relief parts of the basin.

2.6.3 Chlorite: origin and evolution in the Ravenglass estuary sedimentary system

Chlorite in the stream sediments beyond the tidal reach and in suspended material in the estuary at low tide seems to be a mixed Mg-Fe type of chlorite and also given the (001):(002) ratio of 1:2 and dioctahedral chlorite (Figures 2.7 and 2.8) and (Hillier 2003)). In contrast, the chlorite in the cored sediment from the estuary and in the immediate marine environment close to the estuary mouth seems to be a Fe-rich type of chlorite given the (001):(002) ratio of 1:4 (Figures 2.5 and 2.6). Chlorite has been reported to be an alteration and weathering product in the Eskdale granite (Moseley 1978) so it is perhaps not surprising that it is present in the stream sediment samples. The implication from the change of chlorite composition is that the chlorite being fed into the estuary evolves towards an Fe-dominated composition once it is subject to marine influences.

2.6.4 Berthierine in the Ravenglass estuary sedimentary system

The presence of berthierine was not really expected given the received wisdom that the verdine facies seems to be limited to the tropics (Odin 1988). However, the systematic reduction in intensity of the peak at 12.5° on heating to 400°C is difficult to explain unless berthierine is present in the estuarine samples. Estuaries trap most fluvially-transported iron (Boyle et al. 1977b). Much of the iron in rivers is initially in a non-crystalline form occurring as a combination of dissolved Fe and the rather more important colloidal and complex forms of iron (Mayer 1982). It is not fully understood what solid form the iron adopts when it is trapped in estuaries (Sholkovitz 1978). In this case some may be taken up by dioctahedral chlorite and Mg-Fe chlorite, which becomes increasingly Fe-rich into the marine environment. Some may form Fe-oxyhydroxides, goethite, or even haematite, upon river water mixing with seawater (Mylon et al. 2004). It has been proposed that 7Å Fe-clay minerals formed by a reaction between kaolinite and (ill-defined) sources of iron soon after deposition (Ryan and Hillier 2002; Gammon and James 2003). It is possible that a similar process has occurred to produce the berthierine in the Ravenglass estuary given that the estuary will trap the fluvial iron, and that kaolinite is present within the sediment in the estuary. Biofilms on sand and silt grains in rivers have been reported to have berthierine-like compositions (Konhauser and Urrutia 1999) suggesting that the bacterially-mediated synthesis of Fe-clays may commence in the fluvial part of the system although it has been shown that marine and estuarine macrofauna (lug worms, *Arenicola marina*) can also lead to the neoformation of berthierine (Needham et al. 2004; Needham et al. 2005). It seems likely that berthierine can form in the estuarine sediment by

interaction between the flocculated and deposited fluvial Fe and detrital and neoformed alumina-silicate phases. Once formed, however, such berthierine (and indeed kaolinite and illite) will be remobilised by the continual erosion and redeposition processes as well as the burrowing activities of lugworms (and other burrowing creatures) that operate in such active sedimentary environments as estuaries. It is not surprising that berthierine (and kaolinite and illite) is present in the suspended sediment both in the estuary itself (Fig. 2.6) and in the local seawater (Fig. 2.5) that is fed by the river.

2.6.5 Grain coating clay minerals in estuaries

Sand grains in the cored sample are coated with clay-grade material that is dominated by clay minerals (Fig. 2.4). It is impossible to discriminate Fe-chlorite from berthierine using the secondary X-ray analyser (EDAX) in the SEM. Much of the coating is Fe-chlorite, given the size of the chlorite(001) trace in Figure 2.5. However, it is likely that some of the Fe-rich clay mineral particles present in the sample is berthierine. Some of the coating material is illite leading to a mixed mineralogy for clay coats on sand grains in the Ravenglass estuary. Coatings on sand grains in ancient sediments have been reported to be both illite- and chlorite-bearing (Ehrenberg 1993) suggesting that the Ravenglass case study is not especially unusual in this regard.

2.7 Conclusion

1. Berthierine has been identified in estuarine sediment by the systematic reduction in intensity of the peak at 12.5° on heating to 400°C. This was not necessarily expected given the previous emphasis in the literature on berthierine and the verdine facies being limited to the tropics.
2. Chlorite, illite and kaolinite are all present in cored sediment in the Esk estuary, NW England.
3. Chlorite, illite, kaolinite and dioctahedral chlorite are also present in the suspended sediment in the Esk estuary water at low tide and in nearby seawater (fed by the Ravenglass estuary at low tide).
4. Chlorite, dioctahedral chlorite and a minor expandable phase, such as hydroxy-interlayer vermiculite (HIV), are present in the fluvial sediments, beyond the tidal

reach. This suggests that illite, kaolinite and berthierine are all formed in the estuarine or lower fluvial environment.

5. Chlorite evolves to a progressively more Fe-rich composition going from the fluvial to the marine environment suggesting that fluvial colloidal or suspended Fe phases, trapped in the estuary, help to alter the composition of this deposited clay mineral.
6. Berthierine probably forms in the estuarine environment by interaction between fluvial colloidal or suspended Fe phases and aluminosilicate minerals.
7. Sand grains in the estuary are coated with a fine layer of clay minerals including Fe-rich chlorite, berthierine and illite. This suggests that estuaries are sites for not only Fe-clay creation and accumulation but also for the generation of coated grains, which upon subsequent burial and diagenesis, would become chlorite-coated sand grains.

Chapter 3

Chapter 3 Clay mineral distribution in surface sediments from the Ravenglass estuary

3.1 Abstract

Ravenglass estuary in North West England is a trap for the transported and *in situ* clay minerals. A clay mineral study from hinterland geology (granite and Triassic Sandstones) toward estuarine surface sediments has been undertaken using X-ray diffraction (XRD), fourier transform infra red (FTIR) and scanning electron microscopy (SEM/BSE/EDAX) techniques. Samples from (1) fluvial sediments beyond the high tide line, (2) surface sediments at the upper part of the estuary and (3) lower part of the estuary in respect of the clay minerals, have been analysed. Discrimination of the clay minerals using XRD in association with glycolataion salvage and heating treatment to identify the behaviour of 7Å and 14Å peaks have been discussed and concluded that chlorite from hinterland toward the estuary is being changed in quantity and quality from dioctahedral abundant in fluvial sediments to tetrahedral Fe-rich chlorite in surface estuarine sediments. Chlorite, illite and kaolinite and possibly berthierine are all present in surface sediment in the estuary. Chlorite, a minor expandable phase such as hydroxyl-interlayer vermiculite (HIV), dioctahedral chlorite and also illite are present in the fluvial sediments, beyond the tidal reach. Given the abundance of kaolinite and illite within the estuarine sediments in comparison to the fluvial sediment, it seems likely that these minerals were formed within the estuarine environment. Sand grains in the estuarine surface sediments are coated with a fine layer of clay minerals including chlorite, illite, mix of illite-chlorite, Fe-rich chlorite, berthierine and kaolinite.

3.2 Introduction

The transport and deposition of sediment in estuaries is controlled by the interaction of different factors, most notably circulation patterns (Wiley 1978; Schubel and Carter 1984; Phillips 1986; Dyer 2009; Manning et al. 2010). Clay minerals found in estuarine sediments may be derived; (1) from weathering profiles in the catchment soils occurring as detrital clays (2) in their depositional environment as diagenetic clays (Edzwald and O'Melia 1975), or (3) transportation from offshore setting (Stanev et al. 2007; Robins and Davies 2010) . The role of clay mineral associations during burial diagenesis in sediments

is well known especially in the control of the quality of sandstone reservoirs (Rossel 1982; Worden and Morad 2002). Therefore, it is important to understand the mechanisms that control clay mineral formation and distribution in clastic sediments.

During rising sea-level, estuaries are highly efficient sediment traps and their deposits have high preservation potential in the geological record. The distribution of clay minerals in estuaries have been addressed in several studies (Edzwald and O'Melia 1975; Feuillet and Fleischer 1980; Abu-Zeid and Stanley 1990; Petschick et al. 1996). Distribution of clays in estuaries is controlled by various mechanisms such as differential settling, diagenesis, flocculation, hinterland geology and physical processes in the estuary (Feuillet and Fleischer 1980). Studies of other estuaries have revealed that the clay mineral distribution is strongly influenced by diagenetic processes in coastal plain estuaries (Chamley 1989). Gibbs *et al.*, (1989) suggest that the clay mineral distribution is governed with grain size and physical circulation in estuarine–marine systems.

In this study, clay mineral distribution has been mapped using surface sediment from the Ravenglass estuary in Cumbria (UK), which drains Triassic sandstones and Palaeozoic granite and andesite (Bousher 1999). Parameters such as estuary dynamics, diagenetic processes, sediment grain size and hinterland geology have been constrained to help identify the important controls on clay mineral distributions. The Ravenglass estuary is a local name for an area that encompasses the tidal reaches of the three rivers: Esk, Irt and Mite. Common sub-environments found within estuarine systems include tidal channels and sand bars and sandwaves with flood and ebb deltas in the axis and mouth of the estuary, salt marshes, sandy and/or muddy tidal flats with tidal creeks at the margin of the estuary, and bay-head deltas where fluvial inputs meets the estuary (Bousher 1999). Surface sediment samples were taken from across the whole of the Ravenglass estuary especially from the north arm (Irt estuary) and south arm (Esk estuary) in the upper, middle and lower reaches of the estuary. The work presented here forms part of wider research into the estuary water chemistry, suspended sediment materials in the estuary, and estuary-filling sediment.

In this research, the clay mineralogy of the soils and weathered rocks in the hinterland geology and the drainage basin of the Irt and Esk rivers have been investigated. This is critical when trying to understand possible intra-estuarine diagenetic processes and

patterns of distribution. The overall goal of the work presented in this paper is to study the distribution pattern of the clay minerals in the Ravenglass estuary by addressing the following questions:

1- What clay minerals are present in the surface sediments in the estuary?
2- What clay minerals are present in the river catchments that feed the estuary?
3- Does hinterland geology affect clay mineral distribution in surface sediments in this estuary?
4- Is there any spatial clay mineral distribution pattern in the estuary?
5- What is the origin of clay minerals?

To determination the clay mineralogy of the Ravenglass estuary surface sediments and catchment soils, clay mineral qualification and semi-quantification can be accomplished through the use of X-ray diffraction (XRD), fourier transmitted infra red (FTIR) and scanning electron microscopy (SEM/BSE/EDAX) techniques.

3.3 Area of study

The Ravenglass estuary in North West England (Figure 3.1) lies near the small town of Ravenglass town located on the west coast of Cumbria. The Ravenglass Estuary, which encompasses the tidal reaches of the Rivers Esk, Irt and Mite, occupies an area of 5.6 km2 of which 86% is intertidal (Bousher 1999).

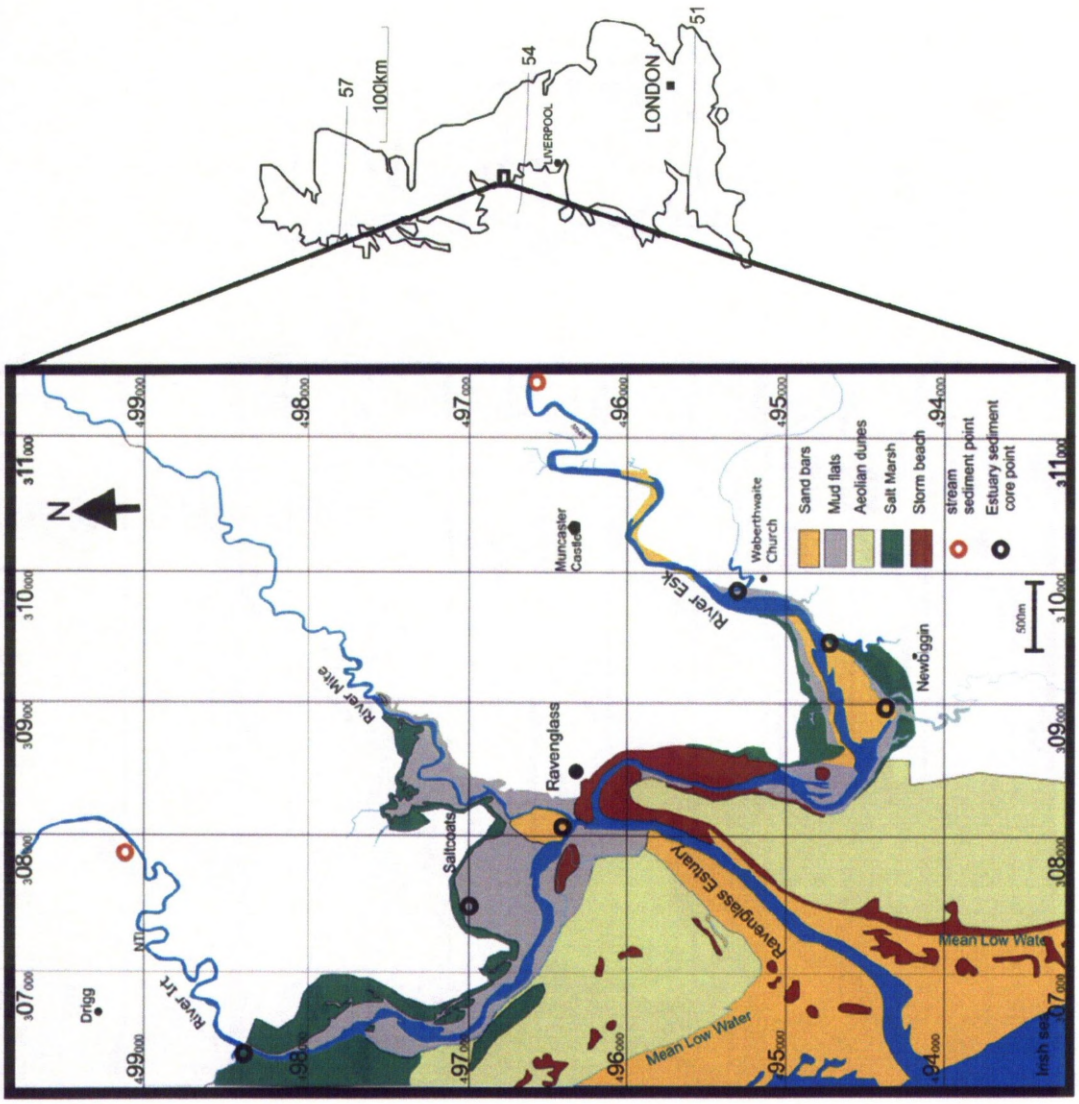

Figure 3.1: Map of the study area, showing the location of the Ravenglass estuary and the sub-estuaries; Esk and Irt estuaries and coring point

The Ravenglass estuary is fed by two main arms; the southerly River Esk drains the Palaeozoic Eskdale granite; the northerly River Irt drains the Triassic Sherwood Sandstone Group (Figure 3.2). Triassic sandstones has been argued and discussed in the name of St Bees sandstone (SBSF) for north west England (Barnes et al. 1994; Strong et al. 1994). This sandstone has mainly covered the north part of the research area (Fig. 3.1) and it is a formation name for Triassic Sherwood sandstones in Cumbria (Colter and Ebbern 1978; Barnes et al. 1994) with a exposure at the St. Bees town 20miles north of the Ravenglass village. SBSF is defined as feldspathic sandstones which is dominated by quartz, K-

feldspars, albite, muscovite and biotite with a carbonatic cement (Barnes et al. 1994) (Table 3.1). The Eskdale granite, the largest exposed intrusion in Cumbria, was emplaced during the late Ordovician related to the final stages of the closure of the Iapetus Ocean and the Caledonian orogeny (Soper 1987). There are two main types of granite; an older biotite-granodiorite in the south and a younger pink-coloured muscovite-granite in the north (Rundle 1979); the Esk River drains mostly the pink-coulored granite (Simpson 1934).Tourmaline occurs as joint-coating and as a replacement of feldspar and biotite, where present, is typically chloritized or replaced by haematite. Overall, the Eskdale granite shows intense chloritization (Brown et al. 1964).

The estuary contains several environments of deposition: tidal channels (mixed wave and river influence), tidal bars, tidal flats (sandy and muddy), aeolian dunes and storm deposits. Subaqueous gravel dune bedforms, made up of shell rich fine/medium gravel, are found at bends in the intertidal part of the rivers. The major part of the estuary is intertidal and, of this, just under half is fine grained sediment (silts and sandy silts).

hinterland geology	drained by:	local formation	major minerals	minor minerals
Triassic sandstones	Irt River	St. Bees sandstones	quartz, feldspars, muscovite, biotite, carbonate	illemnite, haematite
Eskdale granite	Esk River	Cumberland Pink granite	quartz, feldspars, muscovite	Apatite , haematite

Table 3.1: petrology of the Triassic sandstones and Eskdale granite in the research area (Simpson, 1934; Strong et al., 1994).

3.4 Materials and methods

3.4.1 Sampling

Several sediment cores were obtained across the estuary (Fig. 3.1). Samples were taken from the first 10 cm of each core. A combination of Russian corer and window sampler instruments was used to take cores. *Russian corer* is a form of hand corer that is side filling and designed to collect relatively uncompressed sediment samples. The components of the borer include a stainless steel, chambered core tube; extension rods, a stainless steel turning handle; and a core head and bottom point that supports a stainless steel cover plate. The cover plate is curved and sharpened to minimize disturbance when the sampler is driven into the sediment. Once driven to the target depth, the core tube is rotated clockwise to fill the tube by cutting out a half-cylinder segment of sediment. This type of corer can only be used to take samples in loose sediments such as mud and loose sands; it is not suitable for coarser, dense or highly compacted sediment. A Van Walt coring window sampler takes cores of up to 100cm that are preserved in a polythene sleeve that is retracted over the core as the sampler is forced into the sediment. This method preserves the fine sedimentary structures in the core and isolates the sediment from atmosphere. The window sampler was driven into the sediment with an Atlas Copco Cobra TT percussion hammer. Once the polythene sleeve was sliced open, sub-samples were taken every 10cm and preserved in sealed plastic jars. All samples were preserved in sealed plastic bags, and stored at 4°C, pending mineralogical and petrological analysis.

In addition to estuarine sediment samples, fluvial samples (stream sediments) were collected beyond the high tide level on both Rrivers' catchments (Table3.1). All samples from each catchment showed a similar trace in XRD so, one representative fluvial sample were selected for each River.

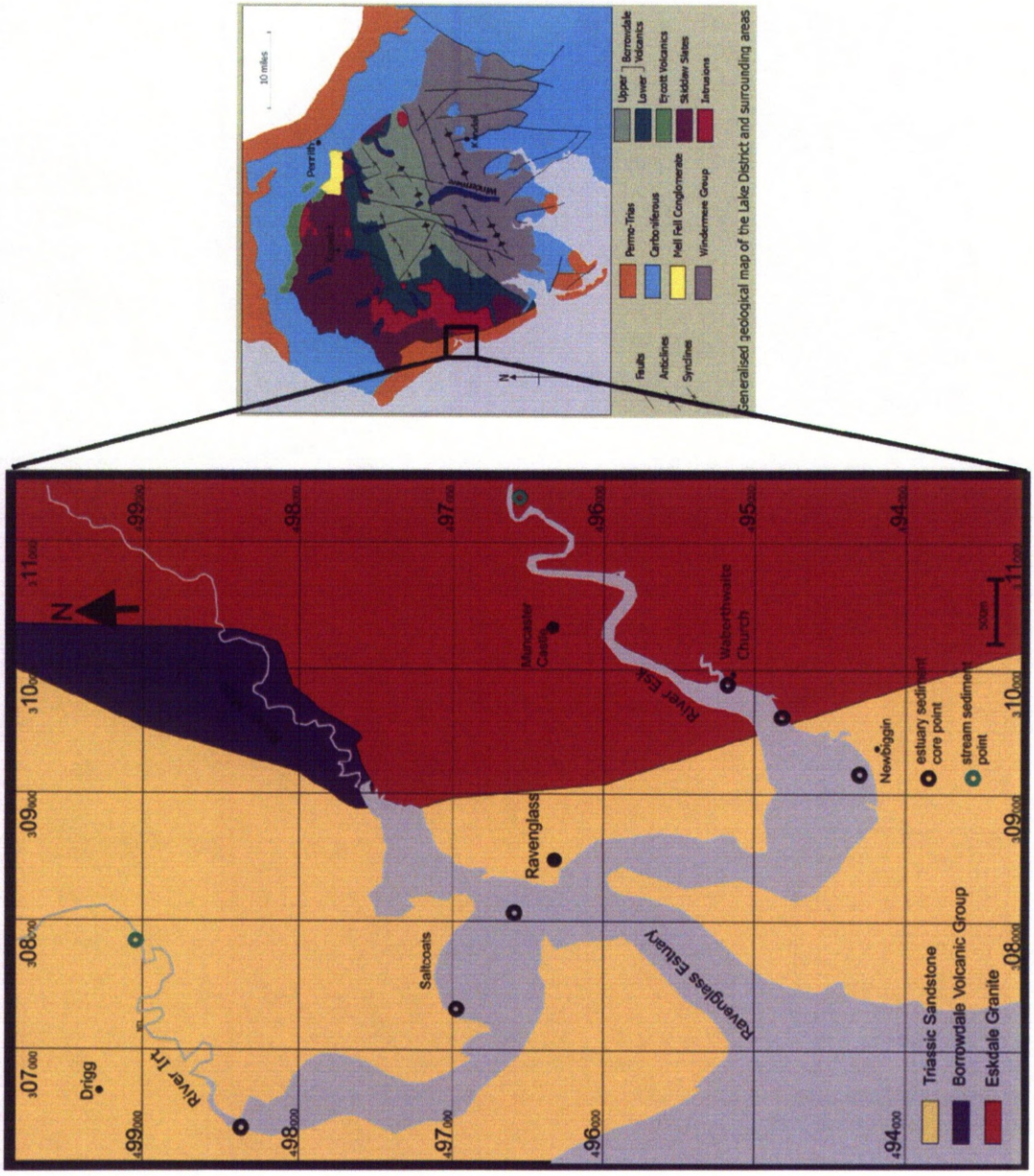

Figure 3.2: Geological map of the Cumbria, UK and the study area. Estuary and fluvial sediment sampling sites marked.

3.4.2 Mineralogical analysis methods

The samples were studied using a combination of X-ray diffraction (XRD), Fourier Transform Infrared Spectroscopy (FTIR) and SEM/BSE/EDAX techniques. The XRD was used to examine the samples in bulk, as well as clay separates. Bulk fractions were crushed using a micromill and distilled water for 10 minutes. The resulting samples were passed through a spray drier (Hillier 1999). The resulting oriented samples were analysed by XRD. In the laboratory, the <2μm fraction of sediment (estuary and fluvial) samples was extracted using an ultrasonic bath in distilled water. This suspended material was separated by settling from a centrifuge after 30 minutes on 3800rpm. The fine fraction material was oven dried at 50°C for 12hours.

Samples for XRD were analysed using a PANalytical X'Pert Pro MPD X-Ray Diffractometer. A copper X-ray source was used operating at 40kV and 40mA. Powder samples were loaded into cavity holders and rotated continuously during the scan, completing one rotation every 2 seconds. Programmable anti-scatter slits and a fixed mask maintained an irradiated sample area of 10x15mm, with an additional 2° incident beam antiscatter slit producing a flat background in raw data from 3.60°. Scans covered the 2Theta range of 3.66-70.00° over a scan time of 1 and half an hour, with 0.04 Rad Soller slits in both the incident and diffracted beam paths. The X'Celerator detector was set to scan in continuous mode with full length active and pulse-height discrimination levels set to 45-80%. Operation of X-Ray Diffractometer and Software was set using a "HighScore Plus®" analysis software and automated Rietveld refinement methods with reference patterns from the International Centre for Diffraction Data, Powder Diffraction File-2 Release 2008.

In order to make an FTIR pellet, 8.0mg of clay separate was ground and mixed with 792mg of KBr in an agate pestle and mortar, then 150mg of this mixture plus 150mg of KBr again were ground and mixed carefully to obtain a 300mg homogenous pellet containing 1.5 mg of sediment (i.e. a 0.5% sample). These amounts were weighed precisely in order to enable quantification. This final mixture was then sintered at 10 tonnes in a Specac press in order to produce an FTIR applicable pellet. The pellets were dried at 140°C for 14 hours in order to remove any absorbed water. These samples were analysed using a Thermoelectron Nicolet 380 infrared spectrometer and OMNIC software

in the range of 230cm^{-1} – 4000cm^{-1}, collecting 32 scans per sample and with a resolution of 4cm^{-1} subsequent to mineral identification in the samples,. The FTIR spectra were run through a band decomposition process in OMNIC and peak areas and were calculated and compared with standards of known quantities that were processed and analysed in the same way as the samples.

3.4.3 Sediment fabric and microanalysis methods

SEM analysis was undertaken using a Philips XL 30 scanning electron microscope equipped with backscattered electron and secondary X-ray detectors used for imaging and microanalysis respectively. Samples were prepared either as gold-coated sediments gently adhered to standard SEM stubs (for SEI work) or as grain mounts, set in resin, cut and polished as standard polished sections (for BSEM and EDAX work).

3.4.4 Worm cast counting

Six intertidal flat areas in the Ravenglass estuary were selected. These areas are the Irt estuary on the mud flats, the Irt estuary at Saltcoats near the mouth of the estuary, the Mite estuary near the channel, the Esk estuary at the channel bank, the Esk estuary on a sand bar, and the Esk estuary on a storm flat. These sites were selected since they are very close to the sediment sampling and coring locations. At each site, a 1m^2 quadrat was thrown randomly at least 15 times for a better coverage of the area and all casts within the quadrat were counted thus revealing the average worm cast density at that site. The newly produced casts of the *Arenicola* were counted using the quadrat when the intertidal area emerged, approximately 3 hours after high tide. Dry days without strong winds had to be selected for field observation due to the fact that the soft *Arenicola* faeces are easily destroyed by wind and water movements. Even during low tide, a few mms to cms of water typically remain on the intertidal flat and casts may be destroyed by waves generated by wind.

3.5 Results

3.5.1 SEM/BSE/EDAX analyses

SEM images reveal poorly sorted, fine sand grains with silt and clay size sediments in the Irt estuary surface sediments (Fig. 3.3). Silt and clay size sediments are abundant in the samples from the mudflat location. SEM images reveal roots and other organic materials were common in mud flat surface sediment samples while shell fragments and diatoms are not abundant. At the Saltcoats locatation, near the mouth of the estuary, fine sand grains with shell fragments and diatoms are abundant and medium sand grains, clay and silt grade sediment, and root plants and other organic materials are rare.

In Esk estuary surface sediments, SEM images revealed poorly to moderately sorted sand grains with sparse clay and silt grade sediment (Fig. 3.3). The amount of the silt and clay grade sediment decreases along the estuary channel toward the mouth of the Esk estuary where it joins the main channel into the sea. SEM images also showed shell fragments and marine fauna, such as diatoms and radiolarians, in association with rare plant material.

In both Irt and Esk estuarine surface sediments, grains have variable clay coating. SEM images also show clastic minerals and particles including carbonate grains (Figs. 3.3c and d). EDAX spectra of coating minerals on sand grains (quartz grains) have a variety of clay minerals from a mineral resembling chlorite to illite as end members and kaolinite. Most of the EDAX spectra seem to reveal the coating minerals to be illite-dominated illite-chlorite and or chlorite-dominated chlorite-illite.

Esk estuary surface sediment EDAX spectra reveal that most minerals that coat sand grains contain Fe. Some minerals resemble the EDAX spectra of chlorite having well-defined Fe peaks and clearly abundant Si, somewhat less Al and much less Mg (Figs. 3.4 a-h). However, most spectra also seem to contain K suggesting either the presence of intergrown illite and chlorite-like material or a smectite phase.

In the Irt estuary surface sediment samples, EDAX spectra reveal mineral coatings with abundant Si, and relatively abundant Al and K and somewhat less Fe. This can be interpreted to reflect more illitic rich intergrown minerals relative to the Esk estuary surface sediment samples (Fig. 3.5 a-h). Kaolinite has been identified with abundant Si and Al peaks (approximately equal peak heights on EDAX spectra) and an absence of K, Fe, or other cations. Illite has been recognized with abundant Si and less Al and K peaks.

The SEM, BSE, and EDAX spectra investigations revealed that the clay minerals in the estuaries' surface sediment are predominantly a chlorite-like Fe-rich mineral, illite and kaolinite, and a combination of illite and chlorite.

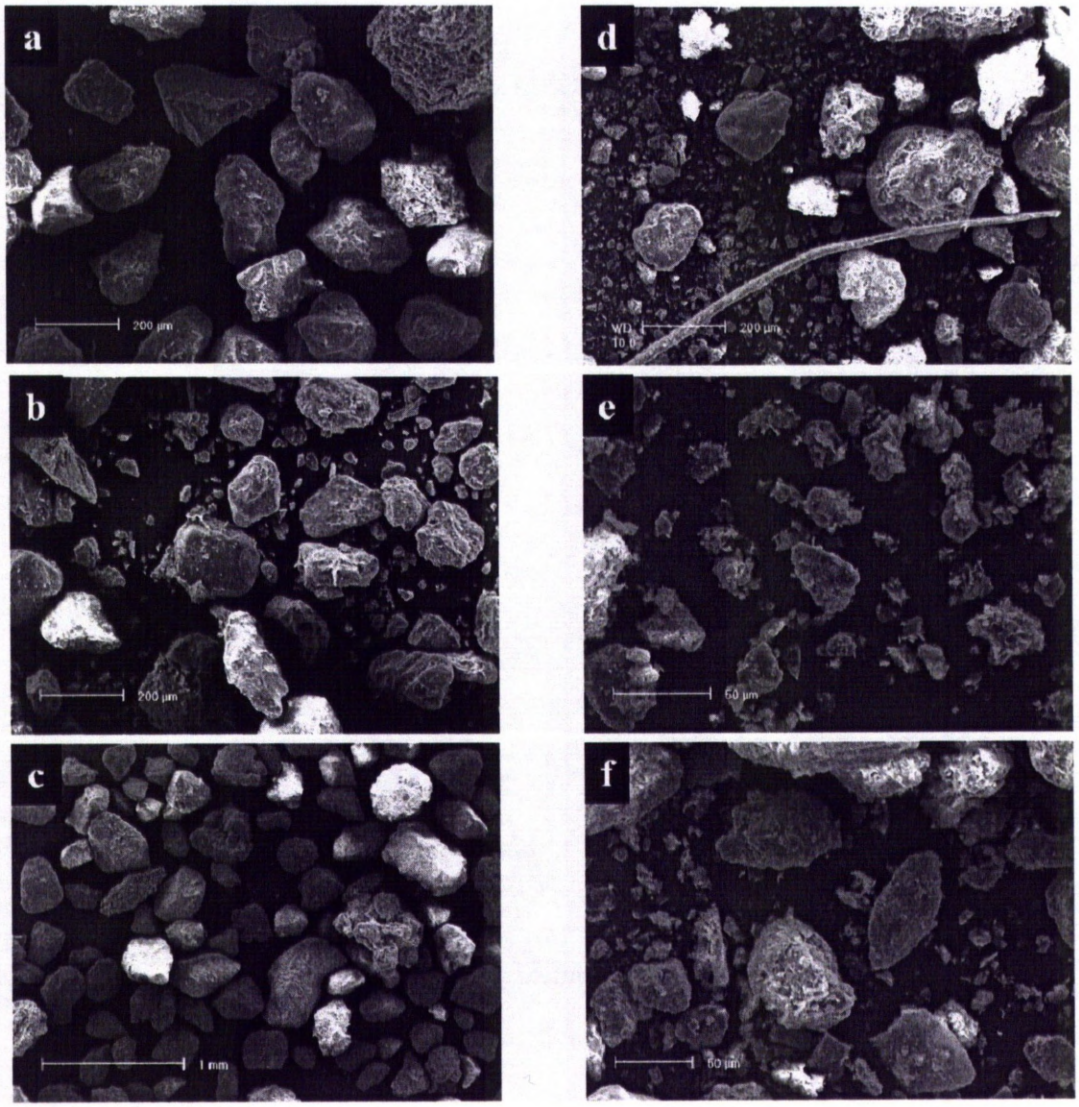

Figure 3.3: SEM images of the Ravenglass estuary surface sediments, a) Upper Esk estuarine surface sediment, channel bank, well sorted medium sands, b) middle of the Esk estuary, sand bars, medium sorted medium sands, c) lower Esk estuarine surface sediments near the train Bridge on sand bars, well sorted medium to coarse sands , d) Irt estuarine surface sediment at the mouth of the estuary, e) middle part of the Irt estuary in mud flat, clay dominant with silt and poor sorted fine sand and f) upper Irt estuarine surface sediment , poorly sorted fine sands and clays.

The presence of K in chlorite can be assumed as smectite or chlorite-smectite; this was then investigated using X-ray diffraction.

3.5.2 XRD analysis of estuarine sediment

The XRD scans of the bulk samples of the surface sediments all across the Ravenglass estuary show these sediments consist of a variety of minerals (Fig. 3.6). X-ray diffraction scans also shows the presence of carbonate minerals, especially calcite, dolomite and siderite. A small peak, which represents pyrite (Fig.3.6), is seen for the Irt estuary surface sediments. X-ray diffraction analyses of the clay fraction samples of the surface sediment show that, in part, all samples have similar clay mineralogy. X-ray diffraction analyses confirms the presence of kaolinite, illite and chlorite. XRD scans of the sample of Esk and Irt estuary surface sediments and heating treatments (Figs. 3.7 and 3.8) show a similar behaviour of clay mineral peaks during heating. For example, 6.2° peaks at the 400°C remains largely unchanged and at the 550°C increases in intensity and became sharper. Peaks at 8.9°at 400°C and 550°C are unchanged and 12.5° and 25.2° peaks show a significant drop about 5-15% (Table 3.2) after 400°C and they collapse with heating to 550°C up to 90%. All traces have peaks at 6.2° and 8.9° and a pair of peaks at 12.3° and 12.5°. Gould et al (2010) reported that kaolinite is difficult to distinguish from chlorite due to an overlapping of the kaolinite (001) and chlorite (002) peaks. Here, however, the kaolinite peaks can be recognized and are clearly differentiated from chlorite at 12.3° and 25° in the analytical work reported here. Chlorite is clearly recognized by the characteristic peaks of chlorite (001) at 6.2°, chlorite (002) at12.5°, chlorite (003) at 18.8° and chlorite (004) at 25.2°. The peak at 8.9° comes from illite. Kaolinite can be confirmed using the 12.3° peak for kaolinite (001) and 25° for kaolinite (002) peaks. The clearly discerned 12.5° peak is plausibly representative of chlorite (002) and other 7Å clay minerals, especially berthierine (001) (Brindley 1982a). Scans of glycolated samples showed no significant changes in peak intensity, especially at 6.2°. This suggests that smectite is negligible and/or below detection limit in surface sediments across the estuary.

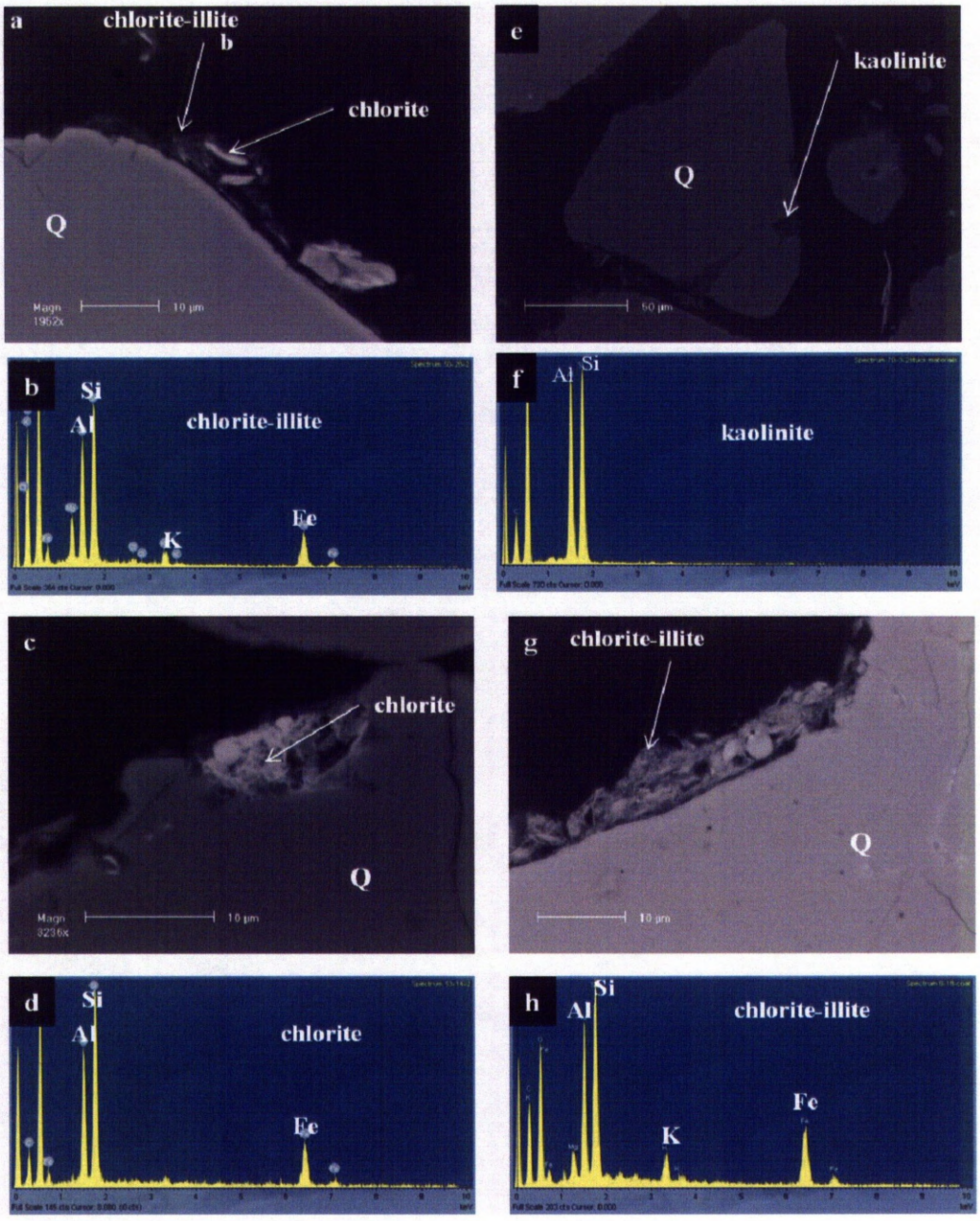

Figure 3.4: Backscattered image (BSE) and spectra analysis of the polished section grain mount samples from the Esk estuarine surface sediment, a) BSE of a sample from the upper part of the estuary, near the channel, Church (Fig. 3.1) at depth 0-5cm, a detrital grain is surrounded with intergrown chlorite-illite as coating and b) is EDAX spectra for clay mineral coating with Al and Si abundant peaks with Fe and K suggesting chlorite-illite mixture, c) BSE of a sample from the lower part of the estuary, Bridge (Fig.3.1) at depth 0-10cm, d) EDAX spectra shows Fe abundant peak in association with abundant Al and Si peaks as well, suggesting Fe-rich chlorite and/or berthierine, e) BSE of a sample from the Church at depth 5-10cm with clay mineral coating, f) EDAX spectra shows abundant Si and Al peaks representing kaolinite, g) BSE of a sample from the church at depth 5-10cm f) EDAX trace shows Al and Si are the dominant peaks in association with K and Fe in which Fe peak relatively is higher than K suggesting chlorite-illite intergrown minerals.

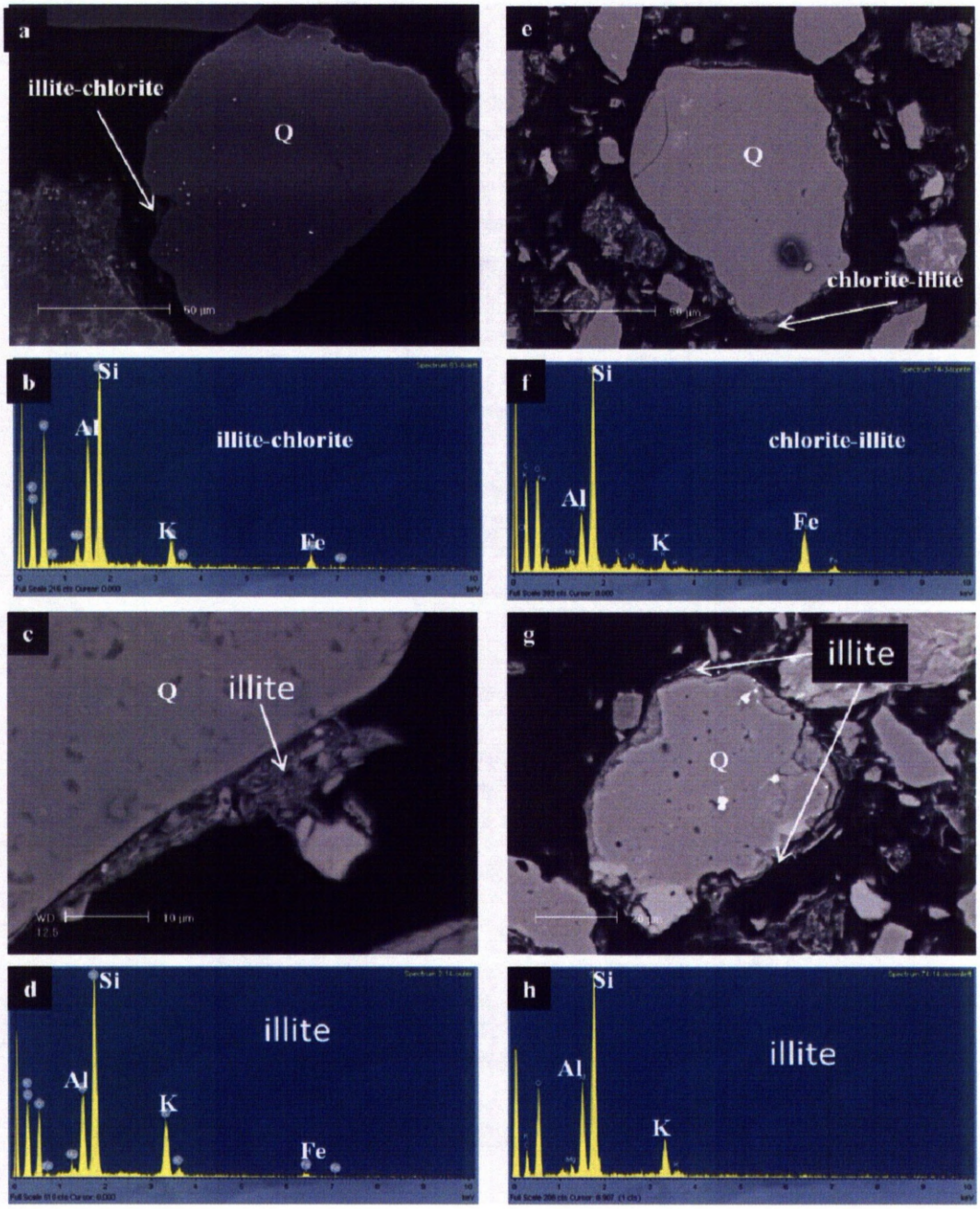

Figure 3.5: Backscattered images (BSE) and EDAX spectra analysis of the polished section grain mount samples from the Irt estuarine surface sediment, a) BSE of a sample from the lower part of the estuary, close to the mouth of the estuay-Saltcoats (Fig. 3.1) at depth 0-10cm, a very thin layer of clay mineral coating is seen b) EDAX spectra for clay mineral coating shows abundant Al and Si peaks with Fe and K, suggesting illite-chlorite mixture, c) BSE of a sample from the Saltcoats at depth 0-10cm , d) EDAX spectra shows Si peak is abundant in association with Al and K and small hint of Fe, suggesting illite, e) BSE of a sample from the upper part of the estuary, Drigg at depth 0-10cm, a quartz grain with coating materials f) EDAX spectra shows abundant Si peak in association with Al, Fe and K in which Fe peak is relatively higher than K it can be chlorite-illite, g) BSE of a sample from the Drigg at depth 0-10cm f) EDAX trace shows Al and Si are the dominant peaks in association with K, suggesting illite.

Scans of samples heated up to 400°C show a slight drop at 12.5° and 12.3° peaks. Chlorite peaks are normally unaffected at 400°C (Starkey et al. 1984); in contrast berthierine (001) typically is sensitive on heating to 400°C (Hillier 2003). Kaolinite peaks sometimes show sensitivity to the temperature around 400°C. A scan of the sample when heated up to 400°C revealed a distinct decrease in intensity for the peaks at 12.3° and 12.5° (equivalent to 7.15Å and 7.07Å respectively). This clearly confirms the presence of kaolinite but further suggests that the peak at 12.5° is not solely due to the chlorite (002) peak. The implication is that 7Å berthierine is present in these samples and that the peak at 12.5° is due to a combination of chlorite (002) and berthierine (001). For the 400°C scan, the intensities of the peaks at 8.9° remain unchanged, which confirms that illite is present. Scans of samples heated up to 550°C shows a significant drop for both the 12.3° and 12.5° peaks while the intensity of the peak at 6.2° increased and sharpened, entirely typical of chlorite. Quantification has been carried out for the XRD scans using area deconvolution of the maximum intensity at peaks: ~14 (6.2°), 9.9 (8.9°), 7.15 (12.3°) and 7Å (12.5°) (Table 3.2). Area quantification of the maximum intensity peak at 6.2° (~14Å) for Esk estuary XRD scan (Fig. 3.6) shows the small change around 10% after heating to 400°C while this loss of intensity is about 30% for the Irt estuary surface sediment. The maximum loss of intensity for this peak is about 90% for the Irt River fluvial sediments. After heating to 550°C, all samples show increasing in intensity (Between 4-40%) from the air dried intensity. Table 3.2 also shows peak at 12.5° (7Å) fall after heating to 400°C from 5% for Esk estuarine sediment to 20% for Irt River fluvial sediments. This loss of intensity for the Esk River fluvial is about 10%.

Normalised maximum peak intensity area quantification of the surface sediments all across the Ravenglass estuary (Table 3.3) shows the maximum number related to 6.2° (14Å) is for fluvial sediments while showing the minimum intensity on 8.9° (9.9Å) and 12.3° (7.15Å). Table 3.4 shows normalised maximum peak intensity area quantification for clay minerals in association with calcite, quartz, and feldspars. The significant loss of feldspar (from 0.41 to 0.10) from the fluvial to the estuary is seen. This decreasing of feldspar content is in contrast with clay mineral in which it increases from fluvial toward the mouth of the estuary.

XRD scans of the surface sediments in different grain size fractions for 5.0-2.0, 2.0-0.2 and <0.2μm in both Esk and Irt estuarine surface sediments (Figs. 3.11 and 12) show a

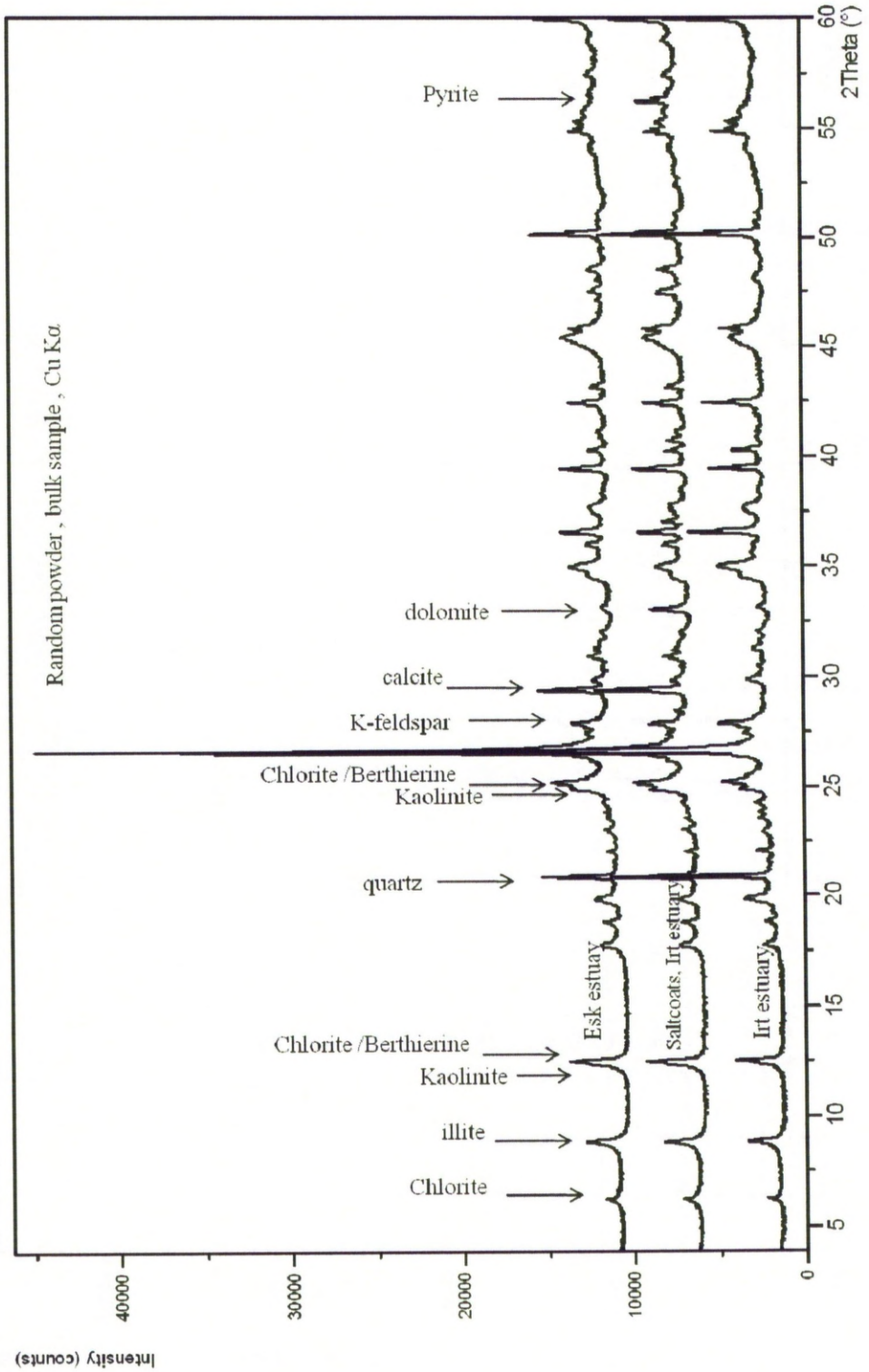

Figure 3.6 XRD patterns of the bulk samples of the Ravenglass estuarine surface sediment showing the minerals present in the estuary. Chlorite, illite, kaolinite are the main clay minerals associate with dolomite and pyrite (just in Saltcoats sample)

difference in intensity for kaolinite peak at 12.3° and 24.9° against fraction size. Increasing in fraction size is in contrast with kaolinite peak intensity. It means the most kaolinite in the surface sediments are present in the very fine size (<0.2μm).

3.5.3 XRD analysis of fluvial sediment

The stream sediment samples beyond the high tide line, from the River Esk, had prominent peaks at 6.2° and 12.5° associated with chlorite and small peaks at 8.9° and 10.5° associated with traces of illite and possibly zeolite (or amphibole) respectively. There is no peak at 12.3° showing that there is no kaolinites present in the sediments of the River Esk (Fig. 3.8). The relative heights of the (001) and (002) peaks (1:2) from the stream sediment sample suggests that this chlorite has a mixed Mg-Fe composition (Hillier 2003). Glycolation led to a slightly bigger effect on 6.2° peak for this sample than the estuarine samples suggesting some sort of expandable phase, such as smectite or possibly vermiculite (Meunier 2007), is present in this sample although expandable clays seem to be broadly absent in the estuarine part of the sedimentary system. Both saturation with magnesium and glycerolation, and potassium saturation produced no noticeable change in the diffraction pattern of the stream sediment sample. However, sequential heating to 300°, 400° and finally 550°C did produce a change in the diffraction pattern, with a gradual collapse and slight shift of a portion of the 14Å peak to ~10Å at 550 C. This behaviour follows the prescribed behaviour of hydroxy-interlayer vermiculite (HIV) (Starkey et al. 1984; Righi et al. 1993; Meunier 2007). The small decrease (15%) in intensity of the 12.5° peak on heating to 400°C can also be fully explained by the presence of HIV; it is thus very unlikely that the decrease in intensity is due to the presence of berthierine in this sample. Heating to 550°C led to substantial collapse of the peak at 12.5° and, as mentioned, a commensurate increase in intensity of the peak at 6.2° suggesting that chlorite is the dominant clay mineral in the sediments of the River Esk. The stream sediment sample, from the River Irt catchment, up beyond the tidal reach, had major peaks at 6.2° and 12.5° probably associated with chlorite and a peak at 8.9° which corresponds to illite. The River Irt sediments seem to contain more illite than the River Esk sediments. There is no peak at 12.3° and 25° showing that there is no kaolinite presents (Fig. 3.9). The relative heights of the (001) and (002) peaks (1:2) from the stream sediment sample suggests that the chlorite has a mixed Mg-Fe composition (Hillier 2003).

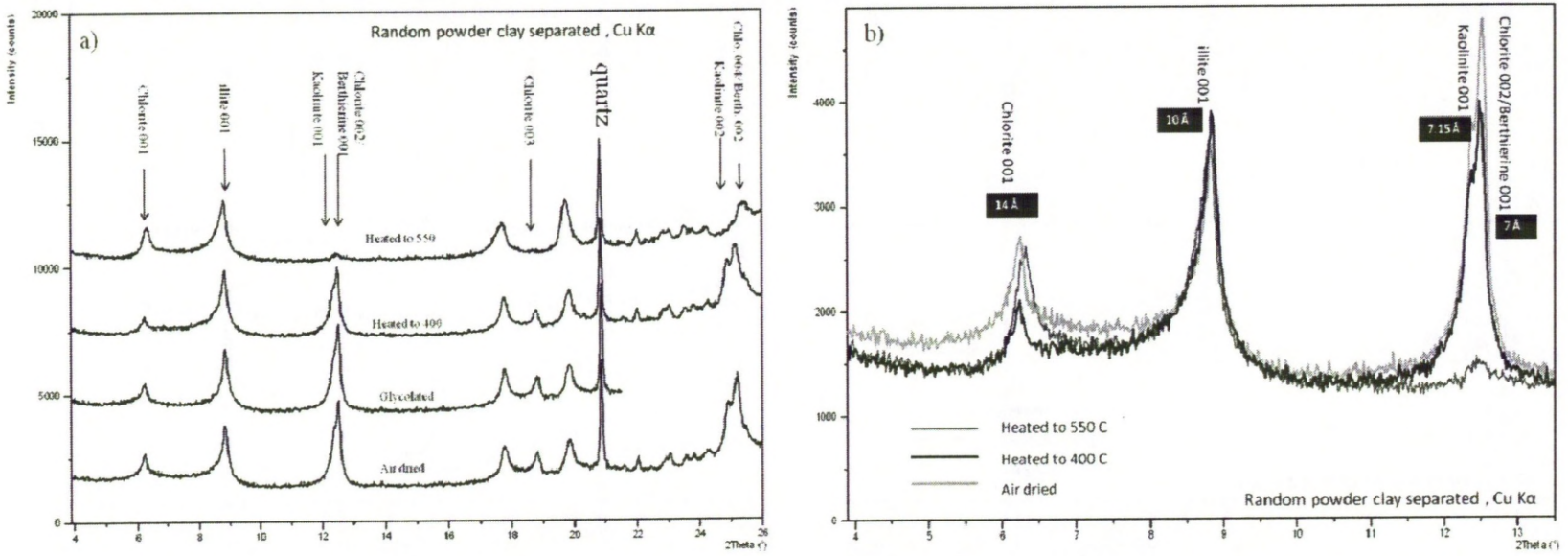

Figure 3.7: XRD patterns of the <2μm fraction of the Esk estuarine surface sediment sample taken at a depth of 5-10cm. a) Collection of patterns arranged from the base: air dried, glycolated, heated to 400°C and heated to 550°C at the top of the stack. b) Overlapping of the XRD data from the low angle end of the pattern to illustrate the drop in intensity of the 7.15 and 7Å peaks during heating to 400°C and their near total collapse at 550°C. Glycolation seems to have little effect on the sample. Note also the broadening of the chlorite(001) peak. The sediment seems to be composed of illite, chlorite, kaolinite and berthierine with negligible smectite present.

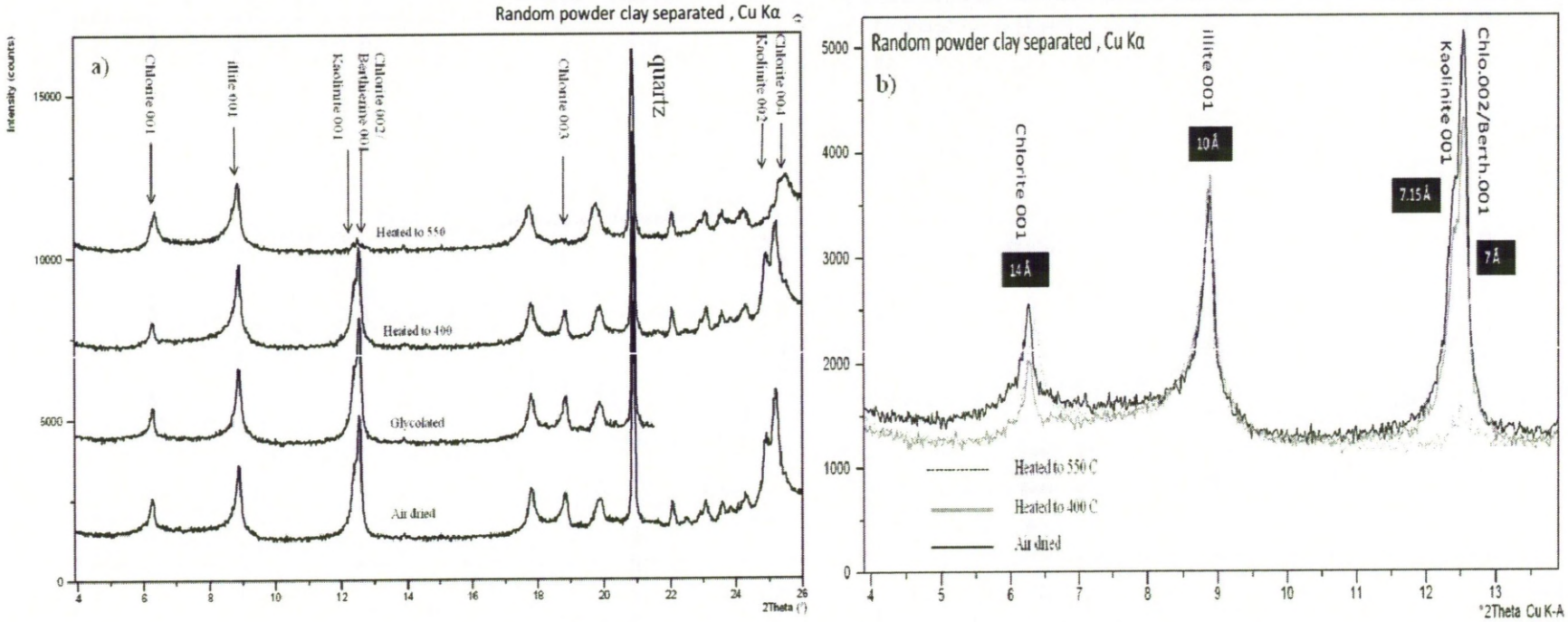

Figure 3.8 : XRD patterns of the <2μm fraction of the Saltcoats near the mouth of the Irt estuarine surface sediment sample taken at a depth of 0-10cm. a) Collection of patterns arranged from the base: air dried, glycolated, heated to 400°C and heated to 550°C at the top of the stack. b) Overlapping of the XRD data from the low angle end of the pattern to illustrate the drop in intensity of the 7.15 and 7Å peaks during heating to 400°C and their near total collapse at 550°C. Glycolation seems to have little effect on the sample. Note also the broadening of the chlorite(001) peak. The sediment seems to be composed of illite, chlorite, kaolinite and berthierine with negligible smectite present.

Glycolation led to a slightly effect on 6.2° peak for this sample suggesting some sort of expandable phase such as smectite, or more likely hydroxyl interlayer vermiculite (HIV), is present in this sample. Both saturation with magnesium and glycerolation, and potassium saturation produced no noticeable change in the diffraction pattern of the Irt stream sediment sample. However, sequential heating to 300°, 400° and finally 550°C produced a change in the diffraction pattern, with a gradual collapse and slight shift of a portion of the 14Å peak to ~10Å at 550 C. The 14Å peak, during heating to 300°C, showed a drop around 70% from the original in intensity and a small shift towards 13.5Å which indicates of the presence of a collapsing vermiculite (HIV) phase. It also shows the general persistence of the 7Å peaks during heating to 300 and 400°C. When the 14Å and 7Å peaks drop (significant drop for 14Å) during heating to 400°C, this is an indication of dioctahedral chlorite (Starkey et al. 1984; Moore and Reynolds 1989) and or hydroxyl-interlayer vermiculite (Meunier 2007) The 7Å and 14Å peaks seem to survive heating to 550°C better than the Irt estuary sample. 14Å peak during 550°C show an increasing in intensity (4-6% greatet than original) and also a new hump around 12.5Å and broader peak at 9.9Å which all indicates the presence of a small quantity of hydroxyl-interlayer vermiculite (HIV). This behaviour follows the prescribed behaviour of HIV (Starkey et al. 1984; Meunier 2007), although unique identification is made difficult by the presence of dioctahedral and trioctahedral chlorite. Heating to 550°C led to substantial collapse of the peak at 12.5° (80-90% removal) and, as mentioned, a commensurate increase in intensity of the peak at 6.2° suggesting that chlorite is the dominant clay mineral in this sediment. In summary, the stream sediment samples are dominated by chlorite in both river systems with no kaolinite present. The River Irt sediments contain rather more illite than River Esk sediments. The River Irt sediment also contains rather more hydroxyl-interlayer vermiculite (Fig. 3.11) than River Esk sediment. The river sediments have quite distinct clay minerals from the estuarine sediments (Table 3.4).

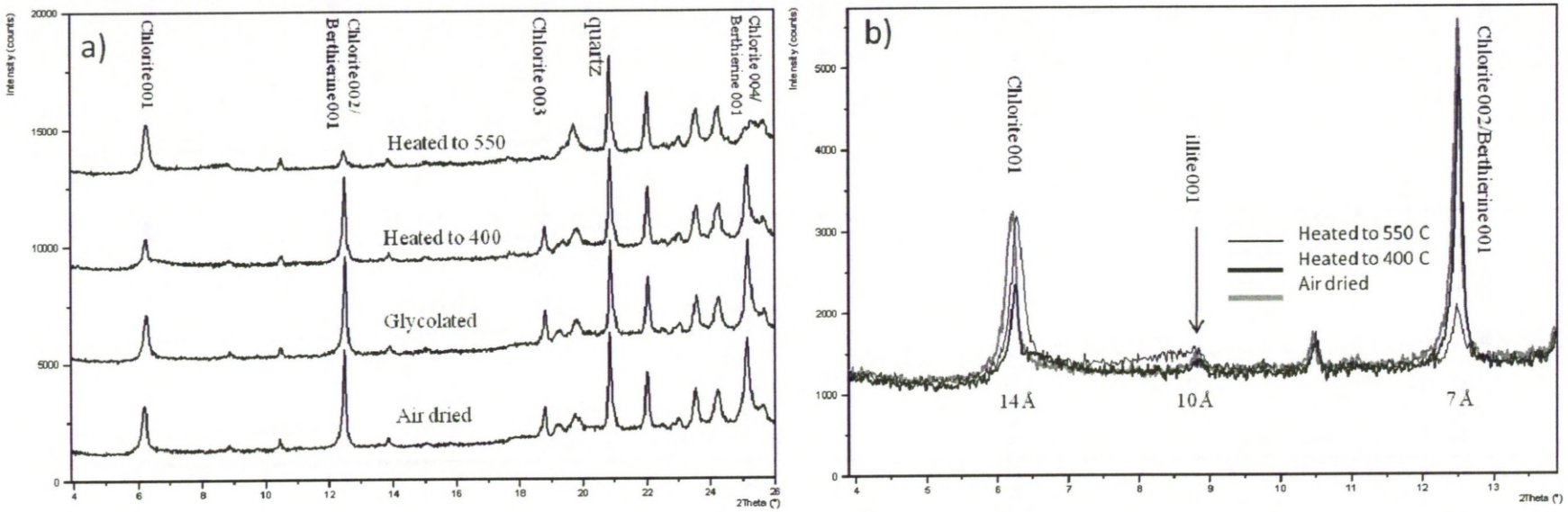

Figure 3.9: XRD patterns of the <2μm fraction of a Esk stream sediment sample taken well beyond the tidal reach of the river. a) Collection of patterns arranged from the base: air dried, glycolated, heated to 400°C and heated to 550°C at the top of the stack. b) Overlapping of the XRD data from the low angle end of the pattern to illustrate the lack of any peak 7.15 and the general persistence of the 7Å peaks during heating to 400°C. The 7Å and 14Å peaks seem to survive heating to 550°C better than the estuary core or suspended sediment samples. Note also the lack of a peak at ~10Å in this sample. The stream sediment seems to be predominantly chlorite with negligible berthierine and no smectite, illite or kaolinite.

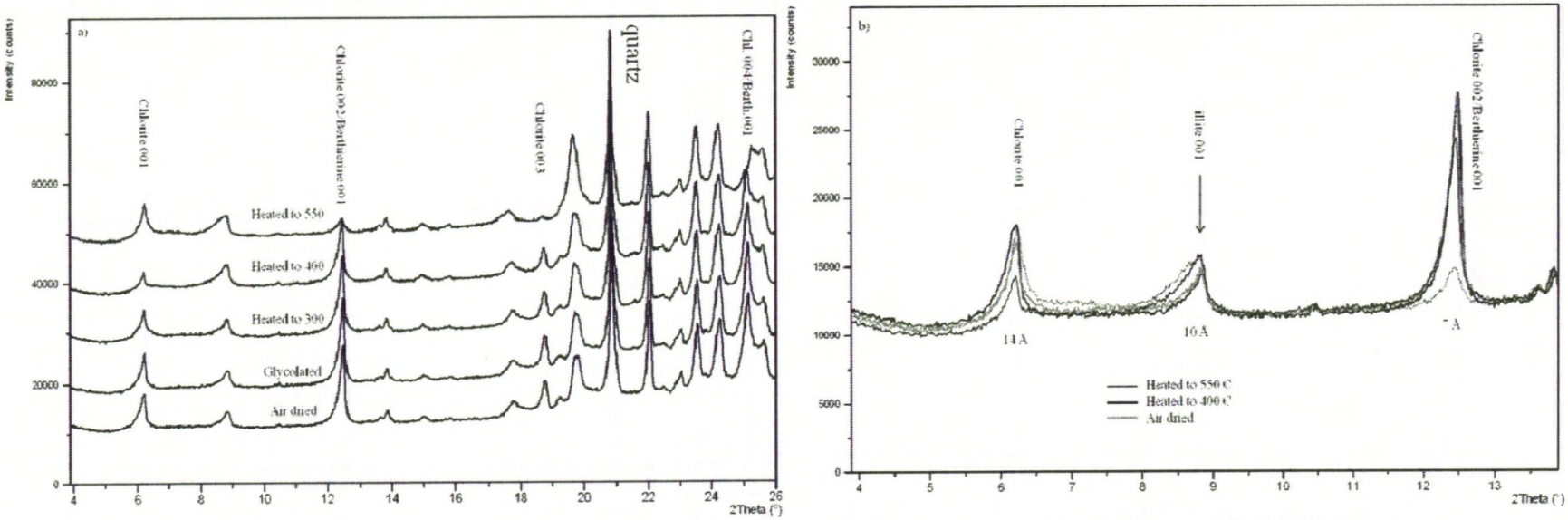

Figure 3.10: Representative XRD patterns of the <2μm fraction of two stream sediment samples taken well beyond the tidal reach of the river Irt(Fig.3.2.1). a) Collection of patterns arranged from the base: air dried, glycolated, heated to 300°C, heated to 400°C and heated to 550°C at the top of the stack. b) Overlapping of the XRD data from the low angle end of the pattern to illustrate the lack of any peak 7.15. The 14Å peak during heating to 300°C shows a small drop in intensity and a tiny shift to the 13.5Å which indicates of small portion of the vermiculite. It also shows the general persistence of the 7Å peaks during heating to 300 and 400°C. While the 14Å and 7Å peaks drop during heating to 400°C, this can be a sign of dioctahedral chlorite. The 7Å and 14Å peaks seem to survive heating to 550°C better than the Irt estuary core samples. 14Å peak during 550°C show an increasing in intensity and also a new hump around 12.5Å and broader peak at 9.9Å which all indicates the presence for small quantity of vermiculite. The stream sediment seems to be predominantly chlorite, some illite with small quantity vermiculite and no smectite and kaolinite.

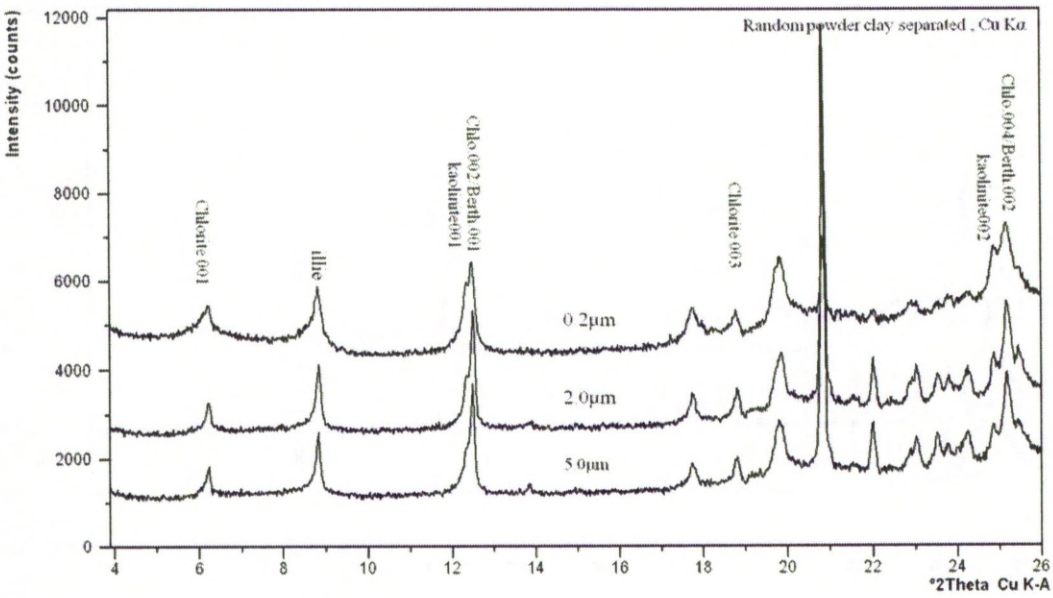

Figure 3.11 XRD patterns of the 5.0-2.0, 2.0-0.2 and <0.2μm fraction of the selected estuarine surface sediment in the Esk estuary samples taken at a depth of 0-10cm. Collection of patterns arranged from the base: 5.0μm, 2.0μm and <0.2μm at the top of the stack.

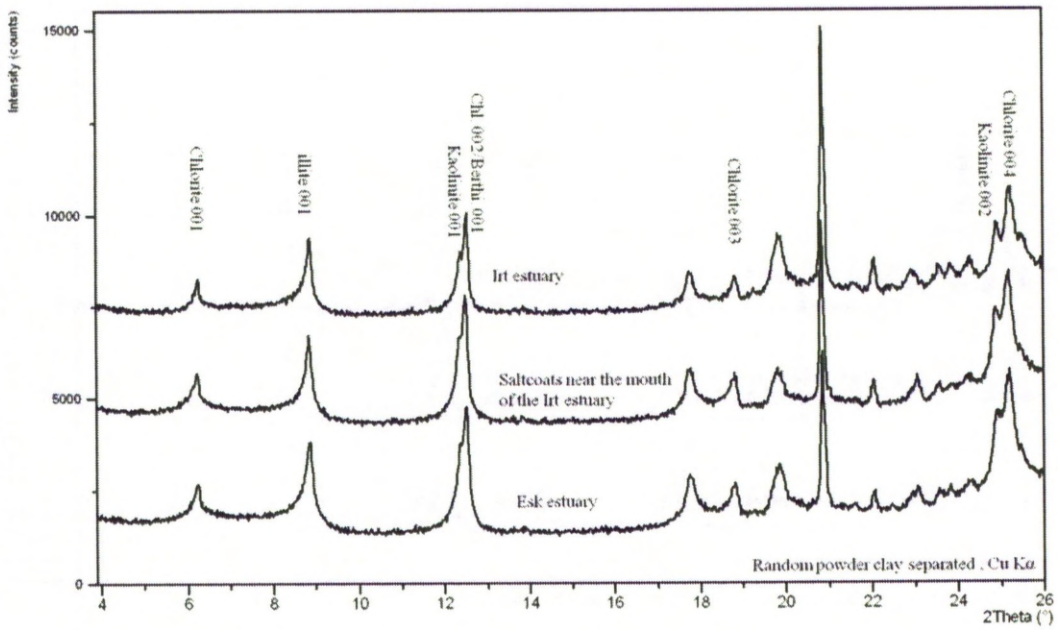

Figure 3.12: Representative XRD patterns of the <2μm fraction of the estuarine surface sediments, collection of patterns arranged from the base: Esk estuary (5-10cm), Saltcoats near the mouth of the estuary (0-10cm) and Irt estuary (0-10cm) at the top of the stack.

	samples	Irt estuary		Esk estuary		Irt fluvial		Esk fluvial	
XRD peaks	treatment	Area of max.Peak intensity	% from original	Area of max.Peak intensity	% from original	Area of max.Peak intensity	% from original	Area of max.Peak intensity	% from original
~14Å	Air dried	171	100	212	100	1337	100	418	100
	300°C	n/a	n/a	n/a	n/a	313	23	n/a	n/a
	400°C	116	68	191	90	70	5	174	42
	550°	243	142	344	162	1388	104	444	106
~7Å	Air dried	472	100	583	100	1846	100	699	100
	300°C	n/a	n/a	n/a	n/a	1506	82	n/a	n/a
	400°C	449	95	497	85	1445	78	628	90
	550°	63	13	63	11	146	8	126	18

Table 3.2: Peak area deconvolution for the surface estuarine and fluvial sediments depends on XRD patterns and sequential heating treatments. Behaviour of the 14Å and 7Å peaks during heating to 300°C, 400°C and 550°C has been quantified for surface sediments in Irt and Esk estuaries and also Irt and Esk River fluvial sediments. The increasing of the 14Å peak after heating to 550°C is a significant sign of chlorite. The small loss (15%) of the 7Å peak for the Esk estuarine sediment while the loss of intensity of 14Å is about 10% can be due to berthierine presense.

samples	~14Å	9.9Å	7.15Å	7Å
Main Ravenglass estuary channel (0-25cm)	0.37	0.17	0.00	0.46
Esk estuary (lower part), Bridge (5-10cm)	0.33	0.26	0.21	0.19
Irt estuary(upper part), Drigg (0-10cm)	0.29	0.20	0.37	0.13
Fluvial sediment (Esk stream sediments)	0.65	0.04	0.00	0.31
Fluvial sediments (Irt stream sediments)	0.64	0.06	0.00	0.30
Irt estuary (mid-part) mudflat (10-20cm)	0.30	0.28	0.31	0.11
Esk estuary (upper part), Church (5-10cm)	0.12	0.37	0.25	0.26
Irt estuary (close to the mouth of the estuary), Saltcoats (0-10cm)	0.34	0.23	0.19	0.24

Table 3.3: normalised peak area quantification of the maximum intensity clay mineral peaks.

samples	quartz	feldspars	calcite	clay mineral
Fluvial sediment (Esk stream sediments)	0 30	0 41	0 00	0 29
Fluvial sediments (Irt stream sediments)	0.57	0.28	0.00	0.15
Main Ravenglass estuary channel (0-25cm)	0.61	0.15	0.13	0 11
Esk estuary (lower part), Bridge (5-10cm)	0.61	0 10	0.00	0.29
Irt estuary(upper part), Drigg (0-10cm)	0 61	0 13	0.06	0.20
Irt estuary (mid-part) mudflat (10-20cm)	0.53	0 09	0 00	0.37
Esk estuary (upper part), Church (5-10cm)	0 26	0.13	0 12	0.49
Irt estuary (close to the mouth of the estuary), Saltcoats (0-10cm)	0 14	0 08	0 23	0 54

Table 3.4: showing normalised peak area quantification of the maximum intensity clay mineral peaks (summation of the 14, 9.9, 7.15 and 7Å peaks), quartz, feldspar and calcite. Feldspar seems decreases from hinterland and fluvial seiment to the open mouth of the estuary. in the same way, clay mineral contents seem increases.

3.5.4 Results of FTIR analysis of clay separates

FTIR can trace a mineral assemblage with small scale features such as atomic positions, mass and bond types and is ideally suited to cryptocrystalline material that may not have long-range crystal structure and so is not suitable for XRD analysis. Using absorbance spectra, rather than the historically-preferred transmission spectra, abundance of a phase is denoted by the relative magnitude of the "peak" height. Peaks at ~3700 (cm^{-1}) represent kaolinite (Lanson et al. 2002), ~3625 (cm^{-1}) represents illite or illite-smectite and a broad peak at 3520 to 3580 (cm^{-1}) corresponds Fe-rich chlorite and berthierine (Madejová 2003).

FTIR graphs of the Irt and Esk surface estuary sediments (Fig.3.13) support XRD results and show peaks representing clays especially kaolinite, illite and Fe-rich clay minerals like chlorite and berthierine. The FTIR analysis of the surface sediments for all across the Irt estuary shows higher absorbance for peaks at 3700 and 3625 (cm^{-1}) relative to the Esk estuary surface sediments. It also shows a hump for Esk estuary around 3520 to 3580 (cm^{-1}) which reveals that some iron-rich chlorite is present in this sample.

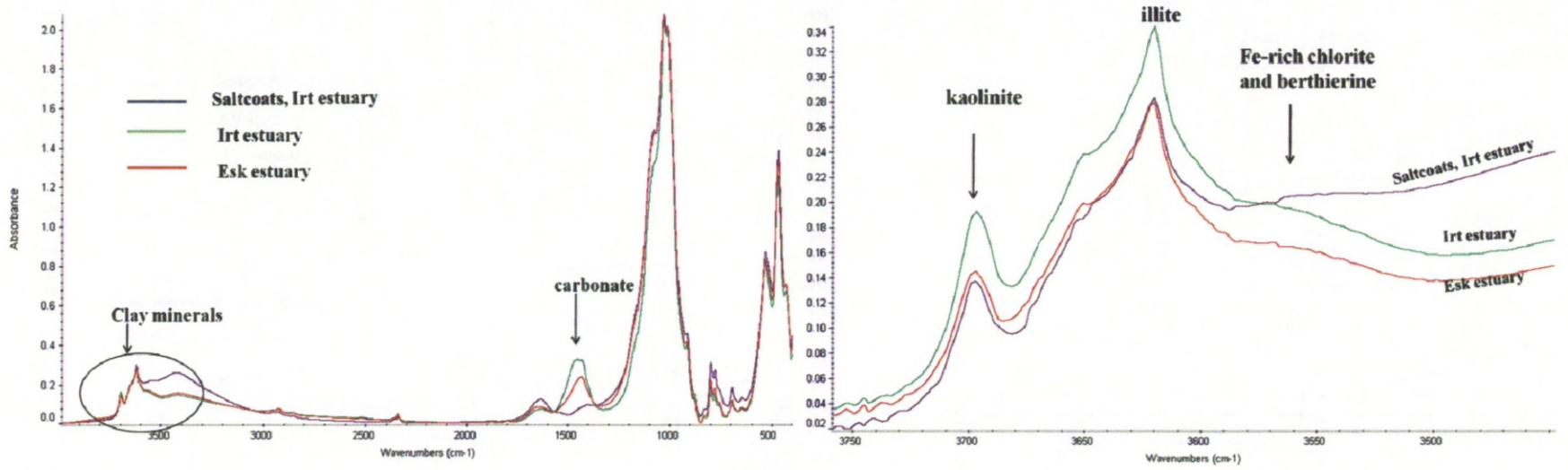

Figure 3.13: FTIR scans of the <2μm fraction of the estuarine surface sediments, (a) collection of patterns Esk estuary-Church (5-10cm) ,Saltcoats near the mouth of the estuary (0-10cm) and Irt estuary, Drigg (0-10cm). (b) showing representative peaks of the kaolinite, illite and Fe-rich chlorite. Scans for the clay minerals relatively showing higher peaks for kaolinite and illite in Irt estuary sediments compare to the Saltcoats (Irt estuary) and Church (Esk estuary).

3.5.5 Results of worm cast counting

Arenicola marina and lugworms have a worldwide distribution (Volkenborn et al. 2007). Bioturbation by these organisms redistributes particles during feeding, burrowing and burrow constructions, however they also lead to alteration of mineralogy and help to generate new minerals (Needham et al. 2005). Mud-flats in the Irt estuary sedimentary system and storm beach deposits in the Esk estuary sedimentary environment do not have any detected lugworm casts suggesting an absence of lugworms in these localities. The other four stations showed variable densities of lugworm casts (Table 3.5). Lugworms are absent in the accumulation of the fine particles and associated organic matter, which characterise the mudflat in the Irt estuary; this is typical of mudflats (Volkenborn et al. 2007). Storm beach deposits, which are composed of gravel and cobble sediment, are also not a suitable habitat for lugworms (Hylleberg 1975). The average lug worm cast population for the Esk estuary in sediment core points show a wide range between 4 to 41 casts/square meter subject to the wet flats and small channels. These range for the Irt estuary on sand bars close to the mouth of the estuary is 8 casts/square meter (Table 3.5)

Lugworm counting location	count	min	max	average	STDEV
Esk estuary-church	15	0	80	41	29
Esk estuary-Bridge	15	0	14	4	4
Irt estuary- Saltcoats	20	2	17	8	5
Irt estuary	10	0	0	0	0
Esk estuary- storm beach, Bridge	5	0	0	0	0

Table 3.5: Worm cast counting statistic measurements in the Ravenglass estuaine sedimentary environment. Lugworm population in mud flat (clay to silt grain size) at Irt estuary and storm beach (gravel abundant and high energy) environment at Esk estuary were not seen while the high population of the lugworms were measured in the

3.6 Discussion

3.6.1 Clay mineral assemblages of surface sediments

In most continental environments, chlorite is typically inherited from ancient rocks and modified by physical or moderate chemical weathering at high latitudes or at altitudes where Quaternary periglacial climatic conditions were prevalent (Sionneau et al. 2008). The dominant clay minerals in the Ravenglass estuarine surface sediment are illite and chlorite (Table 3.3, Figs 3.4 and 5). Chlorite is also abundant in the Irt and Esk stream sediment (Fig. 3.9 and 10). kaolinite and berthierine are also abundant in surface estuarine sediments all across the Ravenglass estuary (Table 3.3, figs 3.7 and 8). Little smectite is found in the Ravenglass sedimentary system although there are some minor effects of glycolation on the stream sediments beyond the tidal reach on Esk and Irt Rivers suggesting that vermiculite is present in the fluvial part of the system. There is a distinct

difference between the sediment found in the fluvial (non marine) and estuarine (marine) parts of the sedimentary system.

Weathering and soil environments are major locations for clay mineral formation. XRD analysis of stream sediments indicated dioctahedral clay minerals (Al-rich chlorite and hydroxyl-inter layer vermiculite) (Figs. 3.9 and 3.10) are present and probably created in the hinterland to the Esk and Irt estuaries. The other major location for clay mineral formation is at depositional environments including estuarine depositional environments. In the Irt and Esk estuaries trioctahedral chlorite including a mix of Fe-Mg and/or Fe chlorite are present along with kaolinite and illite. Chemical weathering, and alteration, subject to specific clay minerals are the major factors that influence clay mineral transformation and creation in the surface sediments all across the Ravenglass estuary.

Sand grains in the surface sediment samples are coated with clay-grade material that is dominated by clay minerals (Fig. 3.4). Much of the coating is Fe-chlorite, given the size of the chlorite (001) trace in Figures 3.6 and 7. Some of the coating material is illite leading to a mixed mineralogy for clay coats on sand grains in the Ravenglass estuary. Coatings on sand grains in ancient sediments have been reported to be both illite and chlorite-bearing (e.g. Ehrenberg, 1993) suggesting that the Ravenglass case study is not especially unusual in this regard. Lugworms in the surface sediments are present as a function of sediment grain size distribution. Lugworms live in shallow depositional environments containing a range of grain sizes; i.e. silt and fine sands to coarse sands, across the estuary. They rework and bioturbate the sediments and also change the chemical properties and mineralogy in sediment as well (Needham 2004; Needham et al. 2004; Needham et al. 2005; Worden et al. 2006). The comparison of the lugworm population and the Fe-rich clay minerals as coating on sand grains (Fig. 3.14) shows the environment of lugworm activity has relatively more Fe-rich clay minerals (Fig. 3.4) in coating patterns compare to the environments with no lugworms (Fig. 3.14).

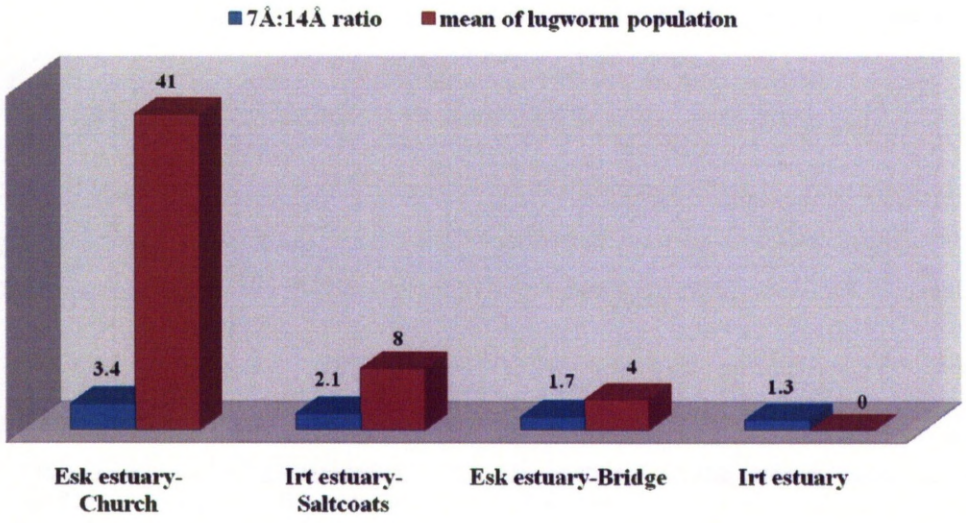

Figure 3.14: Mean worm population against 14Å:7Å ratio in surface Ravenglass estuarine system. Esk estuary Church shows highest mean population with Fe-rich chlorite ratio. Clay minerals at Saltcoats and Bridge seems Fe-Mg chlorite with a ratio ~2, and the Irt estuary with null lugworms shows dioctahedral chlorite in surface sediments.

3.6.2 Chlorite and berthierine origin in the Ravenglass estuary sedimentary system

Chlorite is the only clay mineral that is abundant in both marine and non-marine parts of the Ravenglass estuary system. Chlorite has been reported as an alteration and weathering product in the Eskdale granite (Moseley, 1978), and in the Triassic sandstones (Strong et al. 1994). Therefore, hinterland geology is likely a major source of the chlorite to the Esk and Irt estuary. XRD analysis of the River Esk and River Irt stream sediment samples beyond the high tide line revealed chlorite seems to be a mixed Mg-Fe type of chlorite given the (001):(002) ratio of 1:2 (Figs. 3.9 and 10) (Hillier 2003) as well as dioctahedral chlorite (Al-chlorite) (Table 3.6). This mix of chlorite seems likely dominated by Fe-Mg chlorite for the Esk river sediments and dominated by dioctahedral chlorite (Tables 3.2 and 6)(Figs. 3.9 and 10). The implication from the change of chlorite composition is that the chlorite being fed into the Esk estuary especially and Irt estuary evolves towards a Fe-rich chlorite or berthierine composition (Table 3.6)(Figs. 3.7, 9 and 15) once it is subject to marine influence. On the other hand, the aqueous iron load of rivers typically decreases once rivers enter the estuary and the salinity starts to increase (Boyle et al. 1977a). It seems to be possible that fluvial aqueous Fe, trapped in the estuary, is the source of the increasing Fe-content of chlorite. Up-taking the Fe in association with mobilised cations

can happen in the estuary water and sediment interactions. Fe ions are aggregated and then precipitate as oxide or hydroxide in the estuaries (Eckert and Sholkovitz 1976; Sholkovitz 1978; Mayer 1982), so chlorite and cations especially iron are integrated and segregated and up-taking the Fe controls the new Fe-rich chlorite (berthierine) formation and transformation process.

3.6.3 Illite and kaolinite origin in the Ravenglass estuary sedimentary system

Illite and kaolinite are common weathering products of the feldspar minerals. Feldspar is abundant in the St. Bees sandstones (Strong et al. 1994) and Eskdale granite (Simpson 1934; Soper 1987). The absence of kaolinite in the stream sediment samples (Figs. 3.8, 9 and 15) suggests only a limited degree of chemical weathering in the hinterland (Drever and Zobrist 1992). The presence of kaolinite in the Esk and Irt surface estuarine sediments (Fig. 3.11) suggests that chemical weathering is more advanced in the estuaries. This has been reported in other estuaries in which kaolinite forms through long-term weathering processes (Thiry 2000). Distinguishing between muscovite and illite in the XRD pattern is difficult, however there is a peak at 9.9Å which represents either illite or muscovite in the River sediments beyond the tide line. Muscovite has been reported in the St.Bees sandstones (Strong et al. 1994) and Eskdale granite (Soper 1987), thus it is possible to see the muscovite in the stream sediments, However, there is a small illite peak in the stream sediment samples (Fig. 3.9 and 10) suggesting a limited degree of chemical weathering in the hinterland. Feldspars are abundant in hinterlands and also in the stream sediments (Fig. 3.16) and (Table 3.5). On the other hand, illite-smectite has been reported as a product of chemical weathering reaction on muscovite in soils (Oelkers et al. 2008)).

The presence of illite in the stream sediment might be due to white mica or muscovite (present in both granite and Triassic sandstones) rather than feldspar alteration. The much greater presence of illite in the estuarine and near estuary marine environments (Figs. 3.6-8) suggests that chemical weathering of the feldspar minerals originally derived from either Eskdale granite for Esk estuary and Triassic St.Bees sandstones is more developed in the estuaries than in the rivers and their valleys. In the same way, feldspars decreas from hinterland (40%) toward the estuarine (10%) (Fig. 3.16) and (Table 3.5).

This greater abundance of illite and kaolinite in the estuary relative to the stream sediments might simply be a function of the increased residence time (i.e. more time for

weathering) of the sediment in the lower relief parts of the basin in association with saline water in the estuarine systems.

Another possibility of seeing kaolinite and illite in both estuarine sedimentary surface sediment samples, and their absence (kaolinite in both stream sediments and illite just for Esk River sediments) in the stream sediments could be the transportation of illite and kaolinite by the marine system waters to the Esk and Irt estuary at high tide.

However, grain size fraction analysis on the estuarine surface sediments (Fig. 3.12) reveals <0.2μm kaolinite particle size is abundant in the estuarine surface sediments in contrast to 5.0μm. These very fine kaolinite particles are a product of alteration or chemical weathering within the estuary.

In summary and regards the grain size fraction analysis (Figs. 3.11 and 12) chemical weathering and diagenesis process inside the Ravenglass estuary are interpreted as the main sources of kaolinite in the surface sediments rather than sediment influx from the marine system waters and settling within the estuary.

estuarine sedimentary environment	**7Å:14Å ratio**
Esk estuary-Church	3.4
Irt estuary-Saltcoats	2.1
Esk estuary-Bridge	1.7
Irt estuary	1.3
Esk fluvial sediment	1.7
Irt fluvial sediment	1.4

Table 3.6: showing the chlorite (001):(002) peak ratio related to the estuarine sedimentary environment. The ratio greather than 3 is related to the Fe-rich chlorite and ratio about 1:2 regards Fe-Mg chlorite. The smaller amount are mix of the Fe-Mg chlorite with Al-chlorite and other type of the chlorites.

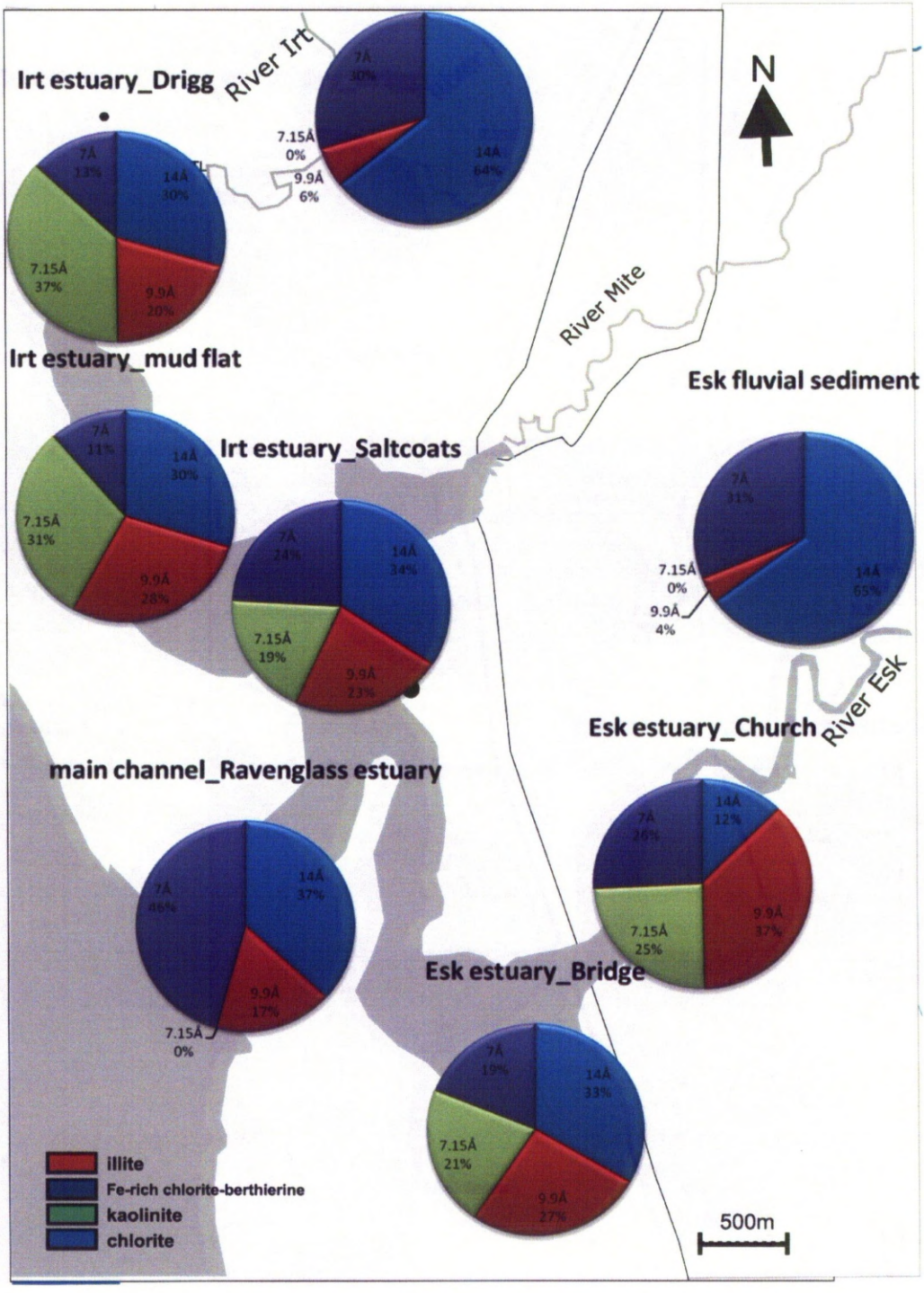

Figure 3.15: schematic map of the Ravenglass estuarine sedimentary system and pie diagram of the normalised quantification of the clay separated (<2μm) clay mineral maximum intensity peaks. Kaolinite is only seen within the estuary and it is absent in the fluvial sediments and in the main channel close to the open sea. Illite is not abundant in the fluvial but is significant within the surface estuarine sediments.

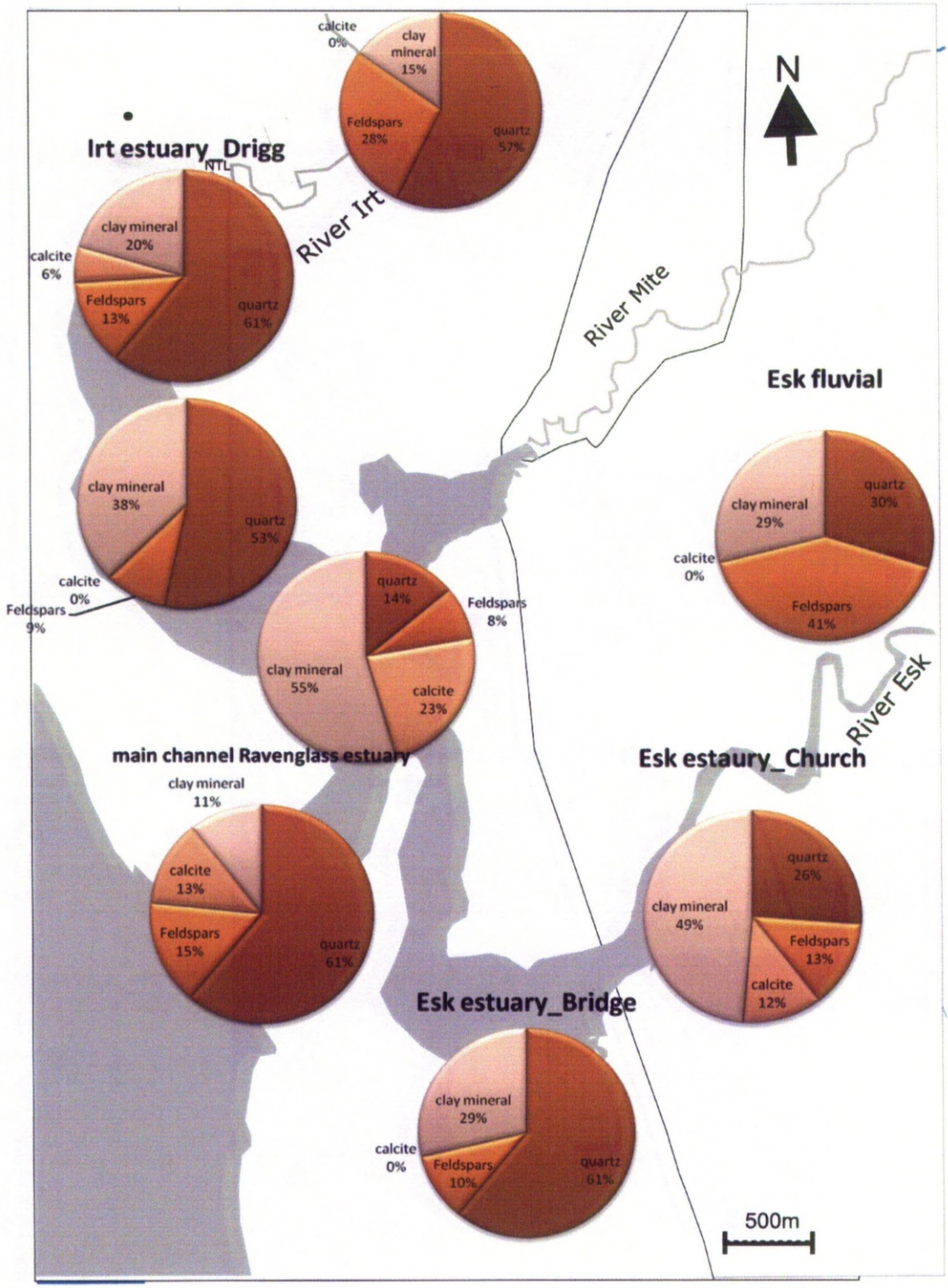

Figure 3.16: schematic map of the Ravenglass estuarunie sedimentary system and pie diagram of normalised maximum intensity peaks of clay separated (<2μm) clay minerals, quartz, feldspars and calcite. Feldspars considerably decreases toward the estuary in contrast with clay minerals. Chemical weathering can alter feldspars to kaolinite mainly and illite as

3.7 Conclusion

1. Chlorite, illite and kaolinite and possibly berthierine are all present in surface sediment in the Ravenglass estuary, NW England.
2. Chlorite, a minor expandable phase such as hydroxyl-interlayer vermiculite (HIV), dioctahedral chlorite and also illite (in the Irt stream sediments), are present in the river sediments, beyond the tidal reach.
3. Chlorite evolves to a progressively more Fe-rich composition (berthierine) from the hinterland and fluvial to the marine environment suggesting that fluvial colloidal or suspended Fe phases, trapped in the estuary, may have helped to alter the composition of this deposited clay mineral.
4. Given the abundance of kaolinite and illite within the estuarine sediments in comparison to the fluvial sediment, it seems likely that these minerals were formed within the estuarine environment.
5. Given the XRD response of the 7Å peak upon systematic heating to 400°C, it is also possible that berthierine was formed within the estuarine environment.
6. Sand grains in the estuarine surface sediments are coated with a fine layer of clay minerals including chlorite, illite, mix of illite-chlorite and kaolinite in the Irt estuary and Fe-rich chlorite, berthierine, chlorite-illite and kaolinite in the Esk estuary. This suggests that estuaries are sites for not only Fe-clay creation and accumulation but also for the generation of coated grains, which upon subsequent burial and diagenesis, would become chlorite-coated sand grains.

Chapter 4

Chapter 4 Stratigraphic variations in clay mineralogy, grain coating pattern and clay mineral alteration in the Ravenglass estuary

4.1 Abstract

The distribution of clay minerals in the Ravenglass estuary (including Irt and Esk estuaries) in the north west England is closely related to the following factors: (i) the petrography of the mother rock in hinterland such as Eskdale granite and Triassic sandstones, (ii) the grain size of the sand grains in very shallow sediment for *in situ* clay mineral coating, (iii) alteration and chemical weathering productions within the estuary. There seem to be strong provenance controls on the proportions of clay minerals in the cores in the two branches of the estuary. The chlorite-rich weathered I-type granite hinterland of the Esk estuary has led to the accumulation of more chlorite (and berthierine) than the chlorite-poor Triassic Sandstone hinterland of the Irt estuary. The clay minerals chlorite, illite, kaolinite, berthierine and vermiculite are all present in the Irt and Esk branches of the Ravenglass estuary as is a gibbsite-like phase and pyrite. Kaolinite and pyrite are more abundant in the Irt estuary cores than the Esk cores while chlorite and berthierine appear to be more abundant in the Esk estuary cores. The Irt estuary cores have slightly increasing chlorite and decreasing illite from base to tops of cores. Esk estuary cores have slightly decreasing chlorite and increasing kaolinite from base to tops of cores. Berthierine abundance broadly decreases up-section. Gibbsite is present at depth, where kaolinite is effectively absent. Grain-coating clay minerals are variably present on sand grains from this estuary. Finer grained sand tends to have more complete clay mineral coats than coarser-grained sand. The degree of coating decreases up-section in the Irt Estuary cores. The degree of grain coating is more variable in the Esk estuary but tends to increase up-sectiones. Fe-clays, chlorite and berthierine, are most abundant in the coarsest sediment where pyrite is absent (where the supply of sulphate is lowest). Grain coatings seem to be best developed in the finest sandy sediments; in this case where illite-chlorite tends to be dominant.

4.2 Introduction

Commonly, three origins of clay minerals in estuarine sedimentary environments have been proposed (Bokuniewicz 1995; Aagaard et al. 2000; Tucker 2001; Burley et al. 2003; Worden and Morad 2003a; Sionneau et al. 2008): (1) inherited from soil and drift deposits in the fluvial hinterland, (2) neoformation (precipitation) and (3) transformation. Estuaries

are highly efficient sediment traps for inherited clay minerals and estuarine deposits, during sea level transgression, have high preservation potential. In estuarine systems clay minerals can form *in situ* either by direct precipitation or transformation. In terms of transformation, inherited clay minerals tend to be modified by ion exchange or cation rearrangement (Berner 1980; Aller and Aller 1998). Clay mineral neoformation and transformation can take place directly within the depositional environment (Berner 1980; Baker et al. 2000a; Burley et al. 2003; Worden and Morad 2003b). For example formation of the kaolinite and/or illite from chemical weathered feldspars, transformation of mix layer chlorite to Fe-rich chlorite and precipitation of gibbsite after kaolinite dissolution and alteration, are all processes that have been invoked previously in estuarine environments (Drever and Hurcomb 1986; Drever and Zobrist 1992; Velde and Church 1999; Worden and Morad 2003b). Here, all these processes will be considered.

Inherited clay minerals, which have formed in the hinterland, can be transported as suspended load through these rivers to the estuary before settling out. The distribution of clay minerals in modern sediments is considered to be largely a reflection of the weathering pattern (Tucker 2001) and clay minerals are altered and replaced by other clay minerals during diagenesis (Worden and Morad 2003b). Estuarine sedimentary processes and stratigraphy have here been investigated in order to obtain a subsurface clay mineral distribution from a cool temperate estuary on the Irish Sea. The Ravenglass estuary on the west coast of Cumbria in north-west England is an area which encompasses the tidal reaches of the three rivers: Esk, Irt and Mite. The Esk River drains the Eskdale granite and the Irt drains Triassic sandstones. The minor Mite River drains a combination of Borrowdale Volcanic Group (mainly andesitic), Eskdale granite and Triassic Sherwood Sandstone Group sandstones. The two dominant rivers, the Irt and Esk, have been selected for this research. Clay mineral distribution and sedimentary depositional environments in the Ravenglass estuarine sediments have been investigated in order to identify the sources of the clay minerals in the estuary, and explain the alteration and early diagenetic processes.

The occurrence, amount and type of clay minerals can alter the porosity and permeability of a deeply burried reservoir (Worden and Morad 2003b) such that they directly control their economic feasibility. Some sandstones with clay-coated grains have been reported to contain anomalously elevated porosity for their depth of burial (Ehrenberg 1993). Chlorite coats on sand grains, in particular, can preserve high porosity to depth of up to 6 km

because they inhibit quartz cementation (Hillier and Velde 1992; Ehrenberg 1993; Aagaard et al. 2000). The accuracy and explanation of the mode of occurrence, and the mechanism(s) that generates the development of the clay mineral coating and therefeore the porosity and permeability of the reservoir, are important issues. Describing and then hopefully explaining the extent of coverage of sand grain by coating clay minerals in modern sedimentary systems is important for understanding subsequent burial diagenesis processes and reservoir quality issues. This research aims to address the following specific questions:

1) What types of clay minerals are present in the Ravenglass estuary; are there differences in the types of clay minerals in different arms of this estuary?
2) Do clay minerals vary with depth (stratigraphically)?
3) Are there different stratigraphic patterns at different locations within the estuary?
4) What is the origin of clay minerals in this estuary? What are the relative roles of primary (sedimentary) and secondary (diagenetic) processes in controlling clay mineralogy?
5) Are there grain-coating clays on sand grains in this estuary?
6) Do grain coating clays vary in terms of mineralogy or extent of grain coverage either with depth or location in the estuary?
7) What controls the mineralogy and extent of grain coating clay minerals?

4.3 Material and method

4.3.1 Sampling

An ideal sediment core is one that remains undisturbed during sampling. Several sediment cores were obtained across the estuary (Fig. 4.1) using a combination of Russian corer and Van Walt window sampler instruments.

A *Russian corer* is a form of hand corer that is side-filling and designed to collect relatively uncompressed sediment samples. The components of the borer include a stainless steel, chambered core tube; extension rods, a stainless steel turning handle; and a core head and bottom point that supports a stainless steel cover plate. The cover plate is curved and sharpened to minimize disturbance when the sampler is driven into the sediment. Once driven to the target depth, the core tube is rotated clockwise to fill the tube by cutting out a half-cylinder segment of sediment. The borer is capable of obtaining samples at depths of 3 meters or more with little sample loss. This corer only takes

sediment samples in loose sediments such as mud and loose sand and it is not suitable for coarser, dense or compact sediment. Sediment samples from the Russian corer were collected every 10 to 20 cm.

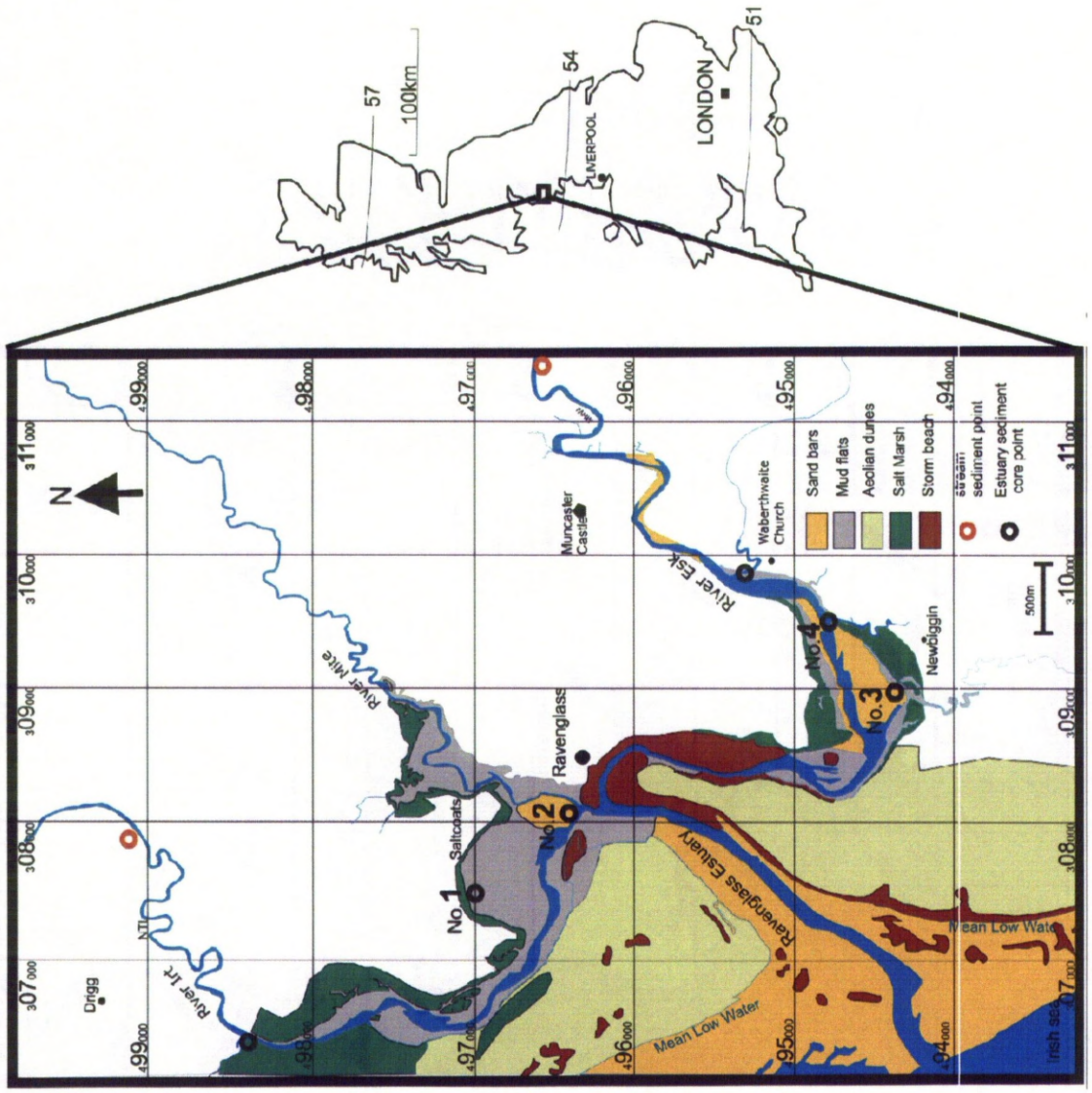

Figure 4.1: Location map of the Ravenglass study area, showing the main estuary and the sub-estuaries; Esk and Irt estuaries and coring localities marked as sites 1, 2, 3 and 4.

A Van Walt window sampler was used for coarse grained and compacted sediments, and is a pneumatic drill-driven corer that recovers ~1m of sediment which preserves entire cores largely undisturbed in a thin filling plastic sleeve. The window sampler was driven into the substrate with an Atlas Copco Cobra TT percussion hammer. Once the polythene sleeve was sliced open, samples were taken every 5-10cm, preserved in sealed plastic jars and then stored in a refrigerator before preparation for mineral and petrological analysis. All samples were preserved in sealed plastic bags, and stored at 4°C, pending mineralogical analysis.

4.3.2 Mineralogical methods

The samples were studied using a combination of electron microscope (SEM/BSE/EDAX), X-ray diffraction (XRD) and infrared spectroscopy (FTIR) techniques.

Backscattered images and Energy-dispersive X-ray spectroscopy (BSE/EDAX)

In order to identify and measure the clay mineral grain coating coverage in polished thin sections, a Philips XL 30 scanning electron microscope equipped with backscattered electron and secondary X-ray detectors were used for imaging and microanalysis respectively. A whole sediment fraction was lightly washed with distilled water and freeze-dried for examination in a Philips XL 30 scanning electron microscopy. Samples were also prepared as grain mounts by setting them in resin under vacuum. These mounted samples were then sliced and prepared as ordinary polished thin sections. The preparation of polished sections enabled clay-grade materials simply resting on the detrital grain surface to be differentiated from surface-attached coatings. Sand grains were selected randomly across the polished thin section and pictured with the highest quality and resolution. Open source image-analysis software "JMicroVision" version 1.2.7 was applied to measure the physical parameters of every selected grain. The BSE images were uploaded to the software media and parameters such as length, width, perimeter and area of every host grain were measured precisely. The perimeter of a host grain which was coated with clay minerals was accurately estimated. The surface of a sand host grains in contact with neighbouring detrital grains was excluded from this calculation.

X-ray diffraction (XRD)

XRD was used to examine the samples in bulk, as well as clay separates. Bulk fractions were crushed using a micromill for 10 minutes. The resulting samples were passed through a spray drier. The spray dryer consists of two parts, the spraying system and the drying chamber (Hillier 1999). The resulting randomly oriented samples were analysed by XRD using a PANalytical X'Pert Pro MPD X-Ray Diffractometer. Clay fractions from portion of the cored sediment sample were suspended by ultrasonic disaggregation in distilled water. Suspended materials were then separated using a centrifuge at 3500 rev/min for 30 minutes. Finally, they were dried out in an oven at 55°C overnight. The separated clay fraction nominally consists of the <2μm fraction although there is considerable variability given the role of grain shape and its effects on settling velocities. Clay fractions of sediment samples were prepared for X-ray diffraction in four ways: (1) air dried, (2) Mg-saturated and then glycolated, (3) heated for one hour at 400°C and (4) heated for one hour at 550°C. A copper X-ray tube at 40kV and 40mA was used. Powder samples were loaded into cavity holders and rotated continuously during the scan, completing one rotation every 2 seconds. Programmable anti-scatter slits and a fixed mask maintained an irradiated sample area of 10x15mm, with an additional 2° incident beam antiscatter slit producing a flat background in raw data from 3.60°. Scans covered the 2Theta range of 3.66-70.00° over a scan time of 13 minutes and 21 seconds, with 0.04 Rad Soller slits in both the incident and diffracted beam paths. The X'Celerator detector was set to scan in continuous mode with full length active and pulse-height discrimination levels set to 45-80%. Operation of the X-Ray Diffractometer and Software was set using a "HighScore Plus®" analysis software, with reference patterns from the International Centre for Diffraction Data, Powder Diffraction File-2 Release 2008.

Quantification of clay minerals was based on the intensity (area) of XRD peaks at ~14Å (~6.2°), 9.9Å (8.9°), ~7.15Å (~12.3°) and 7.07Å (12.5°). Rietveld refinement was not used for quantification due to the low degree of crystallinity of much of the clay grade material and because of problems of variable clay mineral composition (and thus lattice dimensions). The 6.2° peak represents chlorite(001) and possibly a vermiculite phase. The 8.9° peak represents illite and muscovite(001). The 12.3° peak represents kaolinite(001). The 12.5° peak represents either chlorite(002) or berthierine(001) (or a

combination of the two). It was decided to use both the ~6.2° and 12.5° peaks in this approach since it is conceivable that both berthierine and chlorite are present in these samples. If the intensity of the ~6.2° and 12.5° peaks were to vary uniformly with location and stratigraphy then berthierine could be concluded to be absent. If the ~6.2° and 12.5° do not vary sympathetically, this could be the result of either (1) the variable presence of berthierine or (2) chlorite becoming more or less Fe-rich. Variation of the ~6.2° and 12.5° peaks certainly reveals something about the relative abundance of Fe-rich clay minerals. Peak deconvolution of air-dried traces and calculation of peak areas was carried out using the X'pert HighScore Plus 2.2.3. This software is produced by PANalytical B.V. and is licenced to the University of Liverpool. The first task was to deconvolute the overlapping 12.3° and 12.5° peaks and then calculate the areas of these peaks. Next the areas of the 6.2° and 8.9° were calculated. Assuming that the chlorite was Fe-rich led to a correction being applied to the chlorite(001) peak intensity (multiplied by a factor of three given the relative intensity of chlorite(001) to the maximum intensity trace of this mineral; (Hillier, 2003). The next step was to sum the intensities of the ~6.2° (corrected), 8.9°, ~12.3° and 12.5° peaks and then determine a relative proportion for each. This approach assumes that each "mineral" has a equal ability to diffract X-rays (uniform RIR factor). The relative area (approximately equivalent to relative proportions) of the four peaks can then be plotted as a function of depth and compared between cores.

Fourier Transform Infrared Spectroscopy (FTIR)

In order to make an FT-IR pellet, 8.0mg of clay separate was ground and mixed with 792mg of KBr in an agate pestle and mortar, then 150mg of this mixture plus 150mg of KBr again were ground and mixed carefully to obtain a 300mg homogenous pellet containing 1.5 mg of sediment (i.e. a 0.5% sample). These amounts were weighed precisely in order to enable quantification. This final mixture was then sintered at 10 tonnes in a Specac press in order to produce an FTIR applicable pellet. The pellets were dried at 140°C for 14 hours in order to remove any absorbed water. These samples were analysed using a Thermoelectron Nicolet 380 infrared spectrometer and OMNIC software in the range of 230cm^{-1} – 4000cm^{-1}, collecting 64 scans per sample and with a resolution of 4cm^{-1} subsequent to mineral identification in the samples. The FTIR spectra were run through a band decomposition process in OMNIC and peak areas were calculated.

4.4 Results

4.4.1 Core no. 1

Description: Core 1 was obtained from the upper part of the Irt estuary (Fig. 4.2a) on a mud flat using a Russian corer. The core can be split up to six sub units (beds). Below the sediment surface, Unit A (0-3 cm) is light-coloured, silty to fine sand, with interlaminated thin (mm-scale) orange-coloured fine sand. An abrupt change in colour leads to a dark silty sand denotes Unit B (3-5 cm). Unit C is a very dark silt unit (5-20 cm) and is rich in terrestrial organic material (plant materials such as roots and peaty layers). In contrast, there is an absence of the plant materials in unit D (20-35 cm), which changes from the dark colour to light colour downwards over 15cm. Unit E (35-50 cm), is a dark silt layer with terrestrial organic material, and is visually similar to Unit C. Unit F, the thickest unit in this core (50-100 cm), is a clay-rich, dark layer containing abundant organic material.

Overall, this core is interpreted to represent a series of low energy depositional environments, with fine sediment deposited far from the active channel, such as tidal flats where some vegetation could get established.

4.4.2 Core no.2

Description: Core 2 was collected near the confluence of the Irt and Mite rivers in the intertidal zone of the Ravenglass estuary (Fig. 4.2b) using a window sampler. Unit A (0-5 cm) is a clean and light-coloured, moderately to poorly sorted, medium sand. Below an abrupt boundary to dark sediment at 5 cm, Unit B (5-25 cm) is downward-coarsening poorly-sorted, medium-grained sand with silt and clay. This unit is dark coloured and includes several mm-thick dark mud laminae, sub-vertical lugworm burrow-fills, and thin shell fragments. The sediment coarsens downward over 20cm. Unit C (25-35 cm) contains poorly-sorted, medium to coarse sand, which is lighter coloured than Unit B. There are neither mud laminae nor shell fragments. Unit D (35-45 cm) is a light coloured moderately sorted coarse sand with shell fragments. A few gravels mark the abrupt contact with Unit E, a silty clay. Unit E (45-95 cm) is a light-coloured silt- and clay-dominated unit. At the depth 55-65 cm and also 75-90cm multiple mm-scale dark mud laminae are present that contain organic material.

The basal fine grained silty clay sediments are overlain by medium sands. In the lower part of the core the mud laminae indicate low energy conditions, and the shell fragments in the

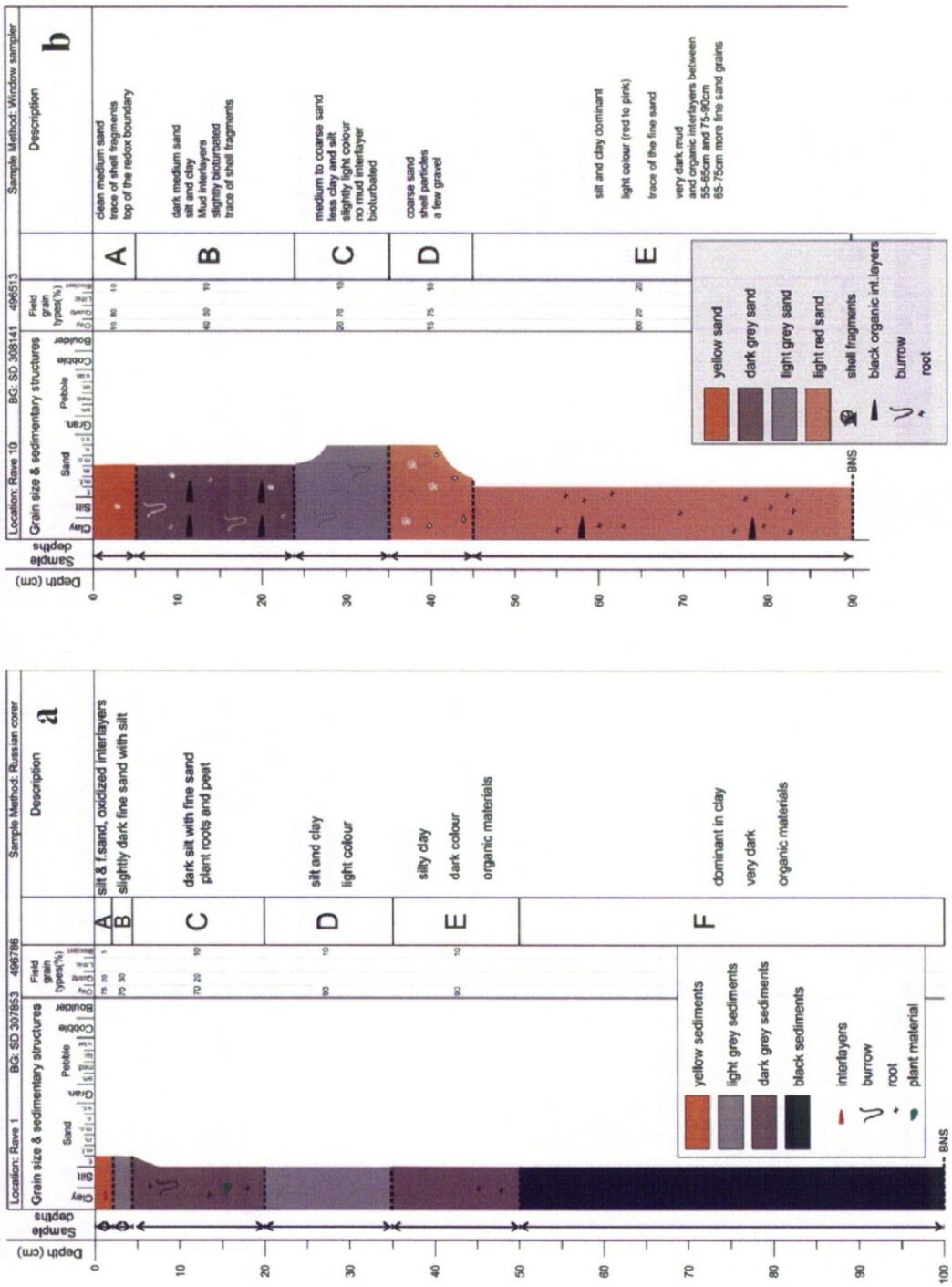

Figure 4.2-a: Detailed stratigraphy of the core from the Ravenglass estuary. (a) **Core no. 1** at the upper part of the Irt estuary in mudflat, (b) **Core no.2** at the immediate marine environment close to the Ravenglass estuary mouth on Irt estuary.

upper core indicate higher energy environments. The overall coarsening upwards in this core could be interpreted as a shallowing in the environment of deposition (regressive). However, the intra-estuary position of the core suggests that the lower fine-grained deposits may be muddy-tidal flat deposits. The coarser sediment is not well sorted, as might be expected in a shoreface setting, and is likely to mark the interplay of river-derived and marine-derived deposits.

4.4.3 Core no.3

Description: Core 3 was obtained near the mouth of the Esk river on an in-channel sand bar close to the pebbly storm beach deposit (Fig. 4.2c) using a window sampler. This core is only ~50cm long (limited by a layer of pebbles of diameter greater than the window sampler aperture) and contains 4 units. Unit A (0-15 cm) is the top 15cm of the core comprising light coloured, moderately- to poorly-sorted medium-grained sand with lugworm burrow-fills. Unit B (15-25 cm) includes dark coloured, poorly–sorted, muddy, medium-grained sand. Organic materials such as plants and root particles can be seen at the top of the unit and a gravel layer sits at 20 cm in this unit. Unit C (25-40 cm) is a 15 cm unit which contains light-coloured mud at the top and moderately sorted sand with gravels at the base. The sediments encountered in the unit D (40-55 cm) are generally moderately-sorted, coarse sands and gravels with abundant shell fragments.

The coarse grain-sizes in this core suggests a relatively high energy environment in part of a channel that is subject to tidal and fluvial processes. The lack of organic material and the low proportion of very fine sand suggests an absence of overbank deposits.

4.4.4 Core no.4

Description: Core 4 was obtained using a window sampler in the Esk estuary on a sand bar near the channel bank (Fig. 4.2d). Unit A (0-5 cm) is a poorly-sorted and bioturbated medium- to fine-grained sand with clay and silt. Unit B (5-20 cm) is a bioturbated, dark, poorly-sorted, medium-grained sand layer with shell fragments and some plant material. Unit C (20-25 cm) is slightly lighter coloured, poorly-sorted, medium-grained sand with a low degree of bioturbation. Unit D (25-35 cm) is dark, moderately-sorted, medium- to fine-grained sand that contains plant materials and in place rootlets. The sediment becomes finer downwards over the 25cm of unit E (35-60 cm). This unit contains dark grey silt and clay-dominant sediments with organic material and roots. Unit F (60-90 cm) coarsens

downwards over 40cm to the base of the core. Unit F is a light-coloured, moderately- to well-sorted, medium-grained sand containing shell fragments.

The basal, well-sorted bioclastic sand suggests a strong marine influence at the environment of deposition, possibly representing a distal to a storm beach deposit. The overlying silt and clay dominated units with plant material suggest a low energy setting, either a muddy tidal flat and/or an overbank setting. The upper bioturbated sand-prone units are interpreted as part of an in-channel tidar bar deposit.

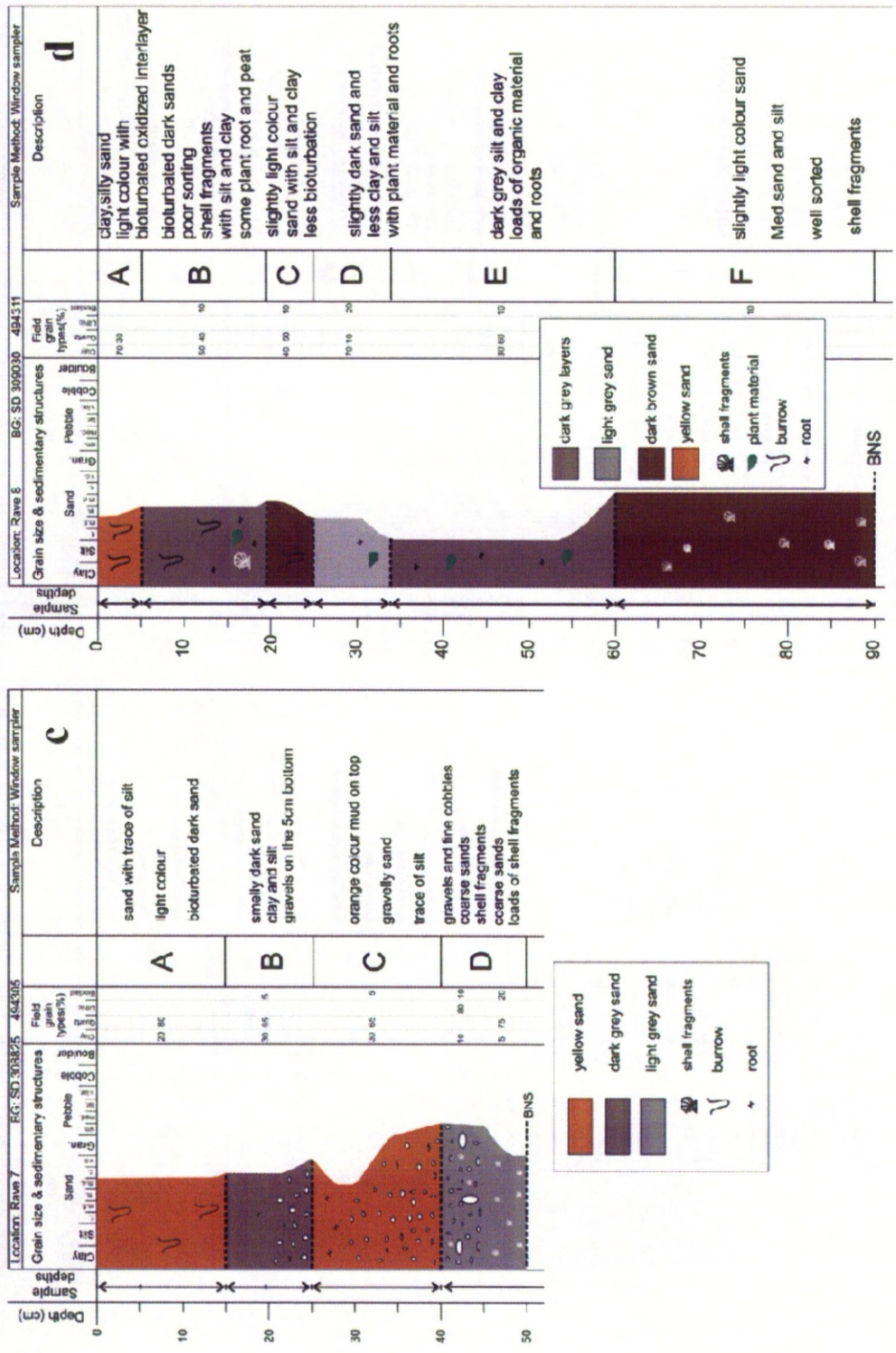

Figure 4.2-b: Detailed stratigraphy of the core from the Ravenglass estuary, (c) **Core no.3** in sand bar close to storm beach on Esk estuary and (d) **Core no.4** in sand bar close to the channel on the Esk estuary.

4.4.5 Mineralogy of core samples: BSE/EDAX Results

Esk core samples

Electron microscope images of the Esk estuary samples (core 3 and 4) reveal moderately-sorted sediment with sand grains that are variably coated with clay minerals. Grains in the lower parts of the core have no clay coating (Figs. 4.3 a and 4.3 b). The BSE and EDAX investigations revealed that the clay minerals present seem to be: kaolinite, illite, chlorite, combinations of these, and gibbsite-like components. The sediment contains a combination of clastic grains and marine, mostly siliceous, bioclasts, such as radiolarians and diatoms, in association with some iron-oxide minerals. The clay minerals present are very fine-grained, tending to be less than a few micrometres in size. They do not occur as masses of monominerallic material, rather they seem to be intergrown with other clay minerals given their variable electron backscatter responses (Figs. 4.3 c and 4.3 d). They are too fine-grained to give high quality, single mineral EDAX spectra and thus represent mixtures of minerals and so must be interpreted with care. Most EDAX spectra of coating minerals on sand grains contain Fe, although some of them have dominant Al peaks suggesting an Al-rich mineral is present (after depth 60cm). Some EDAX spectra of coating minerals resemble spectra of coating clay minerals resemble chlorite having abundant silica (Si), somewhat less Al, a large Fe-peak and rather less Mg (Fig.4.3 b). However, most spectra seem to contain some K suggesting either (1) the presence of intergrown illite and chlorite-like material or (2) the occurrence of some sort of smectite phase. Kaolinite has been identified in places (Fig. 4.3 d) (equal Al and Si peaks and no K or any other cations). Illite has also been identified with abundant Si, somewhat less Al and a sizeable K peak (Fig. 4.4-1 k). Some EDAX spectra show abundant Al in association with oxygen sometimes with minor Si but sometimes without Si (Fig. 4.4-1 g). This could plausibly be Al oxide or an Al hydroxide (gibbsite) type of material. These gibbsite components are abundant at greater than 60 cm depth. EDAX spectra reveal that most grains at the base of the core are coated with the chlorite-illite intergrown components in comparison to grains from the shallower section, which are coated predominantly with illite-chlorite.

Irt core samples

Backscattered electron images on the Irt estuary samples reveal poorly-sorted sediments with sand grains that are variably coated with clay minerals. This coating coverage broadly decreases up-section. The sediments contain a combination of clastic grains and marine microfauna, such as diatoms. The BSE and EDAX investigations revealed that the clay minerals present seem to be: kaolinite, illite, chlorite, combinations of these and a rare gibbsite-like phase. Pyrite is an important authigenic mineral which decreases in abundance upward in the core. The clay minerals present are fine grained and in some part, they occur as masses of monominerallic material. Clay minerals are largely too fine-grained to give high quality, single mineral EDAX spectra. Most EDAX spectra of coating minerals on sand grains contain Fe and K. Some coating minerals resemble EDAX spectra of illite having abundant Si, somewhat less Al and much less Mg as well as Fe and K. Chlorite has also been identified with abundant Si, somewhat less Al and a sizeable Fe peak and less Mg (Fig. 4.4-1 c). However, most spectra seem to contain K suggesting either the presence of intergrown illite and chlorite-like material or some sort of smectite phase. Some EDAX spectra show abundant Al in association with oxygen, and sometimes with Si. These gibbsite-like components occur at > 50 cm depth, although they are not abundant in comparison to the Esk estuary sediments. EDAX spectra also reveal that most grains at the base of the core are coated with the illite with some illite-chlorite, in contrast to grains in the shallow part which are coated more with illite-dominated illite-chlorite.

Some BSE and EDAX clearly revealed the presence of abundant pyrite in the Irt samples and iron oxides in Esk samples (Fig. 4.4-2). Theses investigation is also shown the early chemical weathering process such as dissolution and iron up-taking.

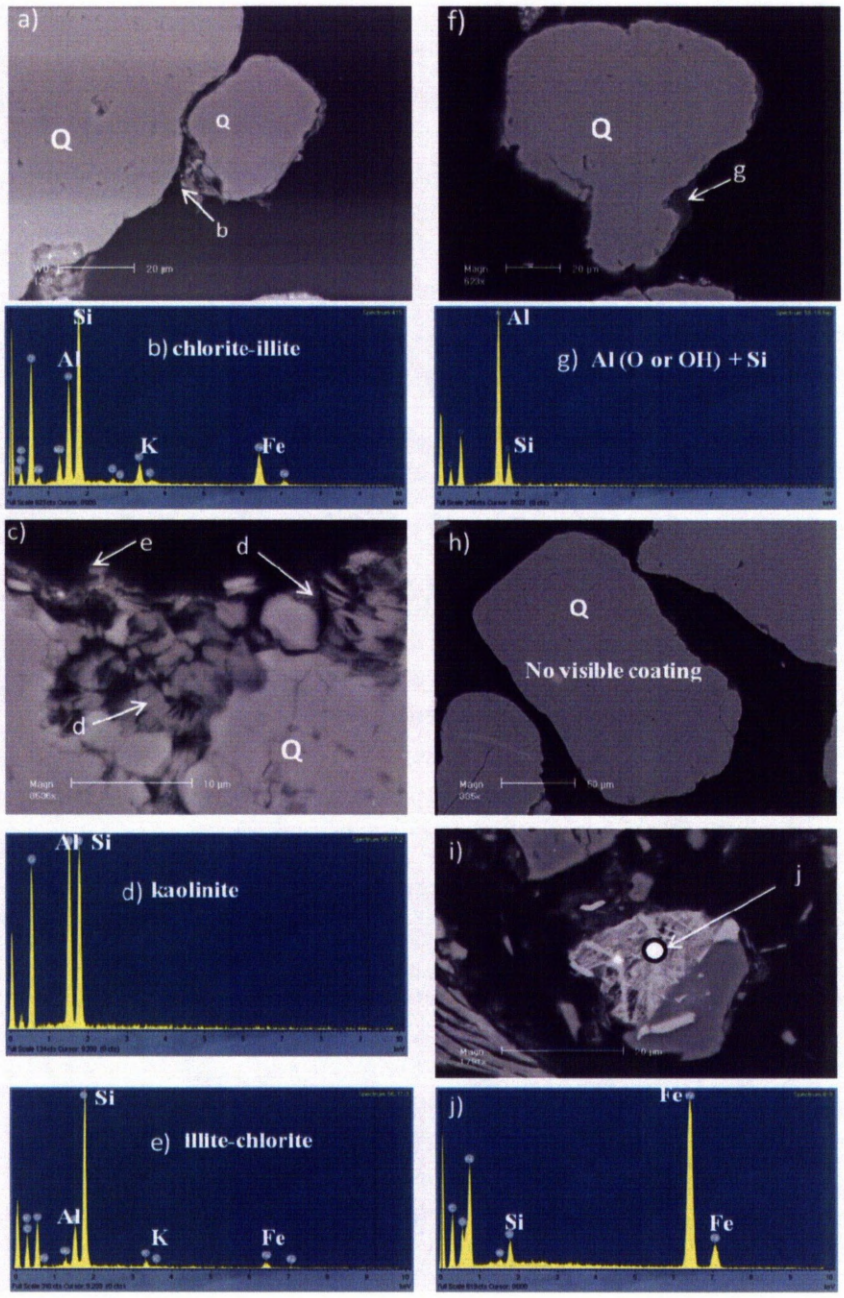

Figure 4.3: Backscattered electron image of polished section grain mount, Esk estuary; quartz (Q) sand grain in the middle is coated with clay grade material. a) BSE image of sample at depth 30-40cm. EDAX spectrum analysis of the flaky shape (b) with clays that contain Si, Al, Mg, K and Fe are dominant. c) 50-58cm depth BSE image of the sand grains with two different age coating with two different compositions. EDAX spectrum analysis of the area (d) indicating kaolinite and EDAX spectrum at (e), which shows Si, Al, Mg, K and Fe. f) BSE image of a sample at 61-70 cm, quartz grain in the middle with coated material. EDAX spectrum for the point (g) indicates an Al dominant peak, which can be a gibbsite-like compound, h) BSE image of a grain at depth 70-80cm shows no visible coating around the sand grain. i) BSE image of a coated sand grain with iron oxide at the depth 50-58cm. j) EDAX spectrum shows abundant Fe and oxygen with minor Si.

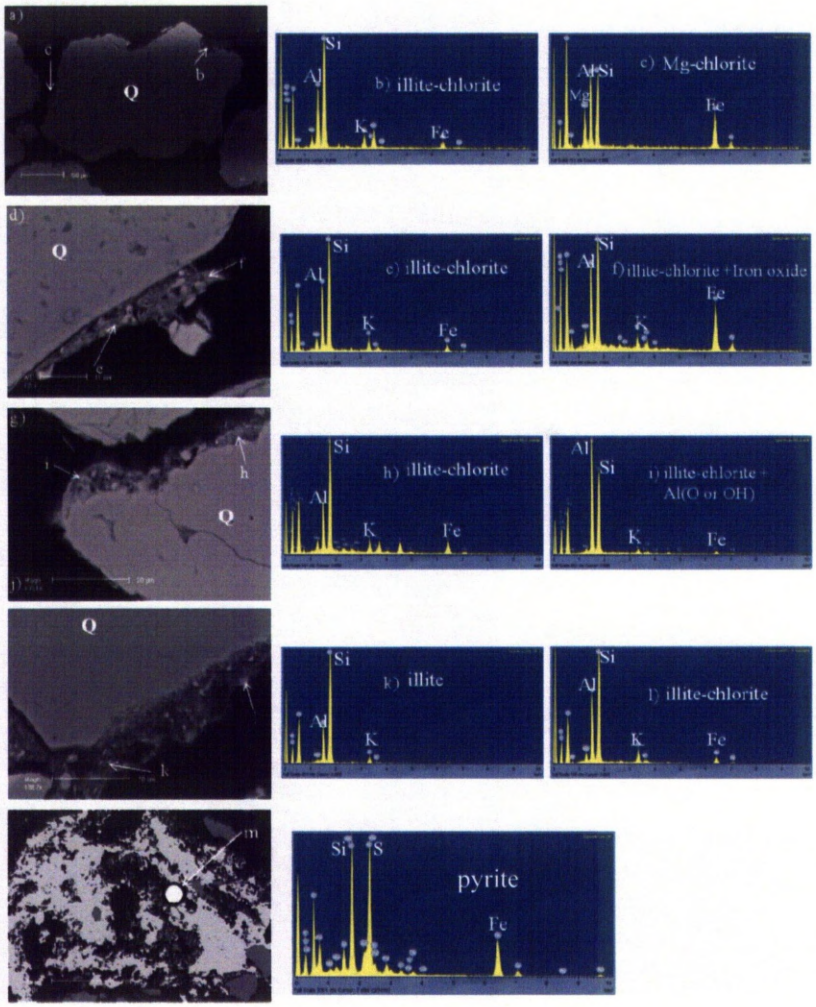

Figure 4.4-1: Backscattered electron image of polished section grain mount, Irt estuary, Saltcoats close to the mouth of the estuary; quartz (Q) sand grain in the middle is coated with clay grade material and the respected spectra. a) BSE image of sample at depth 10-20cm. EDAX spectrum analysis of the area (b) shows clay mineral coating which Si, Al, Mg, K and Fe are dominant peaks. And spectra for area (c) shows Al, Si, Mg and Fe are abundant which indicates chlorite, d)30-40cm depth BSE image of the sand grains with spectra analysis show illitic coating (e) with a chlorite detrital grain. (g) BSE image of a sand grain at depth 40-50cm which EDAX spectrum analyses show as illite-chlorite (h) and an illite-chlorite with abundant Al (i) and Si, j) BSE image of a sand grain at depth 70-80cm. EDAX spectrum analysis of the area (k) indicating Al, Si and K abundant peaks which can indicates illite and EDAX spectrum at (l) which shows Si, Al, Mg, K and Fe can indicate illite-chlorite. A combination of the BSE images and EDAX spectra reveal coating coverage descriptively decreases upward. m) dominant pyrite in the sample at depth 70-80cm.

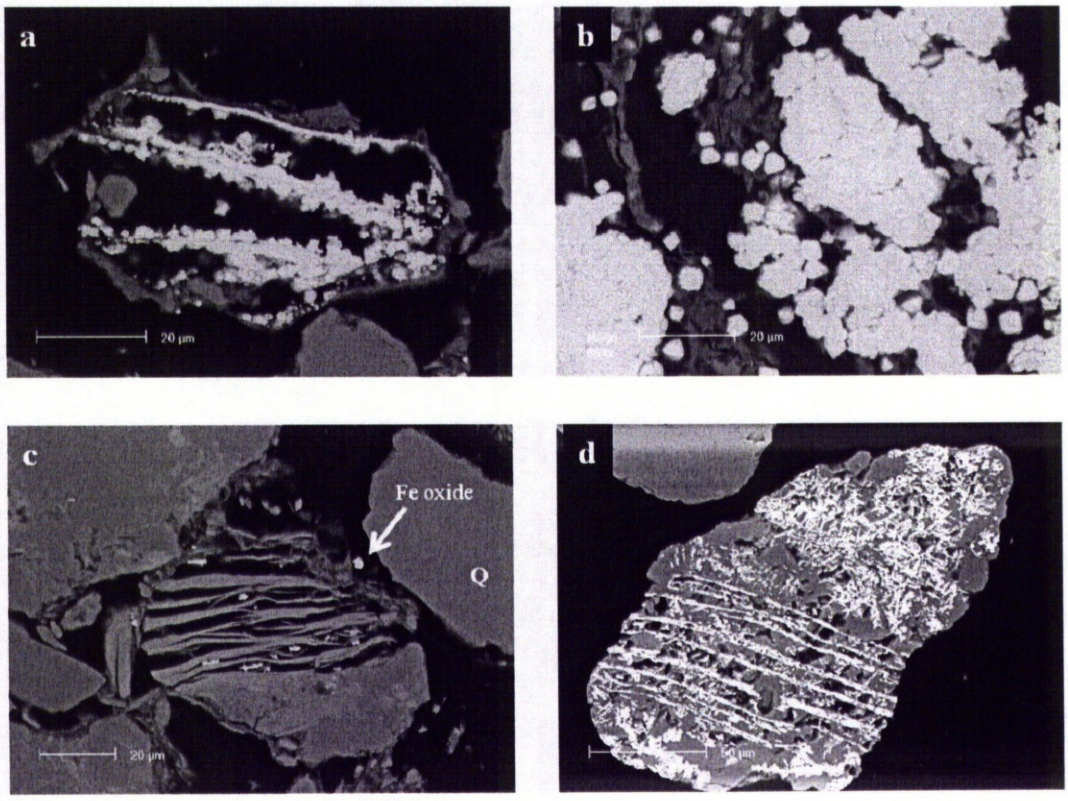

Figure 4.4-2: Backscattered electron image of polished section grain mount showing chemical weathering process within the Ravenglass estuarine sedimentary system; a) residual coated grain with iron oxides. b) Pyrite crystals around the grains which shows well supplied sulphate in a reduction media in Irt estuarine system, c) a K-feldspar grain is torn to strings and Fe-oxide particles between the strings and d) a quartz grain is coverd with the secondary deposition of Fe-oxide in the Esk estuary sediments.

4.4.6 Coverage of the grain coating

The degree of grain coating has been recognised to be an important parameter that controls reservoir quality (Walderhaug 1996). However, the degree of grain coating in modern sedimentary systems has received even less attention than in deeply buried sedimentary rocks.

Esk core samples

In Esk estuary core sediments, the percentage of grain coating coverage increases stratigraphically from the base to 50cm depth, and then decreases to 10cm depth. This trend of decreasing and increasing seems to be the reverse trend of the grain size distribution. Therefore, fine grained sediments in the middle of the core have relatively a greater degree of grain coating compared to the overlying and underlying sandy layers. The shallowest part of the core, which is well-bioturbated, has the highest coverage grain coating percentage (Fig 4.5a).

Irt core samples

Estimation of the grain coating coverage for the Irt estuary core sediments shows the extent of grain coating coverage decreases upward. This trend is in contrast to the sediment grain size which increases upward (Fig. 4.5b). These analyses suggest that surface area of the host grains is an important control on the percentage of grain coating coverage. Increased grain size shows decrease the grain coating coverage in both estuaries (Fig. 4.5).

4.4.7 X-ray diffraction results

The X-ray diffraction analyses of sediment are presented in Figures 4.6 (Esk estuary), 4.7 (Irt estuary) and 4.8 (Saltcoats - close to the mouth of the Irt estuary). These collections of XRD spectra were each analysed using a variety of sample preparation techniques: air-drying, glycolation and heating to 400°C and then heating to 550°C. These data are also represented stacked as a function of depth in each core in Figures 4.9 (Esk estuary), 4.10 (Irt estuary) and 4.11 (Saltcoats - close to the mouth of the Irt estuary). The quantified areas of the 6.2°, 8.9°, 12.3° and 12.5° peaks (in order: 14Å, 9.9Å, 7.15Å, 7Å) are illustrated as a function of depth in Figure 4.12.

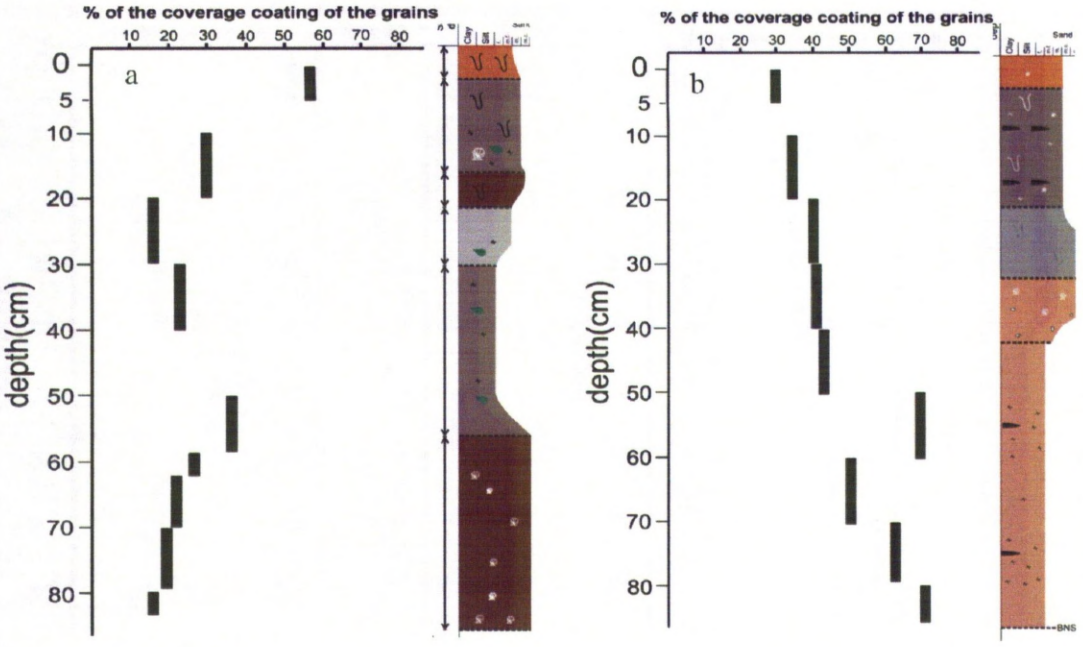

Figure 4.5: Stratigraphic variation in clay mineral grain coating coverage in the selected core samples in the Ravenglass estuary sedimentary system. a) Esk estuary and b) Irt estuary, Saltcoat close to the mouth of the estuary.

Gould et al. (2010) reported that kaolinite can be difficult to distinguish from chlorite due to the overlap of the kaolinite (001) and chlorite (002) peaks but the analytical approach adopted here was sufficient to clearly differentiate the two minerals. The air-dried scans reveal peaks at 6.2°, 8.9° and a pair of peaks at 12.3° and 12.5°. The peak at 6.2° is chlorite (001) while the peak at 8.9° is illite. The peak at 12.3° is the clearly discerned kaolinite (001) peak while the bigger peak at 12.5 is either solely due to the chlorite (002) peak or is a combination of chlorite (002) and berthierine (001) (Brindley, 1982).

Esk estuary

The relative height of the chlorite (001) and (002) peaks (1:4) suggests that the chlorite in the sediment core is Fe-rich (Hillier, 2003). Scans of the glycolated sample showed no discernable changes in peaks intensity suggesting that smectite is negligible in this sediment. Chlorite (002) peaks are reportedly unaffected when heated to 400°C (Starkey et al., 1984). In contrast, berthierine (001) and kaolinite (001) peaks typically show a decrease in intensity on heating to 400°C. A scan of the sample when heated up to 400°C

revealed a distinct decrease in intensity for the peaks at 12.3° and 12.5° (equivalent to 7.15Å and 7.07Å respectively). This confirms the presence of kaolinite but further suggests that the peak at 12.5° is not solely due to the chlorite (002) peak. The implication is that berthierine is present in this and other samples in this core. For the 400°C scan, the intensities of the peaks at 6.2° and 8.9° remain unchanged further confirming that illite and chlorite are present. A scan of the sample heated up to 550°C shows a significant collapse for both the 12.3° and 12.5° peaks while the intensity of the peak at 6.2° increased slightly sharpened entirely typical of chlorite. Figure 4.6 shows the combined intensity of the chlorite(002), berthierine(001) at 12.5°, and chlorite(004), berthierine(002) at 25.3° peaks decrease in intensity up-section. This suggests that the overall quantity of Fe-rich clay minerals decreases up-section.

Irt Estuary

The air-dried scans reveal peaks at 6.2°, 8.9° and a pair of peaks at 12.3° and 12.5°. The peak at 6.2° is from chlorite(001) while the peak at 8.9° is illite(001). The peak at 12.3° is the kaolinite(001) peak while the bigger peak at 12.5 is either solely due to the chlorite(002) peak or is a combination of chlorite(002) and berthierine(001) (Brindley, 1982). The relative heights of the (001) and (002) peaks (about 1:2) suggests that the chlorite has a mixed Mg-Fe composition (Hillier, 2003). Glycolation had negligible effect on these samples suggesting that there was relatively little of any expandable phase such as smectite, in these sediments. Scans of these samples heated up to 400°C revealed a distinct decrease in the intensity for the peaks at 12.3° and 12.5. This confirms the presence of kaolinite but shows that the peak at 12.5° is not solely due to the chlorite (002) peak but also represents the presence of a berthierine component. A change in the diffraction pattern occured at 550°C , with a gradual collapse and slight shift of a portion of the 14Å peak to ~10Å at 550 C suggesting that there was a vermiculite component (1:3) in these samples.

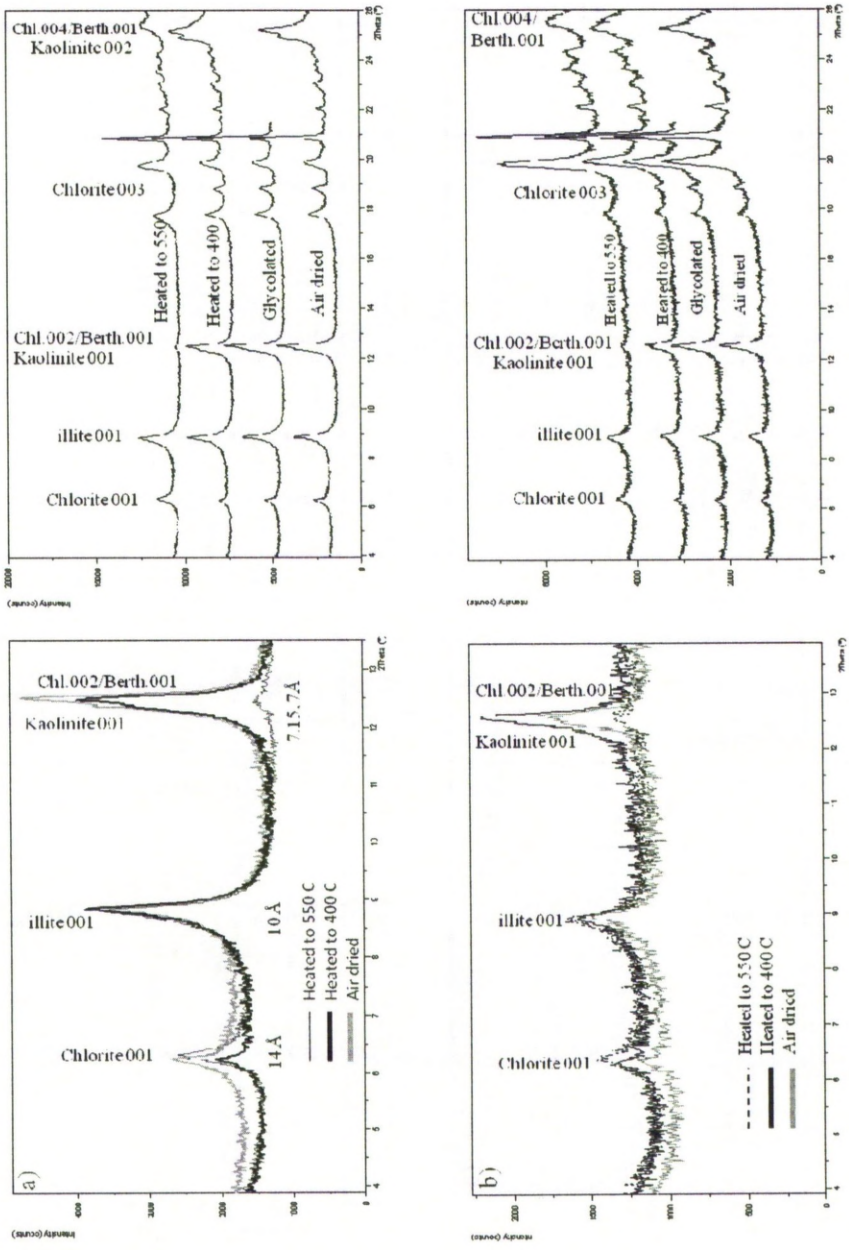

Figure 4.6: XRD patterns of the <2μm fraction of the cored sediment samples in Esk estuary taken at a depth of 5-10cm (a) and 40-50cm (b). Collection of patterns arranged from the base: air dried, glycolated, heated to 400°C and heated to 550°C at the top of the stack (right).Overlapping of the XRD data (left) from the low angle end of the pattern to illustrate the drop in intensity of the 7.15 and 7Å peaks during heating to 400°C and their near total collapse at 550°C. Glycolation seems to have little effect on the sample. Note also the broadening of the chlorite (001) peak. The sediment seems to be composed of illite, chlorite, kaolinite and berthierine with negligible smectite present.

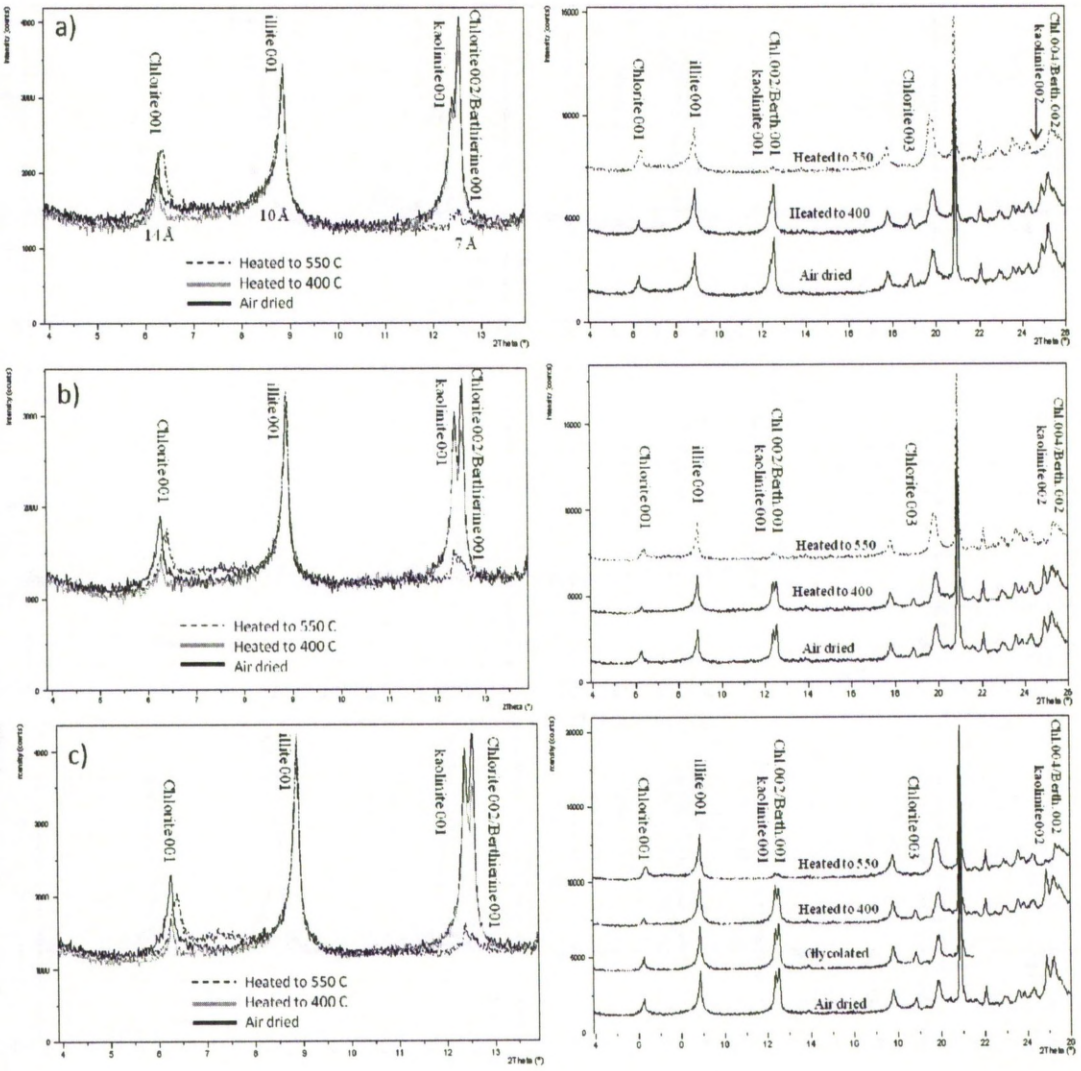

Figure 4.7: XRD patterns of the <2μm fraction of the cored sediment sample at Irt estuary, taken at a depth of 10-20cm (a), 50-60cm (b), and 80-90cm (c). Collection of patterns (right) arranged from the base: air dried, glycolated, heated to 400°C and heated to 550°C at the top of the stack. Overlapping (left) of the XRD data from the low angle end of the pattern to illustrate the drop in intensity of the 14, 7.15 and 7Å peaks during heating to 400°C and peaks at 7.15 and 7Å show near total collapse at 550°C and a significant shift from 14Å to 12Å while 10Å peak is unchanged at 550°C. Glycolation seems to have little effect on the sample. There was a slight collapse of the 14Å trace on heating to 550°C with a broad hump developing at about 12Å. This is characteristic of vermiculite suggesting that the 14Å peak represents a combination of chlorite and vermiculite. The sediments thus seem to be composed of illite, chlorite, dioctahedral chlorite and vermiculite, kaolinite and berthierine with negligible smectite present.

This behaviour follows the prescribed behaviour of dioctahedral vermiculite (Starkey et al., 1984), although unique identification is made difficult by the presence of dioctahedral and trioctahedral chlorite. Heating to 400°C had relatively little effect on the peak at 12.5° suggesting that there is relatively little berthierine in this sample. Heating to 550°C led to substantial collapse of the peak at 12.5° and, as mentioned, a commensurate increase in intensity of the peak at 6.2° suggesting that chlorite is the dominant clay mineral in this sediment. The sequence XRD pattern of the different depth samples reveal that the intensity of the peaks at 8.9° and 12.3° significantly decreases upward relatively to the intensity of the peaks at 12.5° and 25.2° which increasing upward. On the other hand, the relative heights of the (001) and (002) peaks (about 1:2) suggests that chlorite along the depth slightly showing to have more Mg in its structure.

Saltcoats- close to the mouth of the Irt estuary

The X-ray diffraction analysis of the <2μm fraction from the cored sediment on this area yielded a moderately complicated trace for the air-dried sample (Fig. 4.8) with peaks at 6.2°, 8.9° and a pair of peaks at 12.3° and 12.5°. The peak at 6.2° represents chlorite(001). The peak at 8.9° is illite. The peak at 12.3° is the kaolinite(001) peak while the peak at 12.5 is either solely due to the chlorite(002) peak or is a combination of chlorite(002) and berthierine(001) (Brindley, 1982). The relative heights of the (001) and (002) peaks (1:3) suggests the chlorite in the sediment core is more likely Fe-rich than Fe-Mg rich chlorite (Hillier, 2003). Scans of the glycolated sample showed no discernable changes in peaks intensity suggesting that smectite is negligible in these samples. Chlorite(002) peaks are reportedly unaffected when heated to 400°C (Starkey et al., 1984). In contrast, berthierine(001) and kaolinite(001) peaks in general show a decrease in intensity on heating to 400°C. A scan of the sample when heated up to 400°C revealed a distinct decrease in intensity for the peaks at 12.3° and 12.5°. This confirms the presence of kaolinite and is evidence for the presence of berthierine. The sequence of XRD pattern from samples from different depths reveals that the intensity of the peaks at 8.9° and 12.3° significantly decreases up-section relative to the intensity of the peaks at 12.5° and 25.2° which increase up-section.

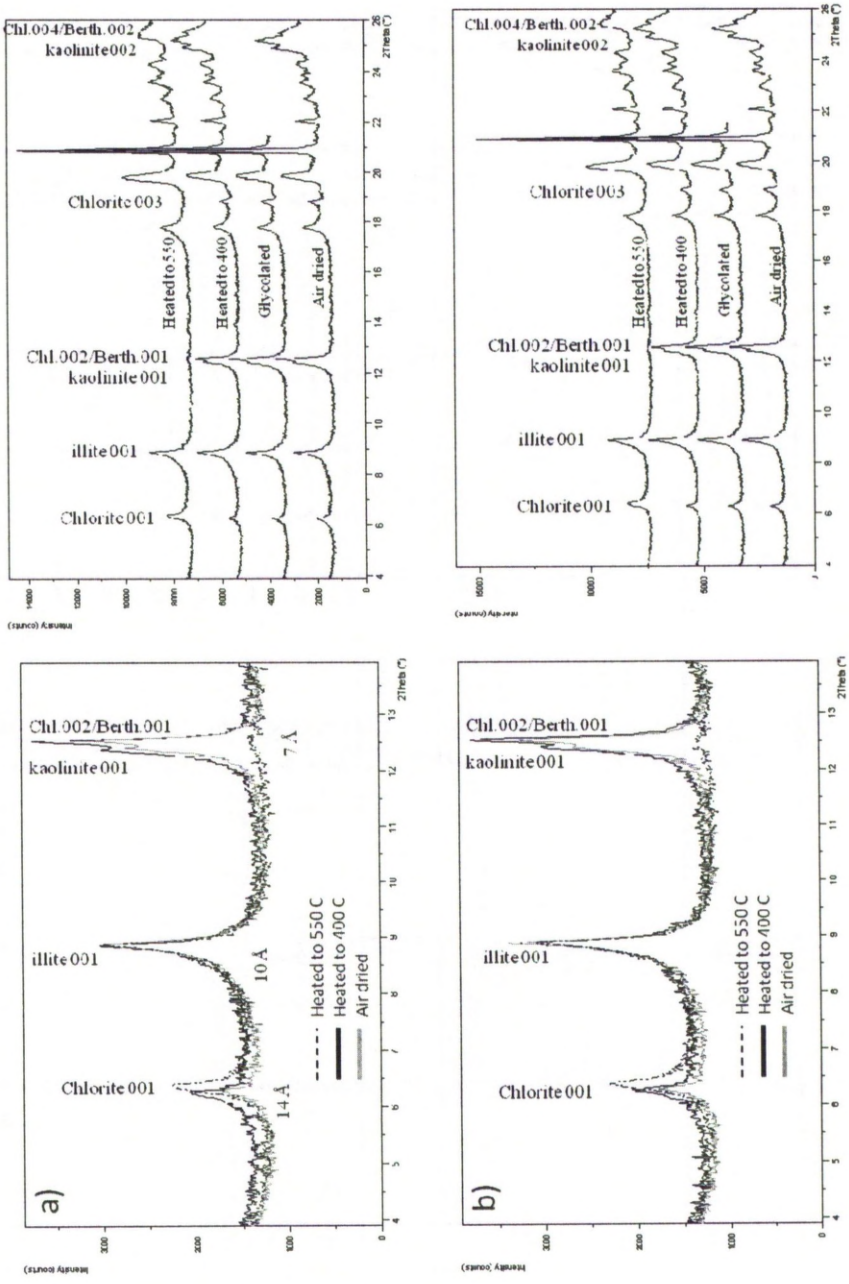

Figure 4.8: Representative XRD patterns of the <2μm fraction of the cored sediment samples in Irt estuary, Saltcoats close to the mouth of the estuary, taken at a depth of 50-60cm (a) and 70-80cm (b). Collection of patterns (right) arranged from the base: air dried, glycolated, heated to 400°C and heated to 550°C at the top of the stack. Overlapping (left) of the XRD data from the low angle end of the pattern to illustrate the drop in intensity of the 14, 7.15 and 7Å peaks during heating to 400°C and peaks 7.15 and 7Å show near total collapse at 550°C. Glycolation seems to have little effect on the sample. Note also the broadening of the chlorite (001) peak. The sediment seems to be composed of illite, chlorite and dioctahedral chlorite, kaolinite and berthierine with negligible smectite present.

Conversely, the ratio of the heights of the chlorite(001) and chlorite(002) (±berthierine(001)) peaks (approximately 1:2) suggests that chlorite along the core slightly showing more Fe-Mg rich. The sequence of XRD patterns by depth (Fig. 4.8) reveals that the intensity of the peak at 8.9° decreases up-section relative to the intensity of the peaks at 12.5° and 25.2° which increase up-section.

Scans of all samples show a peak at 56.23°, representing pyrite. The intensity of the 56.23° peak varies with the location and depth of the samples. In summary, intensity of the pyrite peak at the Saltcoats site, close to the mouth of the Irt estuary decreases up-section. No such pattern was found for the Esk cores which seemed to have negligible pyrite as determined by XRD.

Esk estuary-Church

Depth (cm)	~14Å	9.9Å	7.15Å	7Å
0-5	0.300	0.252	0.107	[illegible]
5-10	0.296	0.300	0.197	[illegible]
20-30	0.265	0.193	0.000	[illegible]
40-50	0.335	0.293	0.195	[illegible]
50-58	0.454	0.147	0.17[illegible]	[illegible]
58-61	0.283	0.255	0.000	[illegible]
61-70	0.240	0.169	0.00[illegible]	[illegible]
70-80	0.276	0.157	0.00[illegible]	[illegible]

Esk estuary-Bridge

Depth (cm)	~14Å	9.9Å	~7.15Å	~7Å
0-5	[illegible]	[illegible]	[illegible]	[illegible]
10-15	[illegible]	[illegible]	[illegible]	[illegible]
20-25	[illegible]	[illegible]	[illegible]	[illegible]
45-50	[illegible]	[illegible]	[illegible]	[illegible]

Irt estuary-Saltcoats

Depth (cm)	~14Å	9.9Å	9.9Å	7Å
10-20	0.341	0.227	0.190	[illegible]
20-30	0.252	0.245	0.327	[illegible]
30-40	0.290	0.271	0.150	[illegible]
40-50	0.282	0.272	0.326	[illegible]
50-60	0.231	0.381	0.228	[illegible]
60-70	0.210	0.409	0.222	[illegible]
70-80	0.136	0.459	0.282	[illegible]

Irt estuary

Depth (cm)	~14Å	9.9Å	7.15Å	7Å
10-20	[illegible]	[illegible]	[illegible]	[illegible]
20-30	[illegible]	[illegible]	[illegible]	[illegible]
30-40	[illegible]	[illegible]	[illegible]	[illegible]
40-50	[illegible]	[illegible]	[illegible]	[illegible]
50-60	[illegible]	[illegible]	[illegible]	[illegible]
60-70	[illegible]	[illegible]	[illegible]	[illegible]
70-80	[illegible]	[illegible]	[illegible]	[illegible]
80-90	[illegible]	[illegible]	[illegible]	[illegible]

Table 4.1: Normalised relative peak area deconvolution of the maximum intensity peak of clay minerals (~14Å, 9.9Å 7.15Å and 7Å) based on the XRD patterns for the Irt and Esk estuary. The protocol for determining these fractional values was described in the XRD part of the methods section

4.4.7 Infrared results

Analysis of the all samples along the Ravenglass estuary reveals similar traces for the clay mineral fraction in the Ravenglass estuary. Peak at 3697 (cm^{-1}) represent kaolinite, 3625 (cm^{-1}) predominantly represents illite or illite-smectite (plus a kaolinite component if there is a band at 3697) and a broad peak at 3520 to 3580 (cm^{-1}) corresponding to Fe-rich clays such as chlorite or berthierine (Madejová 2003). FTIR scans of the Saltcoats, close to the mouth of the Irt estuary, reveal the strong peak at 3697 (cm^{-1}) which is from kaolinite and 3625 (cm^{-1}) which is predominantly from illite and a small hump around the 3550 (cm^{-1})

from Fe-clay such as chlorite. FTIR scans for the Esk estuary sediment samples (Fig. 4.13) also show strong peaks for Fe-rich chlorite and berthierine as well as for kaolinite and illite. The variation of the clay minerals as a function of depth shows a similar pattern as the XRD scans which kaolinite increases upward while the Fe-rich chlorite decreases upward respectively. FTIR scans for the Irt estuary shows a clear trend for decreasing upward for kaolinite and illite. The Fe-rich chlorite is also has an increasing trend upward. FTIR scans for the Saltcoats-close to the mouth of the Irt estuary shows the strong peak for kaolinite at surface sample (0-3cm), and Fe-rich chlorite increases up-section.

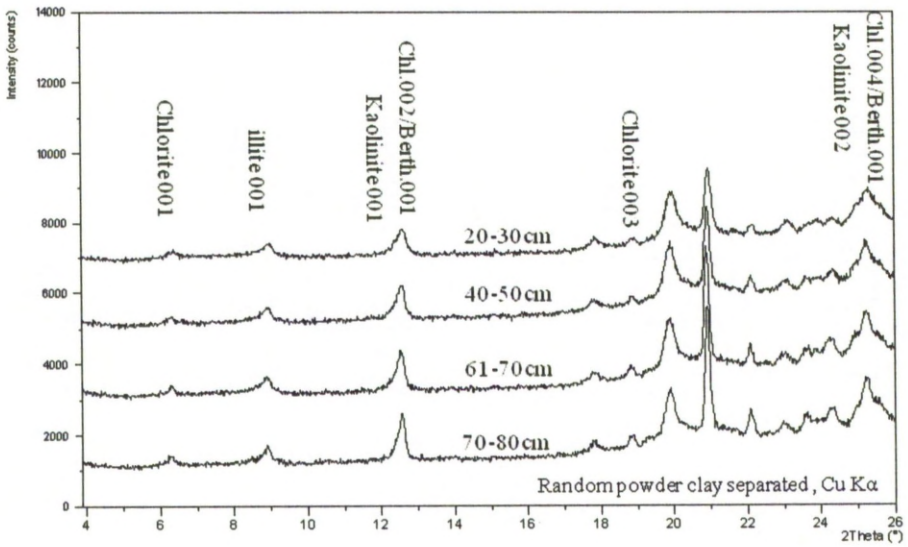

Figure 4.9: XRD patterns of the <2μm fraction of the Esk estuary cored sediment samples taken at a depth of 20-30, 40-50, 61-70, and 70-80cm. The stacked pattern show kaolinite increases upward while the chlorite intensity decreases upward.

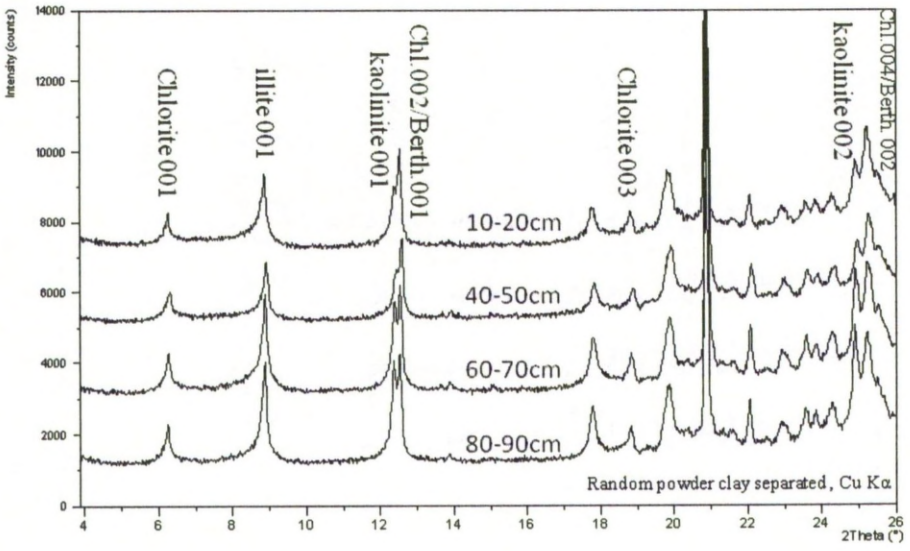

Figure 4.10: XRD patterns of the <2μm fraction of the Irt estuary cored sediment samples taken at a depth of 10-20, 40-50, 60-70, and 80-90cm. The stacked pattern show kaolinite and illite decreases upward while the chlorite intensity increases upward.

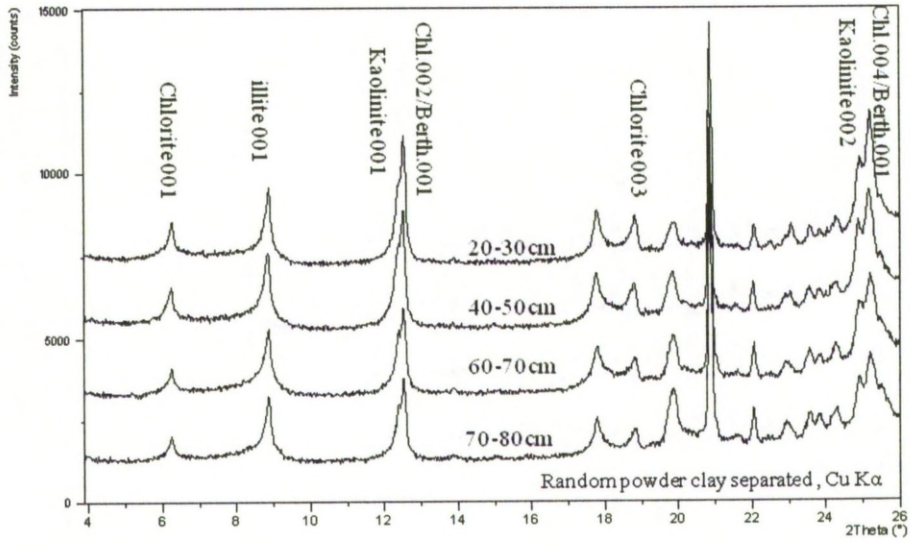

Figure 4.11: XRD patterns of the <2μm fraction of the Saltcoats close to the mouth of the Irt estuary, cored sediment samples taken at a depth of 20-30, 40-50, 60-70, and 70-80cm. The stacked pattern show kaolinite decreases upward while the chlorite intensity increases upward.

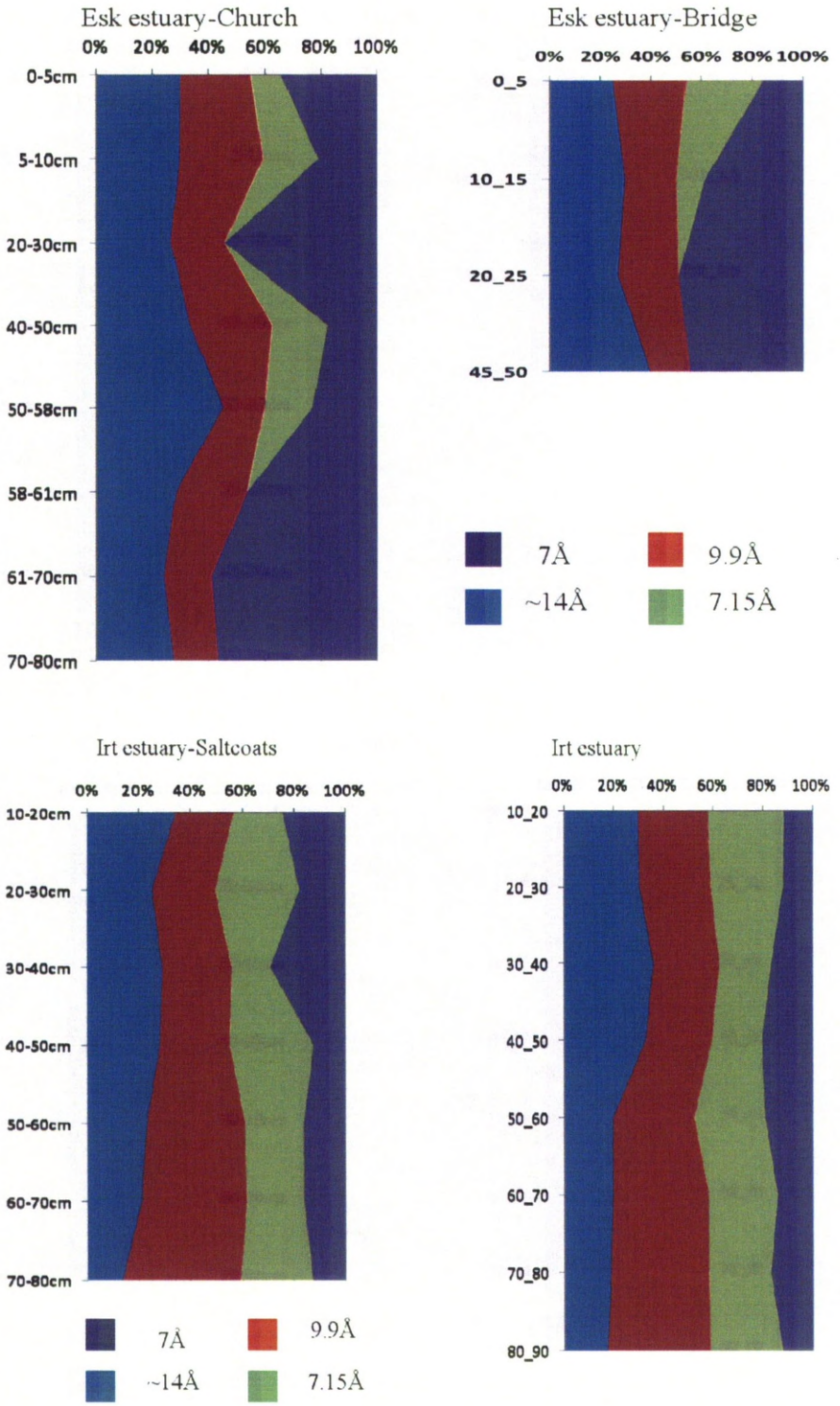

Figure 4.12: stratigraphical variation of the clay mineral peaks in the Ravenglass estuary. Normalised relative quantification of maximum intensity peak of the clay minerals (~14, 9.9, 7.15 and 7Å) based on the XRD pattern for 4 cores across the estuary. In the Esk estuary, 14 and 7Å peaks show a significant decreasing upward while the 9.9 and 7.15 increasing downward suggesting more Fe-rich clay minerals are abundant in the deeper part of the cores. 14 and 7Å peaks in the irt estuary cores show slightly increasing upward while 9.9Å significantly decreasing upward. Deeper part of the Irt estuary cores are abundant in illite.

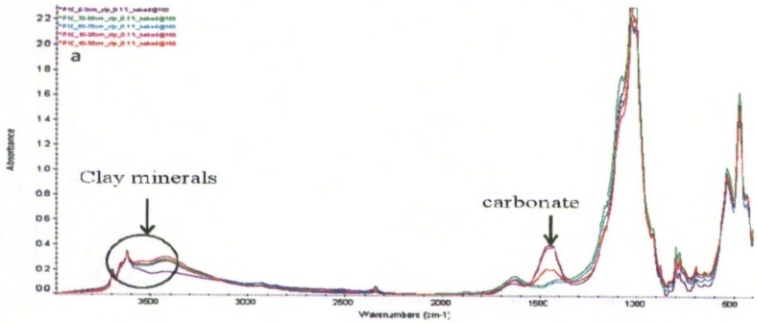
a
Clay minerals
carbonate
Absorbance
Wavenumbers (cm-1)

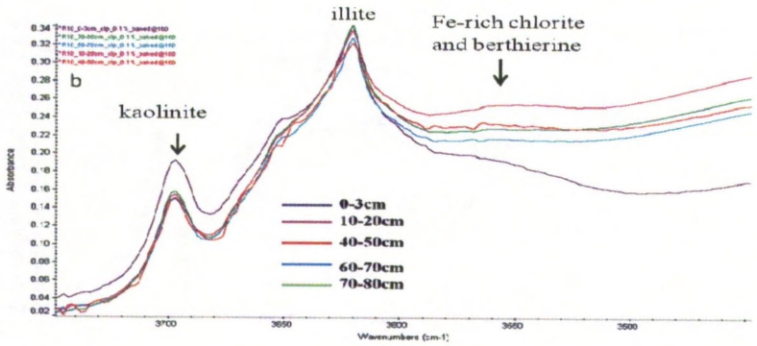
b
illite
Fe-rich chlorite
and berthierine
kaolinite
0-3cm
10-20cm
40-50cm
60-70cm
70-80cm
Absorbance
Wavenumbers (cm-1)

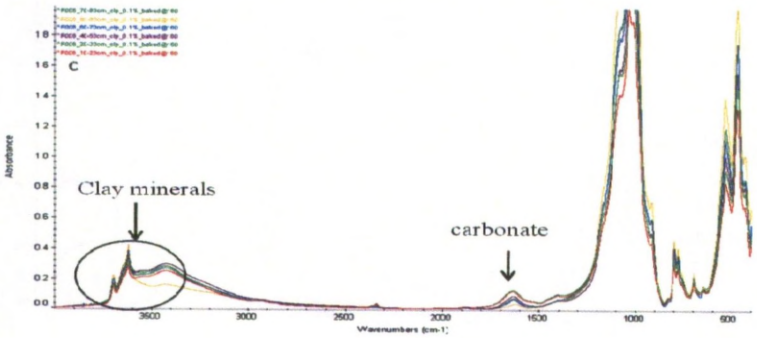
c
Clay minerals
carbonate
Absorbance
Wavenumbers (cm-1)

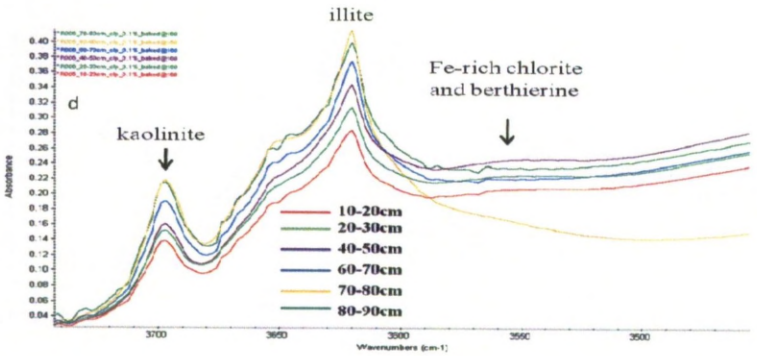
d
illite
Fe-rich chlorite
and berthierine
kaolinite
10-20cm
20-30cm
40-50cm
60-70cm
70-80cm
80-90cm
Absorbance
Wavenumbers (cm-1)

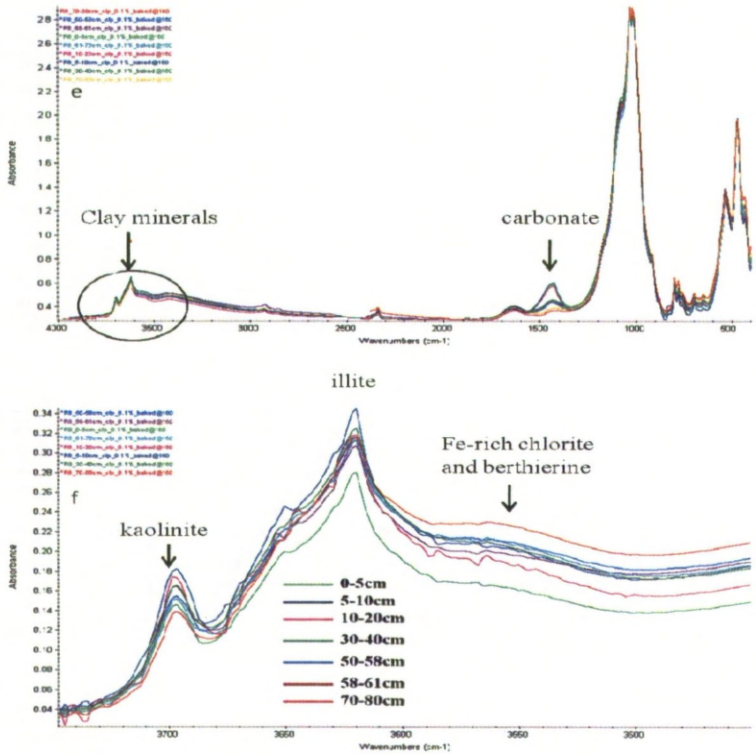

Figure 4.13: FTIR scans of the samples in the Ravenglass estuary.a) the full scan for the Saltcoats_close to the mouth of the Irt estuary and (b) showing representative peaks of the kaolinite, illite and Fe-rich chlorite. The relative peaks for kaolinite showing the highest is for the surface sediments and also the Fe-rich chlorite increases upward. c)full FTIR scan for the Irt estuary samples and (d) is representative clay minerals peaks area, kaolinite and illite decreases upward while the Fe-rich clay minerals increases upward, e) fullscans of the Esk estuary samples and (f) showing representative clay mineral peaks, kaolinite considerably increases upward while Fe-rich chlorite decreases upward.

4.5 Discussion

4.5.1 Clay minerals present in the Ravenglass estuary sedimentary system

A combination of techniques have shown that chlorite and illite are the most common clay minerals present in the cores from the Ravenglass estuary. Kaolinite is also present especially in the Irt estuarine sediments and in the top 50cm of the Esk estuary sediments. Gibbsite seems to be present especially in the Esk cores, revealed during SEM/EDAX studies but presumably at too low concentration for detection by bulk mineralogical analysis. Gibbsite is present where kaolinite is absent in the deeper part of the Esk cores. Berthierine is seems to be present, revealed by very large peaks at 12.5° that diminish on heating to 400°C. Berthierine is especially abundant at depth in the Esk estuary sediment.

Traces of hydroxyl interlayer vermiculite, revealed by shifting of part of the 6.2° peak to higher angles on heating, is only seen in sediments from the Irt estuary.

4.5.2 Vertical variation of the clay minerals in the Ravenglass estuary sedimentary system

The relative proportions of clay minerals can be qualitatively assessed by examining stacked XRD traces from samples all prepared and analysed in exactly the same way (same XRD analysis time and conditions; see Figures 4.8, 4.9, 4.10). It is not so easy to see small changes in overlapping peaks (12.3 and 12.5 especially) so it is rather better to study changes in mineral proportions by examining the quantified peak area data. The quantified areas of the 6.2°, 8.9°, 12.3° and 12.5° peaks (in order: 14Å, 9.9Å, 7.15Å, 7Å) are illustrated as a function of depth in Figure 4.12.

The clay-mineral logs (Fig. 4.12) show that the Irt cores (Saltcoats and estuary) do not vary very much as a function of depth although there is a clear but subtle increase in the relative area of the 14Å peak up the core commensurate with a decrease in the relative area of the 9.9Å peak. The Irt estuary core has a broadly but slightly decreasing area of the 7Å peak relative to the 14Å peak up section. In summary, these plots show that the clay mineral proportions in the Irt cores do not vary hugely as a function of depth but chlorite increases in abundance and illite decreases in abundance up-section. It is hard to detect any major changes in the ratio of the 7Å to 14Å peaks so that while berthierine is present in the Irt samples (Figs. 4.7 and 4.8), there is not much change in the amount of berthierine as a function of depth. The sequential heating experiments revealed that the Irt cores contained a small amount of vermiculite (Figs. 4.7 and 4.8) although it is not easy to discern any variation of vermiculite content with depth. Pyrite, reaching maximum concentrations of up to several percent, decreases in abundance up-section in Irt cores.

In stark contrast, the Esk cores (Church and Bridge) show a decrease in the relative area of the 14Å peak up the cores commensurate with a increase in the relative area of the 7.15Å peak. The area of the 7.15Å peak is variable in the Esk cores but is highest closest to the top of both cores. The Esk cores show approximately constant relative proportions of the 9.9Å peak up the core. The Esk cores have a decreasing area of the 7Å peak relative to the 14Å peak up section. In the Esk cores, the 7Å and 14Å peaks do not strongly co-vary. In

summary, the Esk cores show that the clay mineral proportions vary significantly as a function of depth; chlorite decreases in abundance and kaolinite increases in abundance up-section. There seems to be a major decrease in the ratio of the 7Å to 14Å peaks up the cores so that while berthierine is present in the Esk samples (Fig. 4.6), there is a major change (increase) in the amount of berthierine as a function of depth. Gibbsite, detected by electron microscope investigations (Fig. 4.3), is present only in the deeper part of the Esk cores, significantly where kaolinite is below XRD detection. XRD analysis showed that pyrite is at low concentration throughout the Esk cores.

4.5.3 Illite distribution

Illite seems to be the most constant clay mineral in the Irt and Esk cores typically representing about 20% of the clay fraction (Fig. 4.12). Illite is present in the Eskdale I-type granite hinterland occurring as minor muscovite (Moseley, 1978). Illite is a dominant clay mineral in the Sherwood Sandstone hinterland of the Irt (Strong et al., 1994). The relative uniformity of the illite in all the cores seems to suggest that the dominant illite from the Irt arm of the estuary has contributed to sediment deposited in the Esk arm of the estuary. Intra-estuary sediment and tide dynamics are thus not simply about sediment flux from river to ocean but likely involve some local movements with the estuary, e.g. on a rising tide.

4.5.4 Chlorite: origin and evolution in the Ravenglass estuary sedimentary system

In the following section it will be assumed that the overall (clay) fractional amounts of chlorite and berthierine are represented by the summed areas of the 14Å and 7Å peaks. This is reasonable since the approach captures the variable presence of berthierine (relative to illite and kaolinite as well as chlorite). It should be noted that decreasing the area of the chlorite 14Å peak relative to the 7Å peak can be achieved by making the chlorite more Fe-rich (Hillier, 2003) as well as by adding a 7Å berthierine component to chlorite of fixed composition. However, the detailed work on the effect of sequential heating of the clay minerals has shown that berthierine is variably present in these sediments (Figs. 4.6, 4.7, 4.8) suggesting that the second option is the preferred interpretation of the relative changes of the peak areas of the 14Å and 7Å peaks (Fig. 4.12).

There is more chlorite in the Esk cores than the Irt cores. The concentration of chlorite plus berthierine decreases from being 85% of the clay fraction at 1m to being 40-60% of the clay fraction at the surface in the Esk cores (Table 1, Fig. 4.12). In contrast, the concentration of chlorite and berthierine increases subtly from being 25-30% of the clay fraction at 1m to being 40-45% of the clay fraction at the surface in the Irt cores. Berthierine seems to be most abundant (relative to chlorite as well as other clay minerals) in the deeper part of the Esk cores while the areas of the 14Å and 7Å peaks seem not to vary much with depth in the Irt cores (Fig. 4.12).

Chlorite could have its depth-variation and spatial variation patterns in the Irt and Esk estuary cores controlled by a range of possible origins:

1) Primary sedimentary variations;
    a. Initial differences in chlorite content, and chlorite type,
    b. Initial differences in Fe-oxide content at the time of deposition.
2) Secondary, post-depostional, variations;
    a. Infiltration of different types of clay into different types of sediment at different sites,
    b. Infiltration of different amounts of Fe-oxide (as fines, flocs or colloidal material) at different sites,
    c. Different degrees of circulation of oxygenated or reduced water at different sites,
    d. Different water types dominant at different sites and different depth (sulphate-rich seawater versus sulphate-poor river water).

Chlorite has been reported as an alteration and weathering product in the Eskdale granite (Moseley, 1978) so it is perhaps not surprising that it is present in the stream sediment samples. Also, chlorite in Triassic sandstones has been reported as an authigenic (diagenetic) product (Worden and Morad 2003a; Schmid et al. 2004), but XRD analysis reported by Strong *et al.*(1994) taken from a local Sherwood sandstone outcrop at St.Bees, shows only a trace of chlorite. The Irt sediments contained a trace of vermiculite (Figs. 4.7, 4.8) suggesting that some chlorite-like clay minerals formed in soils in the hinterland. What is certain is that there is primary sedimentary chlorite being fed into both estuaries. Moreover, the elevated amount of chlorite in the Esk estuary may be a result of chlorite being a common weathering product of the Eskdale granite (Moseley, 1978) while chlorite

is only present in small amounts in the Sherwood Sandstone (Strong et al., 1994). Differences in primary sediment supply (option 1 above) could plausibly play a significant role in controlling the relative concentrations of chlorite in this estuary system.

The Irt cores are very fine-grained and so will be relatively impermeable (Fig. 4.2). The Esk cores contain interbedded medium- to coarse-sands and fine silts and so will have variable permeability (Fig. 4.3). The Irt cores will have had little opportunity for any sort of infiltration or lateral movement of water, whether by tidal pumping or down-aquifer subsurface flow. The Esk cores will have had opportunity for infiltration and lateral movement of water along the coarsest and most permeable sand layers. It is thus noteworthy that the coarser units are where there is most chlorite and where there is most berthierine; the coarsest layers have the highest peak area ratios of the 7Å to 14Å peaks. These observations possibly suggest a role for permeability in the generation of berthierine and chlorite at depth in the Esk cores that has not been effective in the low permeability Irt cores.

The aqueous iron load of rivers falls suddenly once rivers enter estuaries as the salinity starts to increase (e.g. Boyle et al., 1977). More than 90% of all aqueous iron is typically trapped within the estuarine environment (Boyle et al. 1977b; Mayer 1982). The mineral form of the flocculated iron is not well known but it is presumably oxidised (ferric) and very fine-grained (clay grade material). Some of this maybe co-deposited with the suspended and bed loads, some may be available for infiltration into permeable beds at low tide (when the sediment was not water-saturated). Solid phase ferric oxides and hydroxides in the estuarine environment can be reduced to ferrous phases in the presence of organic matter (Caccavo Jr et al. 1992; Coleman et al. 1993). In highly reducing (organic matter-rich, (Aller et al. 1986) and seawater-dominated environments in the subsubsurface, sulphate reduction occurs leading to the growth of iron monosulphate or pyrite (Coleman et al. 1993). If reduction of ferric iron occurs in the relative absence of seawater but with abundant oxidising organic matter, the result is likely to be siderite. It is noteworthy that the Irt cores are organic-rich and contain more pyrite than the Esk cores (Figs. 4.2, 4.3, 4,12) suggesting that any available iron (e.g. flocculated iron) has made Fe-sulphide rather than Fe-clay.

The prevalence of berthierine at depth in the Esk cores (Fig. 4.12) suggests some sort of diagenetic alteration process. Kaolinite is absent at depth in these cores; this l-silicate plus

iron phases (derived by flocculation) and SiO_2 (present as detrital quartz as well as highly reactive silica diatoms and radiolarian) could plausibly be the source of at least some of the berthierine in the Esk cores at depth. The flocculated iron phase could be primary (co-deposited with the sediment) or secondary (infiltrated after deposition). The prevalence of the berthierine in the coarser sediment could be a primary depositional factor or could be a function of the higher permeability of the coarser sediment.

In summary, the chlorite (plus berthierine) concentration seems to be affected by provenance given the different quantitites found in the two branches of the estuary. The amount of berthierine (area of the 7Å peak relative to the 14Å peak) is strongly affected by grain size (and maybe permeability) suggesting a post-depositional process (e.g. infiltration of flocculated Fe-oxides or reduction of co-deposited flocculated Fe-oxides) contributes to the creation of Fe-rich clay. Berthierine is only abundant at depth and where pyrite is at low concentrations. Where pyrite is most abundant (at depth in the Irt cores), there is little berthierine. This suggests that berthierine can only develop where sulphate reduction (to sulphide) has been hampered.

4.5.5 Kaolinite dissolution and diagenesis

There is more kaolinite in the Irt cores than the Esk cores (Fig. 4.12). Kaolinite is a more-or-less constant 20% of the clay fraction in the Irt cores while it varies from 20% to 0% with increasing depth in the Esk cores.

Kaolinite could have its depth-variation and spatial variation patterns in the Irt and Esk estuary cores controlled by a range of possible origins:

1) Primary sedimentary variations with initial differences in kaolinite content as a function of provenance or depositional processes.
2) Secondary, post-depostional, variations;
    a. Infiltation of more kaolinite at the Irt sites relative to the Esk sites,
    b. Different degrees of alteration of primary deposited kaolinite (more alteration in the Esk than the Irt sediments) creating other Al-phases such as gibbsite or even berthierine.

Variable infiltration is unlikely to be important since the greatest quantity of kaolinite is found in the finest sediments and the finest cores. The hinterlands of the Esk and the Irt seem to contain little kaolinite so that hinterland geology seems to play little part in controlling the variable quantities of kaolinite in the cores. Variable processes within the depositional environment could partly explain the kaolinite distribution pattern.

SEM studies revealed a new coating Al-hydroxide coating material (Figs. 4.3. f and g) at depths greater than 50cm depth in the Esk cores. It is possible that this originated from the alteration of the primary deposited kaolinite and partially explains the absence of kaolinite in the deeper Esk samples. Berthierine is most abundant at depth in the Esk cores, where kaolinite is absent suggesting that this too could explain the kaolinite depth-variation pattern. A number of experimental studies (Small 1992; Huang 1993; Manning 2003) have addressed the dissolution mechanisms of kaolinite. Dissolution rates of kaolinite are presented by Nagy et al. (1991) who showed in the laboratory dissolution of kaolinite is possible under surface pressure conditions. Huang (1993) also carried out similar experiments and explained the possibility of kaolinite transition, kaolinite dissolution finally generating Al-hydroxide. The laboratory experiments were undertaken <200°C. Formation of an aluminium oxide phase was reported as kaolinite chemical weathering product in lake and stream sediments down the granitic alpine environment (Drever and Zobrist 1992). The composition of this granite and soil clay mineral contents show a similarity to the Eskdale granite and Esk stream sediments. On the other hand, Griffin and Ingram (1954) reported kaolinite transformation to illite and/or chlorite in a modern sedimentary system. Dissolution and transformation of the kaolinite to the gibbsite-like compound in the Esk estuary may thus be due to shallow burial diagenesis processes although clearly further work is required to explain this issue properly.

4.5.6 Grain coating clay minerals in estuaries

Sand grains in the cored sample are coated with a wide-range of the clay minerals. Some of the material coating sand grains is Fe-chlorite (and possibly berthierine), but some is illite leading to a mixed mineralogy for clay mineral coats such as illite-dominated illite-chlorite or chlorite-dominated chlorite-illite depending on the relative proportions of the areas of the K and Fe peaks from EDAX spectra (Figs. 4.3 and 4.4). Sediments from the Irt core revealed that grain-coating clay minerals are mainly illite at depth while the shallower core samples contain illite-dominated illite-chlorite. For the Esk cores, the

deeper coats are mainly chlorite-dominated illite-chlorite while the shallower grain coats are illite-dominated illite-chlorite. Significantly, these patterns seems to mimic the relative changes of the clay minerals in the quantified XRD-depth plots (Fig. 4.12). This suggests that whatever relative proportions of clay minerals are found in the <2 μm fraction of the bulk sediment are found as grain-coating minerals. This broadly seems to suggest that sand grains become coated with whatever clay minerals they are physically close to in the host sediment.

Figure 4.13 shows the extent of coverage of sand grains by clay mineral as a function of sand grain size. The inverse correlation suggest that the degree of grain coating is at least partly a function of grain size. Coarser, moderately sorted sands have a lower degree of clay coat coverage relative to the finer, more poorly sorted sands in the modern sedimentary environment in the Ravenglass estuary system.

In principle, the clay coats on sand grains in the Ravenglass estuary could have a variety of possible origins:

1) Primary inherited coats on sand grains formed in the fluvial hinterland and then washed into the estuary (e.g. Konhauser and Urrutia, 1999).
2) Primary depositional coats, formed at the site of deposition and buried along with the host sediment (Wilson 1992).
3) Secondary coats, due to alteration of the primary sediment by early diagenetic processes including;
    a. Bioturbation by such as lugworms (e.g. Needham et al. 2005, 2006).
    b. Vertical infiltration of water bearing fine suspended material (Matlack et al, 1989, Skolasinska 2006).
    c. Tidal pumping and washing in fine suspended material.
    d. Downstream influx of material along more permeable strata.

The hinterland of the Esk is dominated by chlorite (Moseley, 1978) and yet the Esk coats contain chlorite-dominated illite-chlorite at the base and illite-dominated illite-chlorite at the top of the core. For the Irt estuary, the coats are dominated by illite with illite-dominated illite-chlorite at the top of the cores. This seems to reflect the illite-dominated nature of the clay minerals in the Irt's hinterland (Strong et al., 1994). Moreover, the similarity of the mineralogy of the grain coats to the local bulk-analysed clay minerals for

each sample suggests that the coats were, at most, only partially inherited as clay-coated sand grains from the fluvial part of the system. Clay coat mineralogy certainly reflects the local provenance but also seems to reflect processes in the local environment of deposition.

Grain coats are best developed on finer sand grains (Fig. 4.13). Thus grain coats are best developed in the lower permeability sediments; grain coat development is unlikely to be exacerbated by the ease of water movement suggesting that tidal pumping or downstream flux of material through aquifers are unlikely to becontrols on coat creation. Vertical infiltration would slow down in the finer sediments and possibly permit fines to be deposited on sand grain surfaces, However, the similarity of the clay coat mineralogy and the bulk mineralogy of the fine fraction suggests that the coats are simply composed of the local clays suggesting that the coating clays were co-deposited with the bulk sediment. Bioturbation (sediment ingestion and excretion) has been shown to create clay-coated sand grains (Needham et al., 2005, 2006) and this could plausibly lead to clay coats having much the same mineralogy as the local bulk sediment.

In summary, clay coats are composed of illite, chlorite (and likely berthierine), kaolinite and Al-hydroxide (gibbsite). Clay coats are better developed (are more complete coats) on finer sand grains. Overall, the clay coats reflect the mineralogy of the hinterland but seem to have formed within the environment of deposition rather than as inherited features. They vary in mineralogy in concert with the local bulk sediment mineralogy and are affected by the local diagenetic changes (such as creation of gibbsite and possibly the creation of berthierine).

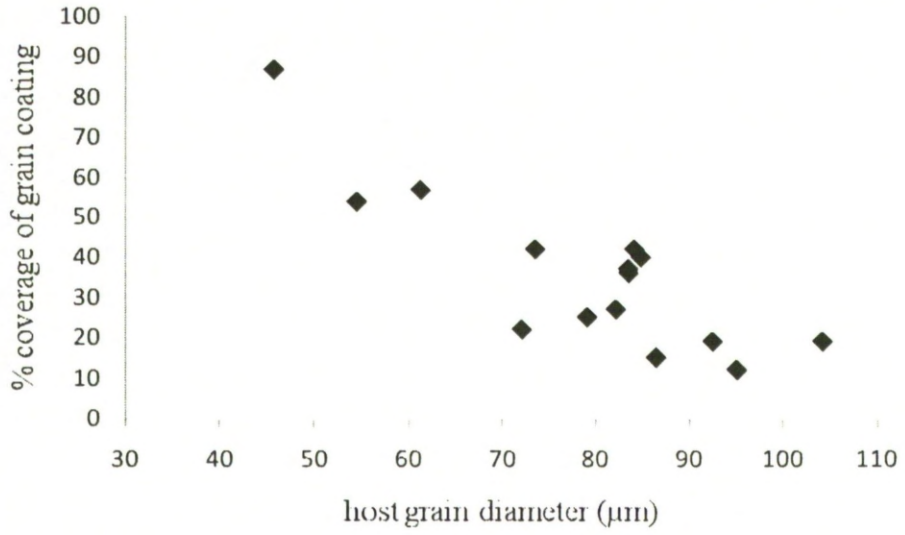

Figure 4.13: clay mineral grain coating coverage *verses* the host grain size or surface area in the Ravenglass estuary sediment samples.

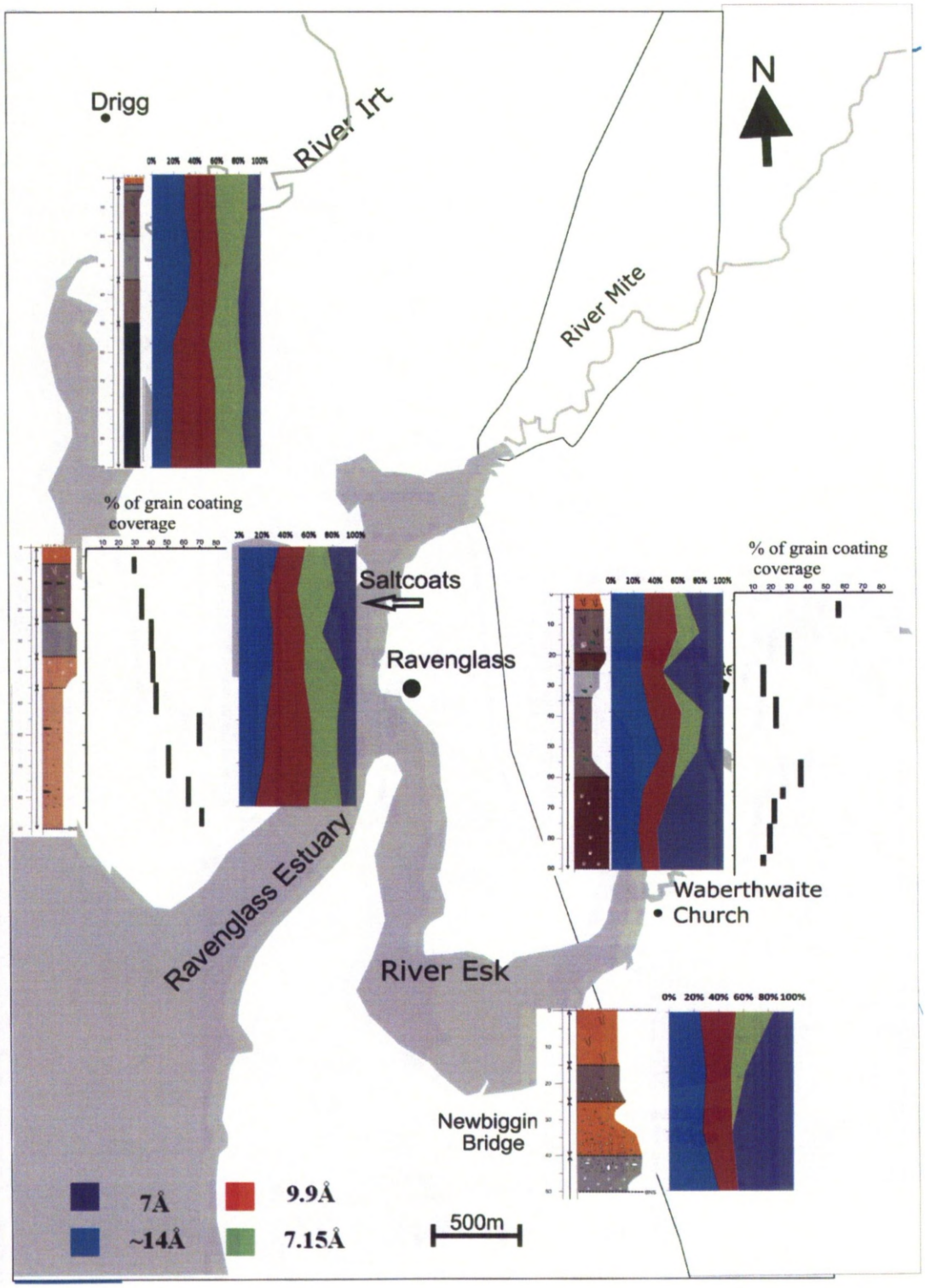

Figure 4.14: Schematic synthesis map of the Ravenglass estuary with the core information and stratigraphic variation of the clay mineral content, percentage of the coating coverage of the sand grains and sedimentary logs.

4.6 Conclusion

1) The clay minerals chlorite, illite, kaolinite, berthierine and vermiculite are all present in the Irt and Esk arms of the Ravenglass estuary, NW England, as is a gibbsite-like phase and pyrite. Kaolinite and pyrite are more abundant in the Irt estuary cores than the Esk cores while chlorite and berthierine appear to be more abundant in the Esk estuary cores.
2) The Irt estuary cores have slightly increasing chlorite and decreasing illite from base to tops of cores. Esk estuary cores have slightly decreasing chlorite and increasing kaolinite from base to tops of cores. Berthierine abundance broadly decreases up-section. Gibbsite is present at depth, where kaolinite is effectively absent.
3) There seem to be strong provenance controls on the proportions of clay minerals in the cores in the two branches of the estuary. The chlorite-rich weathered I-type granite hinterland of the Esk estuary has led to the accumulation of more chlorite (and berthierine) than the chlorite-poor Sherwood Sandstone hinterland of the Irt estuary.
4) The loss of kaolinite and creation of gibbsite in the Esk cores suggests that gibbsite is forming from kaolinite. Berthierine and pyrite are mutually exclusive suggesting that berthierine forms where the aqueous sulphide supply (from bacterial reduction of sulphate) is limited.
5) Grain-coating clay minerals are variably present on sand grains from this estuary. Finer grained sand tends to have more complete clay mineral coats than coarser-grained sand. The degree of coating decreases up-section in the Irt Estuary cores. The degree of grain coating is more variable in the Esk estuary but tends to increase up-section.
6) Grain coatings include berthierine, kaolinite and gibbsite but tend to be dominated by mixtures of illite and chlorite. Grain coatings tend to become more complete where illite is the dominant clay minerals but all coats are illite-chlorite mixtures.
7) Estuaries are sites of clay mineral generation and alteration as a function of primary supply and secondary alteration processes. Fe-clays, chlorite and berthierine, are most abundant in the coarsest sediment where pyrite is absent (where the supply of sulphate is lowest). Grain coatings seem to be best developed in the finest sandy sediments; in this case where illite-chlorite tends to be dominant.

Chapter 5

Chapter 5 Dissolved iron behavior in the Ravenglass estuary waters

5.1 Abstract

The aqueous geochemistry of the Ravenglass estuary and its feeding rivers has been studied to assess if, where and when aqueous iron is lost from the river water and accumulates as part of the sediment in the estuary. Ravenglass estuary waters are conservative mixtures between river water and seawater in terms of chloride, sodium, potassium and magnesium. Alkalinity (bicarbonate), calcium and sulphate are locally non-conservative and are affected by biological and mineral processes. The River Irt contains twice as much dissolved iron as the River Esk but all iron concentrations are much lower in the estuary samples than in the feeding rivers. Aqueous iron undergoes large-scale accumulation in the Ravenglass estuary. Iron concentrations are lowest at high tide at all sampling sites on the Ravenglass estuary. Iron concentrations are highest at low tide for the Irt arm of the estuary but are highest on the falling tide between high and low tide. Iron concentrations in estuary samples decrease rapidly as salinity increases with low iron concentrations in all estuary samples once salinity exceeds 5,000 mg/lit. Iron concentrations also decrease as pH increases. The loss of iron is presumably due to flocculation of colloidal iron oxides, hydroxides and iron-organic complexes. Fluvial aqueous iron does not behave conservatively on mixing with seawater; most iron is lost from the water column at an early stage of river water mixing with estuary water. The site of primary iron-loss from the water occurs towards the heads of estuaries but this site will move as a function of time within the tide cycle. Given that the Esk has highest iron concentrations between high and low tide, it is likely that iron is swept from the iron-rich Irt arm of the estuary into the iron-poor Esk arm soon after high tide.

5.2 Introduction:

The non-conservative behaviour of dissolved iron during estuarine mixing has been well documented (Boyle et al. 1974; Boyle et al. 1977a; Sholkovitz 1978; Mayer 1982; Escoube et al. 2009). Fluvial dissolved iron, sometimes defined as the fraction which passes through a filter size of 0.2μm, comprises mostly colloidal iron on the filter papers (Sholkovitz 1978). On mixing with seawater in an estuary, these colloids are believed to aggregate to create grains that are larger than the filter pore size (Mayer 1982). The aggregation of the Fe colloids is due to an interaction with cations such as Mg^{2+} and Ca^{2+}

which are introduced to the estuary on an incoming tide by seawater (Eckert and Sholkovitz 1976; Boyle et al. 1977a).

There have been several experimental and laboratory-based studies of fluvial Fe removal and aggregation (Boyle et al. 1977a; Sholkovitz 1978; Sholkovitz et al. 1978; Bale and Morris 1981; Mayer 1982; Ouddane et al. 1999). Most of the research involved the experimental mixing of river water with either natural seawater or a mixture of electrolytes simulating the various ions in seawater.

Natural fluvial Fe colloids are more stable and resistant to aggregation by salt when in association with organic matter (humic acid) than synthetic iron hydroxide colloids (Mosley et al. 2003), so it would be expected to not see absolute compatibility between non-conservative behaviour of Fe in natural fluvial systems with experiments. If organic matter were absent from river water, it has been speculated that Fe colloids would precipitate rapidly long before reaching the estuarine mixing zone (Mosley et al. 2003). However, in the presence of seawater ions, binding with ions and organic matter accelerates the aggregation of Fe colloids (Boyle et al. 1977a; Mosley et al. 2003). It has been reported that the salt-induced-aggregation of Fe colloids consists of at least two sequential reactions (Mayer 1982); the first is fairly rapid and occurs early in the river-sea mixing process by interparticle collision and is responsible for loss of a significant portion of the iron. The second occurs more slowly over hours as Fe colloids continue to aggregate due to particle-particle collision (Mayer 1982). Understanding how salinity varies during the tide cycle at different positions within an estuary is therefore an important step in understanding Fe behaviour in estuaries.

In contrast to laboratory experiments, in estuarine environments the distribution of dissolved iron is complicated by strong gradients of several physico-chemical-biological properties such as salinity, turbidity, temperature, dissolved oxygen concentration, pH, and organic matter concentration. The behaviour of iron in the estuarine systems is influenced by all these parameters and the various processes involved in estuaries such as adsorption-desorption, precipitation-dissolution, sedimentation-resuspension and flocculation-coagulation (Sholkovitz 1978; Sholkovitz et al. 1978; Olausson and Cato 1980; Drever 1982; Head 1985; Ouddane et al. 1999). One important biogeochemical process in the estuary, and in sediments at or near to the sediment surface, is bacterial sulphate reduction, since this coverts marine sulphate into sulphide which subsequently removes aqueous iron

in the form of Fe-sulphide. It is also possible that sulphide minerals become oxidised (e.g. during erosion down to the sulphate reduction and sulphide precipitation zone in sediment), thus creating sulphate and, potentially, Fe either released into the water or making new Fe-minerals (such as siderite or Fe-clay minerals)

Water circulation in an estuary is typically controlled by topography, tidal currents and range, and the volume of fresh water discharged from rivers. The transition from fresh to salt water (estuary characteristic) causes some changes in the dissolved and suspended load of rivers (Gibbs et al. 1989; Stow et al. 2003). The most important physical effect is flocculation. Clay minerals, organic matter, and colloidal hydroxides of iron all tend to form stable suspensions in fresh water, but tend to flocculate and sink in seawater (Boyle et al. 1977a; Sholkovitz 1978; Fan et al. 2008). Depending on the type of estuary and the specific details of the mixing of saline and fresh water in an estuary, the floccules either sink to the sediment surface and settle or they are transported to the sea, e.g. as bedload (Drever 1982).

Clay minerals and organic matter as well as iron colloids are transported to estuaries by rivers; clay minerals tend to undergo ion-exchange. Iron becomes mobilised in the presence of cations within the mixing zone of freshwater and seawater, so estuarine natural water (Huthnance et al. 1993)is a suitable place for clay mineral alteration processes (and specifically ion exchange) and Fe flocculation.

This research was designed to address the way aqueous Fe varies in the Ravenglass estuary as function of salinity and water chemistry. The specific questions being addressed are:

1) How do salinity and water geochemistry vary at different sites within the Ravenglass estuary during the tide cycle?
2) Is Ravenglass estuary water a conservative mixture between river water and seawater, or do geochemical processes further alter the estuary water composition?
3) How does dissolved iron vary at different sites within the estuary during the tide cycle?
4) How does the concentration of dissolved iron change when river water enters the estuary?
5) Does fluvial dissolved iron behave conservatively on mixing with seawater?

5.3 Background to the Ravenglass Estuary

The Ravenglass estuary is a local name for an area which encompasses the tidal reaches of the Rivers Esk, Irt and Mite. The estuary is located on the Cumbrian coast in the north-west of England (Fig. 5.1). A single channel connects the confluence of the three rivers to the sea.

The Ravenglass Estuary is a macro-tidal estuary, with a tidal range of over 7m on spring tides. The estuary has relatively high tidal discharges and velocities but the rivers that feed into it have relatively low discharges (Assinder et al. 1985). The estuary thus largely empties of water at low tide.

The evolutionary of geological issue in this estuary has been shown its present morphology, and follows the global rise in sea level following melting of the ice after the last glaciations (Bousher 1999). The Rivers Esk and Irt are primarily fed by small streams from the surrounding hill draining the Eskdale granite (Moseley 1978) and the St. Bees Lower Triassic sandstone Sherwood sandstone Group; (Strong et al. 1994) respectively.

5.4 Sampling and analysis methods

5.4.1 Sampling methods

Water samples from the Ravenglass estuary were collected at various sites at regular intervals through the tidal cycle in the summer of 2009, in sunny normal day. Six stations were selected for water sampling including four sites for estuary waters and two fluvial end member sites and a coastal site about 1000m north of the where the Ravenglass estuary meets the open sea. For each estuary (Irt and Esk arms of the Ravenglass estuary), fresh-water dominated and marine-water dominated sites subject to availability and easy access, were chosen. In the Irt estuary, the Drigg site is fresh water-dominated and the Saltcoats site is marine water-dominated. In the Esk estuary, the Newbiggin bridge (hereafter known as Bridge) is marine water-dominated and the Waberwaith Church (Church) is fresh water-dominated. In addition, Santonbridge from the River Irt and Stockbridge from the River Esk were chosen in order to characterise the fluvial (fresh water) end-members.

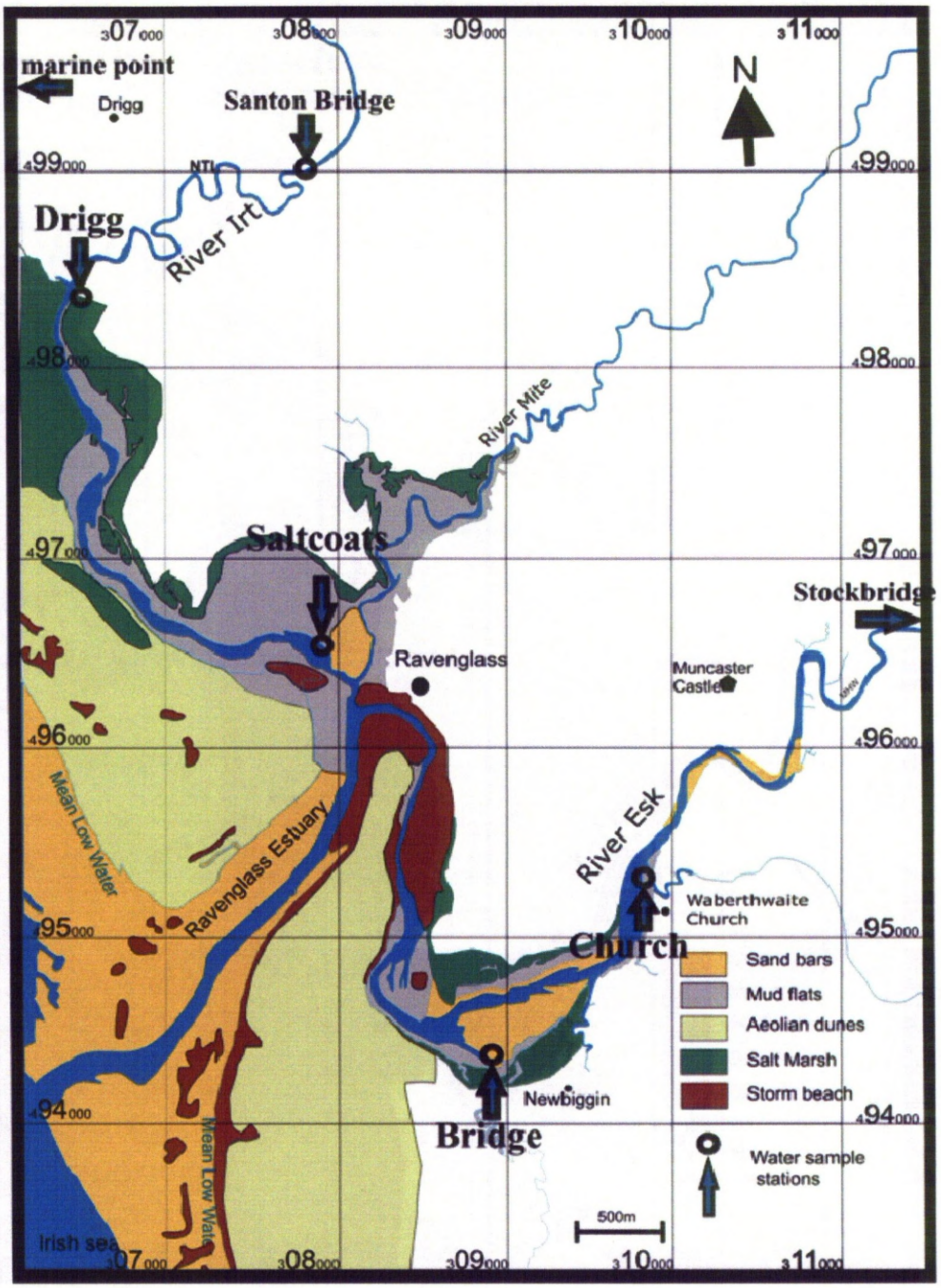

Figure 5.1: The Ravenglass estuary and sub estuaries: Irt, Mite and Esk. Location of the water sample stations in the estuaries and end-members.

A site at Driggholme beach, about 1000m north of the point where the Ravenglass estuary meets the sea, was chosen to sample the marine water end-member.

Twelve estuary water samples were taken during tide cycles for 12 hours at each estuary station. The end-members at Santonbridge, Stockbridge and Driggholme were collected on the same sampling mission. The extra end-members from Santonbridge and Stockbridge were collected later immediately after a storm event.

Water samples were initially collected in 1 gallon polythene canisters by wading out into the estuary (or river or the sea) until the water depth was about 1m. These canisters were half filled with the water from the site and then capped, shaken and emptied. The canisters were then filled to the brim by immersing the neck about 50 cm below the water surface. The canisters were capped and taken to a mobile laboratory (the back of a Ford Transit van) for processing. Note that working in estuaries carries peculiar risks and suitable personal protective equipment was employed during sample collection including; chest-high waders, life jacket, and, in some cases a rope held firmly by a colleague standing on the bank of the estuary.

All water samples were stored in air-tight polyethylene jars that were filled to the brim. Four types of sample were carefully prepared on-site (i.e. in the back of the van), from each site and at each time, for further chemical analysis.

Raw sample: 500ml water samples preserved in a PE jar as an untreated (unfiltered-unacidified) sample (Fig. 5.2).

Filtered-acidified: 500ml raw water samples were filtered using NALGENE filteration set jars in the field, using 0.2μm Whatman cellulose nitrate filters, under pressure using a car battery-driven simple Fisher brand vacuum pumps. Suspended particles and large floccules remained on the filter papers. The samples were acidified with 1% analytical grade nitric acid to reach pH ~3. These types of sample were intended for cation analysis and possibly also iron determination.

Filtered-unacidified: 500ml raw water samples were filtered in the field, using 0.2μm Whatman cellulose nitrate filters, under pressure using car battery driven simple vacuum pumps. These samples were left at its natural pH and were intended for anion analysis in the laboratory.

Acidified-filtered: a 500ml raw water sample was acidified with 1% nitric acid to reach the pH ~2. These samples were then filtered using NALGENE filteration set jars in the field, using 0.2μm Whatman cellulose nitrate filters, under pressure using a car battery-driven simple Fisher brand vacuum pumps. These samples were prepared for iron analysis and were designed to monitor the concentration of aqueous and colloidal iron in the water.

All samples were frozen for further geochemical analysis in the laboratory.

5.4.2 Field analysis methods

Determination of pH, temperature and alkalinity were made as quickly as possible (typically with 15-20 minutes), on site, using unfiltered raw samples. pH and alkalinity were measured with an automated alkalinity meter. The 848 Titrino Plus is a titrator for volumetric titrations for universal applications which is manufactured by Metrohm Company. This titrator was used under Monotonic equivalence point titration (MET) conditions in which the reagent (sulphuric acid 0.01%) was added in constant volume steps by the titrator and pH was continuously measured.

5.4.3 Laboratory analysis methods

All major anions and cations were analysed using ion chromatography (IC). The instrument used was a Metrohm Compact IC Pro 881. The instrument was used for ion chromatography determination of anions with sequential suppression and without the suppression for the determination of cations. The instrument was operated with MagIC Net software 2.1.2. MagIC Net controls and monitors the IC instrument, evaluates the measured data (quality control) and administers it in a database. All water samples were filtered (2μm) before analysis with IC. Filtered, unacidified samples were analysed using a Metrospe A Supp 5-250 column for anion analysis with an eluent of sodium carbonate and bi-carbonate. Filtered acidified samples were analysed using a Metrosep C4 150 column for cation analysis using an eluent of 1% nitric acid and 4.6mM H_3PO_4.

Calibration was set before anion and cation analysis. Quantification in IC requires a calibration that covers the defined measuring range. The necessary calibration standards were prepared from a concentrated standard by appropriate manual dilution. Calibration was run with standard solutions in steps of 1, 5, 10, 50, 100 and 200mg/L of each species to be determined, diluted from an original stock of 1000mg/L. MagIC Net controls all data and components of the intelligent IC. The combination of software and hardware allows the system to compare results and shows graphs and statistic of calibration pattern.

Calibration method was done to appropriate (R^2>=0.999) levels for all anion and cation analyses.

Iron concentration in the acidified-filtered samples was measured at Manchester University. Fe was determined using a VG Elemental ''Horizon'' inductively coupled plasma-optical emission (ICPOES) instrument, following appropriate dilutions.

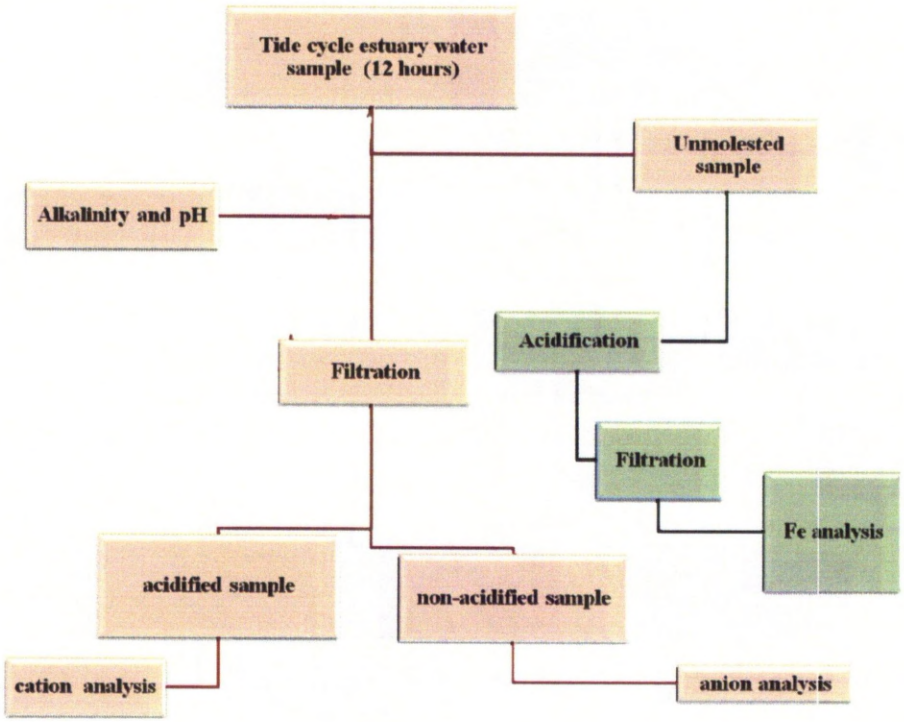

Figure 5.2: Methodology chart for estuary water sample during tide cycle at each station. Every hour on going sampling for 12 hours in each station and then two different types of Fe sample preparation treatment. First filtration and acidification for the "dissolved iron" in the estuary waters and the second is acidification to break the floccules and dissolved ultra fine grained solid phase Fe then filtration to analyse total Fe.

5.5 Results

5.5.1 pH and alkalinity

Alkalinity and pH are two parameters that provide insight into changing water geochemistry in an estuary. Both can be determined by simple tests. pH and alkalinity influence the estuarine carbon cycle, which involves the movement of carbon from the atmosphere into plant and animal tissue and into water bodies (Burton and Liss 1976; Sutcliffe and Carrick 1988). The pH of water is the measure of how acidic or basic it is and it is a master variable controlling chemical speciation in natural waters. Figure 5.3a shows the pH measurement for the four stations in the Esk and Irt branches of the Ravenglass estuary through tide cycles. The highest pH in the all stations occurs approximately at high tide for the less marine Drigg and Church sites. The lowest pH roughly corresponds to low tide conditions. The more marine-dominated parts of the Irt estuary at Saltcoats and the Esk estuary at Bridge have less variable and higher pH than the up-estuary sites. This pattern is in accord with the fact that the Rivers Esk and Irt have pH values of 6.8 and 7.4, respectively, and the nearby seawater sample has a pH of 8.7 (Table 5.1). Thus low tide estuary samples, at least high up the estuary, appear to be river water-dominated while the high tide samples and the more sites closer to the sea tend to be seawater-dominated.

Alkalinity is a measure of water's capacity to neutralize acids and in natural estuary waters is influenced by the presence of alkaline compounds in the water such as bicarbonates, carbonates, and hydroxides (Drever 1982). Alkalinity is reported as mg/l of bicarbonate (HCO_3^-). The alkalinity of the Rivers Esk and Irt is 10 and 14 mg/l respectively, while the nearby seawater has an alkalinity of 126 mg/l (Table 5.1). The alkalinity behaviour in the Irt and Esk estuaries (Figure. 5.3a) broadly follows pH in that it increases at high tide and decreases in a falling tide. The lowest alkalinity occurs at low tide. The two estuary sites closest to the sea develop higher alkalinities than the incoming seawater and have much greater alkalinity than the two sites furthest from the sea (most up-estuary; Fig. 5.3a).

5.5.2 Results of major cation and anion analysis

As would be expected, chloride is relatively low in the two river water samples (24 mg/l in the Esk and 40 mg/l in the Irt) and, of course, is highly concentrated in the nearby seawater sample (18 g/l; Table 5.1). Chloride concentrations increase rapidly at high tide and then fall towards low tide (Fig. 5.3a). The two estuary sites closest to the sea develop higher

chloride concentrations than the incoming seawater and have much higher chloride concentrations than the two sites furthest from the sea (most up-estuary; Fig. 5.3a).

To illustrate the co-variation of the analysed cations and anions, the Na and Cl concentrations were divided by 10 (to prevent those two elements obscuring changes in the less concentrated elements) and then all were plotted as concentration as a function of time through the tide cycle at each site (Figs. 5.3b and c). These diagrams beautifully illustrate how composition of estuary water varies with time during tide cycles.

To further examine the relative concentrations with time, the data at each site were normalised to 100% (again using Na/10 and Cl/10) at each time step and then plotted as a function of relative concentration versus time. To further highlight relative behaviour each river composition and the seawater sample were also normalised and compared to the time data from the two sites in each estuary (Figs. 5.3b and c). These normalised plots versus time show that at high tide, at each site, the water broadly resembles seawater (the relative proportions of the ions in the estuary are much the same as the seawater). However, at low tide, the relative proportions of the ions in the estuary are not particularly like those in the river water samples suggesting the geochemical addition or removal of some species in the estuary. When chloride and sodium are plotted versus TDS, they have excellent correlations (Fig. 5.3d), presumably because they are largely conservative species (i.e., they are not particularly involved in geochemical processes). While the trend is not quite as perfect, there appear to be good 1:1 correlations between magnesium and potassium and TDS suggesting that these cations are also largely conservative in the estuary (Fig. 5.3d). In comparison to species such as chloride, calcium and alkalinity appear to be non-conservative species in the estuary (Figs. 5.3b and c). Sulphate concentrations also appear to be non-conservative developing relatively low concentrations under low tide conditions at the up-estuary Irt-Drigg and Esk-Church sites.

To test this further, all species have been plotted against (x-axis) conservative chloride concentrations for all sites with the nominal 1:1 conservative mixing line added for reference on each graph. Because it is here now assumed that chloride can be neither added nor removed by geochemical processes, values above the line suggest addition of that species while values below that line suggest removal of that species (Figs. 5.4a and b). Thus sodium values all plot on, or very close to, the 1:1 lines, as expected from Figure 5.3d. Similarly, magnesium and potassium values also plot very close to the 1:1 lines.

Sulphate concentrations seem to lie close to the 1:1 line for two up-estuary sites at Esk-Church and Irt-Drigg but there appears to be an excess sulphate at Irt-Saltcoats and a shortfall at Esk-Bridge. Thus the two more marine estuary sites thus show contrasting behaviour. Almost all alkalinity values (HCO_3) lie above the 1:1 mixing line although the low and high chloride concentrations do appear like the fluvial and marine end-members. Overall the alkalinity data describe an arc above the 1:1 line suggesting significant addition of HCO_3 within the estuary itself. Calcium values mostly lie close to the 1:1 line but with some scatter in the values. Calcium values have also been plotted against alkalinity for all sites with a nominal 1:1 conservative mixing line added for reference on each graph; these graphs suggest an excess of HCO_3 relative to calcium in the estuary.

Piper diagrams have been prepared for all estuary sites and the marine and the relevant fluvial end-members (Figs 5.5a to d). These diagrams largely confirm the strongly marine appearance (species proportions) at the down-estuary Irt-Saltcoats and Esk-Church sites but also reveal more scatter in the up estuary Irt-Drigg and Esk-Church sites. The scatter away from a marine to fluvial joining line seems to confirm that there are geochemical processes involved in loss and gain of same species (especially HCO_3, sulphate and calcium, as discussed previously).

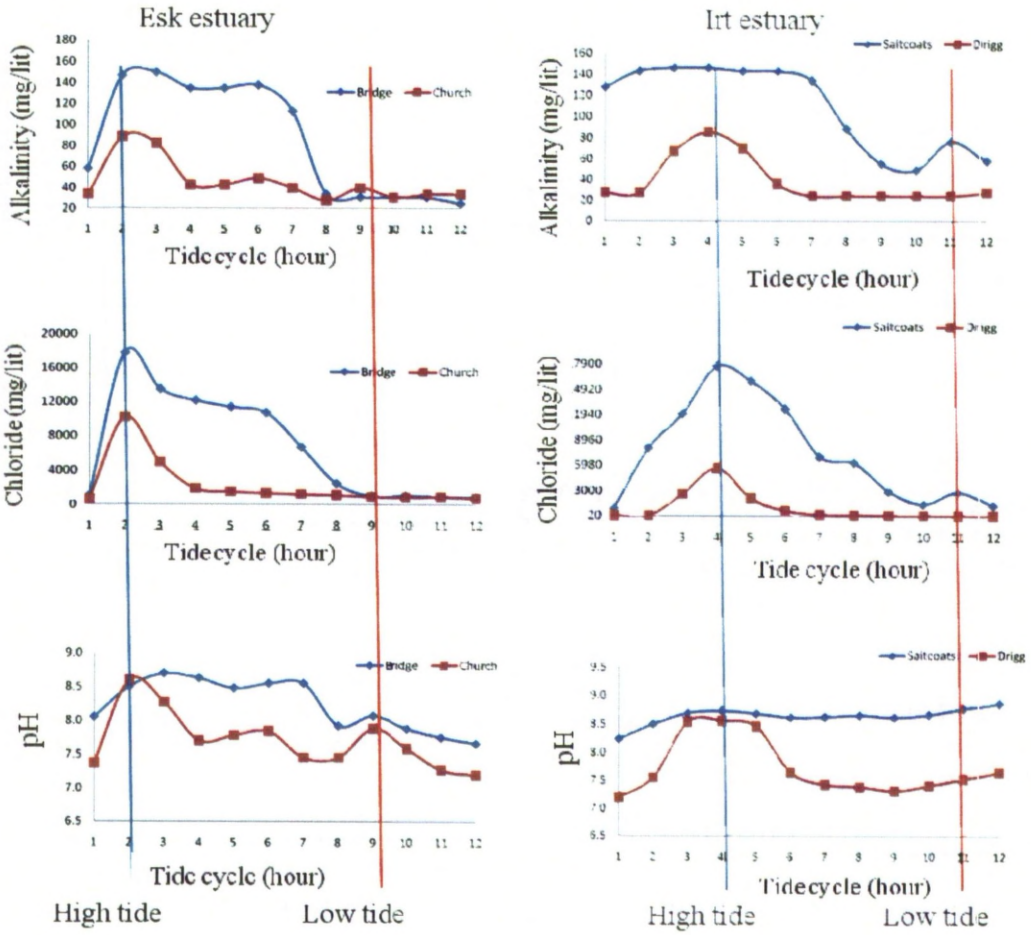

Figure 5.3a: Alkalinity, pH and chloride concentration of the samples during 12 hours tide cycle sampling in the Irt estuary (right) stations (Saltcoats and Drigg) and Esk estuary (left) stations (Bridge and Church). Saltcoats and Bridge are the marine-dominated part of their estuaries. Drigg and Church are the fresh water-dominated part. The marine water-dominated samples show a broad peak around high tide while the fresh-dominated samples had a sharp peak at high tide.

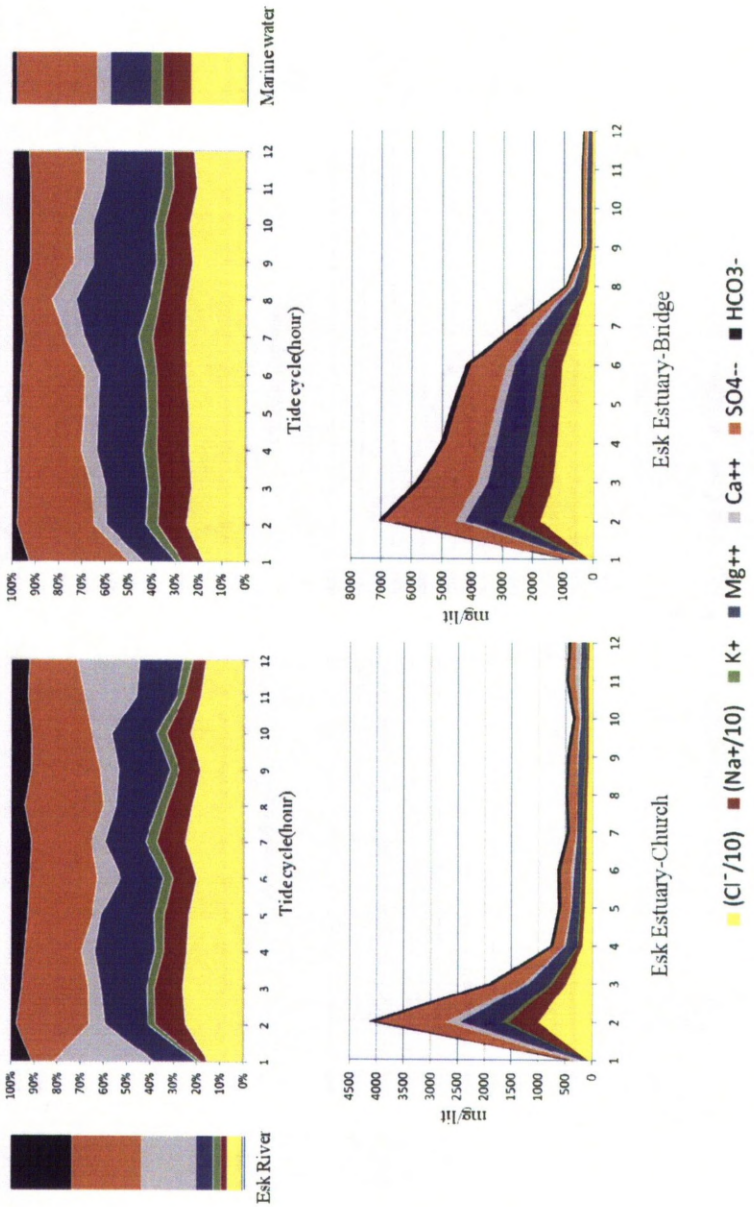

Figure 5.3b: Normalised and absolute concentrations of the common cations and anions at the two sampling stations on the Esk arm of the Ravenglass estuary; Bridge is towards the sea while Church is towards the head of the estuary. The sodium and chloride concentrations were both divided by ten to allow the variations of the other ions to be visible. The normalised data show how the relative concentrations vary with time; the absolute concentrations illustrate the timing of high tide and how quickly the sea water is replaced by river water at the two sampling stations.

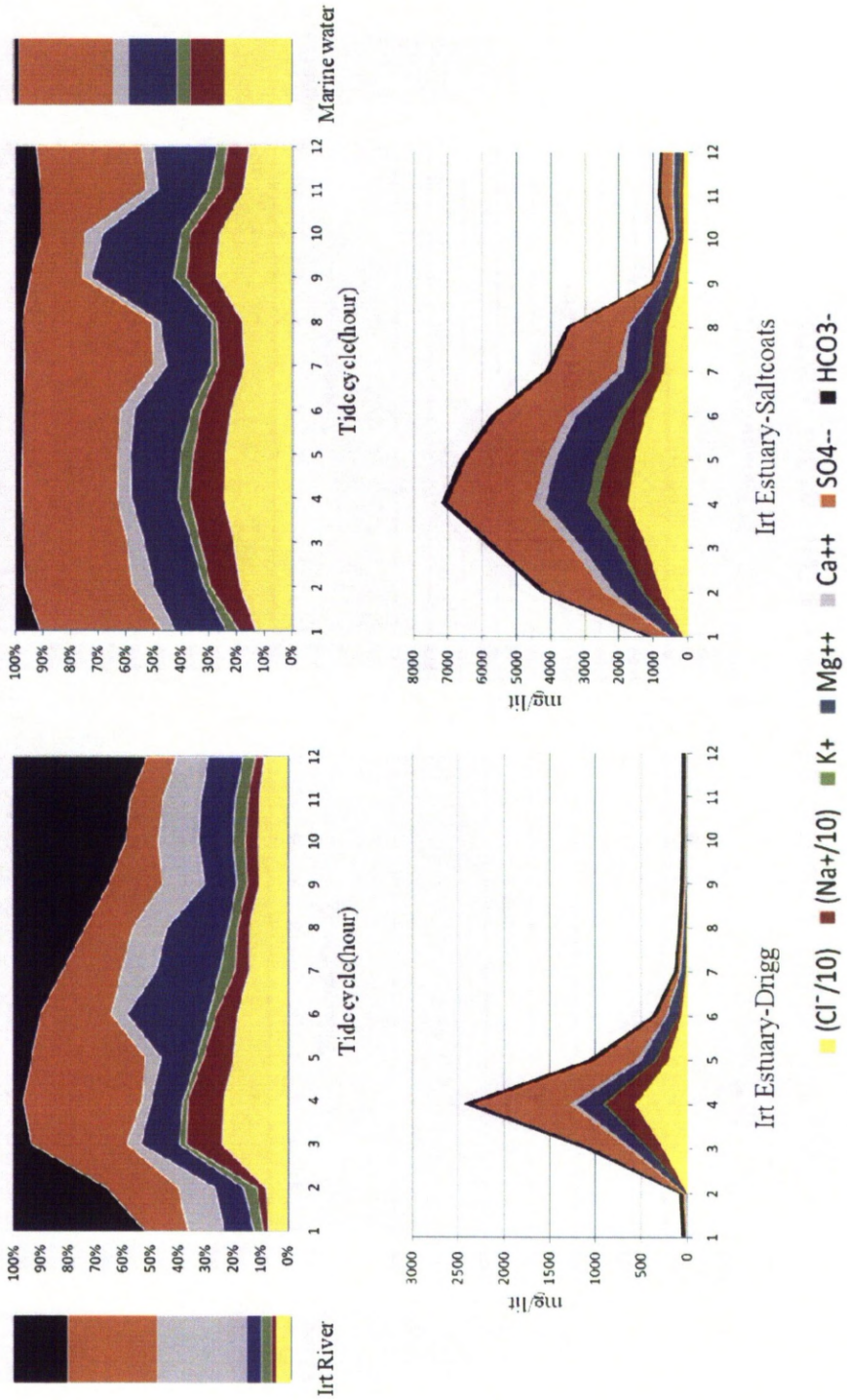

Figure 5.3c: Normalised and absolute concentrations of the common cations and anions at the two sampling stations on the Irt arm of the Ravenglass estuary; Saltcoats is towards the sea while Drigg is towards the head of the estuary. The sodium and chloride concentrations were both divided by ten to allow the variations of the other ions to be visible. The normalised data show how the relative concentrations vary with time; the absolute concentrations illustrate the timing of high tide and how quickly the sea water is replaced by river water at the two sampling stations.

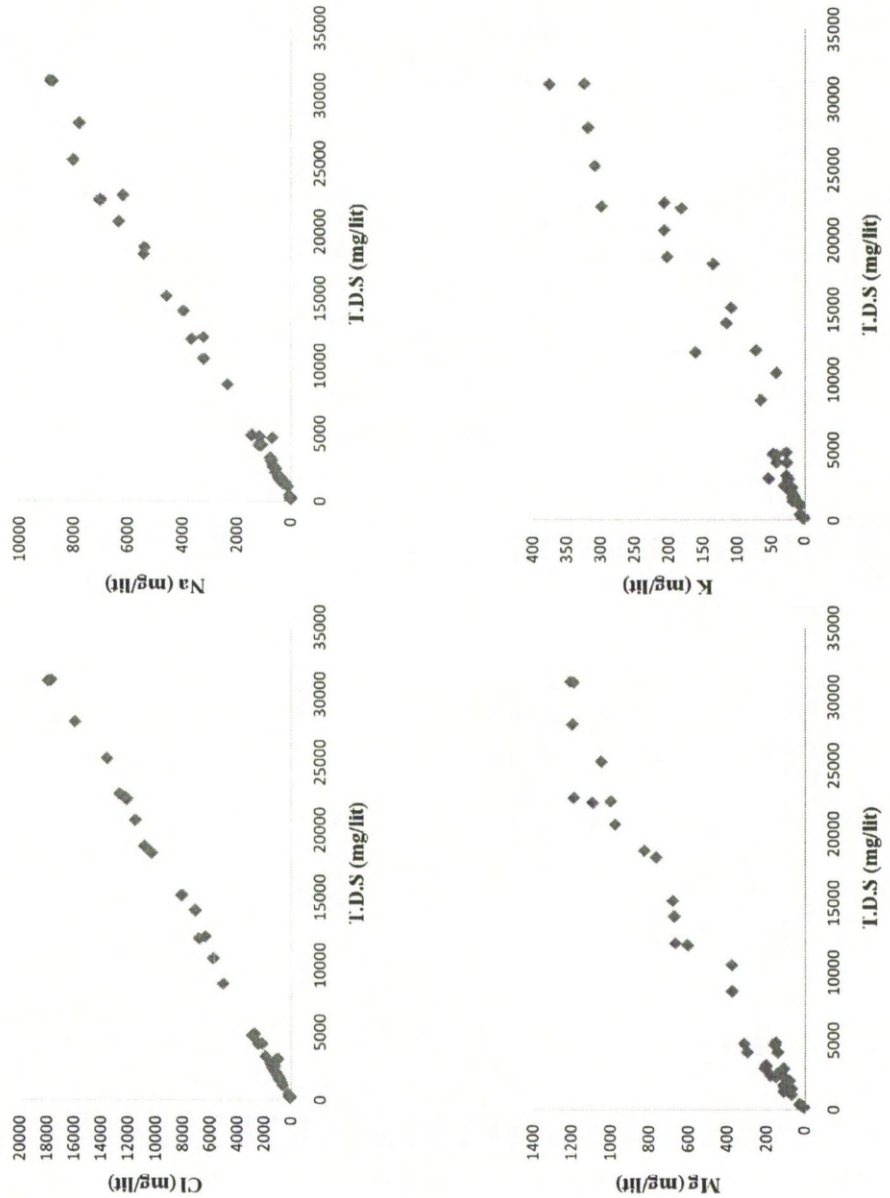

Figure 5.3d: Cross-plot of elemental concentrations (mg/L) versus calculated total solid dissolved (T.D.S) for all samples across the Ravenglass estuary. Chloride and sodium show a strongly linear increase in concentration with T.D.S; inevitable since they are the dominant anion and cation in almost all of the water.

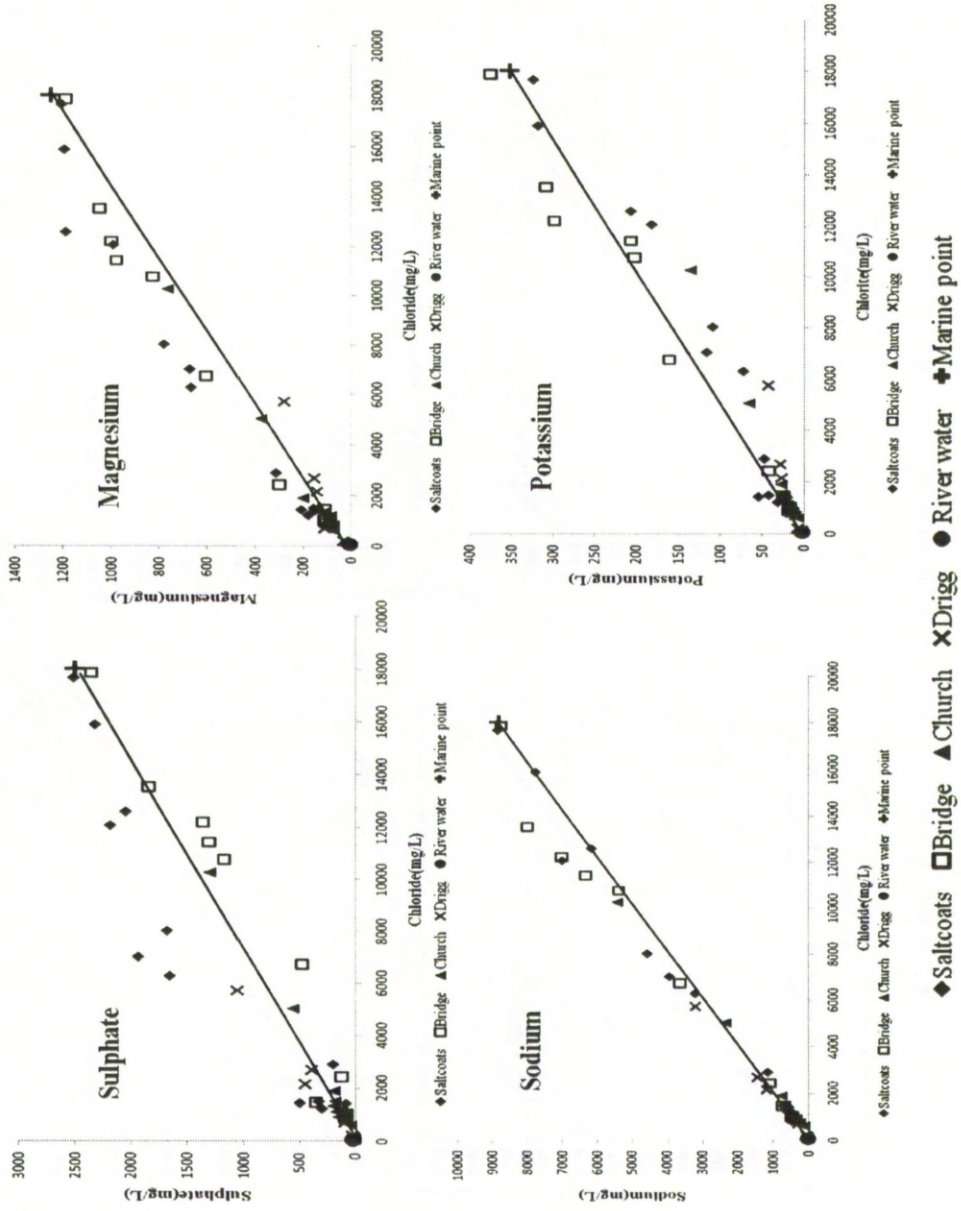

Figure 5.4-a: Ion concentration vs. chloride and modelled 1:1 correlation line that describes the theoretical conservative behaviour of each ion, at the Saltcoats and Drigg from Irt and Church and Bridge from Esk sampling stations. Calcium, alkalinity and Sulphate broadly show a non-conservative behaviour. Sulphate seems is taken from the water at the Esk and is added to the estuarine water at the Irt.

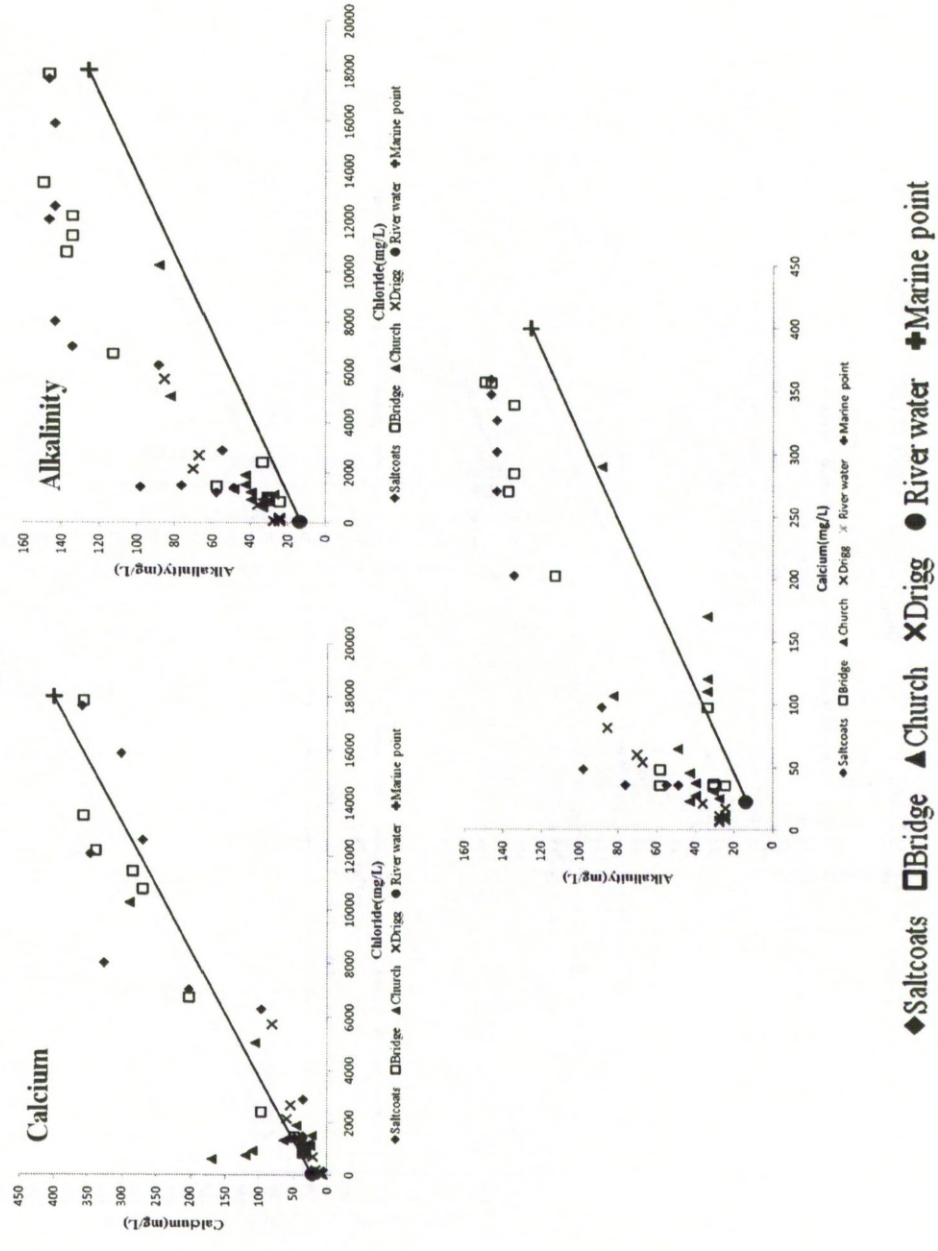

Figure 5.4-b: Ion concentration vs. chloride in association with alkalinity vs. calcium and modelled 1:1 correlation line that describes the theoretical conservative behaviour of each ion, at sampling stations on the River Esk (Bridge and Church) and River Irt (Saltcoats and Drigg).

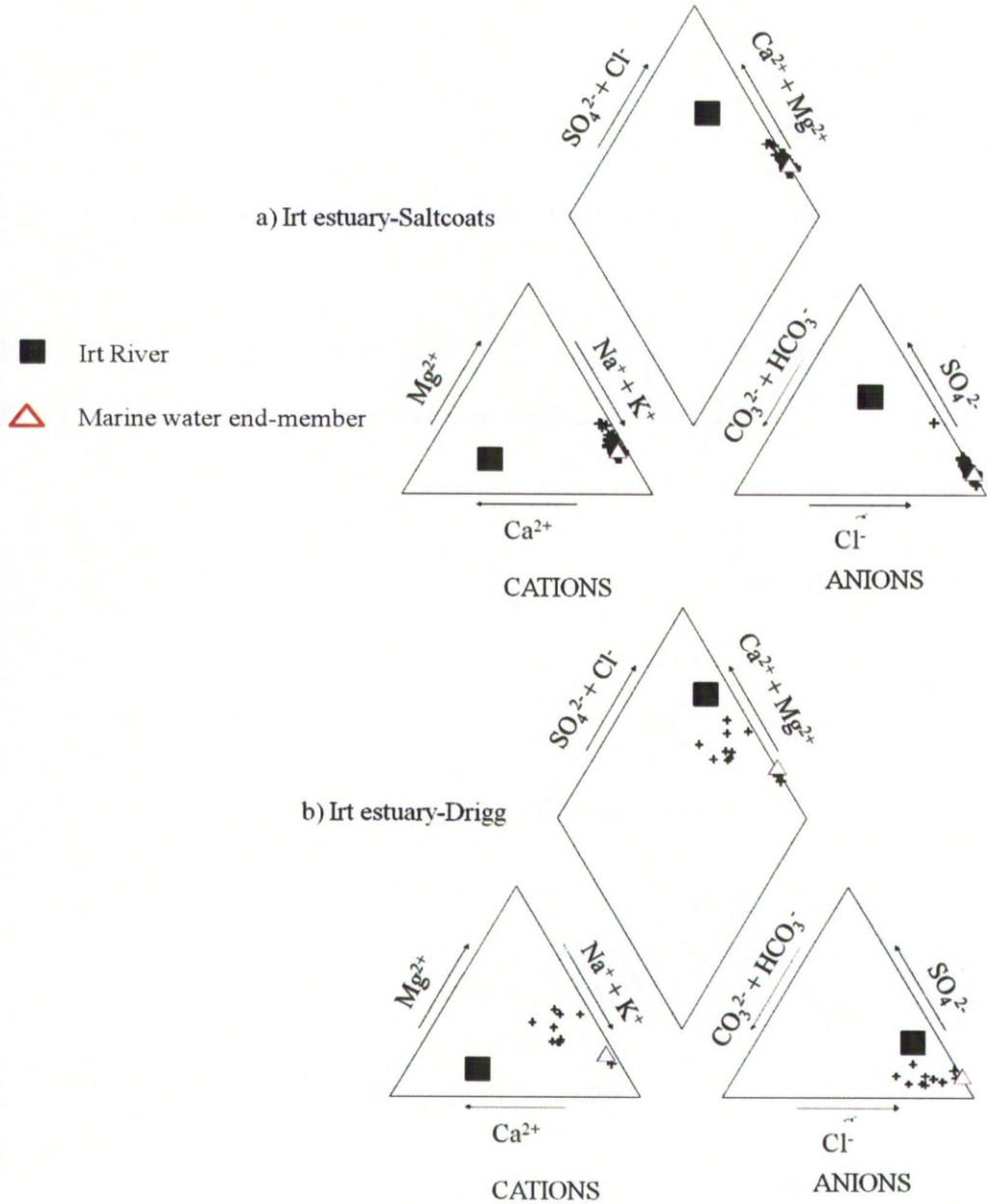

Figure 5.5, part 1: Piper diagram showing overall geochemistry and composition of estuarine water samples during tide cycle at the Irt estuary sampling sites. a) Saltcoats station, marine-dominated part of the Irt estuary is poor in calcium and magnesium at low-tide, overall sodium and chloride are dominated cations, b) Drigg, freshwater-dominated part of the Irt estuary is moderately poor in calcium and magnesium and chloride (except at high-tide).

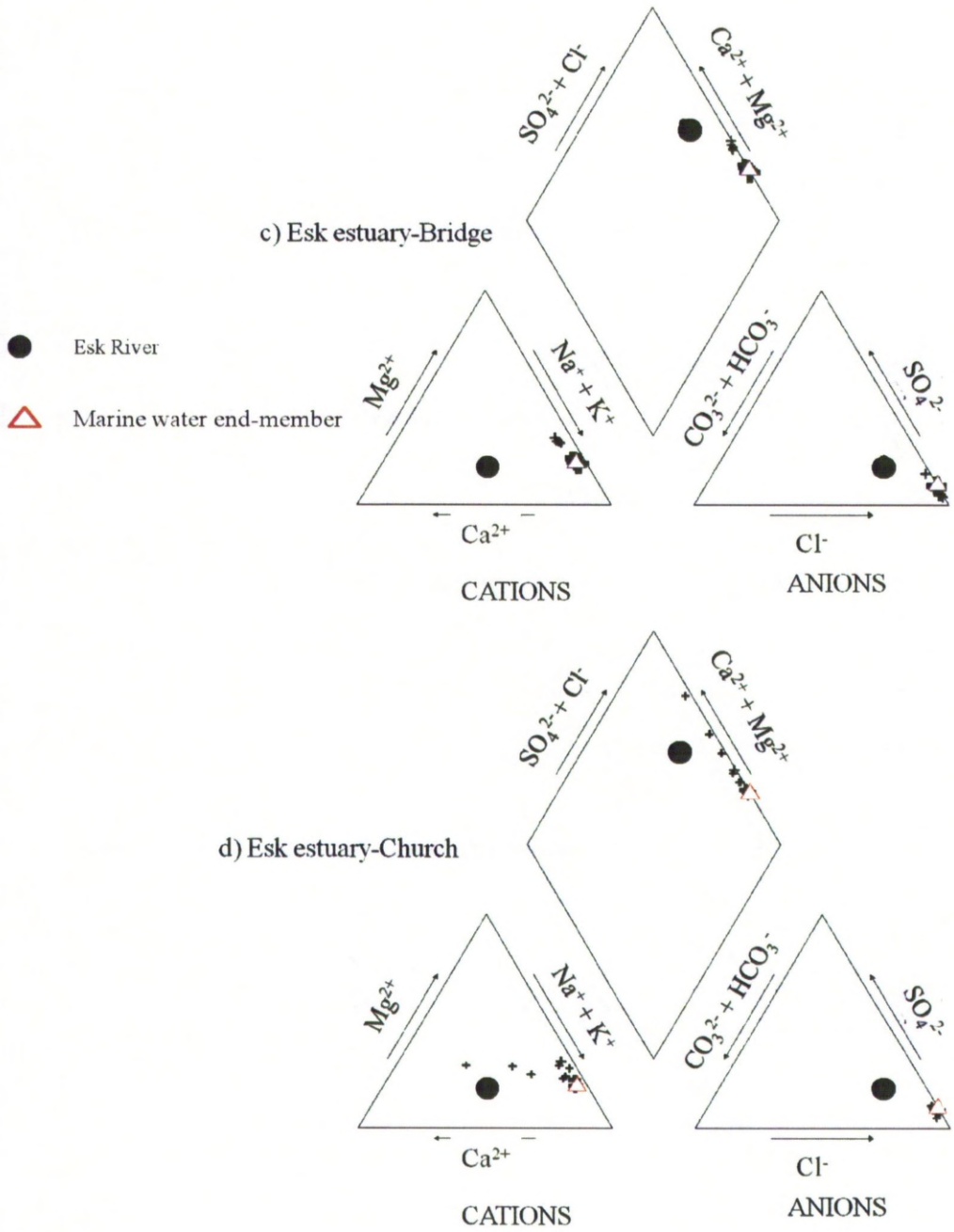

Figure 5.5 – part 2: Piper diagram showing overall geochemistry and composition of estuarine water samples during tide cycles at the Esk estuary sampling sites. c) Bridge, marine-dominated part of the Esk estuary is not rich in calcium and magnesium and it that seems chloride and sodium are the dominant ions, d) Church, freshwater-dominated part of the Esk estuary is slightly depleted with magnesium and rich in sodium and chloride.

5.5.3 Results of iron analysis

The fluvial samples had iron concentrations for waters (acidified to pH 3 and then immediately filtered, i.e. within 5 minutes) of 0.29 mg/L for the River Esk and 0.67 mg/L for the River Irt (Table 5.1). This method releases iron held in colloids and floccules and is a true representation of the amount of aqueous iron transported by the river. The marine-end member is assumed to have an iron concentration of 0.01 mg/L (Bousher, 1999; Table 5.1).

The estuary water samples were also treated in the same way for iron determination. The concentrations of iron, as a function of time through tide cycles at the four stations, are represented in Figure 5.6. For all stations in the estuary, high tide time sees the lowest iron concentrations confirming that the incoming seawater bears very little iron, as expected. For the Esk estuary, the estuary waters seem to have their highest iron concentrations between high and low tide. For the Irt estuary the highest iron concentrations seem to be at low tide, although there are elevated values between high and low tides for both stations on the Irt estuary.

Especially at the Esk-Church site, there is a crude inverse relationship between pH and iron concentration (Fig. 5.7). At high pH, the iron concentration tends to be low while at low pH, the iron concentration tends to be high.

The concentrations of iron in the estuary water samples have been plotted as a function of salinity (total dissolved solids; Fig. 5.8). This shows that high salinity estuary water equates to low iron concentrations. Conversely, low salinity estuary water samples have the highest iron concentrations. Seawater has a very low concentration of iron (0.01 mg/L; Table 5.1) and the river water have much higher iron concentrations (Table 5.1) so that the decrease with salinity in the estuary is not surprising. However, the estuary waters do not lie on a 1:1 conservative mixing line; they have much less iron than would be expected for this situation. Even by the time the estuary waters have mixed with 1/7 seawater (having a salinity of salinity of 5000 mg/L) they have lost the vast majority of their iron (transported in by the rivers). In the case of the River Irt (starting at 0.67 mg/L), the waters have lost 80% of their iron. Almost all the elevated iron concentrations are found in the up-estuary (river-dominated) sites at low to very salinity. The Esk-Bridge site appears to be slightly different to the other three sites having slightly elevated iron concentrations (e.g. in comparison to Irt-Saltcoats), but still having non-conservative behaviour relative to iron.

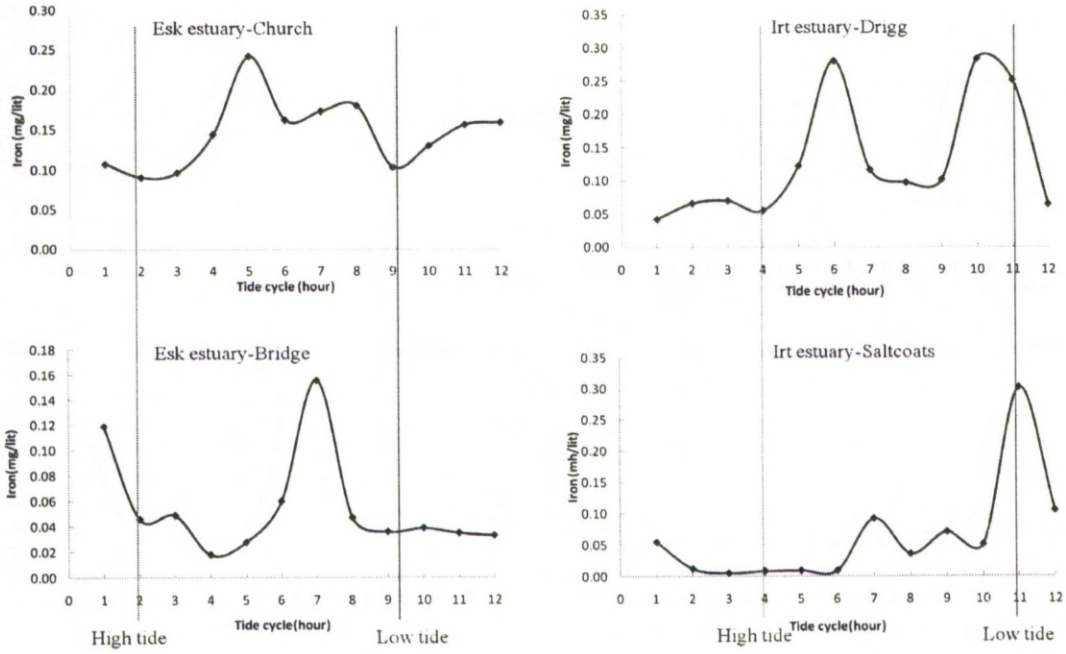

Figure 5.6: Iron concentration (mg/L) in the four Ravenglass estuary water sampling stations during tide cycles. Drigg station in the fresh water-dominated part (up-estuary) of the Irt estuary, iron concentration shows dissolved iron increases after high tide and the maximum concentration is at low tide. Saltcoats, marine water-dominated part (down-estuary) of the Irt estuary, dissolved iron concentration significantly is low at high tide (saline water) and increases toward low tide (fresh waters). Church, fresh water-dominated part (up-estuary) of the Esk estuary, dissolved iron concentration shows variation during the tide cycle with the maximum between high and low tide. Bridge, marine water-dominated part (down-estuary) of the Esk estuary, the highest dissolved iron concentration is before low tide and at high tide, dissolves iron is low as well. Overall, the maximum iron concentration in the Irt estuary system is about twice the iron concentration in the Esk part of the estuary. Also, dissolved iron concentration around high tide is low and increases towards low tide conditions.

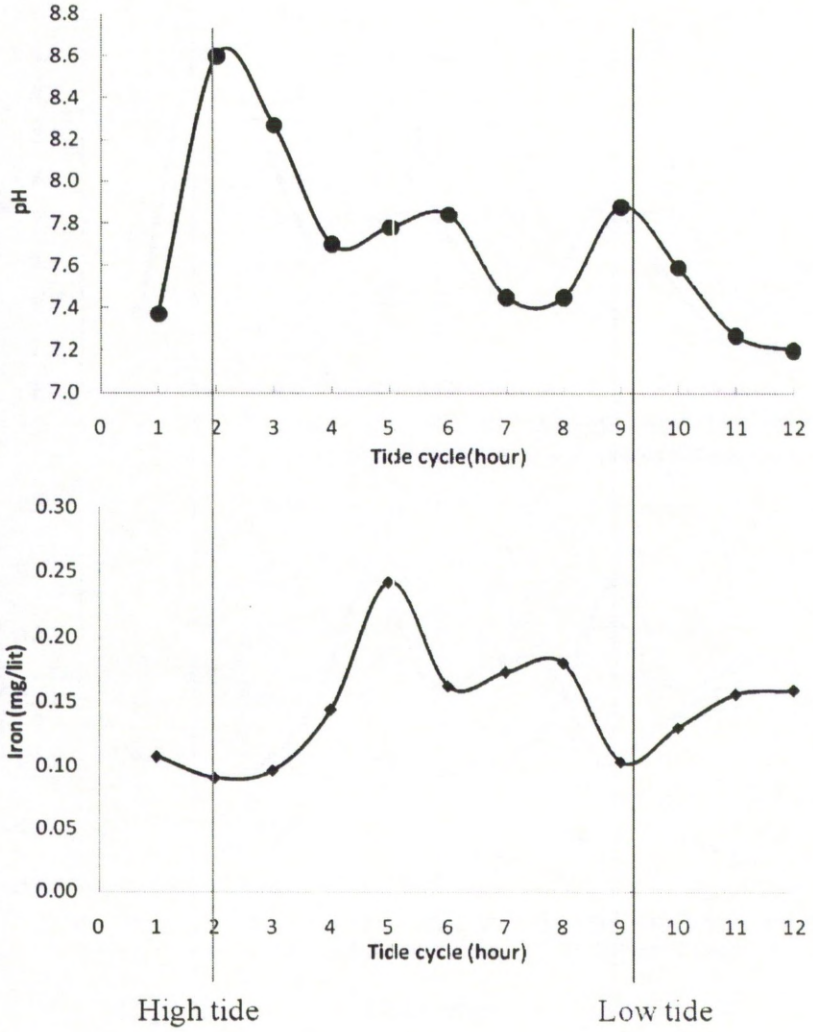

Figure 5.7: Relationship between pH and dissolved iron during a tide cycle in the estuary water at the Church station on the Esk estuary showing the maximum removal of iron from the estuary water occurs when the pH is highest.

Ions (mg/lit)	River Esk (Stock bridge)	River Irt (Santon bridge)	Marine point (Driggholme)
Na	9.41	11.27	8816.90
K	1.18	2.49	352.15
Mg	2.83	3.93	1252.15
Ca	8.82	22.33	399.85
Cl	24.40	40.55	18004.00
SO4	11.19	22.64	2497.10
Fe	0.29	0.67	0.01(filtered)
Alkalinity	10.01	13.80	125.5
pH	6.82	7.41	8.67

Table 5.1: Chemical composition of the end-members. Fresh water was collected beyond the high tide line in each estuary and a marine sample, Stockbridge on the Esk River, Santon Bridge on the Irt River and a coastal path from the Drigg LLNW site for the marine point (marine Fe concentration taken from Bousher, 1999). The fluvial Fe concentrations are from samples that were acidified to ~pH 2 and then filtered through a 0.2 μm filter.

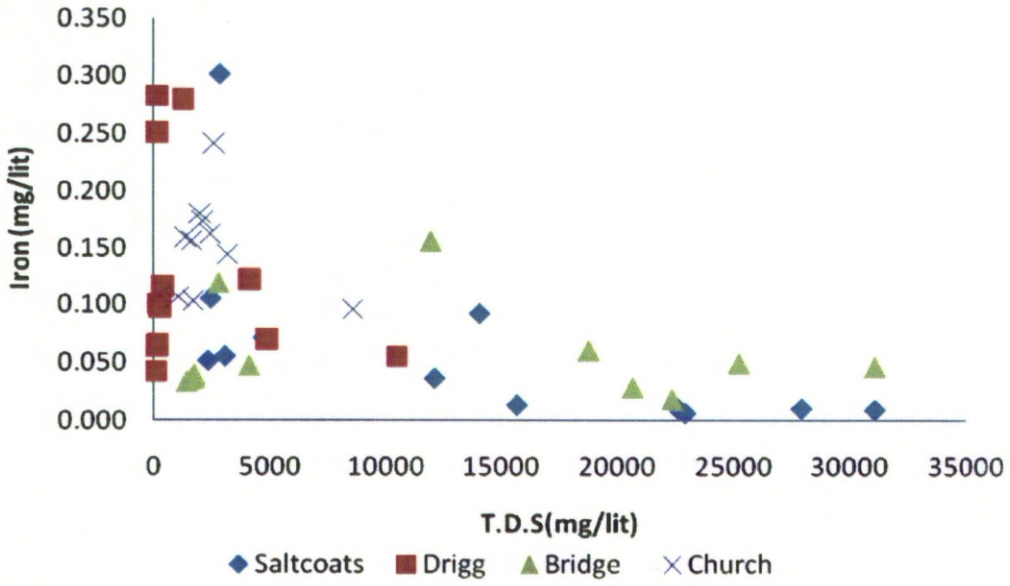

Figure 5.9: Iron concentration *vs.* calculated salinity (total dissolved solids: T.D.S.) for four stations across the Ravenglass estuary. Overall iron behaves non-conservatively in the Ravenglass estuary since the data plot below a mixing line between seawater (35,000 mg/L salinity and 0.01 mg/L iron) and river water samples with their salinity of <100 mg/L and iron concentrations of 0.29 to 0.67 mg/L.

5.6 Discussion

5.6.1 Controls on estuary water geochemistry

Salinity and conservative species (chloride, sodium and possibly magnesium and potassium) increase and decrease in concentration through the tide cycle (Figs. 5.3a, b and c). At high tide, the estuary water at the Esk-Bridge and Irt-Saltcoats sites effectively is pure seawater. The upper estuary Esk-Church and Irt-Drigg sites achieve lower maximum concentrations and overall salinity than the lower estuary Esk-Bridge and Irt-Saltcoats sites.

At high tide, the upper estuary Esk-Church and Irt-Drigg sites have species proportions that makes the estuary look like seawater (compare the marine species proportions on the right of Figs. 5.3b and c to the high tide species proportions at these sites) suggesting that a simple seawater-river water mixing process has occurred (Ixer et al. 1979; Bull and Hall 1986). Although at low tide, the Esk-Church and Irt-Drigg sites fall to very low salinities, the estuary waters are not the same as the incoming river waters in terms of species proportions. Thus, the Irt-Drigg site has an excess of alkalinity suggesting that HCO_3 has

been added, for example by biological processes, while the Esk-Church site approaching high tide has a shortfall of alkalinity and an excess of calcium suggesting that HCO_3 has been removed, for example by calcite precipitation processes.

Sulphate concentrations also seem to be non-conservative with possible relative decreases after high tide at Esk-Bridge especially (Figs. 5.3b and 5.4) and with a possible relative increase at Irt-Saltcoats (Figs. 5.3c and 5.4). Sulphate could be lost from the water by bacterial sulphate reduction (Burton and Liss 1976) leading to the creation of sulphide species and the possible growth of Fe-sulphide minerals. Thus apparent loss of aqueous sulphate could be important since it potentially influences iron geochemistry. Conversely sulphate could be added to the estuary water by oxidation of sulphide minerals (e.g. during sediment erosion down to the redox interface in the sediment) with the concomitant possible release of iron to get involved with non-sulphide geochemical processes.

The non-conservative behaviour of iron on mixing river water with seawater has already been established (Fig. 5.8). This is not surprising since a similar pattern has been illustrated for several other estuaries (e.g. Mayer, 1982) The possible controls on the relative loss of iron and its relationship to water geochemistry, the position this occurs in the estuary and the timing of iron loss during the tide cycle will now be discussed.

5.6.2 Salinity and iron removal

Salinity has an important effect on the surface charge and stability of the colloidal particles; in saline waters, Fe-colloids lose their charge and become less repellent to each other (Mayer 1982; Escoube et al. 2009). It has been suggested that iron agglomerates to form colloids during the mixing of river water and seawater (Sholkovitz 1978; Mayer 1982). Iron concentrations in the River Irt and the River Esk fall as soon as they mix with any estuary water suggesting that elimination of iron from the water thus happens at the earliest stage of rivers entering estuaries, i.e. relatively high up the tidal creeks and channels (Fig. 5.8). River water-seawater mixing occurs at different positions in the estuary as a function of the tide cycle; dissolved iron concentrations at a given site are lowest at high tide (Fig. 5.6). Thus as saline estuary sweeps up the tidal channels at high tide, the point of Fe-loss will also presumably sweep up the tidal channels.

5.6.3 pH and iron elimination

Elimination of dissolved iron by flocculation and precipitation of iron oxides and hydroxides has been reported to be a possible result of increasing pH (Sholkovitz 1978) as

well as salinity (ionic strength). Higher pH values, such as found in seawater relative to river water (Table 5.1), increase the chance of generating solid-phase ferric iron oxide or hydroxide, thus eliminating iron from the water as a direct result of pH change (Sholkovitz 1978). At pH values below 6.5 the oxidation rate is slow, thus when relatively low-pH river mixes with higher-pH marine water, iron is oxidized and precipitated as hydrated ferric oxide (Boyle et al. 1977b; Sholkovitz 1978). pH at high tide tends to be higher than low tide all across the Ravenglass estuary and it is compatible with iron elimination from the water in the estuary at high tide conditions.

5.6.4 Flocculation

Despite the possible role of redox processes, the oxidation of ferrous iron has been reported to be an insignificant mechanism for iron removal in estuaries (Boyle et al. 1977b; Fan et al. 2008). Conversely, flocculation is typically concluded to be the main mechanism of removal iron in the estuaries (Sholkovitz 1976; Boyle et al. 1977a; Sholkovitz et al. 1978; Sholkovitz 1979; Mayer 1982). In this matter, high tide at all stations has the highest pH and salinity, the flocculation and loss of iron in the form of oxide or hydroxide can happen (Balls et al. 1994) (Fig. 5.6 and 5.8). Small and therefore light floccules potentially remain suspended in the estuary water and may be taken out into the sea at low tide. Irt and Esk Rivers supply relatively large amounts of dissolved iron (Table 5.1) to their estuaries and because of the dimension of the estuaries (small estuaries), high energy environments, and variation between high and low tide, the suspended iron floccules can be transported and some of the settled floccules may be washed down the tidal channels and creeks towards the sea at low-tide, and then be flushed back to the estuaries during a rising tide. The River Irt supplies almost twice as much dissolved iron to the estuary relative as the River Esk (Table 5.1).

Dissolved iron concentrations in the Irt at Drigg and Saltcoats fall dramatically at high tide (down to <0.05 mg/L), presumably due to the creation of abundant floccules (Fig. 5.6, 5.8). Elimination of iron in the Esk estuary also shows a drop from fresh water to the saline water, however, the collapse of dissolved iron concentration during high tide is not as dramatic as the Irt estuary possibly because less iron is being supplied by the Esk. The presence of dissolved iron in the marine-dominated part of the Esk estuary (Bridge) soon after high tide, and at a similar time of the river water-dominated Esk-Church site, may be due to the transport of abundant Fe floccules, produced in the Fe-rich Irt at low tide and transported down tidal channels and creeks, then being flushed into the Esk arm of the

estuary by the incoming tide. The Ravenglass estuary is a macro-tidal estuary, with a tidal range of over 7m on spring tides and also the estuary has relatively high tidal discharges and velocities (Bousher 1999), but the rivers that feed into it have relatively low discharges (Assinder et al. 1985). Consequently tidal discharges and velocities in the Ravenglass estuary are relatively high (Assinder et al. 1985), resulting in the penetration of seawater (and mixed seawater-and outgoing Irt River water) far up the Esk arm of the estuary. The saline state persists for long periods after high tide in the middle reaches of the estuaries especially in the Esk estuary Bridge (Fig. 5.3b) but also in the Irt estuary (Fig. 5.3c).

An association between dissolved iron and dissolved organic matter (humic acid) (Fox 1983)in terms of the aggregation of the iron colloids has been reported (Sholkovitz 1976; Ouddane et al. 1999) and also significant role of cation exchange capacities on organic matter flocculation and iron aggregation have been revealed (Sholkovitz 1976). The greatest removal of dissolved iron in the Ravenglass estuary occurs as TDS approaches ~5000 mg/L (Fig. 5.11; (Sholkovitz 1976; Mayer 1982; Assinder et al. 1985).

Iron rich colloids that are flushed from the rivers out into seawater-influenced estuary and altered to aggregates and floccules must be removed from the water column by gravitational settling. The iron leaves the aqueous part of the system once salinity exceeds ~5000 mg/L and the pH starts to increase and presumably becomes part of the sediment (mineral) part of the system.

5.6.5 Sulphate-iron geochemistry

It was noted that sulphate concentrations are relatively depleted in parts of the Ravenglass estuary in comparison to conservative mixtures of seawater and river water (Fig. 5.3b and c, Fig. 5.4). It was concluded that this may be due to localised bacterial sulphate reduction converting sulphate into sulphide. Comparison of dissolved iron and sulphate concentrations (Fig. 5.9) shows that there is a pattern rather similar to the iron-TDS diagram (Fig. 5.8). High iron concentrations are only possible at low sulphate concentrations. It is interesting to speculate that elevated sulphate concentrations leaves the possibility of elevated sulphide concentrations so that at least some dissolved iron may be lost from the water by Fe-sulphide mineral formation. At present the mineral (or at least solid) form of the flocculated iron remains unknown so this possibility cannot be assessed further.

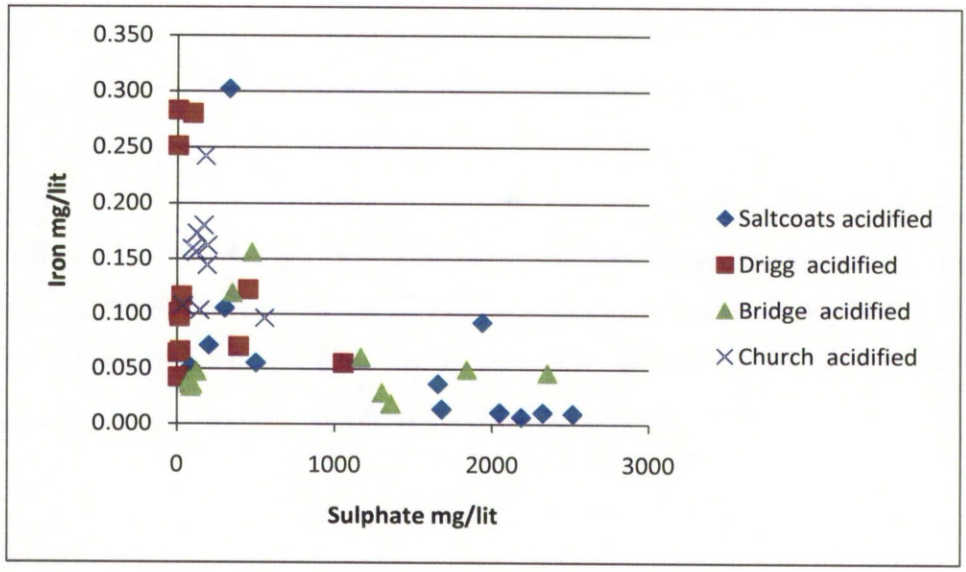

Figure 5.9: Iron concentration *vs.* sulphate concentration for four stations across the Ravenglass estuary. Elevated iron only occurs when sulphate concentrations are low, possibly due to the increased opportunity for sulphate reduction and the creation of Fe-sulphide phases.

5.7 Conclusions

1) In the lower to middle reaches of the Ravenglass estuary at high tide salinity reaches seawater values and remains elevated long after high tide but then falls to very low values at low tide. Salinity reaches between a quarter and a half of seawater salinity about 1km further up-estuary and quickly falls back to low values soon after high tide.
2) Ravenglass estuary water is a conservative mixture between river water and seawater as far as chloride, sodium, potassium and magnesium are concerned, Alkalinity is non-conservative and is added, probably by biogeochemical processes, in the estuary, Calcium is also non-conservative, possibly being lost from the water (as alkalinity increases) due to calcite growth (possibly as shells), Sulphate is present in seawater-like proportions at high but may be lost from the water at low tide, possibly by sulphate reduction processes. It is also possible that there is local sulphate addition, possibly by sulphide mineral precipitation.
3) Iron concentrations are lowest at high tide at all sampling sites on the Ravenglass estuary. Iron concentrations are highest at low tide for the Irt arm of the estuary but are highest on the falling tide between high and low tide

4) The River Irt contains twice as much dissolved iron as the River Esk. Iron concentrations are much lower in the estuary samples than in the feeding rivers so that dissolved iron undergoes large-scale accumulation in the Ravenglass estuary.
5) Iron concentrations in estuary samples decrease rapidly as salinity increases with low iron concentrations in all estuary samples once salinity exceeds 5,000 mg/L. Iron concentrations also decrease as pH increases. The loss of iron is presumably due to flocculation of colloidal iron oxides, hydroxides and iron-organic complexes as increasing salinity reduces the surface charge of colloids and thus permits aggregation. It is also possible that sulphate reduction may locally lead to Fe-sulphide creation within the estuary.
6) Fluvial dissolved iron does not behave conservatively on mixing with seawater; most iron is lost from the water column at an early stage of river water mixing with estuary water. The site of primary iron-loss from the water occurs towards the heads of estuaries but this site will move as a function of time within the tide cycle.
7) Given that the Esk has highest iron concentrations between high and low tide, it is likely that iron, either dissolved or as fine floccules, is swept from the iron-rich Irt arm of the estuary into the iron-poor Esk arm soon after high tide.

Chapter 6

Chapter 6 Suspended clay minerals in the Ravenglass estuary; origin of the clay minerals, their variation during tide cycles and comparison to fluvial suspended clay minerals

6.1 Abstract

Rivers Irt and Esk are the major sediment transporters to the Ravenglass estuary in northwest England. X-ray diffraction (XRD) analyses the oriented particles from the suspended materials from riverine, estuarine, and marine waters show that clay minerals chlorite and hydroxyl-interlayer vermiculite with minor illite are transported from the hinterland to the estuary. Chlorite, illite, kaolinite and possibly berthierine are present within the estuarine water. Chlorite in the fluvial suspended load is dioctahedral, while in the estuary water it tends to trioctahedral chlorite. Kaolinite and berthierine are not present in the river water suspended loads beyond the high tide line. Kaolinite is an *in situ* clay mineral and also increasing illite content in estuarine suspended matters suggesting illite has at least two origins: authigenetic and detrital. Chlorite has two sources in the estuary suspended clays; dioctahedral chlorite is transported from the hinterland via the rivers into the estuary while trioctahedral chlorite seems to be generated *in situ*, presumably in the sediment column, and then mobilised by flood tides. The seawater suspended clay minerals seem to have more kaolinite and less illite than the estuary suspended sediment samples. Also, the seawater chlorite is slightly less Fe-rich than the estuary chlorite, or possibly there is less berthierine in the seawater than the estuary samples. High tide conditions at the more seaward sampling sites in the estuary have the lowest clay content suggesting that seawater, via the incoming tide, does not bring much clay mineral material into the estuary. The incoming tide seems to flush clay-rich waters up stream to the heads of the estuary. The relative proportions of clay minerals do not vary significantly as a function of tides.

6.2 Introduction

A major objective in the study of estuarine clay mineral distribution and sediment is to establish the nature and origin of the estuarine and fluvial suspended materials (Sholkovitz 1979). Suspended material in estuarine water systems comes from many sources (Milliman et al. 1985; Fenn and Gomez 1989). Inorganic material can be sourced from river runoff, from coastal erosion, and from re-suspension of previously deposited sediments from the

surface sedimentary environment of the estuary (Eisma and de Boer 1998). Organic matter is produced mainly in the estuary waters themselves (Meade et al. 1975), and also comes from the hinterland (Sholkovitz 1976). The combination of processes and parameters vary widely in space and time within an estuary and produces a broad range of sedimentary structures. Some researchers have suggested that the identification of specific mineral and chemical fractions of suspended material may be useful as indicators of sedimentological processes in estuaries (Meade et al. 1975; Wiley 1978; Sholkovitz 1979; Zhang et al. 1990).

One of the main problems in understanding the suspended sediment in estuarine waters is the identification and discrimination of material from different sources. Measurement and analysis of the suspended material and sediment mineralogy can reveal the prevalence of fluvial versus marine sources in the supply materials to estuaries (Meade et al. 1975; Sholkovitz 1979). The role of the clay minerals in estuaries has been well documented (Gibbs 1977; Berner 1980; Petschick et al. 1996; Worden and Morad 2003a; Schmid et al. 2004; Sionneau et al. 2008) and the identification using X-ray diffraction (XRD) of transported clay minerals to the estuary as suspended material or wash load can be a way to reveal sedimentary-geochemical (diagenetic) processes in estuaries. X-ray diffraction is the most commonly-employed technique to detect and discriminate clay minerals. Chlorite(002) and kaolinite(001) with a ~7Å basal spacing and chlorite (001) with a ~14Å basal spacing and illite with a ~9.9° basal spacing are theoretically distinguishable in XRD patterns (Moore and Reynolds 1989; Hillier 2003; Manning 2003). Filtration of estuary waters and XRD analysis of the materials deposited on the filter paper is a practical approach to start studying clay mineral distribution, transportation and alteration in estuaries.

The estuary selected for study in this case was the Ravenglass estuary in Cumbria (UK). The Ravenglass estuary is a local name for an area that encompasses the tidal reaches of the three rivers: Esk, Irt and Mite. The Esk River drains the Eskdale granite and the Irt drains Triassic sandstones (Fig. 6.1). The minor Mite River drains a combination of Borrowdale Volcanic Group (mainly andesitic), Eskdale granite and Triassic Sherwood Sandstone Group sandstones (Ixer et al. 1979). Water samples from the Ravenglass estuary were collected at various sites regularly through the tidal cycle from the freshwater end-members, upper estuary stations (freshwater dominated), lower estuary stations (marine dominated) and marine end-member.

The main questions being addressed by this work were:

1) What clay minerals are transported into the Ravenglass estuary by the rivers? Are different clay minerals transported by the two main rivers?
2) What clay minerals are in suspension in the Ravenglass estuary?
3) Do clay minerals in suspension in the estuary vary as a function of time during a tide cycle? Are different clay minerals found at different sites within the estuary?
4) How do the clay minerals in the estuary (and its feeding rivers) relate to what is found in the nearby marine setting?
5) What is the origin of the clay minerals and their distribution pattern in the Ravenglass estuary?

6.3 Materials and methods

6.3.1 Field sampling and collection of suspended clay fraction from water samples

A water sample from Irish Sea (the marine-end member) was collected about 1000 m north of where the Ravenglass estuary meets the sea (Fig. 6.1, Driggholme beach before Sellafield nuclear site). River water samples were taken from both the River Irt (at Santon Bridge) and the River Esk (at Stock Bridge; Fig. 6.1) at two different times. The first river water sampling session occurred during the same sampling mission as the estuarine water and marine end-member during fair weather conditions; the rivers were not in flood at this time. The second river water sampling session was performed during a period of high rainfall will the rivers were in flood.

Water samples were collected from the Ravenglass estuary at four sites through a full tidal cycle. Two stations on the Irt estuary (Saltcoats and Drigg) and two stations on the Esk estuary (Bridge and Church) were chosen. Stations were selected to sample the marine-dominated and the river-dominated parts of the two estuaries. Twelve estuarine water samples were taken at the rate of one an hour to cover the full range of tidal conditions within the estuary.

Water samples were initially collected in 1 gallon polythene canisters by wading out into the estuary until the water depth was about 1m. These canisters were half filled with the water from the site and then capped, shaken and emptied. The canisters were then filled to the brim by immersing the neck about 50 cm below the water surface. The canisters were

capped and taken to a mobile laboratory (the back of a Ford Transit van) for processing. Note that working in estuaries carries particular risks and suitable personal protective equipment was employed during sample collection including; chest-high waders, life jacket, and, in some cases a rope held firmly by a colleague standing on the bank of the estuary.

All water samples were filtered in the field within 20 minutes of collection. 500 ml of raw water, shaken prior to filtering, was poured into the top part of a NALGENE filtering assembly. A vacuum was applied using a Fisher Brand pump, powered by the Transit van battery and the water was drawn through a 47mm diameter, 0.2μm Whatman cellulose nitrate filter. Suspended material remained on the cellulose nitrate filter paper. This filtering process was carried out in duplicate to produce 1000 ml of filtered water and two sets of filter papers for each site. 500 ml of raw, unfiltered, water was collected for further processing in the laboratory. This water sample was frozen in the laboratory until further treatment was required. Cellulose nitrate filter papers were stored for direct analysis by XRD techniques. In addition to analytical processes on the cellulose nitrate and silve filter papers, they are weighed individually for further statistic and hydrological investigations (Appendix 2).

6.3.2 Laboratory separation of clay fraction from water samples

Direct X-ray diffraction analysis of the cellulose filter papers led to a noisy background and contributed a broad pair of humps between about 9 and 50° 2theta using Cu K_α radiation leading to potential problems for interpretation of the XRD traces. Several samples of raw, untreated (unacidified, unfiltered) estuary and river water samples were filtered in the laboratory, using 0.2μm Sterlitech silver filters. The filtrate on these silver filters were also analysed directly by X-ray diffraction. In contrast to the cellulose filters, the silver filters resulted in no additional background noise and only a few very sharp peaks derived the metallic silver. An additional major benefit was that the silver filters could be glycolated and heated to at least 550°C enabling full characterization of the clay minerals while the cellulose filters could not withstand these clay treatment steps. The extra cost of the silver filters is their only disadvantage relative to the cellulose filters.

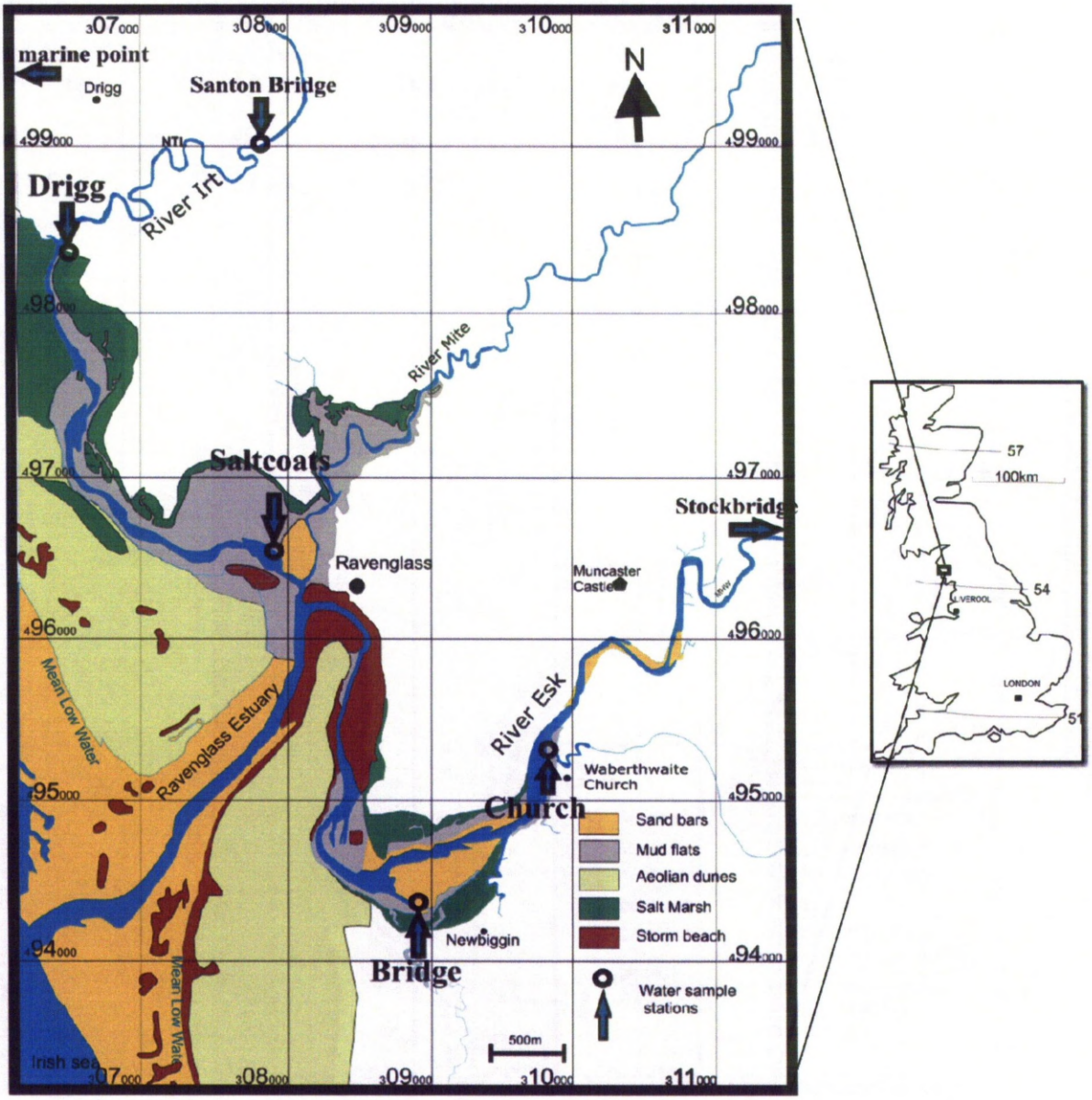

Figure 6.1: Location map of the Ravenglass study area, showing the main estuary and the sub-estuaries; Esk and Irt estuaries and water sampling localities

6.3.3 X-ray diffraction analysis

An X-ray diffractometer (XRD) was used to examine the clay separate samples on both the cellulose and silver filters. All samples were analysed by XRD using a PANalytical X'Pert Pro MPD X-Ray Diffractometer. Cellulose filters could not be treated by, for example, heating to 400C so that only air-dried XRD analysis was possible. Filtrate samples prepared in the laboratory after the field work using silver filters could be processed in a variety of ways due to the durability of the silver in comparison to the cellulose. Clay fractions of suspended sediment samples were thus prepared for X-ray diffraction in four ways: (1) air dried, (2) Mg-saturated and then glycolated, (3) heated for one hour at 400°C and (4) heated for one hour at 550°C. The cellulose and silver filters were placed directly onto standard sample holders and placed in multisample holder racks for analysis.

A copper X-ray tube at 40kV and 40mA was used for XRD analysis in this study. The sample holders were rotated continuously during the scan, completing one rotation every 2 seconds. Programmable anti-scatter slits and a fixed mask maintained an irradiated sample area of 10x15mm, with an additional 2° incident beam antiscatter slit producing a flat background in raw data from 3.60°. Scans covered the 2Theta range of 3.66-70.00° over a scan time of two hours and fifty nine minutes, with 0.04 Rad Soller slits in both the incident and diffracted beam paths. The X'Celerator detector was set to scan in continuous mode with full length active and pulse-height discrimination levels set to 45-80%. Operation of X-Ray Diffractometer and Software was set using a "HighScore Plus®" analysis software. With reference patterns from: International Centre for Diffraction Data, Powder Diffraction File-2 Release 2008.

6.3.4 Processing X-ray diffraction data

Quantification of clay minerals was based on the intensity (area) of XRD peaks at ~14Å (~6.2°), 9.9Å (8.9°), ~7.15Å (~12.3°) and 7.07Å (12.5°). Rietveld refinement was not used for quantification given the low degree of crystallinity of much of the clay grade material and because of problems of variable clay mineral composition (and thus lattice dimensions). The 6.2° peak represents chlorite(001) and possibly a vermiculite phase. The 8.9° peak represents illite and muscovite(001). The 12.3° peak represents kaolinite(001). The 12.5° peak represents either chlorite(002) or berthierine(001) (or a combination of the two). It was decided to use both the ~6.2° and 12.5° peaks in this

approach since it is possible that both berthierine and chlorite are present in these samples. If the intensities of the ~6.2° and 12.5° peaks were to vary uniformly with location and time (at each location) then berthierine could be concluded to be absent. If the ~6.2° and 12.5° peaks do not vary sympathetically, this could be the result of either (1) the variable presence of berthierine or (2) chlorite becoming more or less Fe-rich. Whichever of these two options is correct, variation of the ~6.2° and 12.5° peaks certainly reveals informations about the relative abundance of Fe-rich clay minerals.

Peak deconvolution of air-dried traces and calculation of peak areas was carried out using the X'pert HighScore Plus 2.2.3. This software is produced by PANalytical B.V. and is licensed to the University of Liverpool. The first task was to deconvolute the overlapping 12.3° and 12.5° peaks and then calculate the areas of these peaks. Next the areas of the 6.2° and 8.9° were calculated. Assuming that the chlorite was Fe-rich led to a correction being applied to the chlorite(001) peak intensity (multiplied by a factor of three given the relative intensity of chlorite(001) to the maximum intensity trace of this mineral; Hillier, 2003). The next step was to sum the intensities of the ~6.2° (corrected), 8.9°, ~12.3° and 12.5° peaks and then determine a relative proportion for each. This approach assumes that each "mineral" has a equal ability to diffract X-rays (uniform RIR factor). The relative area (approximately equivalent to relative proportions) of the four peaks can then be plotted as a function of time and compared between cores.

6.4 Results

6.4.1 Estuarine tide-cycle samples

XRD analyses of air-dried, cellulose filter samples of estuarine suspended sediment, the river water-end member (flood time) and marine-end member all revealed a series of peaks at 6.2°, 8.9°, and a pair of peaks at 12.3° and 12.5°. Twelve sets of filtrates of the suspended sediment samples from each complete tide cycle were analysed by XRD for each station. X-ray diffraction analyses of the suspended materials on filter paper are presented in Figures 6.2 (Esk estuary), and Figure 6.3 (Irt estuary). There are clay mineral peaks at 6.2° (chlorite 001), 8.9° (illite 001), 12.3° (kaolinite 001), 12.5° (chlorite 002 and/or berthierine 001), 24.9° (kaolinite 002) and 25.2° (chlorite 004 and/or berthierine 002). The stacked scans of the filtrates sample at Saltcoats (Fig. 6.3a), Drigg (Fig. 6.3b)

and Bridge (Fig. 6.2b) show the intensity of the clay mineral peaks relatively decreases from low-tide to high-tide. Given that all samples were collected in exactly the same way and all analyses were performed under the same conditions for the same length of time, this change in intensity suggests a change in absolute quantities of clay minerals in the suspended sediment. There is an additional peak at 11.8° on the high tide XRD scans which represents gypsum (Starkey et al. 1984). Gypsum is a marine indicator mineral which is understandably present on the filters from marine waters and estuarine high tide samples.

6.4.2 River water end-member samples

XRD scans of a trend from river water under flood conditions, river water under quiet flowing conditions, estuary at low tide and estuary at high tide for four stations are presented (Figs. 6.4 and 6.5). Clay minerals in fresh water samples (normal day under quiet flowing conditions) from the Esk River, appear to be below detection limit (Fig. 6.4). For the sample from the River Irt, clay minerals seem to be present in very small quantities (Fig. 6.5). XRD analyses of samples from the Esk River under flood conditions (Fig. 6.4) show small peaks at 6.2° (chlorite 001) and 12.5° (chlorite 002) and small hint at 8.9° which represents illite (001). XRD analyses from samples from the Irt River water sample during flood conditions (Fig. 6.5) show significant peaks at 6.2° (chlorite 001), 8.9° (illite 001), 12.5° (chlorite 002) and 25.2° (chlorite 004). Kaolinite peaks for all fluvial suspended sediments are below detection although the XRD analyses of the low tide suspended estuarine samples all across the Ravenglass estuary, show that kaolinite is present in the estuary even at low tide (Figs 6.4 and 6.5).

6.4.3 Analysis of estuary and marine samples on silver filters

The X-ray diffraction analyses of the suspended sediment filtrate, separated using silver filters, are presented in Figures 6.6, 6.7 and 6.8, taken from two locations at low tide conditions (Esk estuary-Church and Irt estuary-Saltcoats) and seawater respectively. These samples were also each analysed using air-drying, glycolation and heating to 400°C and then 550°C. As expected, air-dried scans from both seawater and low tide filtrates reveal peaks at 6.2°, 8.9° and a pair of peaks at 12.3° and 12.5°. The peak at 6.2° is chlorite (001) while the peak at 8.9° is illite. The peak at 12.3° is the clearly-discerned kaolinite (001) peak while the bigger peak at 12.5 is either solely due to the chlorite (002)

peak or is a combination of chlorite (002) and berthierine (001) (Bailey 1988; Moore and Reynolds 1989).

The relative heights of the chlorite (001) and (002) peaks from the Esk estuary low tide sample (Fig. 6.6; about 1:2) suggest that the chlorite has a mixed Mg-Fe composition (Hillier, 2003). In contrast, the marine and Irt estuary low tide filtrate samples have higher (001) to (002) ratios (Figs. 6.7 and 6.8; ratio of about 1:3) suggesting that chlorite at this site is more likely to be Fe rich (i.e. Fe-chlorite, (Starkey et al. 1984; Hillier 2003).

Glycolation had negligible effect on the estuarine low-tide filtrate samples (Figs. 6.6 and 6.7) in contrast to the marine filtrate sample (Fig. 6.8) suggesting there was little smectite in the marine-end member suspended sediment.

XRD analyses of three samples (Saltcoats and Church at low tide and marine-end member) samples heated up to 400°C revealed a distinct ~10% decrease in the intensity for the peaks at 12.5° and 12.3° (Figs. 6.6, 6.7 and 6.8) (Table 6.2). This confirms the presence of kaolinite, but shows that the peak at 12.5° is *not* solely due to the chlorite (002) peak since the intensity of the (002) peak of pure trioctahedral chlorite does not fall during heating to 400°C (Moore and Reynolds 1989; Hillier 2003). This suggests that berthierine is present in these samples in trace quantities. A fall in intensity of ~45% for the 6.2° peak for marine-end member after heating to 400°C (Fig. 6.8) (Table 3.2) as well as 12.5° peak suggests that there is a mix of chlorite (trioctahedral and dioctahedral types) and some expandable mineral phases such as smectite and vermiculite.

The scan of the seawater filtrate sample heated up to 550°C shows a total collapse for the 12.3° peak and substantial collapse of the 12.5° peak. In contrast, the intensity of the peak at 6.2° slightly decreased but sharpened, largely typical of chlorite (Figs. 6. 8). The scan of the Esk estuary- Church at low tide filtrate sample heated up to 550°C shows a total collapse for both the 12.3° and 12.5° peaks while the intensity of the peak at 6.2° radically decreased (Table 3.2). This collapse at 6.2° suggests the presence of a mixture of dioctahedral chlorite, berthierine and an expandable phase such as dioctahederal vermiculite (Starkey et al. 1984; Moore and Reynolds 1989; Hillier 2003).

6.4.4 Semi-quantification of the clay mineralogy as a function of time through tide cycles

The quantified areas of the 6.2°, 8.9°, 12.3° and 12.5° peaks (in order: 14Å, 9.9Å, 7.15Å, 7Å) are illustrated as a function of time in Figure 6.8. The 14Å peak area is from chlorite (possibly with a trace of dioctahedral vermiculite) and its area was multiplied by a factor of three to account for the relative intensity of the (001) peak relative to the (002) peak (assuming a Fe-rich forma of chlorite). The 9.9Å peak area represents illite (001). The 7.15Å peak area represents kaolinite (001). The 7Å peak represents a combination of chlorite (002) and berthierine (001).

The presence of berthierine was ascertained during the heating experiments and XRD analyses of the filtrates prepared with silver filters (Figs. 6.6, 6.7, 6.8). It is impossible to discriminate the quantities of chlorite (002) and berthierine (001) using the cellulose filters (since they cannot be heated) although it is sufficient to note that as the 7Å peak area increases relative to the 14Å peak area, either the chlorite is becoming more Fe-rich or there is an increasing amount of berthierine in the clay fraction.

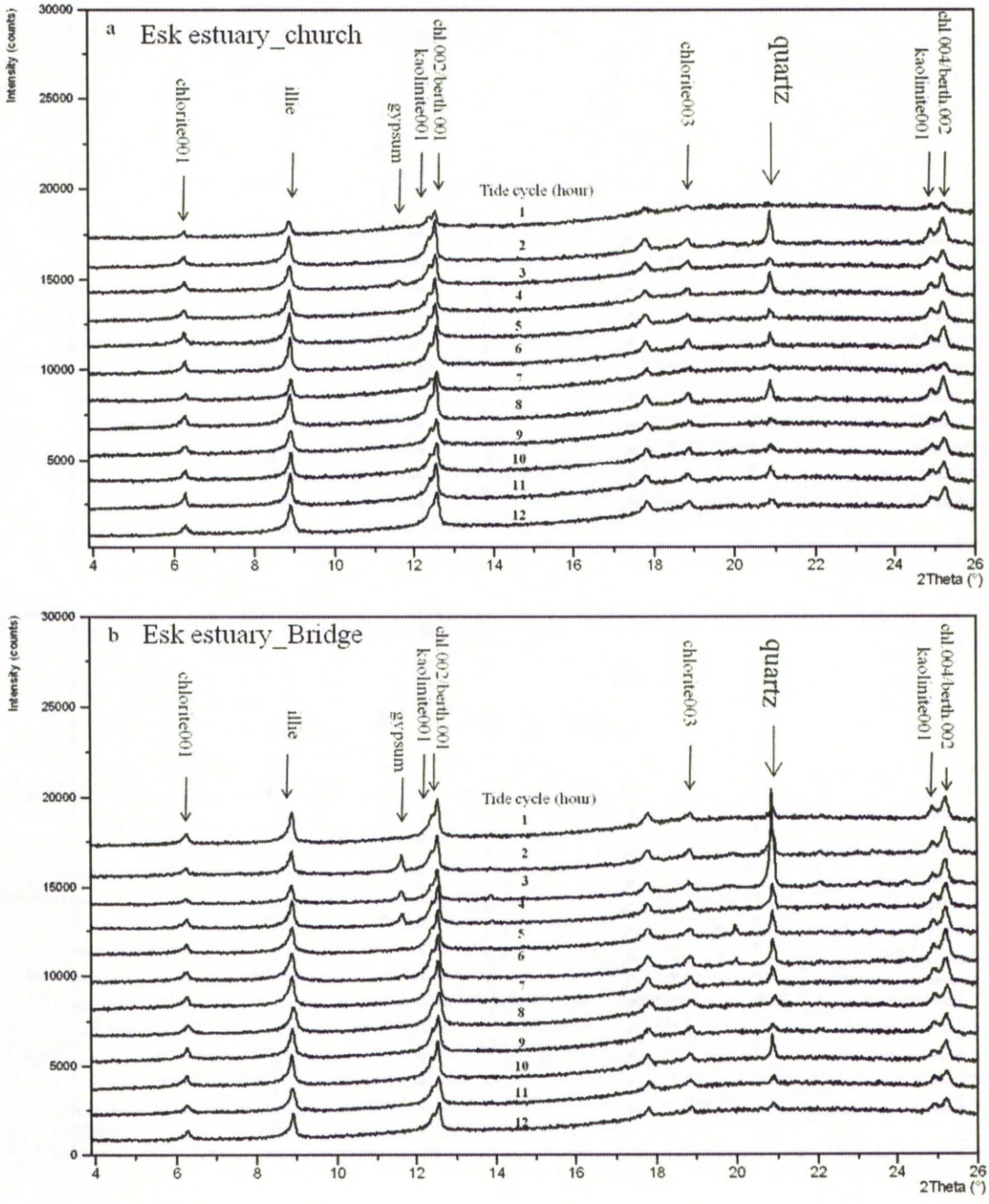

Figure 6.2: XRD patterns of the <2μm fraction of the filtered suspended sediment taken from the Esk estuary water at Church (a) and Bridge (b) from low tide to high tide during a 12hours tide cycle. Collection of patterns arranged from the top of the stack base: first taken sample and last taken sample at the base. Gypsum is an indicator of high waters (marine) to the estuary during the high tide.

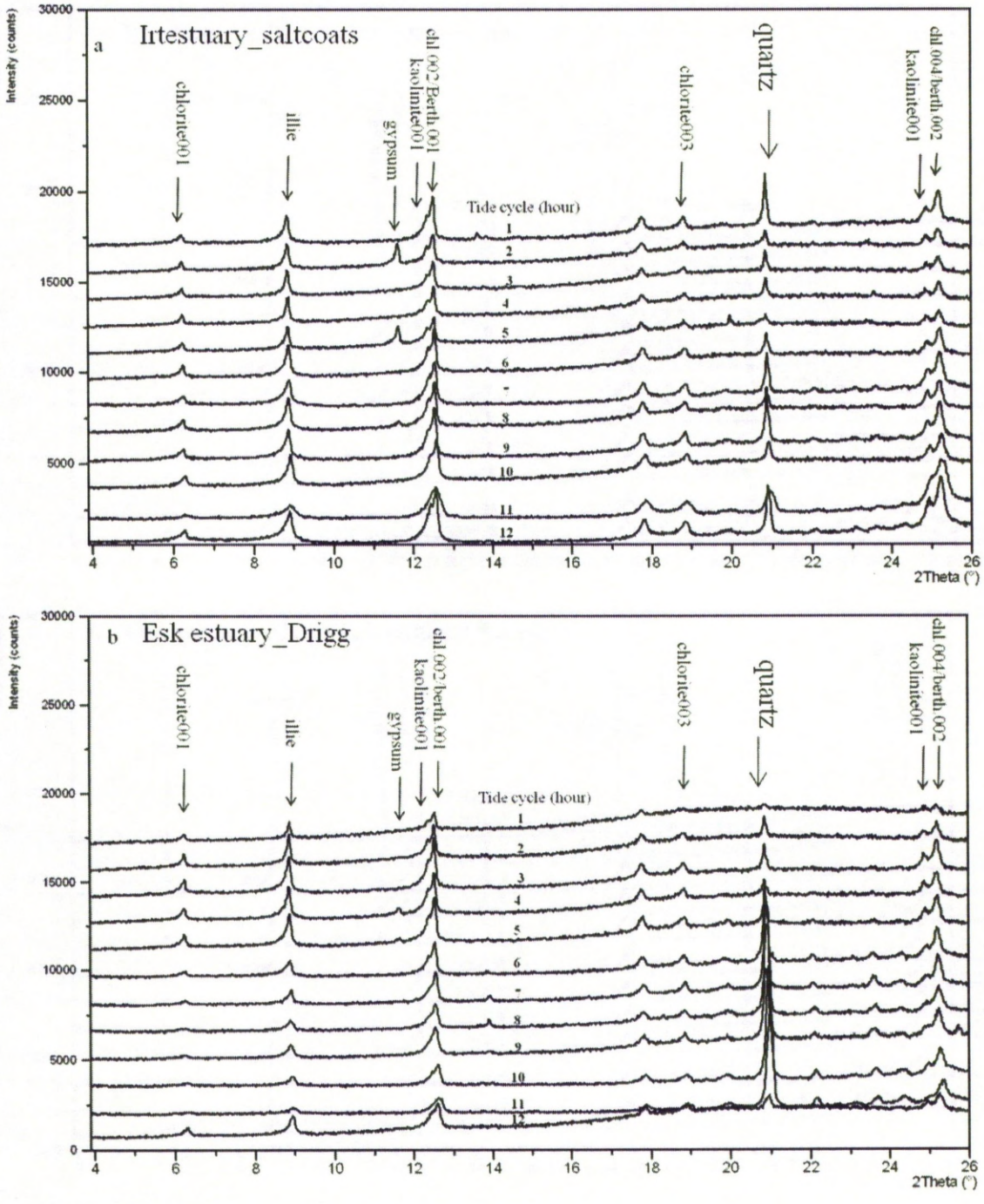

Figure 6.3: XRD patterns of the <2μm fraction of the filtered suspended sediment taken from the Irt estuary water at Saltcoats (a) and Drigg (b) during a tide cycle (12 hours). Gypsum peak is an indicator of marine water or high waters in the estuary. Collection of patterns arranged from the base the last taken sample, and first taken sample at the top of the stack. Comparison of the clay mineral peak intensities show a relative decreasing of the clay mineral peaks from low tide toward high tide in both stations.

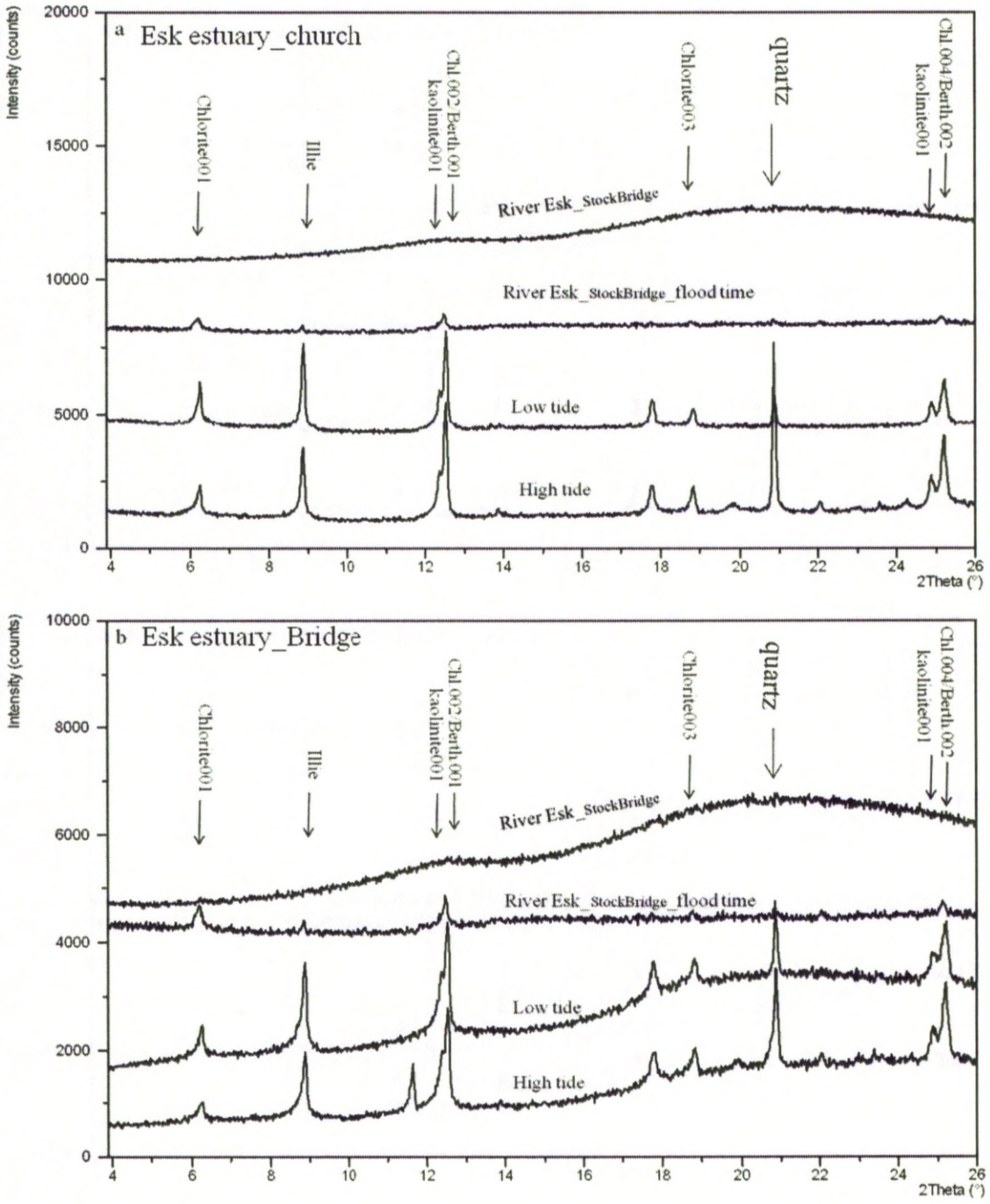

Figure 6.4: XRD patterns of the <2μm fraction of the filtered suspended sediment taken from the Esk river on a normal day and at a flood time and Esk estuary water at Church (a) and Bridge (b). Collection of patterns arranged from the base: high tide, low tide, flood time of the Esk river at StockBridge and normal day at the same point at the top of the stack. Comparison of the clay mineral peak intensities show clay mineral transportation on normal day through Esk river to the Esk estuary is negligible while in flood time a small quantity of clay minerals are transported to the estuary. The river during flood times is carrying dioctahedral chlorite and possibly vermiculite given the elevated (001):(002) ratio (Moore and Reynolds, 1989; Hillier, 2003). A small amount of illite is present but no kaolinite is being transport by the River Esk.

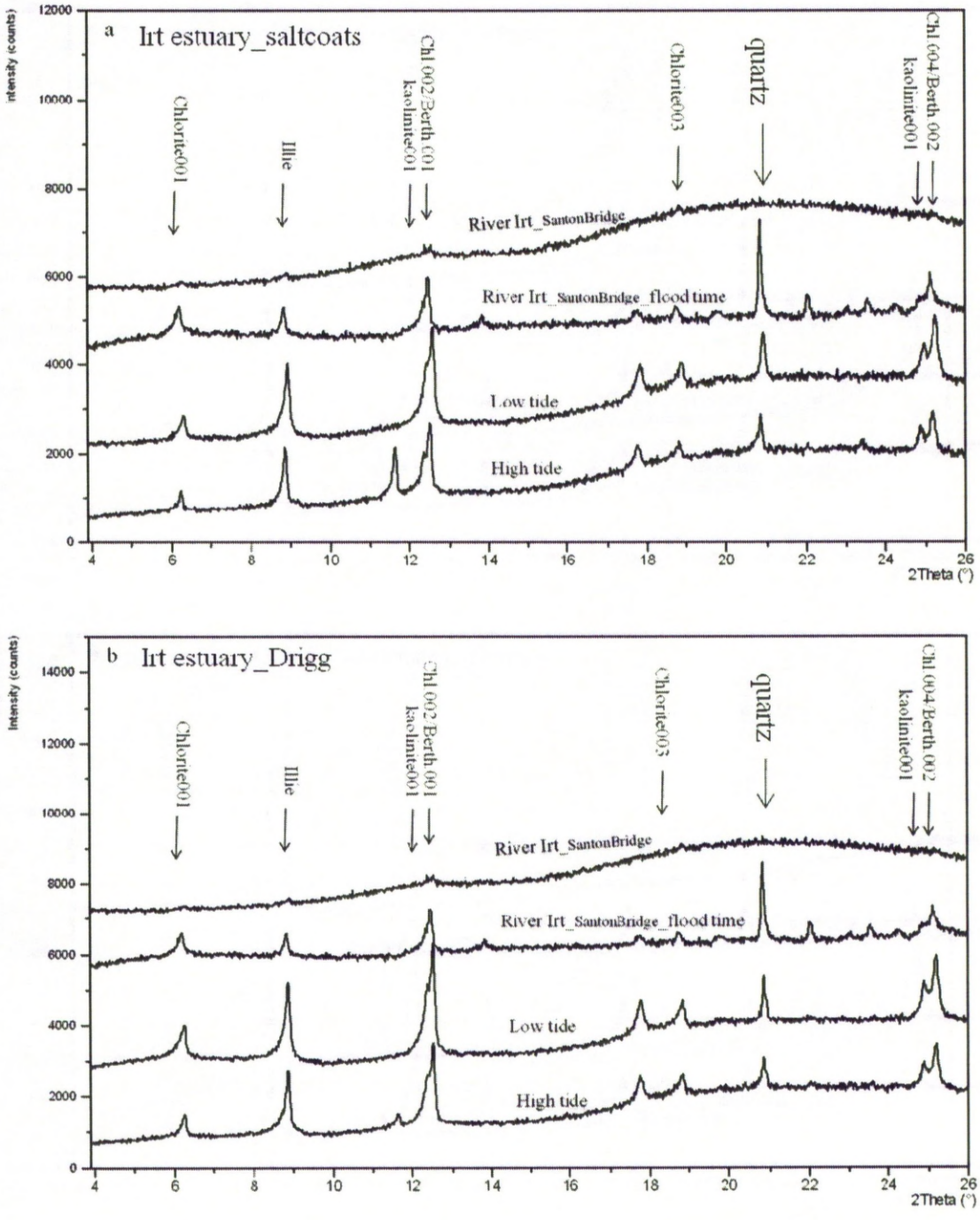

Figure 6.5: XRD patterns of the <2μm fraction of the filtered suspended sediment taken from the Irt river on normal day and a flood time and Irt estuary water at Saltcoats (a) and Drigg (b). Collection of patterns arranged from the base: high tide, low tide, flood time of the Irt river at Santon Bridge and normal day at the same point at the top of the stack. Comparison of the clay mineral peak intensities show clay mineral transportation on a normal day through the Irt river to the Irt estuary is not considerable compared to the quantity of clay minerals are transported to the estuary during flood time. The river during flood times is carrying dioctahedral chlorite but probably with less vermiculite than the Esk (Fig 6.4) given the moderately elevated (001):(002) ratio (Moore and Reynolds, 1989; Hillier, 2003). A moderate amount of illite is present but no kaolinite is being transport by the River Irt.

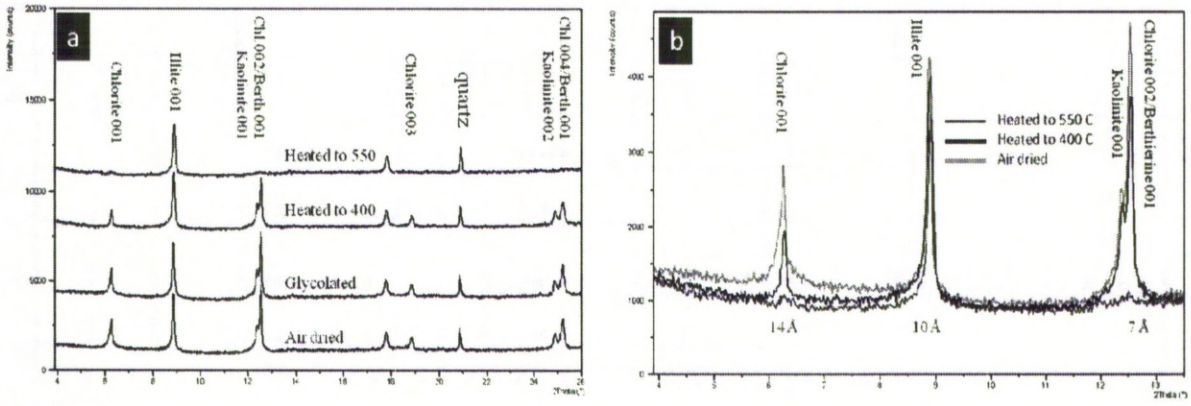

Figure 6.6: XRD patterns of the <2μm fraction of the filtered suspended sediment taken from the Esk river at low tide. a) Collection of patterns arranged from the base: air dried, glycolated, heated to 400°C and heated to 550°C at the top of the stack. b) Overlapping of the XRD data from the low angle end of the pattern to illustrate the drop in intensity of the 7.15 and 7Å peaks during heating to 400°C and their near total collapse at 550°C. Note also the unexpected collapse of the chlorite (001) peak. Heating up to 400°C shows a drop on peak intensity at 6.2°, while the air dried pattern at same peak shows a broad peak, this can lead to expandable mineral presence. Dioctahedral chlorite and HIV (Hydroxy-interlayer vermiculite seems present in the suspended materials at low tide.

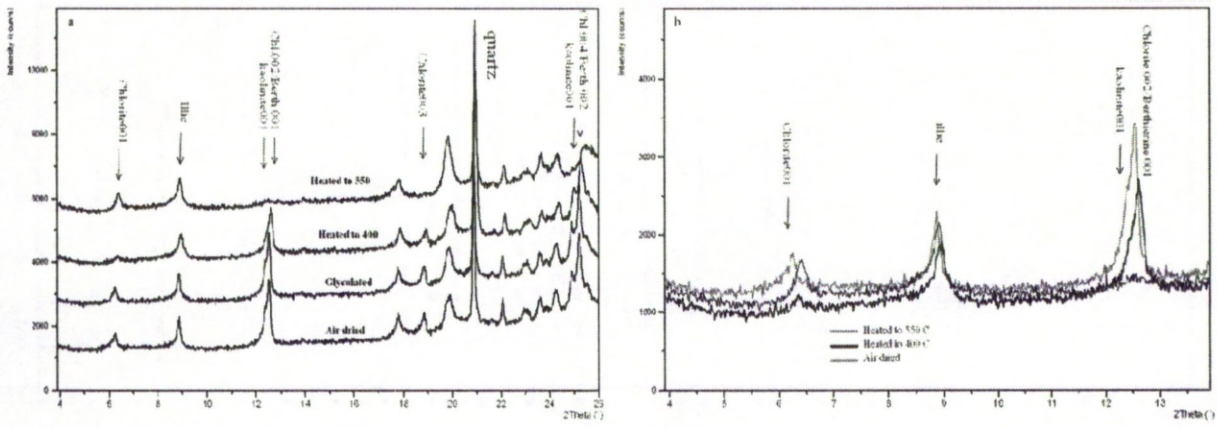

Figure 6.7: XRD patterns of the <2μm fraction of the filtered suspended sediment taken from the river Irt, Saltcoats station at low tide. a) Collection of patterns arranged from the base: air dried, glycolated, heated to 400°C and heated to 550°C at the top of the stack. b) Overlapping of the XRD data from the low angle end of the pattern to illustrate the drop in intensity of the 7.15 and 7Å peaks during heating to 400°C and their near total collapse at 550°C. Note also the unexpected collapse of the chlorite (001) peak. Glycolation seems no affect on the scans. Heating up to 400°C shows a drop on peak intensity at 6.2° while the air dried pattern at same peak shows a broad peak, this can lead to expandable mineral presence. Dioctahedral chlorite and HIV (Hydroxy-interlayer vermiculite seems present in the suspended materials at low tide.

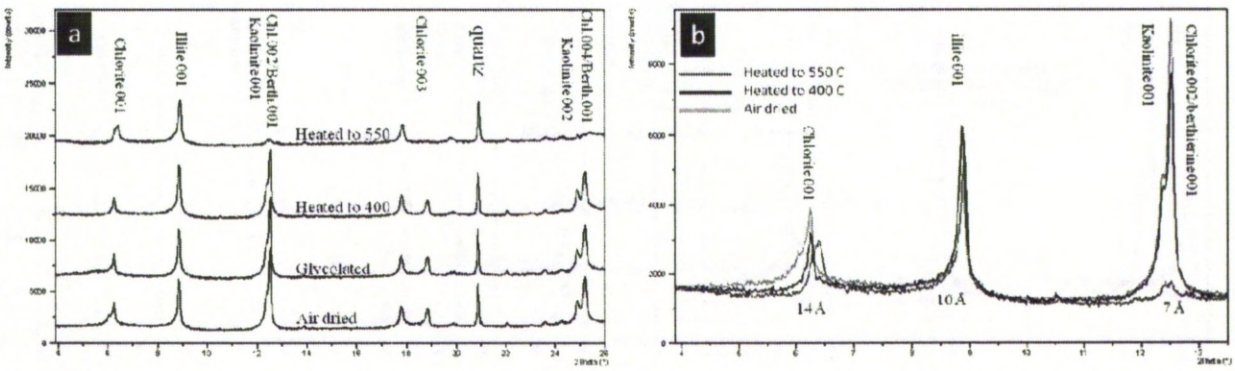

Figure 6.8: XRD patterns of the <2μm fraction of the filtered suspended sediment taken from sea water ~1000m north of where the Ravenglass estuary meets the Irish Sea (Fig. 6.1). a) Collection of patterns arranged from the base: air dried, glycolated, heated to 400°C and heated to 550°C at the top of the stack. b) Overlapping of the XRD data from the low angle end of the pattern to illustrate the drop in intensity of the 7.15 and 7Å peaks during heating to 400°C and their near total collapse at 550°C. Glycolation seems to have little effect on the sample.

Esk estuary-Church

Tide cycle (hour)	~14Å	9.9Å	7.15Å	7Å
1	0.302	0.277	0.193	0.229
2	0.212	0.294	0.232	0.262
3	0.266	0.296	0.208	0.231
4	0.235	0.289	0.233	0.243
5	0.354	0.270	0.203	0.174
6	0.289	0.272	0.223	0.216
7	0.325	0.228	0.162	0.285
8	0.297	0.282	0.245	0.176
9	0.297	0.281	0.228	0.194
10	0.337	0.259	0.198	0.206
11	0.284	0.242	0.246	0.228
12	0.282	0.278	0.236	0.204
Average	0.290	0.272	0.217	0.221
STDEV	0.040	0.020	0.025	0.033

Esk estuary-Bridge

~14Å	9.9Å	7.15Å	7Å
0.255	0.299	0.242	0.204
0.279	0.268	0.248	0.205
0.208	0.271	0.205	0.316
0.258	0.302	0.229	0.211
0.258	0.318	0.203	0.221
0.284	0.267	0.163	0.286
0.278	0.276	0.199	0.247
0.267	0.284	0.232	0.218
0.283	0.295	0.240	0.182
0.278	0.290	0.227	0.206
0.280	0.262	0.267	0.191
0.311	0.259	0.259	0.171
0.270	0.283	0.226	0.221
0.024	0.018	0.028	0.040

Irt River-Saltcoats

Tide cycle(hour)	~14Å	9.9Å	7.15Å	7Å
1	0.234	0.272	0.252	0.241
2	0.243	0.313	0.194	0.249
3	0.286	0.292	0.190	0.232
4	0.259	0.273	0.226	0.241
5	0.359	0.248	0.194	0.199
6	0.300	0.307	0.175	0.219
7	0.243	0.261	0.245	0.250
8	0.235	0.293	0.174	0.298
9	0.223	0.281	0.263	0.232
10	0.236	0.240	0.249	0.275
11	0.151	0.273	0.267	0.309
12	0.152	0.289	0.268	0.291
Average	0.244	0.279	0.225	0.253
STDEV	0.057	0.022	0.037	0.033

Irt River-Drigg

~14Å	9.9Å	7.15Å	7Å
0.320	0.138	0.248	0.293
0.299	0.229	0.226	0.246
0.283	0.248	0.234	0.235
0.232	0.267	0.254	0.247
0.239	0.283	0.253	0.225
0.129	0.273	0.274	0.324
0.227	0.239	0.212	0.322
0.208	0.222	0.220	0.349
0.212	0.263	0.220	0.304
0.145	0.267	0.239	0.350
0.225	0.199	0.265	0.311
0.361	0.222	0.199	0.218
0.240	0.238	0.237	0.285
0.067	0.040	0.023	0.048

XRD peak quantification

End members	~14Å	9.9Å	7.15Å	7Å
Esk River_StockBridge	0.56	0.05	0	0.38
Irt River_SantonBridge	0.48	0.13	0	0.37
Marine-end member, Drigg	0.36	0.22	0.22	0.20

Table 6.1: Peak deconvolution measurements of the maximum intensity peaks at ~14Å (6.2°), 9.9Å (8.9°), 7.15Å (12.3°) and 7Å (12.5°) for 4 stations across the Ravenglass estuary and three end-members (the two feeding rivers and a marine sample) based on the XRD scans of randomly powdered water suspended matters. The results are illustrated and presented in Figures 6.9 and 10.

peak	treatment	Esk estuary-Church at low tide		Marine-end member		Irt estuary- Saltcoats at low tide	
		Peak area	%changes from original	Peak area	%changes from original	Peak area	%changes from original
14Å	air	231	100	486	100	123	100
	400°C	183	79.2	327	52.9	42	34.1
	550°C	53	22.94	366	75.31	134	108.9
7Å	air	310	100	721	100	168	100
	400°C	272	87.7	668	92.6	156	92.8
	550°C	35	11.3	88	10.06	26	15.5

Table 6.2: Peak deconvolution of XRD patterns of air dried, heated to 400°C and heated to 550°C samples from Church and Saltcoats estuary sites, both at low tide, in addition marine end–member suspended sediments. There is fall in intensity of the 14Å peak for all samples during heating to 400°C while for the Church sample; it is about 2 to 3 times lower than the others. On the other hand, loss of intensity of the 7Å peak is roughly same (10%) for all samples (Church falls slightly more than 10% though). Considering the increased intensity of the peak at 14Å after heating 550°C for Saltcoats and the marine samples and also decreasing intensity for Church, this suggests a mix of weak chlorite (dioctahedral, Al-rich chlorite) and strong chlorite (trioctahedral Fe-Mg rich chlorite) with some expandable phases in Saltcoats and marine system suspended sediments and mix of chlorites (weak and strong) with berthierine possibly in addition.

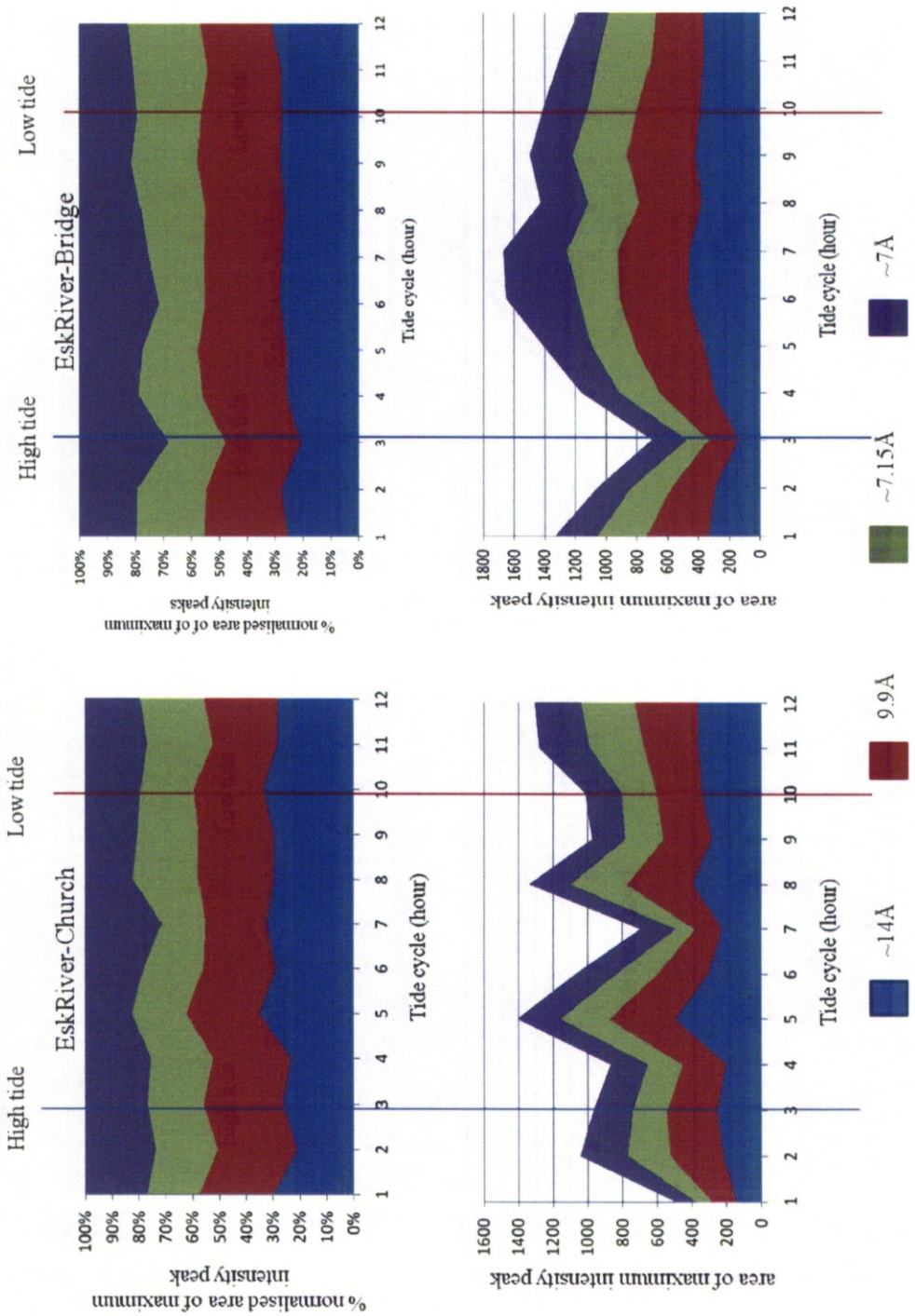

Figure 6.9: Graphs of clay mineral quantification based on XRD maximum intensity peaks at ~14, 9.9, 7.15, 7Å for oriented samples of suspended matters in Esk estuary water. (a) and (c) are the percentage of normalised area (14Å peak area multiplied by 3 to account for the less than maximum intensity of chlorite (001)) measurement of maximum intensity peak at Church and Bridge stations in Esk estuary respectively. (b) and (c) are the area of maximum intensity peak in Church and Bridge stations. These graphs show that suspended clay minerals in the low waters at the Bridge station seems mostly are fed to the estuary from upper part of the estuary.

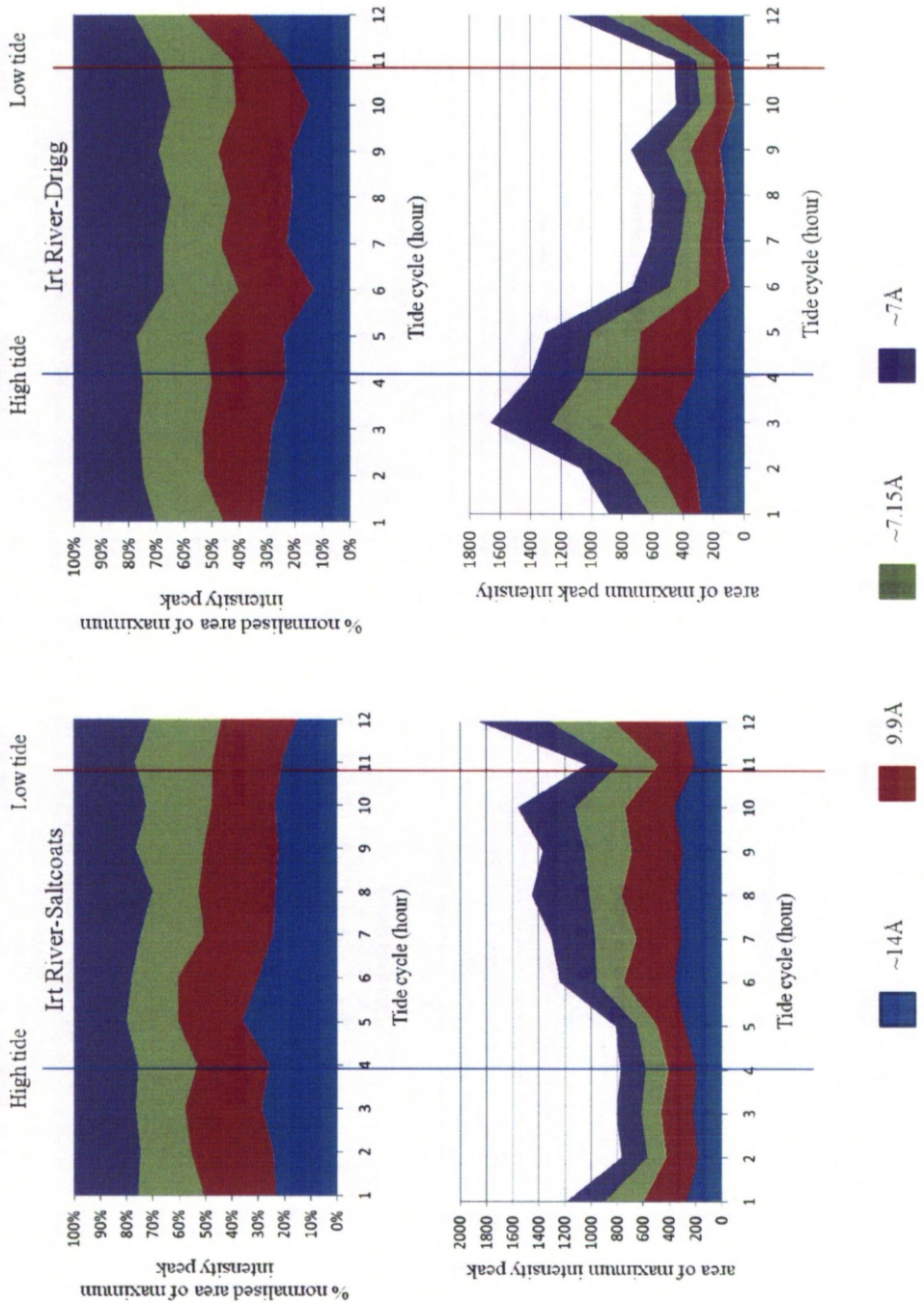

Figure 6.10: Graphs of clay mineral quantification based on XRD maximum intensity peaks at ~14, 9.9, 7.15, 7Å for oriented samples of suspended matters in Irt estuary water. (a) and (c) are the percentage of normalised area (14Å peak area multiplied by 3 to account for the less than maximum intensity of chlorite (001)) measurement of maximum intensity peak at Saltcoats and Drigg stations in Irt estuary respectively. (b) and (c) are the area of maximum intensity peak in Church and Bridge stations. These graphs show that clay minerals at low tide in the Bridge station estuary waters seems abundant relatively compare to the high tide. Most of the suspended clay minerals in the estuary water at Saltcoats are fed to the estuary from the upper part of the estuary while at the Drigg station most of the suspended clay minerals are from the lower part of the estuary during high tide, i.e. flushed upstream. It seems the Saltcoats is likely a potential depositional trap environment for the clay minerals in the estuary.

6.5 Discussion

6.5.1 Clay minerals transported by the two rivers into the estuary

Clay minerals in suspension in the southern River Esk are below detection by the sampling and analytical methods adopted during quiescent conditions but are present and identifiable under flood conditions (Fig 6.4). The clay minerals that come into the estuary via the southern River Esk during flood conditions are predominantly chlorite, possibly with an Al-rich, dioctahedral composition given the relatively high (001) to (002) peak height ratio (Fig. 6.4, Table 6.1 and Hillier, 2003). It is possible that elevated (001) peak is partly due to the presence of vermiculite as well as the Al-rich dioctahedral chlorite (Moore and Reynolds 1989; Hillier 2003). There is a very small peak at 8.9° showing that there is a small amount of illitic clay being fed into the estuary by this river. There is seemingly no kaolinite coming down the River Esk.

The clay minerals that enter the estuary via the northern River Irt during flood conditions are predominantly chlorite possibly with an Al-rich dioctahedral composition given the relatively high (001) to (002) peak height ratio (Fig. 6.5, Table 6.1 and Hillier, 2003). The (001):(002) ratio for the Irt suspended clay is slightly lower for the Irt than the Esk suggesting either that there is more vermiculite or that the chlorite has a less trioctahedral (Mg-Fe enriched) component (Figs 6.4 and 6.5); (Moore and Reynolds 1989; Hillier 2003). There is a larger peak at 8.9° than for the River Esk showing that there is a somewhat more illitic clay being fed into the estuary by the River Irt than the River Esk. There is seemingly no kaolinite coming down the River Irt. Clay minerals in suspension in the northern River Irt are just above detection during quiescent conditions by the sampling and analysis methods adopted here. It can be assumed that more clay minerals are being fed into the estuary by the River Irt (draining mainly the Sherwood Sandstone) than the River Esk (draining the Eskdale Granite).

6.5.2 Clay minerals present in the Ravenglass estuary water

Water samples from the Esk part of the estuary at low tide conditions contain a range of suspended clay minerals (Figs. 6.2, 6.4, 6.6). The air-dried samples revealed the presence of significant illite and kaolinite (Figs. 6.4, 6.6), unlike the River Esk suspended clay mineralogy. Heating to 400°C showed that at least part of the peak at 12.5° is not due to chlorite since the peak collapsed by about 12% (Fig. 6.6, Table 6.2), suggesting the

presence of berthierine (Hillier, 2003; Moore and Reynolds, 1989; Starkey et al., 1984). Heating to 400°C also showed that the 6.2° peak partially collapsed (Fig. 6.6, Table 6.2), behaviour not typical of pure trioctahedral Fe-Mg-rich chlorite. This plausibly suggests that some dioctahedral vermiculite and chlorite are present in the sample. Heating to 550°C showed that the 6.2° peak totally collapsed (Fig. 6.6, Table 6.2), possibly suggesting that the chlorite is an Al-rich dioctahedral chlorite (Starkey et al. 1984; Hillier 2003).

Water samples from the Irt part of the estuary at low tide contain a range of suspended clay minerals (Figs. 6.3, 6.5, 6.7). As for the Esk estuary, the air-dried samples had large peaks for illite and kaolinite (Figs. 6.5, 6.7). Also, heating to 400°C showed that the peak at 12.5° is not solely due to chlorite since the peak collapsed by about 7% (Fig. 6.7, Table 6.2), again suggesting the presence of berthierine (Hillier, 2003; Moore and Reynolds, 1989; Starkey et al., 1984). Heating to 400°had an even greater effect on the 6.2° peak than for the Esk estuary samples (Fig. 6.7, Table 6.2) perhaps suggesting more vermiculite present in the Irt than the Esk estuary suspended clay minerals. Heating to 550°C showed growth of the 6.2° peak (Fig. 6.7, Table 6.2), possibly suggesting that the chlorite is a mixture of Fe-Mg-rich trioctahedral and Al-rich dioctahedral chlorite (Starkey et al. 1984; Hillier 2003).

The biggest differences between the fluvially-transported and the low tide estuary suspended clays are the presence of kaolinite and illite in greater abundance in the estuary samples. Also the ratio of the chlorite (001) peak to the peak at 12.5° is lower in the estuary samples than the river samples (Table 6.1) suggesting either that the chlorite is more Fe-rich in the estuary samples than the river samples and/or that there is a new berthierine component in the estuary samples, absent in the river samples.

6.5.3 Clay minerals suspended in seawater near to the mouth of the estuary

Seawater samples contain a range of suspended clay minerals (Figs. 6.8). As for the estuary samples, the air-dried samples revealed the presence of significant illite and kaolinite. Heating to 400°C showed that at least part of the peak at 12.5° is not due to chlorite since the peak collapsed by about 8% (Fig. 6.8, Table 6.2), again suggesting the presence of berthierine (Starkey et al. 1984; Moore and Reynolds 1989; Hillier 2003). Heating to 400°C showed that the 6.2° peak partially collapsed (Fig. 6.8, Table 6.2),

behaviour not typical of pure trioctahedral Fe-Mg-rich chlorite. Heating to 550°C showed that the 6.2° peak grew slightly relative to the peak at 400°C possibly suggesting that the chlorite is a mixture of Fe-Mg-rich trioctahedral and Al-rich dioctahedral chlorite (Starkey et al. 1984; Moore and Reynolds 1989; Hillier 2003). Seawater suspended clay minerals thus seem to broadly resemble the estuary samples, and especially the Irt estuary sample (Fig. 6.7). There are differences however;

1) The seawater suspended clay minerals seem to have more kaolinite and less illite than the estuary samples (Table 6.1)
2) The ratio of the 6.2 peak to the 12.5 peak is higher for the seawater sample than the estuary samples suggesting either that the chlorite is more Mg-rich or that there is less berthierine in the seawater than the estuary samples (Table 6.1).

6.5.4 Clay minerals in suspension in the estuary at different sites and at different times during tide cycles

The XRD data for the estuary samples taken through tide cycles (Figs. 6.2, 6.3) were semi-quantified by measuring the areas of the peaks at 6.2°, 8.9°, 12.3° and 12.5°. The peak at 6.2° represents chlorite (001); the peak at 8.9° represents illite (001); the peak at 12.3° represents kaolinite (001); the peak at 12.5° represents chlorite (002) and possibly berthierine (001). In fact, the peak at 6.2° possibly represents the sum of dioctahedral and trioctahedral chlorite (001) plus vermiculite (001) but these cannot be discriminated for the samples collected on cellulose filter papers (Figs. 6.2 and 6.3). The semi-quantified data are presented as a function of time through the tide cycles for the four sites (Figs. 6.9 and 6.10). The data are shown in two ways as a function of time: (1) as absolute peak areas, illustrating how the absolute quantities of suspended clay minerals varies through the tide cycle, and (2) as relative peak areas to reveal whether the proportions of the different clay minerals vary with time. The relative peak area data and the averages for each site are given in Table 6.1.

The Esk estuary Church site (fluvial end of the estuary) has a noisy pattern of absolute quantity of clay minerals in the water as function of time (Fig. 6.9). There is no simple pattern of the amount of clay in the water depending on whether the sample was high or low tide. In contrast, the Esk estuary Bridge site (more marine end of the estuary) has the smallest amount of clay at high tide with the greatest quantity half way between high and low tide (Fig. 6.9).

The Irt estuary Drigg site (fluvial end of the estuary) has the greatest quantity of clay minerals in the water just before high tide and the smallest quantity at low tide (Fig. 6.10). In contrast to the Drigg site but similar to the Esk Church site, the Irt estuary Saltcoats site (more marine end of the estuary) has the smallest amount of clay at high tide (Fig. 6.9). This site has the greatest quantity of clay an hour before or after low tide (Fig. 6.10).

The two sites closest to the mouth of the estuary (Saltcoats and Bridge) have the lowest quantities of clay minerals at high tide (Figs. 6.9, 6.10) suggesting that, during the flood tide, the incoming seawater has rather less clay in suspension than the pre-existing water in the estuary. The up-estuary Church site has no simple pattern but the up-estuary Drigg site has the most clays in suspension at high tide (in direct contrast to the marine end of the estuary) suggesting that incoming seawater pushes the pre-existing suspension-laden water in the estuary basin, back up stream. In conclusion, the incoming tide seems to operate like a piston displacing the clay-rich estuary waters back up the estuary. On the outgoing tide, the clay-rich estuary waters then flow back towards the sea leading to greater quantities of suspended clay at the down-stream sites as the "clean" seawater is flushed out of the estuary.

The relative proportions of clay minerals seem to be roughly consistent during the tide cycle at the Esk Bridge and Church sites (Fig. 6.9). On average, the clay peak height ratios (clay proportions) seem to be very similar at the Esk Church and Bridge sites (Table 6.1). There is a vague hint that the ratio of the 14Å to 7Å peak reaches a minimum at about high tide at the Church and Bridge sites possibly suggesting either: (1) that the chlorite is slightly more Fe-rich at high tide or (2) there is slightly more berthierine suspended in the water at high tide (Fig. 6.9).

The relative proportions of clay minerals seem to be roughly consistent during the tide cycle at the Irt Saltcoats and Drigg sites (Fig. 6.10). On average, the clay peak height ratios (clay proportions) seem to be very similar at the Irt Saltcoats and Drigg sites (Table 6.1). In contrast to the Esk estuary, there is a hint that the ratio of the 14Å to 7Å peak reaches a maximum at high tide at the Irt sites possibly suggesting either: (1) that the chlorite is slightly less Fe-rich at high tide or (2) there is slightly less berthierine suspended in the water at high tide. Conversely, the 14Å peak diminishes approaching low tide at both Irt sites while the 7Å peak either stays the same or the relative area gets bigger

suggesting either: (1) that the chlorite is slightly more Fe-rich at low tide or (2) there is slightly more berthierine suspended in the water at low tide.

On average, the suspended clay minerals in the Irt estuary are in similar proportions to the Esk estuary suspended clay minerals (Table 6.1, Figs 6.9, 6.10). However, the 14Å peak is slightly smaller relative to the 7Å peak for the Irt samples suggesting either: (1) that the chlorite is slightly more Fe-rich in the Irt than the Esk or (2) there is slightly more berthierine suspended in the Irt than the Esk.

6.5.5 The origin of the clay minerals in suspension in the Ravenglass estuary and their distribution pattern

Dominant chlorite and subordinate illite are present in suspended sediment in fluvial waters while kaolinite and berthierine are absent. Chlorite, kaolinite and illite are the most common suspended clay minerals throughout the Ravenglass estuary waters, including low tide and high tide water and marine water. Berthierine is another clay mineral which is present in estuarine suspended matters. Al-rich dioctahedral chlorite and some expandable phases minerals such as vermiculite seems to be present within the estuarine waters but Fe-rich chlorite is the dominant chlorite type in the estuary.

Chlorite in the fluvial waters from the Rivers Irt and Esk was sourced from the hinterland and is probably typical of chlorite in the river sediment. Comparing the 14Å peak area to the 7Å peak for the fluvial suspended sediment (Fig. 6.11) revealed that most of the chlorite is dioctahedral chlorite but also seems to contain a component of hydroxyl-interlayered, vermiculite (Figs. 6.4 and 6.5); (Moore and Reynolds 1989; Hillier 2003).

Chlorite in suspended sediment in the estuary seems to be a mix of dioctahedral (weak) and trioctahedral (strong) chlorite plus berthierine (the (chlorite (002) peak gets smaller on heating to 400°C; Fig. 6.6 and 6.7) (Moore and Reynolds 1989; Hillier 2003). In the low tide waters from the estuaries (Esk and Irt), dioctahedral chlorite is abundant given the decrease in the (001) peak on heating to 550°C (Fig. 6.6 and 6.7). This type of chlorite is present in the fluvial samples, and is added to the estuary water and sediment at low tide and thus is likely to be sourced from the hinterland. Chlorite in suspended sediment at high tide and in marine waters seems likely to be an Fe-Mg rich chlorite (Fig. 6.2, 6.3, 6.4, 6.5 and 6.8; (Moore and Reynolds 1989; Hillier 2003) possibly with some berthierine (given the decrease in intensity of the (002) peak on heating to 400°C; Fig. 6.8). In the

high tide estuary waters, Fe-rich trioctahedral (strong) chlorite seems to become more dominant, likely being sourced from the sediment within the estuary basin. The total amount of chlorite, as denoted by the area of the (001) peak, is lowest at high tide for the two most seaward sampling stations within the estuary (Bridge and Saltcoats) suggesting that the in-flooding seawater is not responsible for the chlorite found in the estuary. There are thus two main sources of chlorite-type clay minerals:

(1) Berthierine and trioctahedral Fe-Mg chlorite thus seem to be formed within the estuary basin itself;
(2) Dioctahedral Al chlorite is mainly fed to the estuary via the rivers from hinterland.

There is no detectable kaolinite in the fluvial water samples (Figs. 6.4 and 5) suggesting only a limited degree of chemical weathering in the hinterland. XRD analyses of the suspended sediment in the estuarine water at low tide (Figs. 6.6 and 6.7) show that kaolinite is present. XRD analyses of the high tide estuary water and marine water suspended materials (Figs. 6.6, 6.7, 6.8) also showed that kaolinite is present. The kaolinite content in the suspended sediments is higher in the estuary (Fig. 6.11). It seems that either:

1) kaolinite is being created in the estuary by alteration and diagenetic processes or,
2) kaolinite is being washed into the estuary by the sea at high tide.

There is no significant increase in the relative kaolinite content of the estuary waters at high tide (Figs. 6.9 and 6.10). Indeed, the absolute quantity of kaolinite at the two estuary sampling sites closest to the sea decreases at high tide suggesting that the incoming seawater actually dilutes the more turbid (and kaolinite-rich) estuary waters. It thus seems that option 2 is untenable. The presence of kaolinite in the Esk and Irt estuary low tide water samples (Figs. 6.6 and 6.7) suggests that chemical weathering (e.g. alteration of detrital minerals such as feldspars) has had more opportunity to progress in the estuarine surface sediments than in the weathering zones and soils of the hinterland (chapter 3; (Thiry 2000). It must be concluded that the kaolinite in the estuarine water is due to the local generation of kaolinite (e.g. in estuary sediments) which is then remobilised by currents (e.g. during flood tides) and washing the kaolinite out from the surface sediments to the estuary waters.

Illite is a common clay mineral in suspended sediment in the Ravenglass estuarine waters (Figs. 6.2, 6.3, 6.6 and 6.7) while it is not abundant in the suspended materials from the

fluvial systems. Suspended sediments from the River Irt at SantonBridge have about twice the illite content of the suspended sediment from the River Esk at Stockbridge (Figs 6.1, 6.4, 6.5, 6.11). The quantity of illite in suspended sediment increases from the fluvial system to the estuarine system (from ~7% to ~30%; Fig. 6.11). While the amount of illite is roughly the same in the estuary and the marine suspended sediments (both ~30%; Fig. 6.11). This trend of increasing toward the estuary then approximately constant into the marine setting suggests that the formation of illite is likely to occur within the estuarine sedimentary systems (especially Irt estuary) and that this adds considerable new illite to the water over and above the small amount of illite being flushed out of the hinterland by the Rivers Irt and Esk. In summary, suspended illite seems to have two origins in the estuary waters:

(1) supplied directly from the hinterland,

(2) *in situ* alteration and weathering product within the estuarine depositional environments.

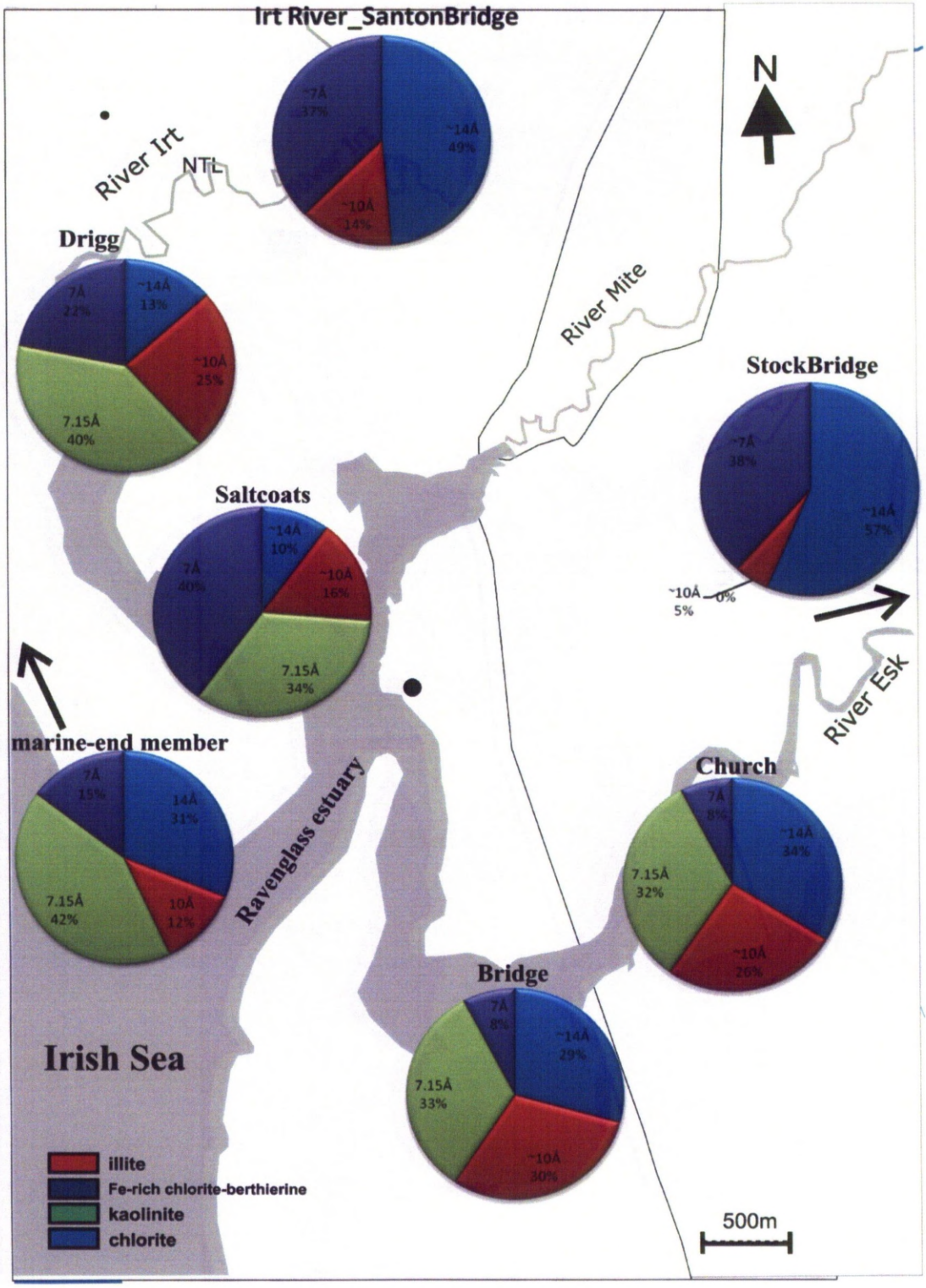

Figure 6.11: Schematic picture of the Ravenglass estuary and suspended matters in estuarine waters and end-members. Clay proportions from estuarine suspended sediment are from low tide and the fluvial-end members were collected after a storm (i.e. during a flood event). These results are normalised to maximum intensity peak values and so have the chlorite (001) area multiplied by 3 to account for the chlorite (001) having lower intensity than (002). Kaolinite (or the 7.15Å peak) is absent in the suspended matters beyond the high tide line (NTL) while kaolinite in suspended sediments is present within the estuary.

6.6 Conclusion

1) The clay minerals being transported into the Ravenglass estuary by both the River Irt and River Esk are dominated by dioctahedral chlorite. The River Esk transports a trace of illite and probably a substantial fraction of dioctahedral vermiculite to the estuary while the River Irt transports a somewhat greater amount of illite but only a trace of vermiculite into the estuary.
2) Both the Esk and Irt arms of the estuary contain abundant kaolinite and illite in the suspended sediment. The Esk arm of the estuary also contains abundant chlorite, possibly dioctahedral, as well as berthierine and some dioctahedral vermiculite. The Irt arm of the estuary also contains abundant chlorite, possibly mixed trioctahedral and dioctahedral types, as well as berthierine and even more dioctahedral vermiculite than the Esk estuary.
3) High tide conditions at the more seaward sampling sites in the estuary have the lowest clay content suggesting that seawater, via the incoming tide, does not bring much clay mineral material into the estuary. The incoming tide seems to flush clay-rich waters up stream to the heads of the estuary. The relative proportions of clay minerals do not vary significantly as a function of tides.
4) The seawater suspended clay minerals seem to have more kaolinite and less illite than the estuary suspended sediment samples. Also, the seawater chlorite is slightly less Fe-rich than the estuary chlorite, or possibly there is less berthierine in the seawater than the estuary samples (Table 6.1).
5) Chlorite has two sources in the estuary suspended clays; dioctahedral chlorite and vermiculite is transported from the hinterland via the rivers into the estuary while trioctahedral chlorite seems to be generated in situ, presumably in the sediment column, and then mobilised by flood tides.
6) Kaolinite seems to be generated *in situ*, presumably within the sediment column by alteration or diagenetic processes and subsequently mobilised by flood tide currents.
7) Illite has two sources in the estuary suspended clays; a trace is transported from the hinterland via the rivers (especially the Irt) into the estuary while elevated illite quantities in the suspended fraction seem to be generated *in situ*, presumably in the sediment column by alteration processes, presumably then mobilised by flood tides.

Chapter 7

Chapter 7 Synthesis discussion and general conclusions

7.1 General discussion and response to key scientific questions

7.1.1 How do estuarine sedimentary processes impact clay distributions, and potentially influence reservoir quality in analogous estuarine rocks?

Estuarine systems are commonly interpreted in the stratigraphic record, and typically are associated with incised valley-fills or parts of fluvio-deltaic systems. Clay minerals are trapped, transformed and/or formed within the estuarine sedimentary system which their distribution imply the reservoir quality. Chlorite is one the most important clay mineral in reservoir quality estimation. The analytical results of the estuarine surface sediments, estuarine very shallow burial sediments, and estuarine suspended materials show that kaolinite, illite, berthierine and Fe-rich chlorite are the main clay minerals inside the Ravenglass estuary. Differences in primary sediment supply could plausibly play a significant role in controlling the relative concentrations of chlorite in this estuary system. The prevalence of berthierine at depth in the Esk cores (Fig. 4.12) suggests some sort of diagenetic alteration process. Estuarine sedimentology and sedimentary processes that influence clay mineral distribution in estuaries are controlled by various processes such as differential settling, diagenesis, flocculation, source area variation and physical properties of estuaries (Feuillet and Fleischer 1980). The distribution and types of clay minerals in ancient estuarine rocks cannot be predicted with present levels of understanding. The distribution and types of clay minerals in modern estuarine systems is also largely unknown so modern systems cannot be used as way to help understand ancient estuarine rock clay mineral distribution. Clay minerals can strongly alter porosity and permeability. The effects of clay minerals, especially kaolinite, illite, and chlorite, on reservoir properties are not always uniform (Edzwald and O'Melia 1975; Eberl et al. 1993; Worden and Morad 2003a). Local characteristics, such as crystal shape, distribution and amount, govern the specific effect of a clay mineral on reservoir quality.

7.1.2 What clay minerals are transport into, formed in (neo-formation) and transported out of the estuary?

With the integration of analytical results of fluvial sediment and suspended riverine materials, kaolinite and berthierine are the main absent clay minerals in such environments

compared to the in-estuary clay mineral assemblage (Fig. 7.1). Illite is also minor in river sediments inland of the high tide mark. Dioctahedral chlorite and expandable phases such as smectite and hydroxyl-interlayer vermiculite are the main clay minerals in the fluvial system beyond the estuary. These clay minerals are transported to the estuary through the fluvial system. The analytical results of the estuarine surface sediments, estuarine very shallow burial sediments, and estuarine suspended materials show that kaolinite, illite, berthierine and Fe-rich chlorite are the main clay minerals inside the Ravenglass estuary.

Illite and kaolinite are common weathering products of the feldspar minerals (Drits et al. 1997) that are abundant in the Eskdale granite, which is exposed in the Esk drainage basin, and the St. Bees Triassic sandstones in the Irt River catchment. The absence of kaolinite in the stream sediment samples suggests a limited degree of chemical weathering in the hinterland. The presence of kaolinite in the estuarine system suggests that chemical weathering has had more opportunity to progress. There is a small illite peak in the XRD traces of stream sediment sample suggesting a limited degree of chemical weathering in the hinterland. This illite peak might be due to an input of some muscovite (Burley et al. 2003), which is present in the Eskdale granite (Branney and Soper 1988) and St. Bees Triassic sandstones (Strong ; Strong et al. 1994). However, only minor diagenetic illite from St. Bees Triassic sandstone has been reported (Strong et al. 1994; Cowan and Bradney 1997; Greenwood and Habesch 1997). The greater presence of illite in the estuary suggests, as for kaolinite, that chemical weathering of various feldspar minerals has had more opportunity to progress in the estuary than in the hinterland. The greater abundance of illite and kaolinite in the estuary relative to the stream sediments might simply be a function of the increased residence time (more time for weathering) of the sediment in the lower relief parts of the basin. Chlorite in the stream sediments beyond the tidal reach, and in suspended material in the estuary at low tide, seems to be a mixed Mg-Fe type of chlorite given the (001):(002) ratio of 1:2 and also likely contains a component of dioctahedral chlorite (Hillier 2003). In contrast, the chlorite in the cored sediment from the Esk estuary seems to be an Fe-rich type of chlorite given the (001):(002) ratio of 1:4.

Chlorite has been reported as an alteration and weathering product in the Eskdale granite (Moseley 1978) so it is perhaps not surprising that it is present in the stream sediment samples. Dioctahedral chlorite in the Irt fluvial sediments can be interpreted as due to formation in soil. However, chlorite has not been reported in the local outcrops of St. Bees

Triassic sandstones (Cowan and Bradney 1997; Greenwood and Habesch 1997). The implication from the apparent change of chlorite composition is that the chlorite being fed into the estuary evolves towards a Fe-dominated composition once it is subject to estuarine influences.

Chlorite could have its depth-variation and spatial variation patterns in the Irt and Esk estuary cores controlled by a range of possible origins:

1) Primary sedimentary variations;
    a. Initial differences in chlorite content, and chlorite type,
    b. Initial differences in Fe-oxide content at the time of deposition.
2) Secondary, post-depositional, variations;
    a. Infiltration of different types of clay into different types of sediment at different sites,
    b. Infiltration of different amounts of Fe-oxide (as fines, flocs or colloidal material) at different sites,
    c. Different degrees of circulation of oxygenated or reduced water at different sites,
    d. Different water types dominant at different sites and different depth (sulphate-rich seawater versus sulphate-poor river water).

Differences in primary sediment supply (option 1 above) could plausibly play a significant role in controlling the relative concentrations of chlorite in this estuary system.

The Irt cores are very fine-grained and so will be relatively impermeable (Fig. 4.2). The Esk cores contain interbedded medium- to coarse-sands and fine silts and so will have variable permeability (Fig. 4.3). The Irt cores will have had little opportunity for any sort of infiltration or lateral movement of water, whether by tidal pumping or down-aquifer subsurface flow. The Esk cores will have had opportunity for infiltration and lateral movement of water along the coarsest and most permeable sand layers. It is thus noteworthy that the coarser units are where there is most chlorite and berthierine; the coarsest layers have the highest peak area ratios of the 7Å to 14Å peaks. These observations possibly suggest a role for permeability (flux of water) in the generation of berthierine and chlorite at depth in the Esk cores that has not been effective in the low permeability Irt cores.

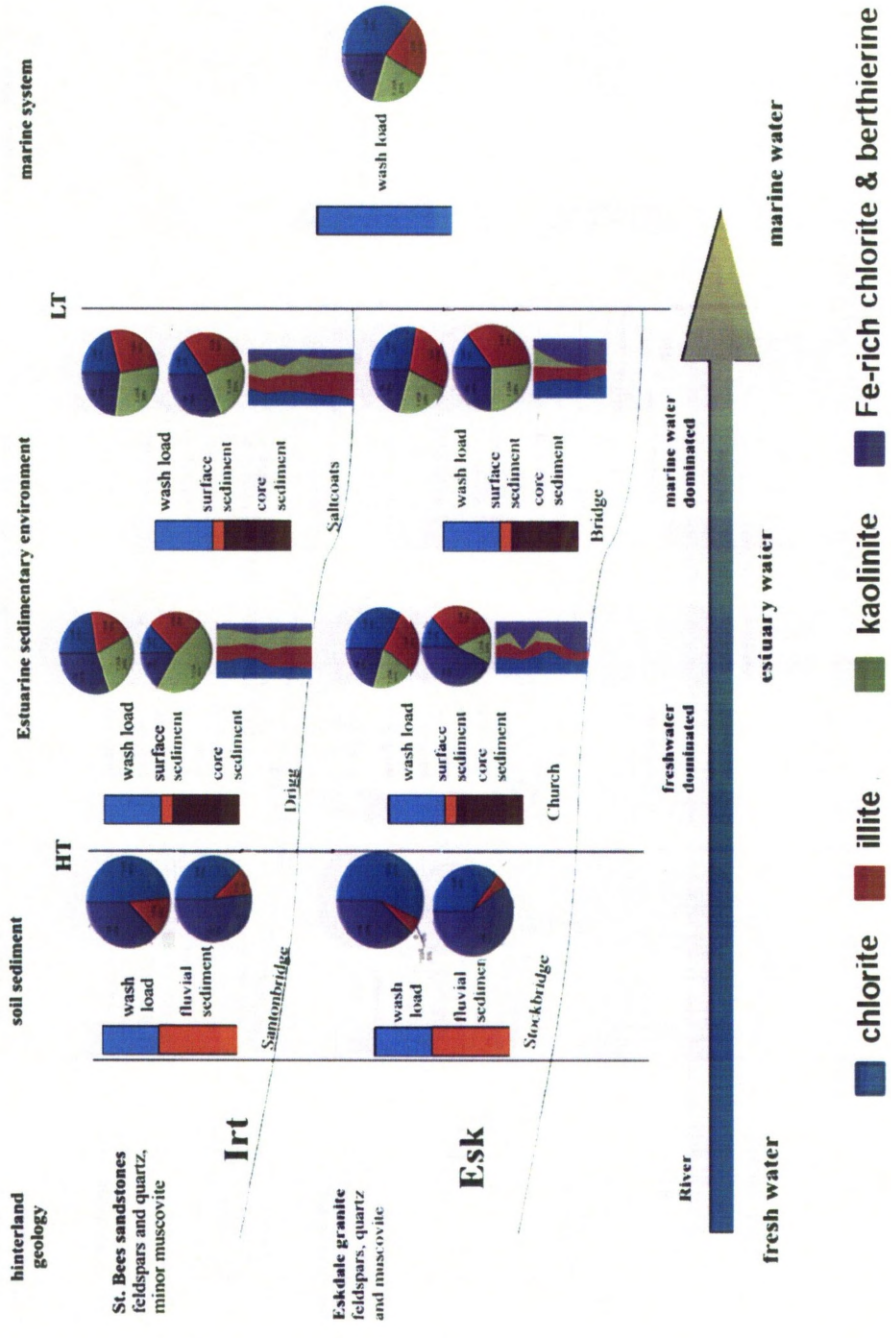

Figure 7.1: Synthesis diagram to show the clay mineral distribution from hinterland geology toward the marine system. In this system, clay minerals have been studied in fluvial sediments and fluvial wash loads, estuarine surface and core sediments in addition with estuarine water suspended matters and in marine water suspended materials.

The aqueous iron load of Irt and Esk rivers falls suddenly once rivers enter their estuaries as the salinity starts to increase (Fig. 5.9 and Boyle et al., 1977). More than 80% of all aqueous iron is typically trapped within the Ravenglass estuarine environment (Fig. 5.11 (Boyle et al. 1977b; Mayer 1982) and it must precipitate as some form of oxidised iron, e.g. as an iron(III) oxide or hydroxide. Some of this maybe co-deposited with the suspended and bed loads, some may be available for infiltration into permeable beds at low tide (when the sediment was not water-saturated). Solid phase ferric oxides and hydroxides in the estuarine environment can be reduced to ferrous phases in the presence of organic matter (Caccavo Jr et al. 1992; Coleman et al. 1993). In highly reducing, organic matter-rich, (Aller et al. 1986) and seawater-dominated environments in the subsurface, sulphate reduction occurs leading to the growth of iron monosulphate or even pyrite (Coleman et al. 1993). If reduction of ferric iron occurs in the relative absence of seawater but with abundant oxidising organic matter, the result is likely to be siderite ($FeCO_3$). It is noteworthy that the Irt cores are organic-rich and contain more pyrite than the Esk cores (Figs. 4.2, 4.3, 4,12) suggesting that any available iron (e.g. flocculated iron) has created Fe-sulphide rather than Fe-clay. On the other hand, it was noted that sulphate concentrations are relatively depleted in parts of the Ravenglass estuary in comparison to conservative mixtures of seawater and river water (Fig. 5.3b and c, Fig. 5.5). It was suggested that this may be due to localised bacterial sulphate reduction converting sulphate into sulphide. Comparison of dissolved iron and sulphate concentrations (Fig. 5.12) shows that there is a pattern rather similar to the iron-TDS diagram (Fig. 5.11). High iron concentrations are only possible at low sulphate concentrations. It is interesting to speculate that elevated sulphate concentrations leaves the possibility of elevated sulphide concentrations so that at least some dissolved iron may be lost from the water by Fe-sulphide mineral formation.

The prevalence of berthierine at depth in the Esk cores (Fig. 4.12) suggests some sort of diagenetic alteration process. Kaolinite is absent at depth in these cores; this Al-silicate plus iron phases (derived by flocculation) and SiO_2 (present as detrital quartz as well as highly reactive silica diatoms and radiolaria) could plausibly be the source of at least some of the berthierine in the Esk cores at depth. The flocculated iron phase could be primary (co-deposited with the sediment) or secondary (infiltrated after deposition). The prevalence of the berthierine in the coarser sediment could be a primary depositional factor or could be a function of the higher permeability of the coarser sediment.

In summary, the chlorite (plus berthierine) concentration seems to be affected by provenance given the different quantities found in the two branches of the estuary. The amount of berthierine (area of the 7Å peak relative to the 14Å peak) is strongly affected by grain size (and maybe permeability) suggesting that a post-depositional process (e.g. infiltration of flocculated Fe-oxides or reduction of co-deposited flocculated Fe-oxides) contributes to the creation of Fe-rich clay. Berthierine is only abundant in the lower parts of the shallow cores and where pyrite is at low concentrations (Fig. 4.12). Where pyrite is most abundant (at depth in the Irt cores), there is little berthierine. This suggests that berthierine can only develop where sulphate reduction (to sulphide) has been hindered.

Analysis of suspended materials revealed kaolinite, illite and chlorite are in the marine-end member and high tide. There is the possibility that these clay minerals are flushed into the sea through the estuarine sediments. However, high tide waters in the estuary are the cleanest of all the estuary waters (they have the smallest quantity of suspended sediment; Figs. 6.9 and 6.10) suggesting that net marine influx of sediment will be minimal. Some part of the estuarine depositional systems with coarse grain sediments (more porous and permeable) is likely to be subject to interstitial washing during tidal cycles. The results of coating coverage analysis showed the coarser host grains have less clay mineral coating (Fig 4.13).

7.1.3 How does fluvial iron form floccules and aggregates in suspended materials in estuary waters and how can these affect clay minerals and so influence reservoir quality?

Chlorite is one of the most important clay minerals for the preservation of anomalously high porosity in deeply buried sandstones. Authigenic Fe-rich chlorite and possibly a small fraction of the detrital chlorite in estuarine sedimentary depositional systems occur as grain coating. Transformation of a precursor Fe rich-clay phase into Fe-chlorite during burial diagenesis has been experimentally illustrated (Aagaard et al. 2000). Furthermore, chlorite coats can preserve high porosity to depths of up to 6 km because they can inhibit quartz cementation (Hillier and Velde 1992; Ehrenberg 1993). The occurrence and amount of chlorite can alter the porosity and permeability of a reservoir (Worden and Burley 2003; Worden and Morad 2003b) such that they directly control their economic feasibility.

Iron agglomeration forms colloids during the mixing of fresh water and saline water (Sholkovitz 1978; Mayer 1982). Estuaries are the best natural place for mixing the saline and fresh water. Iron concentrations in Irt and Esk Rivers decrease as soon as the river water mixes with saline water in the estuary basins (Fig. 5.11). The Irt and Esk Rivers supply high concentrations of dissolved iron (Table 5.1) to their estuaries. Aqueous Fe, during non-conservative behaviour, becomes mobilised in presence of cations during the mixing of freshwater and seawater in associate with organic matters at the estuaries, so estuarine water is a suitable place for clay mineral alteration and specifically cation up-take. Analysis of suspended material in riverine waters and also fluvial sediment investigation showed dioctahedral chlorite and expandable phases beyond the high tide line are dominant (Figs. 6.4 and 6.5), while trioctahedral chlorite is the main chlorite inside the estuary (Figs. 6.6 and 6.7). Suspended materials in the estuarine water at high tide and in the marine–end member showed that trioctahedral chlorite is likely dominant over dioctahedral chlorite (Figs 6.6 to 6.8). Estuarine surface sediment revealed a hinterland–to-estuary increase in trioctahedral Fe-rich chlorite (berthierine is present only in estuarine sediments) (Figs. 3.7 and 3.8). With sources of mobilised iron inside the estuary, up-take of cations and iron can occur. Iron can be taken up into the mineral structure of chlorite and transformation of Fe-Mg chlorite to Fe-rich chlorite is possible. It is probably significant that there is a clear correlation between the lugworm population and the 7Å:14Å peak area ratio (Fig. 3.14); this strongly suggests that animal-sediment interaction is playing a major part in helping to create Fe-rich clay minerals in the Ravenglass estuary (Needham et al. 2004; Worden et al. 2006). If the redox conditions changed from oxidising at the surface to reducing just below the surface, if sulphate were present and if it were reduced to sulphide then pyrite would form. Thus even in reduced states the presence of high concentrations of sulphate and sulphide, chlorite will likely remain a mixed Mg-Fe chlorite and berthierine is unlikely to be formed.

In summary, Fe-clay is created in the estuary at the expense of transported aqueous Fe. Fe-clay is most abundant at the sites of greatest lugworm activity suggesting that biological processes are important for Fe-clay generation and accumulation. Fe-clay is not abundant where pyrite is found suggesting that availability of sulphate, and so sulphide, limits the chance for Fe to be incorporated into silicate minerals. Fe-clay is also more abundant in fine to medium sands (as opposed to silt and mud) suggesting that either vertical infiltration (at low tide) or lateral flow is important.

7.1.4 How hinterland geology, diagenetic and alteration processes, grain-size, and biological activity impact clay mineral distribution in the estuary, and can these controls by discriminated?

The Eskdale granite, the largest exposed intrusion in Cumbria (Soper 1987) comprises two main types of granite; an older biotite-granodiorite in the south and a younger pink-coloured muscovite-granite in the north (Rundle 1979). The River Esk drains mostly the pink-coloured granite (Simpson 1934). Tourmaline occurs as joint-coating and as a replacement of feldspar. Biotite, where present, is typically chloritized or replaced by haematite. Overall, the Eskdale granite shows intense chloritization (Brown et al. 1964).

Triassic sandstones are given the name St. Bees Sandstone Formation (SBSF) in Cumbria (Barnes et al. 1994; Strong et al. 1994). This sandstone crops out in the northern part of the Ravenglass estuary (Fig. 3.1) and it is a local formation name for the Triassic Sherwood sandstones (Barnes et al. 1994) with an exposure at the St. Bees town 20miles north of the Ravenglass village. SBSF is defined as a feldspathic sandstone. The dominant minerals are quartz, K-feldspars, albite, muscovite and biotite with a carbonate cement (Barnes et al. 1994) (Table 3.1).

Chlorite is the only clay mineral that is abundant in both marine and non-marine parts of the Ravenglass estuary system. Chlorite has been reported as an alteration and weathering product in the Eskdale granite (Moseley, 1978), and in the Triassic sandstones (Turner and Ixer 1977; Strong et al. 1994). Therefore, the hinterland geology is likely a major source of the chlorite to the Esk and Irt estuaries. XRD analysis of the River Esk and River Irt stream sediment samples beyond the high tide line revealed chlorite seems to be a mixed Mg-Fe type of chlorite given the (001):(002) ratio of 1:2 (Figs. 3.9 and 10) (Hillier 2003) as well as dioctahedral chlorite (Al-rich chlorite) (Table 3.6). This mix of chlorite seems likely dominated by Fe-Mg chlorite for the Esk river sediments (Tables 3.2 and 6) (Figs. 3.9 and 10). The implication from the change of chlorite composition is that the chlorite being fed into the Esk (especially) and Irt estuaries evolves towards a Fe-rich type of chlorite or berthierine composition (Table 3.6) (Figs. 3.7, 3.9 and 3.15) once it is subject to marine influence. On the other hand, the aqueous iron load of rivers typically decreases once rivers enter the estuary and the salinity starts to increase (Fig. 5.11) (Boyle et al. 1977a). It is possible that fluvial aqueous Fe, trapped in the estuary, is the source of the increasing Fe-content of chlorite. Up-take of the Fe by clay minerals seems to be occurring in the estuary water or sediment. Fe ions are aggregated and then precipitate as

oxide or hydroxide in the estuaries (Eckert and Sholkovitz 1976; Sholkovitz 1978; Mayer 1982), so chlorite and cations, especially iron, are integrated and segregated and up-taking the Fe leads to the new Fe-rich chlorite (berthierine) formation and transformation process.

Feldspar is abundant in the Eskdale granite (Simpson 1934; Soper 1987) and St. Bees sandstones (Strong et al. 1994). However, illite and kaolinite are common weathering products of the feldspar minerals. So, the absence of kaolinite in the stream sediment samples (Figs. 3.8, 9 and 15) and also fluvial suspended materials (Figs. 6.3 and 4) suggests only a limited degree of chemical weathering in the hinterland (Drever and Zobrist 1992).

The presence of kaolinite in the Esk and Irt surface estuarine sediments (Fig. 3.11) suggests that chemical weathering is more advanced within the estuaries. There is a peak (in the XRD pattern) at 9.9Å which represents either illite or muscovite in the river sediments and suspended loads beyond the tide line (Figs. 3.9 and 6.3). Muscovite has been reported in the Eskdale granite (Soper 1987) and St. Bees sandstones (Strong et al. 1994) thus it is possible to see the muscovite in the stream sediments and wash loads. However, there is a small illite peak in the stream sediment samples (Fig. 3.9 and 10) and fluvial wash load as well (Fig. 6.3) suggesting a limited degree of chemical weathering in the hinterland. Feldspars are abundant in the hinterland and also in the stream sediments (Fig. 3.16) and (Table 3.5). On the other hand, illite-smectite has been reported as a product of chemical weathering reaction on muscovite in soils (Oelkers et al. 2008). The much greater abundance of illite in the estuarine and near estuary marine environments (Figs. 3.6-8) (6.11) suggests that chemical weathering of the feldspar minerals originally derived from Eskdale granite for Esk estuary and St. Bees sandstones for Irt estuary is more developed in the estuaries than in the river and its valleys. In the same way, feldspars decrease from hinterland (40%) toward the estuary (10%) (Fig. 3.16) (Table 3.5). However, grain size fraction analysis on the estuarine surface sediments (Fig. 3.12) reveal <0.2μm kaolinite particle size is abundant in the estuarine surface sediments in contrast to the 5.0μm fraction. These very fine-grained kaolinite particles thus seem to be a product of alteration or chemical weathering within the estuary.

In summary and in regards to the grain size fraction analysis (Figs. 3.11 and 12), chemical weathering and diagenesis processes inside the Ravenglass estuary are interpreted to be the

main sources of kaolinite in the surface sediments rather than sediment influx from the marine system waters and settling within the estuary.

In conclusion, hinterland geology has a direct control in clay mineral distribution spatially and stratigraphically in the estuary sediments. Hinterland geology can control the grain size distribution, types of the transported detrial clay minerals to the estuary and also in direct role on alteration of the clay minerals.

Grain size of the estuarine sediment can control the porosity and permeability of the sediment columns in which they also control the quantity of clay mineral coating on sand grains. Grain size distribution of shallow sediments has indirect role on alteration of the clay minerals and finally distribution of the clay minerals across the estuary.

Alteration, chemical weathering and diagenesis processes can change the clay mineralogy content of the estuarine sediments in surface and cores and this can lead the clay mineral distribution inside the estuary.

7.1.5 What are the quality, quantity, and mineralogy of grain coats across an estuary?

Sand grains in the cored samples are coated with a wide-range of the clay minerals. However, the cause of coating remains elusive. Reworking by lugworms can also produce clay rims on detrital grains (Needham et al. 2005) although it is unclear how continuous these rims are. Adhesion of fine clay particles on wetted surfaces and *in situ* disintegration of mud clasts can introduce clay minerals into sand grain coating (Wilson 1992). Sediment ingestion processes represent a new mechanism in which clay mineral rims can form (Needham et al. 2004), but it is not the only mechanism. Infiltration processes can often form continuous clay mineral coating in continental environments (Wilson 1992).

Some of the material coating sand grains in the Ravenglass estuary is Fe-chlorite (and possibly berthierine), but some is illite leading to a mixed mineralogy for clay mineral coats such as illite-dominated illite-chlorite or chlorite-dominated chlorite-illite depending on the relative proportions of the areas of the K and Fe peaks from EDAX spectra (Figs. 4.3 and 4.4). Figure 4.13 shows the extent of sand grain coating by clay mineral as a function of sand grain size. The inverse correlation suggests that the degree of grain

coating is at least partly a function of grain size. Coarser, moderately sorted sands have a lower degree of clay coat coverage relative to the finer, less well sorted sands in the modern sedimentary environment in the Ravenglass. Sediments from the Irt core revealed that grain-coating clay minerals are mainly illite at depth while the shallower core samples contain illite-dominated illite-chlorite. For the Esk cores, the deeper coats are mainly chlorite-dominated illite-chlorite while the shallower grain coats are illite-dominated illite-chlorite. Significantly, these patterns seem to mimic the relative changes of the clay minerals in the quantified XRD-depth plots (Fig. 4.12). This suggests that whatever relative proportions of clay minerals are found in the <2 μm fraction of the bulk sediment are found as grain-coating minerals.

The estuarine Esk sediment grain coats contain chlorite-dominated illite-chlorite at the base and illite-dominated illite-chlorite at the top of the core. For the Irt estuary, the coats are dominated by illite with illite-dominated illite-chlorite at the top of the cores. This seems to reflect the illite-dominated nature of the clay minerals in the Irt's hinterland (Strong et al., 1994). Moreover, the similarity of the grain coat mineralogy to the local bulk-analysed clay minerals for each sample suggests that the coats were, at most only partially inherited as clay-coated sand grains from the fluvial part of the system. Clay coat mineralogy certainly reflects the local provenance but also seems to reflect processes in the local environment of deposition. Sand grains in the surface sediment samples are coated with clay-grade material that is dominated by clay minerals (Fig. 3.4). Much of the coating is Fe-chlorite, given the size of the chlorite (001) trace in Figures 3.6 and 3.7. Some of the coating material is illite leading to a mixed mineralogy for clay coats on sand grains in the Ravenglass estuary. Coatings on sand grains in ancient sediments have been reported to be both illite- and chlorite-bearing (e.g. Ehrenberg, 1993) suggesting that the Ravenglass case study is not especially unusual in this regard. Lugworms in the surface sediments are present as a function of sediment grain size distribution. Lugworms live in shallow depositional environments containing a range of grain sizes; i.e. silt and fine sands to coarse sands, across the estuary. They rework and bioturbate the sediments and also change the chemical properties and mineralogy in sediment as well (Needham 2004; Needham et al. 2004; Needham et al. 2005; Worden et al. 2006). The comparison of the lugworm population and the Fe-rich clay minerals as coating on sand grains (Fig. 3.14) shows the environment of lugworm activity has relatively more Fe-rich clay minerals (Fig. 3.4) in coating patterns compared to the environments with no lugworms (Fig. 3.14). This

broadly seems to suggest that sand grains become coated with whatever clay minerals they are physically close to in the host sediment and animal-sediment interaction has a specific role in clay mineral coating pattern in case of mineralogy. Reworking animals such as lugworms tend to change the sand grain coating to the Fe-rich clay minerals.

7.2 General Conclusion

Estuaries are sites of clay mineral generation and alteration as a function of primary supply and secondary alteration processes. In the Ravenglass estuary, in general, Fe-clays, chlorite and berthierine, are most abundant in the coarsest sediment where pyrite is absent (where the supply of sulphate is lowest). Grain coatings seem to be best developed in the finest sand sediments where illite-chlorite tends to be dominant.

7.2.1 Clay minerals in fluvial sediments

Chlorite, and a minor expandable phase such as hydroxyl-interlayer vermiculite (HIV), dioctahedral chlorite and also illite (in the Irt stream sediments), occur in the fluvial sediments, beyond the tidal reach.

The clay minerals being transported into the Ravenglass estuary by both the River Irt and River Esk are dominated by dioctahedral chlorite. The River Esk transports a trace of illite and probably a substantial fraction of dioctahedral vermiculite to the estuary while the River Irt transports a somewhat greater amount of illite but only a trace of vermiculite into the estuary (Fig. 7.1).

7.2.2 Clay minerals in estuarine system

Both the Esk and Irt arms of the estuary contain abundant kaolinite and illite in the suspended sediment (Fig. 7.1). The Esk arm of the estuary also contains abundant chlorite, possibly dioctahedral, as well as berthierine and some dioctahedral vermiculite. The Irt arm of the estuary also contains abundant chlorite, possibly mixed trioctahedral and dioctahedral types, as well as berthierine and even more dioctahedral vermiculite than the Esk estuary.

Chlorite, illite and kaolinite and possibly berthierine are all present in surface sediment and also chlorite, illite, kaolinite, berthierine and vermiculite are all present in the Irt and Esk arms of the Ravenglass estuary, NW England, as is a gibbsite-like phase and pyrite (Fig. 7.1). Kaolinite and pyrite are more abundant in the Irt estuary cores than the Esk cores

while chlorite and berthierine appear to be more abundant in the Esk estuary cores (Fig. 7.1).

Berthierine has been identified in estuarine sediment by the systematic reduction in intensity of the peak at 12.5° on heating to 400°C. This was not expected given the previous emphasis in the literature on berthierine and the verdine facies being limited to tropical climates.

Given the abundance of kaolinite and illite within the estuarine sediments in comparison to the fluvial sediment, it seems likely that these minerals formed within the estuarine environment.

7.2.3 *In situ* forming clay minerals

Chlorite has two sources in the estuary suspended clays; dioctahedral chlorite and vermiculite is transported from the hinterland via the rivers into the estuary while trioctahedral chlorite seems to be generated *in situ*, presumably in the sediment column mobilised during flood tides.

Kaolinite seems to be generated *in situ*, presumably within the sediment column by alteration or diagenetic processes and subsequently mobilised by flood tide currents.

Illite has two sources in the estuary suspended clays; a trace is transported from the hinterland via the rivers (especially the Irt) into the estuary while elevated illite quantities in the suspended fraction seem to be generated *in situ*, presumably in the sediment column by alteration processes, then mobilised by flood tides.

Given the XRD response of the 7Å peak upon systematic heating to 400°C, it is also possible that berthierine was formed within the estuarine environment. Berthierine probably forms in the estuarine environment by interaction between fluvial colloidal or suspended Fe phases and aluminosilicate minerals.

7.2.4 Stratigraphic variation of clay minerals

Chlorite evolves to a progressively more Fe-rich composition (berthierine) from the hinterland and fluvial to the marine environment suggesting that fluvial colloidal or suspended Fe phases, trapped in the estuary, may have helped to alter the composition of this deposited clay mineral.

The Irt estuary cores have slightly increasing chlorite and decreasing illite from base to tops of cores. Esk estuary cores have slightly decreasing chlorite and increasing kaolinite

from base to tops of cores. Berthierine abundance broadly decreases up-section. Gibbsite is present at depth, where kaolinite is effectively absent.

The loss of kaolinite and creation of gibbsite in the Esk cores suggests that gibbsite is forming from kaolinite. Berthierine and pyrite are mutually exclusive suggesting that berthierine forms where the aqueous sulphide supply (from bacterial reduction of sulphate) is limited.

There seem to be strong provenance controls on the proportions of clay minerals in the cores in the two branches of the estuary. The chlorite-rich weather I-type granite hinterland of the Esk estuary has led to the accumulation of more chlorite (and berthierine) than the chlorite-poor Sherwood Sandstone hinterland of the Irt estuary.

7.2.5 Estuarine water chemistry

Ravenglass estuary water is a conservative mixture between river water and seawater as far as chloride, sodium, potassium and magnesium are concerned. Alkalinity is non-conservative and is added, probably by biogeochemical processes, in the estuary. Calcium is also non-conservative, possibly being lost from the water (as alkalinity increases) due to calcite growth (possibly as shells). Sulphate is present in seawater-like proportions at high tide but may be lost from the water at low tide, possibly by sulphate reduction processes. It is also possible that there is local sulphate addition, possibly by sulphide mineral precipitation.

Dissolved Iron in waters

Iron concentrations are lowest at high tide at all sampling sites on the Ravenglass estuary. Iron concentrations are highest at low tide for the Irt arm of the estuary but are highest on the ebb tide between high and low tide on the Esk arm of the estuary.

The River Irt contains twice as much dissolved iron as the River Esk. Iron concentrations are much lower in the estuary samples than in the feeding rivers so that dissolved iron undergoes large-scale accumulation in the Ravenglass estuary.

Iron concentrations in estuary samples decrease rapidly as salinity increases with low iron concentrations in all estuary samples once salinity exceeds 5,000 mg/L. Iron concentrations also decrease as pH increases. The loss of iron is presumably due to flocculation of colloidal iron oxides, hydroxides and iron-organic complexes as increasing salinity reduces the surface charge of colloids and thus permits aggregation. It is also

possible that sulphate reduction may locally lead to Fe-sulphide creation within the estuary.

Fluvial dissolved iron does not behave conservatively on mixing with seawater; most iron is lost from the water column at an early stage of river water mixing with estuary water. The site of primary iron-loss from the water occurs towards the heads of estuaries but this site will move as a function of time within the tide cycle.

Given that the Esk has highest iron concentrations between high and low tide, it is likely that iron, either dissolved or as fine floccules, is swept from the iron-rich Irt arm of the estuary into the iron-poor Esk arm soon after high tide.

7.2.6 Grain coating quality and quantity

Grain-coating clay minerals are variably present on sand grains from this estuary. Finer grained sand tends to have more complete clay mineral coats than coarser-grained sand. The degree of coating decreases up-section in the Irt Estuary cores. The degree of grain coating is more variable in the Esk estuary but tends to increase up-section. Sand grains in the estuarine surface sediments are coated with a fine layer of clay minerals including chlorite, illite, a mix of illite-chlorite and kaolinite in the Irt estuary and Fe-rich chlorite, berthierine, chlorite-illite and kaolinite in the Esk estuary. This suggests that estuaries are sites not only for Fe-clay creation and accumulation but also for the generation of coated grains, which upon subsequent burial and diagenesis (or transport and burial in other environments of deposition), would become chlorite-coated sand grains.

7.3 Suggestions for future work

The experiments and analysis in this PhD has raised many issues. Not all of these can be answered in one thesis. There is much scope for future work within the field of geochemistry and mineralogy.

7.3.1 Mineralogy

All data and mineralogical data about the Eskdale granite were extracted from the literature. It would be helpful if systematic sampling from the exposed granite in the Esk River catchment could be undertaken and these samples to be prepared and analysed using consistent techniques and procedures such as those employed on the estuarine and fluvial

sediment analysis. Analysis of more fluvial sediments from different reaches in the catchment is also suggested.

Scanning electron microscope analysis on the filter papers could plausibly reveal the natural ingredients of the suspended (non-crystalline) material in the waters which are not analysable with XRD techniques. Analysis and quantification of dissolved organic matter, marine water indicators such as diatoms and radiolarians, Fe-floccules, and clay minerals are also recommended.

The diatom population could reveal marine water influence on the shallow estuarine sediments. The investigation on the diatoms population and other marine water indicators in the samples are thus recommended.

Examining more and deeper cores from different positions in the Irt and Esk estuaries would broaden out the picture of the distribution of clay minerals. More analyses of grain coats as a function of depth and location in the estuary would also be useful. Specifically, it would be good to help better define where (depth, site) Fe-rich clay coats are most abundant. The data suggest finer sands have more clay coats, they also suggest that Fe-coats are prevalent at depth and away from a major source of marine sulphate. It would be good to take more cores in the upper reaches of the Esk (especially) and Irt estuaries to confirm these patterns, with the intention of coring finer sand units.

Transmission electron microscopy (TEM) analysis of the Fe-rich clay samples would possibly help to confirm that berthierine is present in the Ravenglass estuary. TEM includes electron diffraction, lattice imaging and secondary X-ray analytical approaches to help define the crystallography and chemistry of the berthierine although the stability of berthierine in a TEM is unknown. Samples for analysis could include the most deeply buried core samples (from the Esk) where the 7:14 angstrom XRD peak height ratio is highest. Suspended sediment samples from the estuary could also be examined. Clay separate samples could be examined, after being dispersed on a holey-carbon TEM grid.

The kaolinite-to-gibbsite reaction interpreted from the deeper parts of the cores requires further examination. High resolution SEM examination with a FEG-SEM may help this as may examination in a dedicated electron microprobe. TEM analysis may also help although sample preparation may be a challenge, dispersed samples on a holey-carbon grid

may be problematic since the gibbsite is not abundant it may be like looking for a needle in a hay stack).

7.3.2 Geochemistry

A broad climatology and hydrology investigation on both Rivers Irt and Esk catchments would be helpful. Knowledge of surface water run-off (to quantify the bulk of suspended material) and rain precipitation for example, in the catchments can help to better understand the physical and geochemical parameters which control the estuarine sedimentary systems and role of the hinterland geology in clay mineral distribution.

On the other hand, chemical analysis of the water contents such as Br, F, nitrate and nitrite, phosphate, REE and transition metals could better reveal the geochemical behaviour of the sediment and water and the alteration processes.

Analysis of pore waters in the cores (or some form of depth-specific water sampling in lined boreholes) in shallow estuarine sediments is highly recommended to understand the stratigraphy of reactions and geochemical changes in the cores. For this issue, water sampling during a tide cycle from different depths must be considered. Downhole or core-depth specific temperature, pH, alkalinity, dissolved oxygen and carbon, salinity and chloride concentrations are the parameters which should be performed in the field along the other geochemical parameters in the laboratory.

Sulphur isotope analysis of the dissolved sulphate in the estuary waters, from different sites through the tide cycles, should help to reveal whether sulphate reduction is occurring in the estuary; δ34S of the remaining sulphate would increase if sulphate reduction had happened. Similarly, sulphate δ34S would decrease is sulphide oxidation had happened.

Carbon isotope analysis of the dissolved bicarbonate (alkalinity) in the estuary waters, from different sites through the tide cycles, may help to reveal whether biologicaly-derived HCO3 has been added to the estuary. δ13C of the dissolved bicarbonate would need to be characterised in the river systems and in the sea as well as determining the δ13C of the bicarbonate in the estuary.

Repeating the water sampling, filtration and analysis through tide cycles at the same sites at different times of the year would help support the conclusions reached here. Sampling

during neap and spring tides may show different patterns. Sampling the estuary during/after a major rain storm would reveal the impact of different run-off conditions. Sampling estuary waters during strong on-shore winds would also help reveal a stronger influx of marine sediment, a sediment source down-played as a result of the work presented here.

Fe isotope analysis of aqueous and solid phase Fe may help reveal any biological impact on Fe flocculation and Fe mineralisation.

References

Aagaard P, Jahren J, Harstad AO, Nilsen O & Ramm M (2000) Formation of grain coating chlorite in sandstones: laboratory synthesized vs. natural occurrences. *Clay mineral*, **35**,261-269.

Abu-Zeid M & Stanley D (1990) Temporal and spatial distribution of clay minerals in late Quaternary deposits of the Nile delta, Egypt. *Journal of Coastal Research*, **6**,677-698.

Allan J & Komar P (2009) Climate controls on US West Coast erosion processes. *Journal of Coastal Research*, **22**,511-529.

Aller R & Aller J (1998) The effect of biogenic irrigation intensity and solute exchange on diagenetic reaction rates in marine sediments. *Journal of Marine Research*, **56**,905-936.

Aller R, Mackin J & Cox R (1986) Diagenesis of Fe and S in Amazon inner shelf muds: apparent dominance of Fe reduction and implications for the genesis of ironstones. *Continental Shelf Research*, **6**,263-289.

Arthur J, Ball M & Reclamation USBo (1978) *Entrapment of suspended materials in the San Francisco Bay-Delta estuary*, US Dept. of the Interior, Bureau of Reclamation.

Assinder DJ, Kelly M & Aston SR (1985) Tidal variations in dissolved and particulate phase radionuclide activities in the Esk Estuary, England, and their distribution coefficients and particulate activity fractions. *Journal of Environmental Radioactivity*, **2**,1-22.

Bailey S (1980) Summary of recommendations of AIPEA nomenclature committee on clay minerals. *American Mineralogist*, **65**.

Bailey SW (1988) Odinite, a new dioctahedral-trioctahedral Fe3+-rich 1:1 clay Mineral. *clay Minerals*, **23**,237-247.

Baker JC, Havord PJ, Martin KR & Ghori KAR (2000a) Diagenesis and petrographysics of the early Permian Moogooloo sandstone, southern Carnarvon basin, western Australia. *AAPG Bull.*, **84**,250-265.

Baker JC, Havord PJ, Martin KR & Ghori KAR (2000b) Diagenesis and petrophysics of the early permian moogooloo sandstone, Southern carnarvon basin, Western Australia. *Aapg Bulletin-American Association of Petroleum Geologists*, **84**,250-265.

Bale A & Morris A (1981) Laboratory simulation of chemical processes induced by estuarine mixing: the behaviour of iron and phosphate in estuaries. *Estuarine, Coastal and Shelf Science*, **13**,1-10.

Balls P, Laslett R & Price N (1994) Nutrient and trace metal distributions over a complete semi-diurnal tidal cycle in the Forth estuary, Scotland. *Netherlands Journal of Sea Research*, **33**,1-17.

Banfield J, Barker W, Welch S & Taunton A (1999) Biological impact on mineral dissolution: application of the lichen model to understanding mineral weathering in the rhizosphere. *Proceedings of the National Academy of Sciences of the United States of America*, **96**,3404.

Barnes R, Ambrose K, Holliday D & Jones N (1994) Lithostratigraphical subdivision of the Triassic Sherwood sandstone group in west Cumbria. In, Geological Society of London, **50**, 51.

Barnhisel R & Bertsch P (1989) Chlorites and hydroxy-interlayered vermiculite and smectite. *Minerals in soil environments*, **2**,729–788.

Baumfalk Y (1979) Heterogeneous grain size distribution in tidal flat sediment caused by bioturbation activity of Arenicola marina (Polychaeta). *Netherlands Journal of Sea Research*, **13**,428-440.

Belzunce-Segarra M, Wilson M, Fraser A, Lachowski E & Duthie D (2002) Clay mineralogy of Galician coastal and oceanic surface sediments: contributions from terrigenous and authigenic sources. *clay Minerals*, **37**,23.

Berner R (1980) *Early diagenesis: A theoretical approach*, Princeton Univ Pr.

Beukema J & De Vlas J (1979) Population parameters of the lugworm, Arenicola marina, living on tidal flats in the Dutch Wadden Sea. *Netherlands Journal of Sea Research*, **13**,331-353.

Biggs R (1970) Sources and distribution of suspended sediment in northern Chesapeake Bay. *Marine Geology*, **9**,187-201.

Bjolykke K (1998) Clay mineral diagenesis in sedimentary basins-a key to the prediction of rock properties. Examples from the North Sea Basin. *clay Minerals*, **33**,15-34.

Bokuniewicz H (1995) Sedimentary systems of coastal-plain estuaries. *Developments in Sedimentology*, **53**,49-67.

Bousher A (1999) Ravenglass Estuary: Basic characteristics and evaluation of restoration options. *Restrad-Td*, **12**,03.

Boyle E, Collier R, Dengler A, Edmond J, Ng A & Stallard R (1974) On the chemical mass-balance in estuaries. *Geochimica Et Cosmochimica Acta*, **38**,1719-1728.

Boyle E, Edmond J & Sholkovitz E (1977a) The mechanism of iron removal in estuaries. *Geochimica Et Cosmochimica Acta*, **41**,1313-1324.

Boyle EA, Edmond JM & Sholkovitz ER (1977b) The mechanism of iron removal in estuaries. . *Geochim. Cosmochim. Acta.*, **41**,1313-1324.

Branney M & Soper N (1988) Ordovician volcano-tectonics in the English Lake District. *Journal of Geological Society*, **145**,367.

Brindley GW (1982a) Chemical composition. *Clay mineral*, **5**,153-155.

Brindley GW (1982b) Chemical composition of berthierines - a review. *Clays and Clay Minerals*, **30**,153-155.

Brown P, Soper N & Miller J (1964) Age of the principal intrusions of the Lake District. In, Geological Society of London, **34**, 331.

Bull K & Hall J (1986) Aluminium in the Rivers Esk and Duddon, Cumbria, and their tributaries. *Environmental Pollution Series B, Chemical and Physical*, **12**,165-193.

Burley S, Worden RH & Blackwell (2003) *Sandstone Diagenesis: Recent and Ancient*, Blackwell Pub.

Burton J & Liss P (1976) *Estuarine chemistry*, Academic. London. GB.

Caccavo Jr F, Blakemore R & Lovley D (1992) A hydrogen-oxidizing, Fe (III)-reducing microorganism from the Great Bay Estuary, New Hampshire. *Applied and Environmental Microbiology*, **58**,3211.

Cadee GC (1976) Sediment Reworking by Arenicola Marina on Tidal Flats in Dutch Wadden Sea. *Netherlands Journal of Sea Research*, **10**,440-460.

Carpenter-Boggs L, Kennedy A & Reganold J (2000) Organic and biodynamic management: effects on soil biology. *Soil Science Society of America Journal*, **64**,1651-1659.

Carpenter D, Hodson M, Eggleton P & Kirk C (2007) Earthworm induced mineral weathering: Preliminary results. *European Journal of Soil Biology*, **43**,S176-S183.

Chamley H (1989) *Clay sedimentology*, Springer-Verlag, Berlin.

Coleman M, Hedrick D, Lovley D, White D & Pye K (1993) Reduction of Fe (III) in sediments by sulphate-reducing bacteria. *Nature*, **361**,436-438.

Colter V & Ebbern J (1978) The petrography and reservoir properties of some Triassic sandstones of the Northern Irish Sea Basin. *Journal of Geological Society*, **135**,57.

Cowan G & Bradney J (1997) Regional diagenetic controls on reservoir properties in the Millom accumulation: implications for field development. *Geological Society London Special Publications*, **124**,373.

Curtis C, Murchison D, Berner R, Shaw H, Sarnthein M, Durand B, Eglinton G, Mackenzie A & Surdam R (1985) Clay Mineral precipitation and transformation during burial diagenesis and discussion. *Philosophical Transactions of the Royal Society of London. Series A, Mathematical and Physical Sciences*,91-105.

Dalrymple R, Zaitlin B & Boyd R (1992) Estuarine facies models; conceptual basis and stratigraphic implications. *Journal of Sedimentary Research*, **62**,1130.

De Hon R, Washington P, Glawe L, Young L & Morehead E (2001) Formation of northern Louisiana ironstones. *Transcation-Gulf Coast Association of Geological Societies*,55-62.

De Wilde P & Berghuis E (1979) Laboratory experiments on growth of juvenile lugworms, Arenicola marina. *Netherlands Journal of Sea Research*, **13**,487-502.

Deer W, Howie R & Zussman J (1997) *Rock-forming minerals: Single-chain silicates*, Geological Society.

Domenico P, Schwartz F & Zhang H (1998) *Physical and chemical hydrogeology*.

Drever J (1982) *Geochemistry of natural waters*. New Jersey, Prentice-Hall, Inc., Englewood Cliffs

Drever J & Hurcomb D (1986) Neutralization of atmospheric acidity by chemical weathering in an alpine drainage basin in the North Cascade Mountains. *Geology*, **14**,221.

Drever J & Zobrist J (1992) Chemical weathering of silicate rocks as a function of elevation in the southern Swiss Alps. *Geochimica Et Cosmochimica Acta*, **56**,3209-3216.

Drits V, Sakharov B, Lindgreen H & Salyn A (1997) Sequential structure transformation of illite-smectite-vermiculite during diagenesis of Upper Jurassic shales from the North Sea and Denmark. *clay Minerals*, **32**,351.

Dyer K (2009) *ESTUARINE CIRCULATION*. London, Elsevier.

Eberl D, Velde B & McCormick T (1993) Synthesis of illite-smectite from smectite at earth surface temperatures and high pH. *clay Minerals*, **28**,49-49.

Eckert J & Sholkovitz E (1976) The flocculation of iron, aluminium and humates from river water by electrolytes. *Geochimica Et Cosmochimica Acta*, **40**,847-848.

Edzwald J & O'Melia C (1975) Clay distributions in recent estuarine sediments. *Clays and Clay Minerals*, **23**,39-44.

Ehrenberg S (1993) Preservation of anomalously high porosity in deeply buried sandstones by grain-coating chlorite: examples from the Norwegian continental shelf. *AAPG Bulltein*, **77**,1260-1260.

Eisma D (1986) Flocculation and de-flocculation of suspended matter in estuaries. *Netherlands Journal of Sea Research*, **20**,183-199.

Eisma D & de Boer P (1998) *Intertidal deposits: river mouths, tidal flats, and coastal lagoons*, CRC.

Escoube R, Rouxel OJ, Sholkovitz E & Donard OFX (2009) Iron isotope systematics in estuaries: The case of North River, Massachusetts (USA). *Geochimica Et Cosmochimica Acta*, **73**,4045-4059.

Essington M (2004) *Soil and water chemistry: An integrative approach*, CRC.

Fairbridge RW (2002) The estuary: its definition and geodynamic cycle. *North American Coasts: Reading on Evolution, Processes & Policy*,58.

Fan D, Neuser R, Sun X, Yang Z, Guo Z & Zhai S (2008) Authigenic iron oxide formation in the estuarine mixing zone of the Yangtze River. *Geo-Marine Letters*, **28**,7-14.

Fenn C & Gomez B (1989) Particle size analysis of the sediment suspended in a proglacial stream: Glacier de Tsidjiore Nouve, Switzerland. *Hydrological Processes*, **3**,123-135.

Feuillet J & Fleischer P (1980) Estuarine circulation; controlling factor of clay mineral distribution in James River estuary, Virginia. *Journal of Sedimentary Research*, **50**,267.

FitzGerald D, Knight J & SpringerLink (2005) *High resolution morphodynamics and sedimentary evolution of estuaries*, Springer.

Fox L (1983) The removal of dissolved humic acid during estuarine mixing. *Estuarine, Coastal and Shelf Science*, **16**,431-440.

Gammon PR & James NP (2003) Paleoenvironmental controls on Upper Eocene biosiliceous sediments, Southern Australia. *Journal of Sedimentary Research*, **73**,957-972.

Gibbs R (1977) Clay mineral segregation in the marine environment. *Journal of Sedimentary Research*, **47**,237.

Gibbs R, Tshudy D, Konwar L & Martin J (1989) Coagulation and transport of sediments in the Gironde Estuary. *Sedimentology*, **36**,987-999.

Gould K, Pe-Piper G & Piper W (2010) Relationship of diagenetic chlorite rims to depositional facies in lower Cretaceous reservoir sandstones of the Scotian basin. *Sedimentology*, **57**,587-610.

Greenwood P & Habesch S (1997) Diagenesis of the Sherwood sandstone group in the southern east Irish Sea basin (Blocks 110/13, 110/14 and 110/15): constraints from preliminary isotopic and fluid inclusion studies. *Geological Society London Special Publications*, **124**,353.

Griffin G & Ingram R (1954) *Clay minerals of the Neuse River estuary*, University of North Carolina at Chapel Hill.

Head P (1985) *Practical estuarine chemistry: a handbook*, Cambridge University Press.

Hillier S (1993) Origin, diagenesis, and mineralogy of chlorite minerals in Devonian lacustrine mudrocks, Orcadian Basin, Scotland. *Clays and Clay Minerals*, **41**,240-240.

Hillier S (1994) Pore-lining chlorites in siliciclastic reservoir sandstones; electron microprobe, SEM and XRD data, and implications for their origin. *clay Minerals*, **29**,665.

Hillier S (1999) Use of an air brush to spray dry samples for X-ray powder diffraction. *clay Minerals*, **34**,127.

Hillier S (2003) *Quantitative analysis of clay and other minerals in sandstones by X-ray powder diffraction (XRPD)*, Blackwell.

Hillier S & Velde B (1992) Chlorite interstratified with a 7 Å mineral: an example from offshore Norway and possible implications for the interpretation of the composition of diagenetic chlorites. *clay Minerals*, **27**,475-486.

Hornibrook E & Longstaffe F (1996) Berthierine from the lower cretaceous clearwater formation, Alberta, Canada. *Clays and Clay Minerals*, **44**,1-21.

Huang W (1993) Stability and kinetics of kaolinite to boehmite conversion under hydrothermal conditions. *Chemical Geology*, **105**,197-214.

Huthnance J, Allen J, Davies A, Hydes D, James I, Jones J, Millward G, Prandle D, Proctor R & Purdie D (1993) Towards Water Quality Models and Discussion. *Philosophical Transactions: Physical Sciences and Engineering*, **343**,569-584.

Hylleberg J (1975) Selective feeding by Abarenicola pacifica with notes on Abarenicola vagabunda and a concept of gardening in lugworms. *Ophelia*, **14**,113-137.

Ixer R, Turner P & Waugh B (1979) Authigenic iron and titanium oxides in triassic red beds:(St. Bees Sandstone), Cumbria, Northern England. *Geological Journal*, **14**,179-192.

Jeans C (2006) Clay mineralogy of the Jurassic strata of the British Isles. *clay Minerals*, **41**,187.

Jeans C & Merriman R (2006) Clay minerals in onshore and offshore strata of the British Isles: origins and clay mineral stratigraphy. *clay Minerals*, **41**,1.

Komar P & Enfield D (1987) Short-term sea-level changes and coastal erosion. *Society of Economic Paleontologists and Mineralogists Special Publication*, **41**,17–28.

Konhauser K (2007) *Introduction to geomicrobiology*, Wiley-Blackwell.

Konhauser K & Urrutia M (1999) Bacterial clay authigenesis: a common biogeochemical process. *Chemical Geology*, **161**,399-413.

Krauskopf K & Bird D (1995) *Introduction to geochemistry*, McGraw-Hill New York.

Kristensen E (2000) Organic matter diagenesis at the oxic/anoxic interface in coastal marine sediments, with emphasis on the role of burrowing animals. *Hydrobiologia*, **426**,1-24.

Lanson B, Beaufort D, Berger G, Bauer A, Cassagnabere A & Meunier A (2002) Authigenic kaolin and illitic minerals during burial diagenesis of sandstones: a review. *clay Minerals*, **37**,1.

Lowenstam H & Weiner S (1983) *Mineralization by organisms and the evolution of biomineralization*, Springer.

Madejová J (2003) FTIR techniques in clay mineral studies. *Vibrational Spectroscopy*, **31**,1-10.

Maes E, Vielvoye L, Stone W & Delvaux B (1999) Fixation of radiocaesium traces in a weathering sequence mica vermiculite hydroxy interlayered vermiculite. *European Journal of Soil Science*, **50**,107-115.

Maire O, Duchene J, Gremare A, Malyuga V & Meysman F (2007) A comparison of sediment reworking rates by the surface deposit-feeding bivalve Abra ovata during summertime and wintertime, with a comparison between two models of sediment reworking. *Journal of Experimental Marine Biology and Ecology*, **343**,21-36.

Manning A, Langston W & Jonas P (2010) A review of sediment dynamics in the Severn Estuary: Influence of flocculation. *Marine pollution bulletin*, **61**,37-51.

Manning DAC (2003) *Experimental studies of clay mineral occurrence*, Blackwell.

Mayer L (1982) Retention of riverine iron in estuaries. *Geochimica Et Cosmochimica Acta*, **46**,1003-1009.

McIlroy D, Worden R & Needham S (2003) Faeces, clay minerals and reservoir potential. *Journal of the Geological Society*, **160**,489.

McSween H, Richardson S & Uhle M (2003) *Geochemistry: Pathways and processes*, Columbia Univ Pr.

Meade R, Sachs P, Manheim F, Hathaway J & Spencer D (1975) Sources of suspended matter in waters of the Middle Atlantic Bight. *Journal of Sedimentary Research*, **45**,171.

Meadows PS (1991) *The environmental impact of burrows and burrowing animals—conclusions and a model*, Oxford University Press, USA.

Meunier A (2007) Soil hydroxy-interlayered minerals: a re-interpretation of their crystallochemical properties. *Clays and Clay Minerals*, **55**,380.

Meunier A & Velde B (2004) *Illite: origins, evolution, and metamorphism*, Springer Verlag.

Meybeck M (1987) Global chemical weathering of surficial rocks estimated from river dissolved loads. *American Journal of Science*, **287**,401.

Michalopoulos P & Aller R (1995) Rapid clay mineral formation in Amazon delta sediments: reverse weathering and oceanic elemental cycles. *Science*, **270**,614.

Milliman J, Huang-Ting S & Zuo-Sheng Y (1985) Transport and deposition of river sediment in the Changjiang estuary and adjacent continental shelf. *Continental Shelf Research*, **4**,37-45.

Moore D & Reynolds R (1989) *X-ray Diffraction and the Identification and Analysis of Clay Minerals*, Oxford University Press Oxford.

Moseley F (1978) *the geology of the lake district.*

Mosley L, Hunter K & Ducker W (2003) Forces between colloid particles in natural waters. *Environ. Sci. Technol*, **37**,3303-3308.

Mylon S, Chen K & Elimelech M (2004) Influence of natural organic matter and ionic composition on the kinetics and structure of hematite colloid aggregation: Implications to iron depletion in estuaries. *Langmuir*, **20**,9000-9006.

Nagy K & Lasaga A (1993) Simultaneous precipitation kinetics of kaolinite and gibbsite at 80 C and pH 3. *Geochimica Et Cosmochimica Acta*, **57**,4329-4335.

Nahon D (1991) *Introduction to the petrology of soils and chemical weathering*, Wiley-Interscience.

Needham S (2004) Interactive comment on "Animal-sediment interactions: the effect of ingestion and excretion by worms on mineralogy" by SJ Needham et al. *Biogeosciences Discussions*, **1**,S292-S295.

Needham S, Worden RH & McIlroy D (2004) Animal-sediment interactions: the effect of ingestion and excretion by worms on mineralogy. *Biogeosciences*, **1**,113-121.

Needham S, Worden RH & McIlroy D (2005) Experimental production of clay rims by macrobiotic sediment ingestion and excretion processes. *Journal of Sedimentary Research*, **75**,1028.

Odin G (1988) *Green marine clays: oolitic ironstone facies, verdine facies, glaucony facies, and celadonite-bearing facies: a comparative study*, Elsevier Science Ltd.

Oelkers E, Schott J, Gauthier J & Herrero-Roncal T (2008) An experimental study of the dissolution mechanism and rates of muscovite. *Geochimica Et Cosmochimica Acta*, **72**,4948-4961.

Officer C (1981) Physical dynamics of estuarine suspended sediments. *Marine Geology*, **40**,1-14.

Olausson E & Cato I (1980) *Chemistry and biogeochemistry of estuaries*, John Wiley of Sons.

Ouddane B, Skiker M, Fischer J & Wartel M (1999) Distribution of iron and manganese in the Seine river estuary: approach with experimental laboratory mixing. *Journal of Environmental Monitoring*, **1**,489-496.

Pache T, Brockamp O & Clauer N (2008) Varied pathways of river-borne clay minerals in a near-shore marine region: A case study of sediments from the Elbe-and Weser rivers, and the SE North Sea. *Estuarine, Coastal and Shelf Science*, **78**,563-575.

Perillo G (1995) Geomorphology and sedimentology of estuaries: An introduction. *Developments in Sedimentology*, **53**,1-16.

Petschick R, Kuhn G & Gingele F (1996) Clay mineral distribution in surface sediments of the South Atlantic: sources, transport, and relation to oceanography. *Marine Geology*, **130**,203-229.

Phillips J (1986) Coastal submergence and marsh fringe erosion. *Journal of Coastal Research*, **2**,427-436.

Prothero D & Schwab F (2004) *Sedimentary geology: an introduction to sedimentary rocks and stratigraphy*, WH Freeman.

Righi D, Petit S & Bouchet A (1993) Characterization of hydroxy-interlayered vermiculite and illite/smectite interstratified minerals from the weathering of chlorite in a Cryorthod. *Clays and Clay Minerals*, **41**,484-484.

Robins P & Davies A (2010) Morphological controls in sandy estuaries: the influence of tidal flats and bathymetry on sediment transport. *Ocean Dynamics*,1-15.

Rohrlich V, Price N & Calvert S (1969) Chamosite in the recent sediments of Loch Etive, Scotland. *Journal of Sedimentary Research*, **39**,624.

Rossel NC (1982) Clay mineral diagenesis in Rotliegend aeolian sandstones of the southern North Sea. *clay Minerals*, **17**,69-77.

Rowden A, Jones M & Morris A (1998) The role of Callianassa subterranea (Montagu)(Thalassinidea) in sediment resuspension in the North Sea. *Continental Shelf Research*, **18**,1365-1380.

Ruggiero P, Komar P, McDougal W, Marra J & Beach R (2001) Wave runup, extreme water levels and the erosion of properties backing beaches. *Journal of Coastal Research*,407-419.

Rundle C (1979) Ordovician intrusions in the English Lake District. *Journal of Geological Society*, **136**,29.

Ryan P & Hillier S (2002) Berthierine/chamosite, corrensite, and discrete chlorite from evolved verdine and evaporite-associated facies in the Jurassic Sundance Formation, Wyoming. *American Mineralogist*, **87**,1607.

Schmid S, Worden RH & Fisher Q (2004) Diagenesis and reservoir quality of the Sherwood Sandstone (Triassic), Corrib Field, Slyne Basin, west of Ireland. *Marine and Petroleum Geology*, **21**,299-315.

Scholle P & Spearing D (1982) *Sandstone depositional environments*, American Association of Petroleum Geologists.

Schubel J & Carter H (1984) Estuary as a Filter for Fine-Grained Suspended Sediment. *Academic Press, The Estuary as a Filter*,81-105.

Sholkovitz E (1978) The flocculation of dissolved Fe, Mn, Al, Cu, Ni, Co and Cd during estuarine mixing. *Earth and Planetary Science Letters*, **41**,77-86.

Sholkovitz E (1979) Chemical and physical processes controlling the chemical composition of suspended material in the River Tay Estuary. *Estuarine and Coastal Marine Science*, **8**,523-545.

Sholkovitz E, Boyle E & Price N (1978) The removal of dissolved humic acids and iron during estuarine mixing. *Earth and Planetary Science Letters*, **40**,130-136.

Sholkovitz ER (1976) Flocculation of Dissolved Organic and Inorganic Matter during Mixing of River Water and Seawater. *Geochimica Et Cosmochimica Acta*, **40**,831-845.

Simpson B (1934) The petrology of the Eskdale (Cumberland) granite. *Proceedings of the Geologists' Association*, **45**,17-34.

Sionneau T, Bout-Roumazeilles V, Biscaye P, Van Vliet-Lanoe B & Bory A (2008) Clay mineral distributions in and around the Mississippi River watershed and Northern Gulf of Mexico: sources and transport patterns. *Quaternary Science Reviews*, **27**,1740-1751.

Skidmore M, Anderson S, Sharp M, Foght J & Lanoil B (2005) Comparison of microbial community compositions of two subglacial environments reveals a possible role for microbes in chemical weathering processes. *Applied and Environmental Microbiology*, **71**,6986.

Skinner B, Porter S & Park J (2004) *Dynamic Earth: an introduction to physical geology (ed.)*, John Wiley & Sons, Inc.

Small J (1992) Experimental determination of the rates of precipitation of authigenic illite and kaolinite in the presence of aqueous oxalate and comparison to the K/Ar ages of authigenic illite in reservoir sandstones. *Clays and Clay Minerals*, **41**,191-208.

Soper N (1987) The Ordovician batholith of the English Lake District. *geological magazine*, **124**,481-484.

Srodon J (1999) Use of clay minerals in reconstructing geological processes: recent advances and some perspectives. *clay Minerals*, **34**,27-27.

Srodon J, Drits V, McCarty D, Hsieh J & Eberl D (2001) Quantitative X-ray diffraction analysis of clay-bearing rocks from random preparations. *Clays and Clay Minerals*, **49**,514.

Stanev E, Brink-Spalink G & Wolff J (2007) Sediment dynamics in tidally dominated environments controlled by transport and turbulence: A case study for the East Frisian Wadden Sea. *Journal of Geophysical Research*, **112**,C04018.

Starkey HC, Blackmon PD & Hauff PF (1984) The routine mineralogical analysis of clay_bearing samples. *U.S. Geological Survey Bulltein*, **1563**.

Stow C, Roessler C, Borsuk M, Bowen J & Reckhow K (2003) Comparison of estuarine water quality models for total maximum daily load development in Neuse River Estuary. *Journal of Water Resources Planning and Management*, **129**,307.

Strong G Milodowski, AE, Pearce, JM. Kemp, SJ, Prior, SV & Morton. AC 1994. The petrology and diagenesis of Permo-Triassic rocks of the Sellafield area, Cumbria. *Proceedings of the Yorkshire Geological Society*, **50**,77-89.

Strong G, Milodowski A, Pearce J, Kemp S, Prior S & Morton A (1994) The petrology and diagenesis of Permo-Triassic rocks of the Sellafield area, Cumbria. In: *Yorkshire Geological Society*, Geological Society of London, **50**, 77.

Sutcliffe D & Carrick T (1988) Alkalinity and pH of tarns and streams in the English Lake District (Cumbria). *Freshwater Biology*, **19**,179-189.

Thiry M (2000) Palaeoclimatic interpretation of clay minerals in marine deposits: an outlook from the continental origin. *Earth-Science Reviews*, **49**,201-221.

Thom B, Wright L & Coleman J (1975) Mangrove ecology and deltaic-estuarine geomorphology: Cambridge Gulf-Ord River, Western Australia. *The Journal of Ecology*, **63**,203-232.

Tucker M (2001) *Sedimentary petrology: an introduction to the origin of sedimentary rocks*, Wiley-Blackwell.

Turner P & Ixer R (1977) Diagenetic development of unstable and stable magnetization in the St. Bees Sandstone (Triassic) of northern England. *Earth and Planetary Science Letters*, **34**,113-124.

Velde B (1985) *Clay minerals: a physico-chemical explanation of their occurrence*, Elsevier Publishing Company.

Velde B & Church T (1999) Rapid clay transformations in Delaware salt marshes. *Applied Geochemistry*, **14**,559-568.

Volkenborn N, Hedtkamp S, Van Beusekom J & Reise K (2007) Effects of bioturbation and bioirrigation by lugworms (Arenicola marina) on physical and chemical sediment properties and implications for intertidal habitat succession. *Estuarine, Coastal and Shelf Science*, **74**,331-343.

Walderhaug O (1996) Kinetic modeling of quartz cementation and porosity loss in deeply buried sandstone reservoirs. *Aapg Bulletin-American Association of Petroleum Geologists*, **80**,731-745.

Weaver C & Pollard L (1973) *The chemistry of clay minerals*, Elsevier.

White A & Brantley S (1995) Chemical weathering rates of silicate minerals: An overview. *Chemical weathering rates of silicate minerals*, **31**,1–22.

Wiley ML (1978) *Estuarine interactions*. New York, Academic Press Inc.
Wilson M (1999) The origin and formation of clay minerals in soils; past, present and future perspectives. *clay Minerals*, **34**,7.
Wilson MD (1992) Inherited grain-rimming clays in sandstones from eolian and shelf environments: their origin and control on reservoir properties. *Pittman, eds., Origin, diagenesis, and petrophysics of clay minerals in sandstones: SEPM Special Publication*, **47**,209–225.
Worden R & Morad S (2002) Clay minerals in sandstones: controls on formation, distribution and evolution. *Clay mineral cements in sandstones*,3–41.
Worden RH & Burley SD (2003) *Sandstone diagenesis: the evolution of sand to stone*, Blackwell publishing.
Worden RH & Morad S (2003a) *Clay minerals in sandstones: a review of the detrital and diagenetic sources and evolution during burial. In (Worden, R, H, and Morad, S. eds.)*.
Worden RH & Morad S (2003b) Clay minerals in sandstones: controls on formation, distribution and evolution. *Clay mineral cements in sandstones*,3–41.
Worden RH, Needham SJ & Cuadros J (2006) The worm gut; a natural clay mineral factory and a possible cause of diagenetic grain coats in sandstones. *Journal of Geochemical Exploration*, **89**,428-431.
Zhang J, Wen Huang W & Chong Shi M (1990) Huanghe (Yellow River) and its estuary: sediment origin, transport and deposition. *Journal of Hydrology*, **120**,203-223.

Appendices